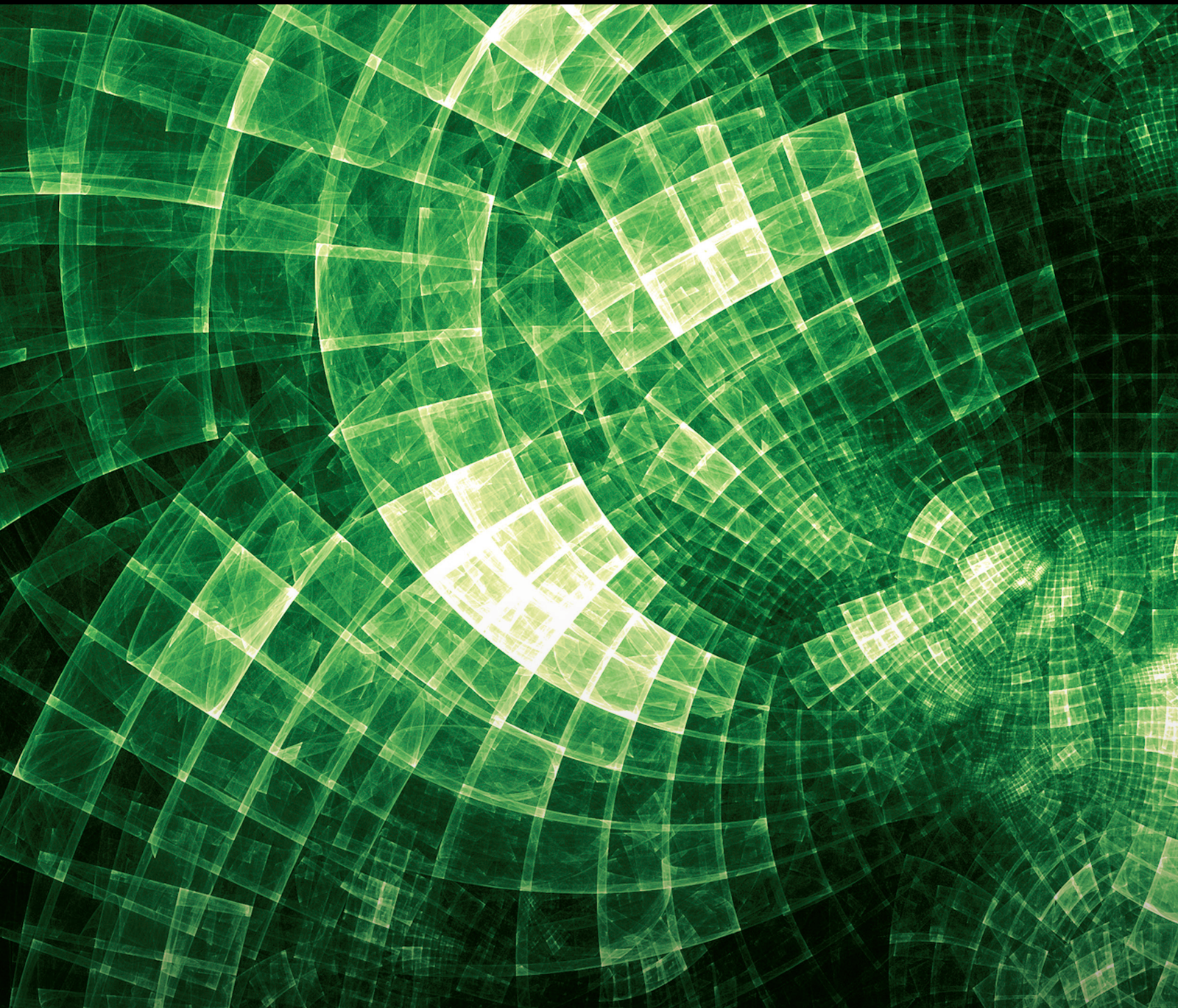# Fractional Operators in Modelling Chaotic and Real-World Problems

Lead Guest Editor: Ndolane Sene
Guest Editors: José Francisco Gómez Aguilar and Kolade M. Owolabi

Fractional Operators in Modelling Chaotic and Real-World Problems

Fractional Operators in Modelling Chaotic and Real-World Problems

Lead Guest Editor: Ndolane Sene
Guest Editors: José Francisco Gómez Aguilar and
Kolade M. Owolabi

Contents

Research Article

Conversion of Fructose to 5-Hydroxymethyl Furfural: Mathematical Solution with Experimental Validation

Muhammad Sajid [iD],[1,2] **Apu Chowdhury,**[1] **Ghulam Bary,**[3] **Yin Guoliang,**[1] **Riaz Ahmad** [iD],[3] **Ilyas Khan** [iD],[4] **Waqar Ahmed,**[5] **Muhammad Farooq Saleem Khan,**[6] **Aisha M. Alqahtani,**[7] **and Md. Nur Alam** [iD][8]

[1]*Faculty of Materials and Chemical Engineering, Yibin University, Yibin 644000, Sichuan, China*
[2]*Department of Chemical Engineering, University of Gujrat, Gujrat 50700, Pakistan*
[3]*Faculty of Science, Yibin University, Yibin 644000, Sichuan, China*
[4]*Department of Mathematics, College of Science Al-Zulfi, Majmaah University, Al-Majmaah 11952, Saudi Arabia*
[5]*Department of Bionanotechnology, Hanyang University, Ansan 155-88, Republic of Korea*
[6]*Faculty of International Applied Technology, Yibin University, Yibin 644000, Sichuan, China*
[7]*Department of Mathematical Sciences, College of Science, Princess Nourah bint Abdulrahman University, P. O. Box 84428, Riyadh 11671, Saudi Arabia*
[8]*Department of Mathematics, Pabna University of Science & Technology, Pabna-6600, Bangladesh*

Correspondence should be addressed to Muhammad Sajid; engr.sajid80@gmail.com, Riaz Ahmad; riazgill2007@gmail.com, and Md. Nur Alam; nuralam.pstu23@gmail.com

Conversion of fructose to furan aldehydes is a rapidly developing concept considering the emergent scenario of the replacement of fossil-derived components to biomass-derived green precursors. 5-hydroxymethyl furfural (HMF) and levulinic acid (LA) are the two most important bio-precursors with expanded downstream utilization in modern industries. Their production from biomass-derived sugars is a complex reaction due to competitive side reactions with a variety of byproducts. Therefore, their simulated optimization is an important tool that can help for process optimization in an economical way. In this article, we have developed a mathematical solution for fructose conversion, HMF production, and levulinic acid (LA) formation in a reactive environment. The accuracy of the developed model is further verified through experiments and found satisfactory with high accuracy. Therefore, the developed model can be used to simulate the reaction environment and product optimization under a given set of conditions.

1. Introduction

The alarming phenomena of global warming and environmental pollution have compelled individuals to shift production processes from fossil-derived to C-neutral feedstock [1–3]. Hence, this compelling problem has expounded the use of lignocellulosic biomass as an efficient and green alternative [4–6]. Lignocellulosic biomass, in this regard, is an abundantly available natural resource of carbohydrates, which is extensively available as forest residues, agricultural waste, and in the form of macro/microalgae [7, 8]. This paradigm shift explored the comprehensive dissolution and fractionation of lignocellulosic biomass to polysaccharides and monosaccharides for further conversion into different downstream expedient commodity chemicals [9–11].

Fructose is the simplest C6 sugar which is obtained by the hydrolysis of cellulose, the major constituent of lignocellulosic biomass [6, 12]. Fructose is versatile platform sugar that has extended utilization due to its biodegradability, environmentally friendly characteristics as well as abundant availability in nature [13, 14]. A long range of different biochemicals can be produced from fructose by employing multiple catalytic routes [15, 16]. Extensive experimental work has been performed on the catalytic

conversion of fructose to 5-hydroxymethyl furfural (HMF) and levulinic acid (LA) [15–17]. In our previous study, it was concluded experimentally that the reaction steps involved in the conversion of fructose are (i) dehydration of fructose to 5-hydroxymethyl furfural and (ii) rehydration of produced HMF to LA and formic acid (FA) consuming two H_2O molecules under a protonic environment, as shown in Scheme 1 [18]. However, the formation of HMF and LA/FA depends strongly on the reaction environment. The proton concentration $[H^+]$, in particular, plays a significant role with strong temperature dependency.

Experimental research is time-consuming and requires extensive financial support [19–21]. To address such challenges, the reaction environment can be optimized using artificial intelligence by developing a similar computational environment [22–26]. Computational analysis is an economical and efficient approach to solving many time-consuming problems [27–30]. Optimized parameters achieved during computational investigations can be used for the performance of experimental work [31, 32]. A reliable balance between computational and experimental results will help to develop a process with less energy and financial affliction [13, 33–35]. However, the computational study needs detailed kinetic data and mathematical modeling for the establishment of a reaction environment similar to experimental conditions [23, 36]. HMF and LA are the two most important bioprecursor components [37, 38]. These can be produced by the catalytic dehydration of C6 sugars under a protonic environment (Scheme 1). Although extensive experimental work has been performed for the conversion of fructose to HMF and LA/FA, however, commercial production of HMF has not been realized yet [39–41]. Mathematical modeling and kinetic data evaluation will help to establish a computational reaction environment for the conversion of fructose to HMF and LA/FA.

Based on this motivational aspect, we have developed a comprehensive kinetic model to sketch the reaction process based on our experimental work [18]. A detailed mathematical model is developed considering the established reaction sequence and reaction stoichiometry. Employing kinetic and mathematical modeling, the theoretical solution of reaction species is developed which will help to establish a real reaction environment in a computational framework. The developed model will help to optimize the dehydrated conversion of lignocellulosic biomass-derived sugar to platform chemicals. This model can be used as a base tool to develop a reaction network model for other sugars, which will ultimately help to convert lignocellulosic biomass to platform chemicals. Replacing the feedstock fructose with other sugars, the same model can be used to elaborate the reaction environment of conversion of various C5 and C6 sugars.

2. Kinetic Modeling

It has been observed that the conversion of fructose proceeded through the dehydration of fructose to HMF followed by the rehydration to LA/FA as shown in Scheme 1 [18]. The mechanistic step took place by the removal of one

water molecule in each step under a protonic environment as shown in Scheme 2.

Hence, the first step is dehydration of fructose to HMF.

$$C_6H_{12}O_6 \xrightarrow[H^+]{k_1} C_6H_6O_3 + 3H_2O \qquad (1)$$
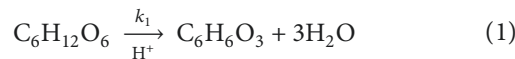
Accordingly, this conversion of fructose to HMF does not proceed in a single step but proceeded through three elementary reactions with the removal of one water molecule in each step as follows:

$$C_6H_{12}O_{6(sol)} \xrightarrow[H^+]{k_1'} [C_6H_{10}O_5]_{(sol)} + H_2O$$

$$[C_6H_{10}O_5]_{(sol)} \xrightarrow[H^+]{k_1''} [C_6H_8O_4]_{(sol)} + H_2O \qquad (2)$$

$$[C_6H_8O_4]_{(sol)} \xrightarrow[H^+]{k_1'''} [C_6H_6O_3]_{(sol)} + H_2O$$
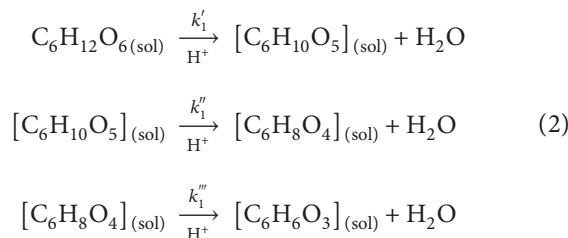
whereas the second step is the hydration of HMF to LA and FA with the consumption of two water molecules.

$$C_6H_6O_{3(sol)} + 2H_2O \xrightarrow[H^+]{k_3} CH_2O_2 + C_5H_8O_3 \qquad (3)$$
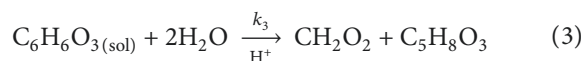
Again, the consumption of two water molecules for the conversion of HMF to LA/FA does not proceed in a single step as shown in Scheme 2. Instead, rehydration proceeded through the following elementary steps:

$$C_6H_6O_{3(sol)} + H_2O \xrightarrow[H^+]{k_3'} [C_6H_8O_4]^+_{(sol)}$$

$$[C_6H_8O_4]^+_{(sol)} + H_2O \xrightarrow[H^+]{k_3''} [C_6H_{10}O_5]^{++}_{(sol)} \qquad (4)$$

$$[C_6H_{10}O_5]^{++}_{(sol)} \xrightarrow[H^+,H_2O]{k_3'''} CH_2O_2 + C_5H_8O_3$$
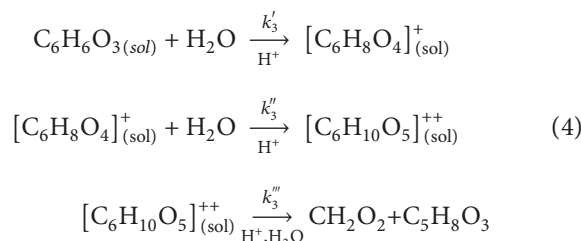
Besides this principal route, fructose degrades through some side reactions yielding unproportioned products. Similarly, the nascent HMF is also degraded sometimes through dimerization or some other nonstoichiometric reactions. All these products are summarized as humin [42, 43]. Therefore, the formation of humin from fructose and HMF can be represented as follows:

$$C_6H_{12}O_6 \xrightarrow[H^+]{k_2} HUMIN \qquad (5)$$

$$C_6H_6O_{3(sol)} \xrightarrow[H^+]{k_4} HUMIN \qquad (6)$$

Following the principles of elementary reactions defined by Espenson and O. Levenspiel [44, 45], the mechanistic elementary reactions of fructose conversion to HMF are as shown in equation (1). HMF conversion to LA/FA is as shown in equation (3) and formation of Humin from fructose as well as from freshly produced HMF can be summarized as shown in equations (7) to (10). [40, 46].
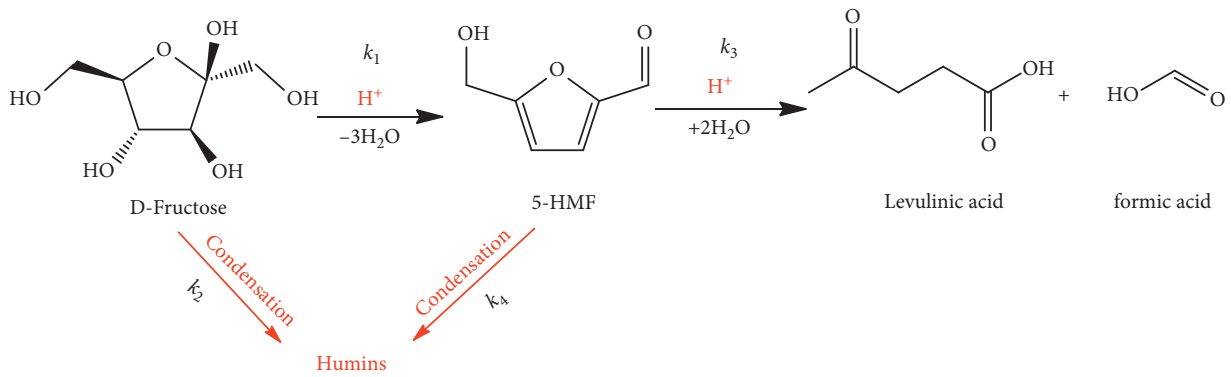
Scheme 1: Reactions pathway of conversion of fructose to 5-HMF and LA/FA [18].
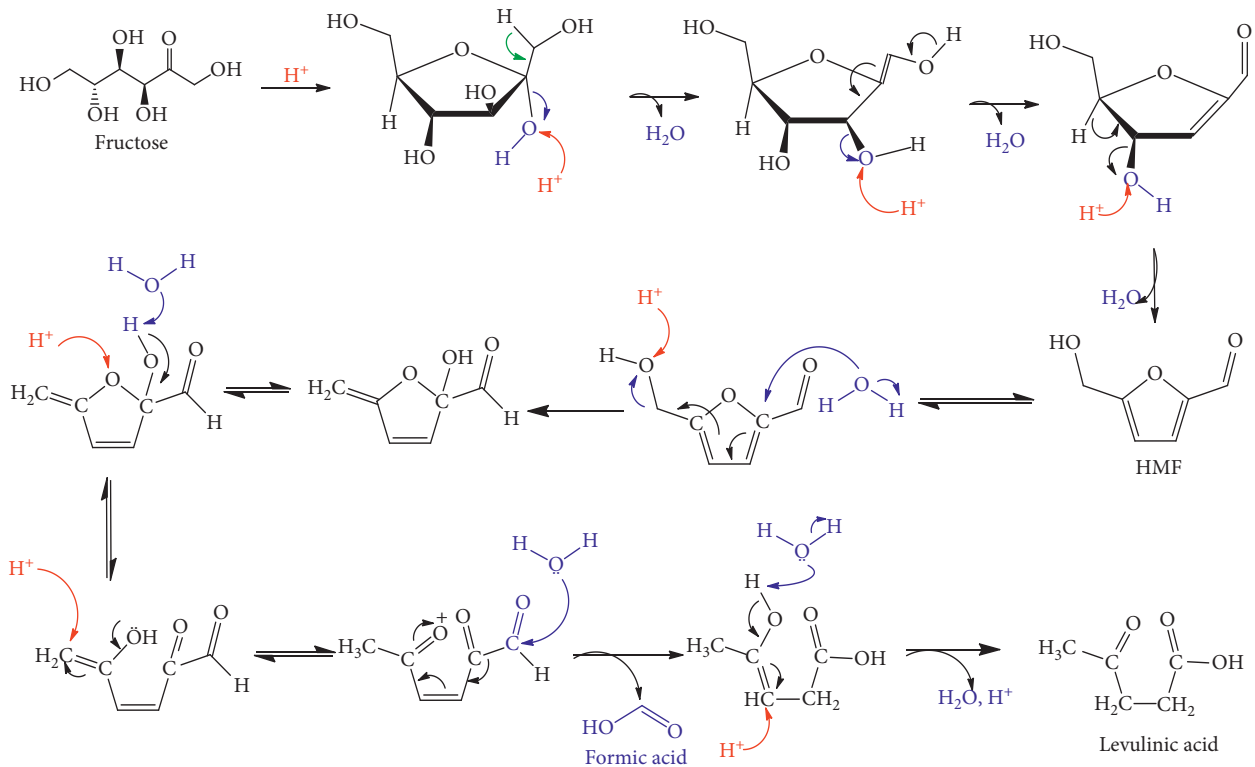
Scheme 2: Complete conversion sequence of fructose conversion to HMF and LA/FA in [H$^+$] environment [18].

$$-\frac{dC_F}{dt} = (k_1 + k_2)C_F, \tag{7}$$

$$\frac{dC_{HMF}}{dt} = k_1 C_F - (k_3 + k_4)C_{HMF}, \tag{8}$$

$$\frac{dC_{LA/FA}}{dt} = k_3 C_{HMF}, \tag{9}$$

$$\frac{dC_H}{dt} = k_2 C_F + k_4 C_{HMF}, \tag{10}$$

where C represents the molar concentration, F is fructose, H is humin, and HMF is 5-hydroxymethyl furfural. k_1, k_2, k_3, and k_4 represent the rate constants as shown in Scheme 1.

3. Mathematical Modeling

Fructose concentration decreases with time as the reaction proceeds. The instantaneous concentration of fructose can be calculated with the integration of the rate equation with respect to time "t" [44, 45, 47]. Hence, from equation (7),

$$-\frac{dC_F}{dt} = (k_1 + k_2)C_F,$$

$$-\frac{1}{C_F}\frac{dC_F}{dt} = (k_1 + k_2). \tag{11}$$

Integrating from the start of the reaction to time interval "t", i.e., between $t = 0$ to $t = t$,

$$\int_0^t \frac{dC_F}{C_F} = -(k_1 + k_2)\int_0^t dt,$$

$$\ln\left(\frac{C_{F(t)}}{C_{F(0)}}\right) = -(k_1 + k_2)t,$$

$$\left(\frac{C_{F(t)}}{C_{F(0)}}\right) = e^{-(k_1+k_2)t}, \tag{12}$$

$$C_{F(t)} = C_{F(0)}\, e^{-(k_1+k_2)t}.$$

Hence, equation (12) represents the analytical solution of fructose concentration. The concentration of fructose at any time (t) can be calculated using this equation (12). Here, $C_{F(t)}$ is the concentration of fructose at a time "t", $C_{F(0)}$ is the initial fructose concentration when $t = 0$, k_1 and k_2 are rate constants as shown in Scheme 1, and "t" is the time of reaction.

Similarly, the instantaneous concentration of HMF can be calculated by the analytical solution of equation (8) implying time limits similar to the fructose equation (7). Hence, from equation (8),

$$\frac{dC_{HMF}}{dt} = k_1 C_F - (k_3 + k_4)C_{HMF},$$

$$\frac{dC_{HMF}}{dt} = C'_{HMF}, \tag{13}$$

$$C'_{HMF} = k_1 C_F - (k_3 + k_4)C_{HMF},$$

$$C'_{HMF} + (k_3 + k_4)C_{HMF} = k_1 C_F.$$

Let $y'(t) = a(t)y(t) = r(t)$.
Therefore,

$$C_{HMF} = y_S + y_H,$$

$$y_H = Ce^{-A(t)}. \tag{14}$$

Here,

$$C = C_{HMF(0)},$$

$$t_0 = 0,$$

$$A(t) = \int_0^t a(t)dt = \int_0^t (k_3 + k_4)dt = (k_3 + k_4)t,$$

$$y_H = C_{HMF(0)}e^{-(k_3+k_4)t}, \tag{15}$$

$$y_S = e^{-A(t)}\int_0^t r(t)e^{A(t)}dt,$$

$$r(t) = k_1 C_F.$$

Putting the value of C_F from equation (12),

$$r(t) = k_1 C_F = k_1 C_F e^{-(k_1+k_2)t},$$

$$\int_0^t r(t)e^{A(t)}dt = \int_0^t k_1 C_{F(0)} e^{(-k_1-k_2+k_3+k_4)t}$$

$$= \frac{k_1 C_{F(0)}}{(-k_1 - k_2 + k_3 + k_4)}\left(e^{(-k_1-k_2+k_3+k_4)t} - 1\right),$$

$$y_S = \frac{k_1 C_{F(0)}}{(-k_1 - k_2 + k_3 + k_4)}\left(e^{-(k_1+k_2)t} - e^{-(k_3+k_4)t}\right), \tag{16}$$

$$C_{HMF(t)} = \frac{k_1 C_{F(0)}}{(-k_1 - k_2 + k_3 + k_4)}\left(e^{-(k_1+k_2)t} - e^{-(k_3+k_4)t}\right) + C_{HMF(0)}e^{-(k_3+k_4)t},$$

$$C_{HMF(t)} = \left[\frac{k_1 C_{F(0)}}{-k_1 - k_2 + k_3 + k_4}\left(e^{(-k_1-k_2+k_3+k_4)t} - 1\right) + C_{HMF(0)}\right]e^{-(k_3+k_4)t},$$

equation (16) represents the analytical explanation for HMF yield concentration. HMF concentration can be calculated using this equation at any time interval (t) during a reaction. Through equations (12) and (16), the concentration profiles of reactant (fructose) and product (HMF) can be developed through simulation. In these models, we have the following assumptions:

(a) The process is acid-catalysed and $[H^+]$ is unchanged during the time course of a reaction

(b) The reaction is assumed to proceed at a fixed temperature

(c) All the unproportioned products are summarized as humin (H)

TABLE 1: Calculated kinetic parameters of organic acid-catalysed dehydration of fructose to HMF. The initial fructose and acid-catalyst concentrations were 1.0 M. The reaction was performed in 50 ml solvent for 3 hours with continuous stirring.

Acid catalyst	Solvent	Temp (°C)	Rate constant (min^{-1})				Goodness of fit (R^2)			
			k_1	k_2	k_3	k_4	Fructose	HMF	LA	Humin
Oxalic acid	Water	100	1.1×10^{-3}	9.7×10^{-4}	1.5×10^{-3}	4.2×10^{-14}	0.9525	0.9849	0.9911	0.8665
pTSA	Water	100	2.1×10^{-3}	1.97×10^{-3}	3.7×10^{-3}	4.4×10^{-13}	0.9576	0.9247	0.9713	0.764

4. Experimental Evolution

Based on these developed models, a control experiment was performed in the laboratory. Oxalic acid was selected as a weak organic acid and p-toluenesulfonic acid (pTSA) as a strong organic acid. Water was selected as a reaction solvent due to its excellent sugar solvation capacity and recognition as a universal solvent; hence, selectively adopted as a solvent in organic reactions. The reaction was proceeded for a long enough time to determine the reaction parameters with high accuracy. The experimental data were used to calculate the kinetic parameter employing developed models in MAT-LAB2016a and presented here in Table 1. With the help of these predicted values, a dynamic simulation of this process was performed. Results thus obtained are then compared with experimental results in Figure 1 and Figure 2 for oxalic acid-catalysed reaction and pTSA catalysed reaction, respectively. Here, the lines are showing the simulated values and symbols are representing experimental results.

Figure 1 elucidates a good relationship between experimental results and model-predicted values. Briefly, there is a difference between model-predicted values and experimental results for fructose conversion and humin formation in the first 120 minutes. This is because of intermediate formation (as shown in Scheme 2). Here, all the unaccounted species formed through different side reactions (condensation, polymerization, and degradation) are termed as humin and calculated by mass difference [48]. Therefore, all the intermediates, whether desired or undesired, were accounted as humin which made the difference. After the first two hours, a good relationship exists for fructose conversion as well as for humin formation. However, for HMF and LA formation, a satisfactory balance can be observed in Figure 1 which proved the model's accuracy and applicability. Additionally, the linear comparison of experimental results and modeled predicted values shows high goods of fit as all the R^2 values are >0.9 (Table 1). Hence, it can be validated that the developed model is appropriate for fructose conversion reactions influenced by weak acids.

It can be observed from Figure 2 that there is a high difference between the experimental value and model-predicted results during the first hour of the reaction, which rapidly decreased in the second hour. After two hours, both values coincide and show high accuracy. However, an overlap of experimental results and model values can be observed for HMF production and LA formation throughout the reaction similar to the oxalic acid-catalysed process (Figure 1). This proved the developed model accuracy for relatively strong acid (pTSA) catalysed fructose conversion reaction. Hence, it can be validated that the developed is equally applicable to both for strong acid as well
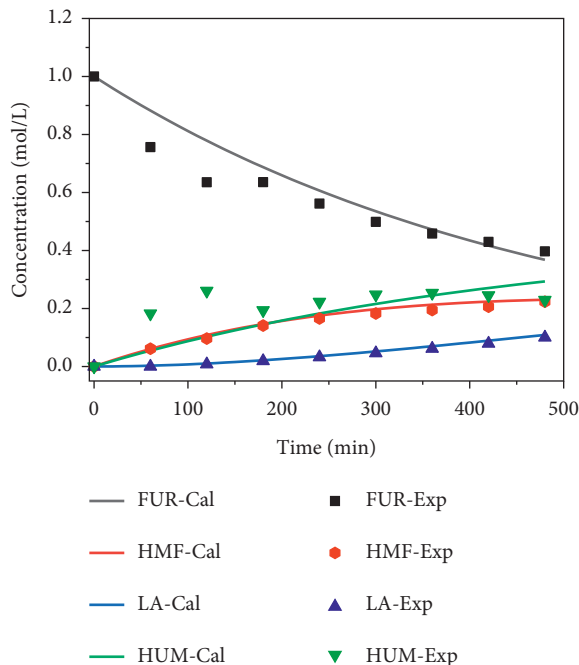
FIGURE 1: Plots of oxalic acid-catalysed conversion of fructose in water solvent. Reaction conditions: 1.0 M oxalic acid with 1.0 M fructose in 50 ml deionized water; FUR: fructose; HMF: 5-hydroxymethylfurfural; LA: levulinic acid; HUM; humin.

as for weak acid-catalysed sugar conversion reactions. Kinetic investigation of the conversion of sucrose solution to HMF employing homogenous catalysts was performed by Abdilla-Santes et al. [49]. The hydrolysis of sucrose yields equimolar concentrations of glucose and fructose. These sugars are then dehydrated to HMF. Therefore, sucrose conversion data are logical to compare with this study because fructose is a common dehydration feedstock in both reactions. It was observed during data analysis that most of the experimental data is comparable with modeled data. The only minor exception was observed with HMF formation during the first hour of the reaction [49]. This anomaly can be explained because the employed catalyst was mineral acid (H_2SO_4) which is more reactive at a reaction temperature of 180°C during the initial phase of the reaction. Overall, the tested model was accurate which was proved with high compatibility of experimental and modeled data-based parity plot. The results presented by Guo et al. [29] are as accurate as shown in this study; however, the catalyst used was again H_2SO_4 and the use of mineral acids as catalysts has severe environmental concerns [50]. Mostly, the use of environmentally friendly catalysts is the primary choice which can be achieved either using organic acid catalysts or
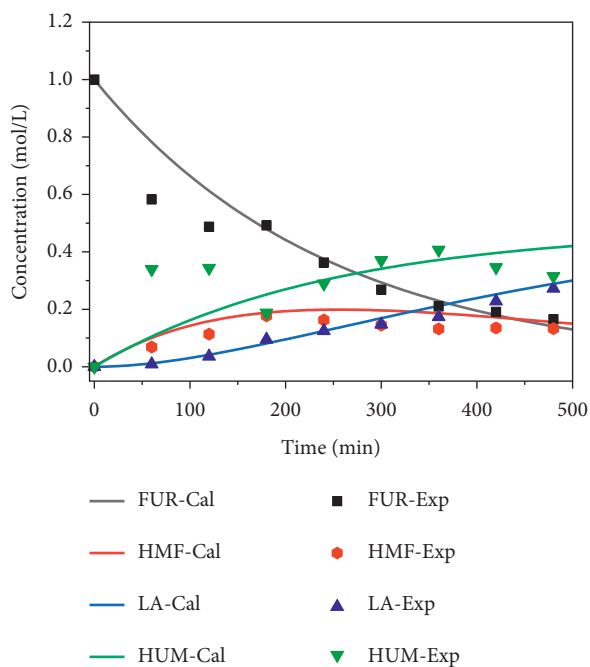
FIGURE 2: Plots of pTSA catalysed conversion of fructose in a water solvent. Reaction conditions: 1.0 M acid with 1.0 M fructose in 50 ml deionized water; FUR: fructose; HMF: 5-hydroxymethylfurfural; LA: levulinic acid; HUM; humin.

recoverable heterogeneous catalysts [51, 52]. Therefore, this study was aimed to use organic acids catalysts to substitute mineral acids as a homogenous catalyst.

It can be observed that most of the model-predicted data are in satisfactory equilibrium with experimental data (Figures 1 and 2). Furthermore, the linear comparison between experimental concentrations with model-predicted values gives very high accuracy as all the R^2 values are >0.9 (Table 1). Hence, a good relationship with high R^2 proved the accuracy of this model. For that reason, this model can be used to predict the experimental outcomes with relatively high accuracy both for strong acids as well as for weak acids catalysed reactions.

5. Conclusions

Conversion of fructose can be optimized using a mathematical model prior to the experimental study. In this paper, an analytical solution for the instantaneous concentration of reacting fructose and products HMF has been developed using kinetic and mathematical modeling. These developed relationships can be used to determine the extent of reaction in a protonic [H$^+$] environment at any time (t) and for the development of concentration profiles in a computational environment. The developed models were further verified with a detailed experiment employing oxalic acid and pTSA as catalysts. The results are elucidated.

(i) The instantaneous concentration of reactant fructose can be calculated theoretically using $C_{F(t)} = C_{F(0)} e^{-(k_1+k_2)t}$.

(ii) The instantaneous concentration of product HMF can be calculated theoretically using $C_{\mathrm{HMF}(t)} = [(k_1 C_{F_{(0)}}$ $/ - k_1 - k_2 + k_3 + k_4)$ $(e^{(-k_1-k_2+k_3+k_4)t} - 1) + C_{\mathrm{HMF}_{(0)}}] e^{-(k_3+k_4)t}$.

(iii) The comparison analyses of experimental data with modeled predicted values elucidated that the developed model is accurate to predict the concentrations because all the values of R^2 are >0.9. Hence, it can be validated that the developed solutions are a good tool to predict the reaction outcomes.

(iv) This model can be used to demonstrate the actual computational environment and reaction behavior during fructose conversion schemes.

(v) This model can be used as a baseline to develop the new specific models for the elaboration of lignocellulosic biomass-derived sugars (C5 and C6) and their derivatives to useful platform chemicals. Further extension of these models will help to demonstrate the computational environment of biomass-derived disaccharides and polysaccharides. Additionally, the model can be extended to elaborate the effect of reaction temperature on concentration profiles of reactants, intermediates, and products.

Data Availability

The required data are included in the manuscript.

Conflicts of Interest

The authors declare that they have no conflicts of interest to report regarding the present study.

Authors' Contributions

Muhammad Sajid, Apu Chowdhury, and Riaz Ahmad conceptualized the study. Muhammad Sajid, Ghulam Bary, and Ilyas Khan developed methodology. Muhammad Sajid, Yin Guoliang, and Riaz Ahmad were responsible for formal analysis. Muhammad Sajid, Waqar Ahmed, and Apu Chowdhury investigated the study. Muhammad Sajid, Yin Guoliang, and Ghulam Bary were responsible for data curation. Muhammad Sajid, Riaz Ahmad, and Muhammad Farooq Saleem Khan prepared the original draft. Muhammad Sajid, Aisha M. Alqahtani, and Md. Nur Alam reviewed and edited the manuscript. Md. Nur Alam, Muhammad Farooq Saleem Khan, and Ilyas Khan supervised the study. Aisha M. Alqahtani and Ilyas Khan were responsible for project administration. Md. Nur Alam and Aisha M. Alqahtani were responsible for funding acquisition. All authors have read and agreed to the published version of the manuscript.

Acknowledgments

References

[1] S. Ge, P. N. Y. Yek, Y. W. Cheng et al., "Progress in microwave pyrolysis conversion of agricultural waste to value-added biofuels: a batch to continuous approach," *Renewable and Sustainable Energy Reviews*, vol. 135, Article ID 110148, 2021.

[2] A. A. Arpia, W.-H. Chen, S. S. Lam, P. Rousset, and M. D. G. de Luna, "Sustainable biofuel and bioenergy production from biomass waste residues using microwave-assisted heating: a comprehensive review," *Chemical Engineering Journal*, vol. 403, Article ID 126233, 2021.

[3] U. Farooq, M. Sajid, A. Shan, X. Wang, and S. Lyu, "Role of cysteine in enhanced degradation of trichloroethane under ferrous percarbonate system," *Chemical Engineering Journal*, vol. 423, Article ID 130221, 2021.

[4] M. Sajid, M. Rizwan Dilshad, M. Saif Ur Rehman et al., "Catalytic conversion of xylose to furfural by p-toluenesulfonic acid (pTSA) and chlorides: process optimization and kinetic modeling," *Molecules*, vol. 26, no. 8, p. 2208, 2021.

[5] C. E. Bounoukta, C. Megías-Sayago, F. Ammari et al., "Dehydration of glucose to 5-Hydroxymethlyfurfural on bifunctional carbon catalysts," *Applied Catalysis B: Environmental*, vol. 286, Article ID 119938, 2021.

[6] S. L. Barbosa, M. D. S. Freitas, W. T. P. dos Santos et al., "Dehydration of d-fructose to 5-hydroxymethyl-2-furfural in DMSO using a hydrophilic sulfonated silica catalyst in a process promoted by microwave irradiation," *Scientific Reports*, vol. 11, no. 1, p. 1919, 2021.

[7] Q. Hou, X. Qi, M. Zhen et al., "Biorefinery roadmap based on catalytic production and upgrading 5-hydroxymethylfurfural," *Green Chemistry*, vol. 23, no. 1, pp. 119–231, 2021.

[8] E. Calcio Gaudino, G. Cravotto, M. Manzoli, and S. Tabasso, "Sono- and mechanochemical technologies in the catalytic conversion of biomass," *Chemical Society Reviews*, vol. 50, 2021.

[9] N. Wu, M. Zhang, X. Pan, J. Zhang, L. Gao, and G. Xiao, "An effective and inexpensive Hf/ZSM-5 catalyst for efficient HMF formation from cellulose," *Catalysis Letters*, vol. 154, 2020.

[10] M. Tan, L. Ma, M. S. U. Rehman et al., "Screening of acidic and alkaline pretreatments for walnut shell and corn stover biorefining using two way heterogeneity evaluation," *Renewable Energy*, vol. 132, pp. 950–958, 2019.

[11] X. Li, K. Peng, Q. Xia, X. Liu, and Y. Wang, "Efficient conversion of cellulose into 5-hydroxymethylfurfural over niobia/carbon composites," *Chemical Engineering Journal*, vol. 332, 2018.

[12] M. Sajid, Y. Bai, D. Liu, and X. Zhao, "Conversion of glucose to 5-hydroxymethylfurfural by Co-catalysis of p-toluenesulfonic acid (pTSA) and chlorides: a comparison based on kinetic modeling," *Waste and Biomass Valorization*, vol. 12, no. 6, pp. 3271–3286, 2021.

[13] X. Zhang, H. Liu, A. Samb, and G. Wang, "CFD simulation of homogeneous reaction characteristics of dehydration of fructose to HMF in micro-channel reactors," *Chinese Journal of Chemical Engineering*, vol. 26, no. 6, pp. 1340–1349, 2018.

[14] H. Li, Y. Zhong, L. Wang et al., "Functionalized metal-organic frameworks with strong acidity and hydrophobicity as an efficient catalyst for the production of 5-hydroxymethylfurfural," *Chinese Journal of Chemical Engineering*, vol. 33, pp. 167–174, 2021.

[15] J. Esteban, A. J. Vorholt, and W. Leitner, "An overview of the biphasic dehydration of sugars to 5-hydroxymethylfurfural and furfural: a rational selection of solvents using COSMO-RS and selection guides," *Green Chemistry*, vol. 22, no. 7, 2020.

[16] C. Thoma, J. Konnerth, W. Sailer-Kronlachner, P. Solt, T. Rosenau, and H. W. G. van Herwijnen, "Current situation of the challenging scale-up development of hydroxymethylfurfural production," *ChemSusChem*, vol. 13, pp. 3544–3564, 2020.

[17] H. Wang, C. Zhu, D. Li et al., "Recent advances in catalytic conversion of biomass to 5-hydroxymethylfurfural and 2, 5-dimethylfuran," *Renewable and Sustainable Energy Reviews*, vol. 103, pp. 227–247, 2019.

[18] M. Sajid, Y. Bai, D. Liu, and X. Zhao, "Organic acid catalyzed production of platform chemical 5-hydroxymethylfurfural from fructose: process comparison and evaluation based on kinetic modeling," *Arabian Journal of Chemistry*, vol. 13, no. 10, pp. 7430–7444, 2020.

[19] M. K. Pasha, L. Dai, D. Liu, M. Guo, and W. Du, "An overview to process design, simulation and sustainability evaluation of biodiesel production," *Biotechnology for Biofuels*, vol. 14, no. 1, p. 129, 2021.

[20] R. Šivec, M. Grilc, M. Huš, and B. Likozar, "Multiscale modeling of (Hemi)cellulose hydrolysis and cascade hydrotreatment of 5-hydroxymethylfurfural, furfural, and levulinic acid," *Industrial and Engineering Chemistry Research*, vol. 58, pp. 16018–16032, 2019.

[21] A. E. Demet, N. Tanchoux, G. Centi et al., "On the R&D landscape evolution in catalytic upgrading of biomass," in *Studies in Surface Science and Catalysis*, vol. 178, pp. 149–171, Elsevier, Amsterdam, Netherlands, 2019.

[22] O. Rosales-Calderon and V. Arantes, "A review on commercial-scale high-value products that can be produced alongside cellulosic ethanol," *BioMed Central*, vol. 12, 2019.

[23] R. S. Assary, T. Kim, J. J. Low, J. Greeley, and L. A. Curtiss, "Glucose and fructose to platform chemicals: understanding the thermodynamic landscapes of acid-catalysed reactions using high-level ab initio methods," *Physical Chemistry Chemical Physics*, vol. 14, no. 48, pp. 16603–16611, 2012.

[24] C. C. Santana Junior, M. C. D. Rambo, R. F. Teófilo, W. J. Cardoso, D. A. Bertuol, and M. K. D. Rambo, "Production of levulinic acid from coconut residues (cocos nucifera) using differents approaches," *Waste and Biomass Valorization*, vol. 12, 2021.

[25] B. Liu, S. Xu, M. Zhang et al., "Electrochemical upgrading of biomass-derived 5-hydroxymethylfurfural and furfural over oxygen vacancy-rich NiCoMn-layered double hydroxides nanosheets," *Green Chemistry*, vol. 23, no. 11, pp. 4034–4043, 2021.

[26] N. Sene, "Fractional model for a class of diffusion-reaction equation represented by the fractional-order derivative," *Fractal and Fractional*, vol. 4, pp. 1–12, 2020.

[27] C. Triebl, V. Nikolakis, and M. Ierapetritou, "Simulation and economic analysis of 5-hydroxymethylfurfural conversion to 2,5-furandicarboxylic acid," *Computers and Chemical Engineering*, vol. 52, 2013.

[28] M. A. Kougioumtzis, A. Marianou, K. Atsonios et al., "Production of 5-HMF from cellulosic biomass: experimental results and integrated process simulation," *Waste and Biomass Valorization*, vol. 9, no. 12, pp. 2433–2445, 2018.

[29] W. Guo, Z. Zhang, J. Hacking, H. J. Heeres, and J. Yue, "Selective fructose dehydration to 5-hydroxymethylfurfural from a fructose-glucose mixture over a sulfuric acid catalyst in a biphasic system: experimental study and kinetic modelling," *Chemical Engineering Journal*, vol. 409, Article ID 128182, 2021.

[30] N. Sene, "Fractional input stability and its application to neural network," *Discrete & Continuous Dynamical Systems - S*, vol. 13, no. 3, pp. 853–865, 2020.

[31] M. Sajid, G. Bary, M. Asim et al., "Synoptic view on P ore beneficiation techniques," *Alexandria Engineering Journal*, vol. 61, no. 4, pp. 3069–3092, 2022.

[32] Q. Chu, W. Tong, S. Wu, Y. Jin, J. Hu, and K. Song, "Eco-friendly additives in acidic pretreatment to boost enzymatic saccharification of hardwood for sustainable biorefinery applications," *Green Chemistry*, vol. 23, no. 11, pp. 4074–4086, 2021.

[33] T. Chakraborti, A. Desouza, and J. Adhikari, "Prediction of thermodynamic properties of levulinic acid via molecular simulation techniques," *ACS Omega*, vol. 3, pp. 18877–18884, 2018.

[34] J. Zhang, S. Zheng, C. Chen, X. Wang, Z. ur Rahman, and H. Tan, "Kinetic model study on biomass pyrolysis and CFD application by using pseudo-Bio-CPD model," *Fuel*, vol. 293, 2021.

[35] N. Sene and A. Atangana, "Integral-balance methods for the fractional diffusion equation described by the caputo-generalized fractional derivative," in *Methods of Mathematical Modelling*, pp. 83–104, CRC Press, Boca Raton, FL, USA, 2020.

[36] Z. Cheng, J. L. Everhart, G. Tsilomelekis, B. Nikolakis, B. Saha, and D. G. Vlachos, "Structural analysis of humins formed in the Brønsted acid catalyzed dehydration of fructose," *Green Chemistry*, vol. 20, no. 5, pp. 997–1006, 2018.

[37] E. J. Cho, L. T. P. Trinh, Y. Song, Y. G. Lee, and H.-J. Bae, "Bioconversion of biomass waste into high value chemicals," *Bioresource Technology*, vol. 298, p. 122386, 2020.

[38] G. C. Hayes and C. R. Becer, "Levulinic acid: a sustainable platform chemical for novel polymer architectures," *Polymer Chemistry*, vol. 11, no. 25, pp. 4068–4077, 2020.

[39] A. Mittal, H. M. Pilath, and D. K. Johnson, "Direct conversion of biomass carbohydrates to platform chemicals: 5-hydroxymethylfurfural (HMF) and furfural," *Energy and Fuels*, vol. 34, no. 3, pp. 3284–3293, 2020.

[40] M. Sayed, N. Warlin, C. Hulteberg et al., "5-Hydroxymethylfurfural from fructose: an efficient continuous process in a water-dimethyl carbonate biphasic system with high yield product recovery," *Green Chemistry*, vol. 22, no. 16, pp. 5402–5413, 2020.

[41] G. Portillo Perez and M.-J. Dumont, "Production of HMF in high yield using a low cost and recyclable carbonaceous catalyst," *Chemical Engineering Journal*, vol. 382, Article ID 122766, 2020.

[42] S. K. R. Patil and C. R. F. Lund, "Formation and growth of humins via aldol addition and condensation during acid-catalyzed conversion of 5-hydroxymethylfurfural," *Energy and Fuels*, vol. 25, no. 10, pp. 4745–4755, 2011.

[43] M. S. Singhvi, A. R. Deshmukh, and B. S. Kim, "Cellulase mimicking nanomaterial-assisted cellulose hydrolysis for enhanced bioethanol fermentation: an emerging sustainable approach," *Green Chemistry*, vol. 23, no. 14, pp. 5064–5081, 2021.

[44] Espenson, *Chemical Kinetics and Reaction Mechanisms*, McGraw-Hill, New York, NY, USA, 2nd edition, 1981.

[45] O. Levenspiel, *Chemical Reaction Engineering*, John Wiley & Sons, Hoboken, NJ, USA, 3rd edition, 2004.

[46] H. Chang, I. Bajaj, A. H. Motagamwala et al., "Sustainable production of 5-hydroxymethyl furfural from glucose for process integration with high fructose corn syrup infrastructure," *Green Chemistry*, vol. 23, no. 9, pp. 3277–3288, 2021.

[47] P. Körner, D. Jung, and A. Kruse, "The effect of different Brønsted acids on the hydrothermal conversion of fructose to HMF," *Green Chemistry*, vol. 20, pp. 2231–2241, 2018.

[48] T. Chhabra, A. Bahuguna, S. S. Dhankhar, C. M. Nagaraja, and V. Krishnan, "Sulfonated graphitic carbon nitride as a highly selective and efficient heterogeneous catalyst for the conversion of biomass-derived saccharides to 5-hydroxymethylfurfural in green solvents," *Green Chemistry*, vol. 21, no. 21, pp. 6012–6026, 2019.

[49] R. M. Abdilla-Santes, J. G. M. Winkelman, I. Van Zandvoort et al., "5-Hydroxy-2-Methylfurfural from sugar beet thick juice: kinetic and modeling studies," *ACS Sustainable Chemistry & Engineering*, vol. 9, no. 7, pp. 2626–2638, 2021.

[50] J. Pang, B. Zhang, Y. Jiang et al., "Complete conversion of lignocellulosic biomass to mixed organic acids and ethylene glycol via cascade steps," *Green Chemistry*, vol. 23, no. 6, pp. 2427–2436, 2021.

[51] M. Sajid, U. Farooq, G. Bary, M. M. Azim, and X. Zhao, "Sustainable production of levulinic acid and its derivatives for fuel additives and chemicals: progress, challenges, and prospects," *Green Chemistry*, vol. 23, no. 23, 2021.

[52] Y. Wang, Z. Hu, G. Fan, J. Yan, G. Song, and J. Li, "Catalytic conversion of glucose to 5-(hydroxymethyl)furfural over phosphotungstic acid supported on SiO2-coated Fe3O4," *Waste and Biomass Valorization*, vol. 10, no. 8, pp. 2263–2271, 2019.

Research Article

The Consensus of Different Fractional-Order Chaotic Multiagent Systems Using Adaptive Protocols

Masoumeh Firouzjahi [ID], Bashir Naderi [ID], and Yousef Edrisi Tabriz [ID]

Department of Mathematics, Payame Noor University, Tehran, Iran

Correspondence should be addressed to Bashir Naderi; b_naderi@pnu.ac.ir

This paper is concerned with the adaptive consensus problem of incommensurate chaotic fractional order multiagent systems. Firstly, we introduce fractional-order derivative in the sense of Caputo and the classical stability theorem of linear fractional order systems; also, algebraic graph theory and sufficient conditions are presented to ensure the consensus for fractional multiagent systems. Furthermore, adaptive protocols of each agent using local information are designed and a detailed analysis of the leader-following consensus is presented. Finally, some numerical simulation examples are also given to show the effectiveness of the proposed results.

1. Introduction

Study of multiagent systems over the past decades in various fields such as biology, mechanics, physics, and, more recently, control theories have been found (see [1]). As one of the most fundamental issues of multiagent systems, the consensus problem has attracted extensive research from various perspectives. Consensus of multiagent systems can be used to solve many complex problems in the control community and have been widely used in sensor network (see [2]), flocking (see [3]), formation control (see [4]), mobile robots (see [5]), and so on. In general, in multiagent systems, consensus means that agents with the arbitrary initial conditions converge to the desired target (position, attitude, speed, phase, etc.) by interacting information with their neighboring agents. In these systems, to achieve the conditions of consensus, graph theory, matrix theory, and the classical stability theorem of fractional-order system have been used, and in terms of classification, there are two general types, consensus with leader and consensus without leader; the latter is more challenging in terms of stability and connected topology than the former (see [6]). In a leader-following consensus, the control signals of the agents are appropriately selected such that their state trajectories follow the leader state, which can be achieved by local information exchanging from the leader and other agents. Prior to 2008, most articles related to multiagent systems worked on consensus of integer-order dynamics, such as consensus algorithms of first-order dynamic systems (see [7–9]) as well as second-order dynamics (see [10]) or even high order dynamic systems (see [11]). However, since many phenomena cannot be accurately explained by integer-order dynamics, such as macromolecule fluids and porous media, a clear example of the fractional order model is the relationship between heat flow and temperature in heat diffusion of a semi-infinite solid (see [12]); also, many systems in the nature can be described and more precisely modeled by a coordinated behavior of agents with fractional-order dynamics(see [13,14]); for instance, the group movement of bacteria in fatty and microbial environments (see [15]) and the coordination of submarines in stagnant water and the movement of land vehicles on sandy, muddy, or grassy roads (see [16]) amongst others, and moreover, compared to the integer-order model, fractional-order systems can provide an excellent method in description the characteristics of the system well; based on these facts, studying the consensus of fractional-order systems has become very important and was fully examined for the first time in [16–18]. Successively, the

convergence speed of consensus for fractional-order multiagent systems was also discussed further in [19] and in [20] and presented the consensus of fractional-order multiagent systems with varying-order $[0 < \alpha < 1, 1 < \alpha < 2]$. The consensus problem of fractional-order systems with input delays and heterogeneous multiagent systems in [21, 22] was also examined.

An interesting issue in fractional-order multiagent systems is that agents follow a leader, where the leader is a special agent and his movement is independent of other agents. It has been reported that such models are an energy-saving mechanism (see [23]), which was found in many biological systems and can also strengthen group communication and orientation. Through the observer method, consensus of multiagent systems with the leader was given by the second-order model and the followers depicted differential order less than two, which was concerned in [24]. In [25], leader-following consensus of fractional-order multiagent systems under fixed topology has been studied.

As we know, the behavior of some fractional dynamical systems in nature can be often chaotic. Chaotic systems are a class of nonlinear deterministic systems and describe numerous complex and unusual behaviors. At first, it has been found that a large number of fractional-order differential systems exhibit chaotic behavior, such as the fractional-order Lorenz system (see [26]), the fractional-order Rossler system (see [27]), the fractional-order Chua system (see [28]), the fractional-order Lü system (see [29]), and the fractional-order Chen system (see [30]). Therefore, control and consensus of fractional-order chaotic systems have attracted great attention. According to one type of classification in terms of the derivative order, consensus in leader-following chaotic fractional systems is divided into two categories. The first group of two dynamic systems have the same order, which is introduced to the commensurate order system, and in the second group, the fractional order of the two systems is different, which is called incommensurate order system, and it is desirable that, by exercising control, the follower system follows the behavior of the leader system. In recent years, many successful attempts have been made to consensus of chaotic commensurate fractional-order systems, but in applied and practical systems, two chaotic systems cannot necessarily be assumed to be the same orders. On the contrary, the methods used to consensus of the same orders' chaotic systems are not easily applicable to consensus of different orders chaotic systems, and also, the incommensurate order system has advantages compared to the previous case. One of them is that the fraction derivative order of the state variables in the follower system, which are to be consensus, is freed from the derivative order component in the leader system, and this can create more flexibility in the choice of leader and follower system. As a result, due to the many applications of chaotic systems consensus in data security in fuzzy systems (see [31]), secure communication (see [32]), the effect of market trust on the financial system (see [33]), and the study and treatment of some diseases, such as the study of tumor cell chaos in the tumor immunity fractional model (see [34]) and its application in neural networks to solve fractional differential

equations (see [35]), motivated us in this paper to deal with the consensus of the different fractional-order chaotic systems using adaptive control.

Adaptive control is a technique of applying some systems' identification techniques to obtain a model and using this model to design a controller (see [36]). The parameters of the controller are adjusted automatically during the operation.

The rest of this paper is organized as follows. In Section 2, the graph theory notations, Caputo fractional operator and one kind of it, the commensurate and incommensurate fractional order system, and some necessary lemmas and theorems are introduced. In Section 3, the main results on adaptive consensus for chaotic fractional multiagent systems with $0 < \alpha \leq 1$ are presented. In Section 4, the corresponding simulation results are provided in this section to demonstrate the effectiveness of the proposed method. Finally, the concluding remarks are given in Section 5.

2. Preliminaries

In this section, first, some basic definitions of algebraic graph theory and Caputo fractional operator will be mentioned. Then, fractional systems with different orders and some necessary lemmas and theorems for the stability of such systems were discussed.

2.1. Graph Theory. Using graphs is the simplest and most effective way to model the exchange of information between factors in multiagent systems with a leader and N agents. Each graph is a pair of $G = (V, \varepsilon)$ that $V = (v_0, v_1, v_2, \ldots, v_N)$ which is a set of empty and finite nodes and $\varepsilon = \left\{ (v_i, v_j), v_i \neq v_j \right\} \subseteq V \times V$ is a set of edges of a graph that connect nodes to each other. Each edge of the graph is shown as an ordered pair (v_i, v_j) which means that the agent j can transfer its information to the agent i, but not necessarily the opposite. An undirected graph has the property that $(v_i, v_j) \in \varepsilon$ implies $(v_j, v_i) \in \varepsilon$. The set of neighbors of node v_i is denoted by $N_i = \left\{ v_j \in V \colon (v_i, v_j) \in \varepsilon \right\}$. Edges of graph can be weighted or weightless. Weight can indicate cost, time, relocation, or any other factor. The weighted adjacency matrix $W = [w_{ij}] \in R^{N \times N}$ of G with nonnegative entries is defined as $w_{ii} = 0, w_{ij} > 0$ if $(v_i, v_j) \in \varepsilon$ and $w_{ij} = 0$, otherwise. The degree matrix of G is $D = \text{diag}(d_1, \ldots, d_N) \in R^{N \times N}$, where diagonal elements $d_i > 0$ if the i agent is a neighbor of the leader and $d_i = 0$, otherwise. The Laplacian matrix $L = [l_{ij}] \in R^{N \times N}$ of the weighted graph G is defined as $l_{ii} = \sum_{j \neq i} w_{ij}$ and $l_{ij} = -w_{ij}$ for $i \neq j$.

Lemma 1 (see [25]). *For any undirected graph G, matrix $H = L + D$ is positive definite if there is at least one directed path from v_0 (the leader) to all the other nodes. Also, it is obvious that all the elements on the main diagonal of the matrix H are all positive.*

2.2. Caputo Fractional Derivative. At present, there are several different definitions regarding the fractional derivative of order $\alpha \geq 0$; Caputo and Riemann–Liouville (R–L)

fractional operators are the two most commonly used in different fields of fractional dynamic systems. The main advantage of the Caputo fraction derivative over the R-L fraction derivative is that the initial conditions for fractional differential equations with the Caputo derivatives are the same as the integer order for the differential equations. Therefore, in this paper, we will adopt the Caputo fractional derivative to model the multiagent systems' dynamics. The Caputo fractional derivative of $f(t)$ with order α can be written as follows (see [13]):

$$_a^c D_t^\alpha = \frac{1}{\Gamma(n-\alpha)} \int_a^t \frac{f^{(n)}(\tau)}{(t-\tau)^{\alpha-n+1}} d\tau, \tag{1}$$

where $n - 1 < \alpha < n, n \in \mathbf{Z}^+$, and $\Gamma(.)$ is the Gamma function:

$$\Gamma(\alpha) = \int_0^\infty e^{-t} t^{\alpha-1} dt. \tag{2}$$

For simplicity, the Caputo derivative $_a^c D_t^\alpha$ is replaced by notation D^α in this paper.

One of the important concepts in fractional systems' theory is stability, where necessary and sufficient conditions for the stability of these systems have been thoroughly studied in (see [37, 38]). For this object, we consider the following linear system of fractional differential equations:

$$D^\alpha x(t) = Ax(t), x(0) = x_0, \tag{3}$$

where $x \in R^n$, the matrix $A \in R^n \times R^n, \alpha = [\alpha_1, \alpha_2, \ldots, \alpha_N]$ indicates the fractional orders, and $\alpha_i = k_i/m_i, (k_i, m_i) = 1, k_i, m_i \in N, 0 < \alpha_i \le 1$, for $i = 1, 2, \ldots, N$, and M is the least common multiple of the denominators m_i.

Theorem 1 (see [37]). *If $\alpha_1 = \alpha_2 = \ldots = \alpha_N$, then system (3) is called a commensurate fractional-order system. In this case, system is asymptotically stable if and only if $|\arg(\lambda_i)| > \alpha\pi/2$ is satisfied for all eigenvalues λ_i matrix $A (\arg(\lambda_i) = \tan^{-1}(\operatorname{Im}(\lambda_i)/\operatorname{Re}(\lambda_i)))$.*

Theorem 2 (see [38]). *If α_i are not identically equal to each other, then system (3) is called an incommensurate fractional-order system. In this case, the system is asymptotically stable if all roots λ_i of the equation $\det(\operatorname{diag}[\lambda^{M\alpha_1}, \lambda^{M\alpha_1}, \ldots, \lambda^{M\alpha_1}] - A) = 0$ satisfy $|\arg(\lambda_i)| > \pi/2M$.*

3. Main Results

In this section, the leader-following consensus problem of incommensurate fractional-order chaotic multiagent systems is discussed, and a distributed adaptive protocol is designed to achieve consensus under an undirected interaction fixed graph. We first consider the different fractional-order multiagent system consisting of N agents and a leader. The dynamics of each agent is given by

$$D^\beta x_i = Bx_i + G(x_i) + U, \tag{4}$$

and the dynamics of the leader(labeled as $i = 0$) is depicted by

$$D^\alpha x_0 = Ax_0 + F(x_0), \tag{5}$$

where D^α means the Caputo fractional derivative of order α, $0 < \beta \le \alpha \le 1$, and $x_i = (x_{i1}, x_{i2}, \ldots, x_{iN}) \in R^N$, $x_0 = (x_{01}, x_{02}, \ldots, x_{0N}) \in R^N$, and $U = (u_1, u_2, \ldots, u_N) \in R^N$ represent the state of ith agent, the state of the leader, and the control input, respectively. $A = (a_{ij})_{N \times N}, B = (b_{ij})_{N \times N}$ are the system matrices and $F(x_0) = (f_1(x_0), f_2(x_0), \ldots, f_N(x_0))^T, G(x_i) = (g_1(x_i), g_2(x_i), \ldots, g_N(x_i))^T$ denote the nonlinear part of the leader-following system.

Remark 1. The leader's dynamic is independent of others. We take the different nonlinear dynamical functions $F(x)$ and $G(x)$ for leader and all the agents, respectively.

Definition 1. The leader-following consensus of systems (4) and (5) will be achieved if, for each agent $i \in \{1, 2, \ldots, N\}$, there is the appropriate control u_i of $\{x_j: j \in N_i\}$ such that the closed-loop system satisfies

$$\lim_{x \to \infty} \|x_i(t) - x_0(t)\| = 0, i = 1, 2, \ldots, N. \tag{6}$$

Theorem 3. *Consider the leader-following multiagent systems (4) and (5), where $\alpha \ne \beta$, but α_i are equal to each other if we define the distributed adaptive control law as follows:*

$$U = \left[D^{-(\alpha-\beta)} - I\right]Bx_i - G(x_i) + D^{-(\alpha-\beta)}\left[(A - B)x_0 + F(x_0)\right.$$
$$\left. -(B + I + \gamma H)(x_i - x_0)\right], \tag{7}$$

such that

$$\gamma > \frac{-1}{\lambda_{\text{Max}}}, \tag{8}$$

where γ is feedback control gain and λ_{Max} is the largest eigenvalue of H; then, all the agents follow the leader under any initial conditions.

Proof. Consider the following system (4), and now, by substituting U from (7) in (4), we have

$$D^\beta x_i = Bx_i + G(x_i) + \left[D^{-(\alpha-\beta)} - I\right]Bx_i - G(x_i) + D^{-(\alpha-\beta)}\left[(A - B)x_0 + F(x_0) - (B + I + \gamma H)(x_i - x_0)\right]$$
$$= D^{-(\alpha-\beta)}Bx_i + D^{-(\alpha-\beta)}\left[(A - B)x_0 + F(x_0) - (B + I + \gamma H)(x_i - x_0)\right]. \tag{9}$$

By taking the fractional derivative of order $\alpha - \beta$ from the above relation, we will have

$$D^{\alpha}x_i = Bx_i + (A - B)x_0 + F(x_0) - (B + I + \gamma H)(x_i - x_0). \tag{10}$$

Let us define the state error between the agents and the leader as $e = x_i - x_0$. Then, the dynamics of e is

$$\begin{aligned} D^{\alpha}e &= Bx_i + Ax_0 - Bx_0 + F(x_0) - (B + I + \gamma H)e \\ &\quad - Ax_0 - F(x_0) \\ &= B(x_i - x_0) - (B + I + \gamma H)e \\ &= -(I + \gamma H)e. \end{aligned} \tag{11}$$

Thus, according to Theorem 1, system (11) is asymptotically stable if

$$\left|\arg\left(\lambda_{i(-I-\gamma H)}\right)\right| > \frac{\alpha\pi}{2}, \forall i \in \{1, 2, \ldots, N\} \tag{12}$$

We select γ so that the following relation is established:

$$-1 - \gamma\lambda_{i(H)} < 0, \forall i \in \{1, 2, \ldots, N\} \tag{13}$$

and on the contrary, from Lemma 1, all eigenvalues of matrix H are nonnegative which implies that

$$-\gamma < \frac{1}{\lambda_{i(H)}}. \tag{14}$$

By definition, $\lambda_{\text{Max}} = \text{Max}(\lambda_H)$, all the agents follow the leader from any initial conditions; it is enough $\gamma > (-1/\lambda_{\text{Max}})$.

The main purpose of this controller is to convert the following system to a fractional-order system equivalent to the leader system so that the derivative order is equal in the corresponding state variables in the two systems. □

Corollary 1. *Consider Theorem 3 under the control law (7). If*

$$\gamma < \frac{-1}{\lambda_{\text{Min}}}, \tag{15}$$

where λ_{min} is the smallest eigenvalue of H, the agents never follow the leader.

Theorem 4. *Consider the leader-following multiagent systems (4) and (5), where $\alpha = \beta$, but α_i are not necessarily equal to each other if we define the distributed adaptive control law as follows:*

$$\begin{aligned} U &= (A - B)x_0 + F(x_0) - G(x_0) - JG(x_0)(x_i - x_0) \\ &\quad - (B + I)(x_i - x_0) - \gamma \operatorname{diag}(H)(x_i - x_0), \end{aligned} \tag{16}$$

such that

$$\gamma > \frac{-1}{\text{Max}(h_{ii})}, \tag{17}$$

where γ is feedback control gain and $\text{Max}(h_{ii})$ and matrix $\operatorname{diag}(H)$ are shown as the largest elements and the elements on the main diagonal of the matrix H, respectively. Matrices L, D and JG are the Laplacian matrix and degree matrix of graph and Jacobian matrix G, respectively. Then, all the agents follow the leader under any initial conditions.

Proof. Consider system (4), and assuming $\alpha_i = \beta_i, \forall i \in \{1, 2, \ldots, N\}$, now, by substituting U from (16) in (4), we have

$$\begin{aligned} D^{\alpha}x_i &= Bx_i + G(x_i) + (A - B)x_0 + F(x_0) - G(x_0) \\ &\quad - JG(x_0)(x_i - x_0) \\ &\quad - (B + I)(x_i - x_0) - \gamma \operatorname{diag}(H)(x_i - x_0). \end{aligned} \tag{18}$$

Now, if we define the state error between the agents and the leader as $e = x_i - x_0$, then the dynamics of e is

$$\begin{aligned} D^{\alpha}e &= Bx_i + G(x_i) + (A - B)x_0 + F(x_0) - G(x_0) - JG(x_0)e \\ &\quad - (B + I)e - \gamma \operatorname{diag}(H)e - Ax_0 - F(x_0) \\ &= Bx_i + G(x_i) - Bx_0 - G(x_0) - JG(x_0)e - (B + I)e \\ &\quad - \gamma \operatorname{diag}(H)e. \end{aligned} \tag{19}$$

By using Taylor expansion around $x_i = x_0 + e$, the following statement is obtained:

$$G(x_i) = G(x_0) + JG(x_0)e + o(\|e\|^2). \tag{20}$$

By combining equations (19) and (20), we have

$$\begin{aligned} D^{\alpha}e &= Bx_i + G(x_0) + JG(x_0)e + o(\|e\|^2) - Bx_0 - G(x_0) - JG(x_0)e - (B + I)e - \gamma \operatorname{diag}(H)e \\ &= -Ie - \gamma \operatorname{diag}(H)e + o(\|e\|^2) \\ &= -\operatorname{diag}(I + \gamma H) + o(\|e\|^2). \end{aligned} \tag{21}$$

Since, α_i are not assumed to be equal, so according to Theorem 2, all roots λ of the equation $\det(\operatorname{diag}[(\lambda^{M\alpha_1}, \lambda^{M\alpha_1}, \ldots, \lambda^{M\alpha_1}) + (I + \gamma H)]) = 0$ satisfy $|\arg(\lambda)| > \pi/2M$ in which λ_i are obtained as follows:

$$\left(\lambda^{M\alpha_1} + 1 + \gamma h_{11}\right)\left(\lambda^{M\alpha_2} + 1 + \gamma h_{22}\right)\ldots\left(\lambda^{M\alpha_N} + 1 + \gamma h_{NN}\right) = 0. \tag{22}$$

So, λ_i holds in at least one of equations $(\lambda^{M\alpha_1} + 1 + \gamma h_{11}) = 0$,

$(\lambda^{M\alpha_2} + 1 + \gamma h_{22}) = 0, \ldots, (\lambda^{M\alpha_N} + 1 + \gamma h_{NN}) = 0.$ Suppose $\lambda = r(\cos\theta + i\sin\theta)$ to get n'th roots of a complex number; we have

$$\begin{cases} \lambda^{M\alpha_1} = -1 - \gamma h_{11} \Longrightarrow \lambda_k = \left(\cos\dfrac{2k\pi + \pi}{M\alpha_1} + i\sin\dfrac{2k\pi + \pi}{M\alpha_1}\right), & k = 0, 1, \ldots, M\alpha_1 - 1, \\[4mm] \lambda^{M\alpha_2} = -1 - \gamma h_{22} \Longrightarrow \lambda_k = \left(\cos\dfrac{2k\pi + \pi}{M\alpha_2} + i\sin\dfrac{2k\pi + \pi}{M\alpha_2}\right), & k = 0, 1, \ldots, M\alpha_2 - 1, \\[4mm] \vdots \\[2mm] \lambda^{M\alpha_N} = -1 - \gamma h_{NN} \Longrightarrow \lambda_k = \left(\cos\dfrac{2k\pi + \pi}{M\alpha_N} + i\sin\dfrac{2k\pi + \pi}{M\alpha_N}\right), & k = 0, 1, \ldots, M\alpha_N - 1. \end{cases} \tag{23}$$

On the contrary, all the elements on the main diagonal of the matrix H are all positive, and as can be seen, if the relation is $\gamma > (-1/\text{Max}(h_{ii}))$, then the condition $|\text{Min}(\arg\lambda_k)| = (\pi/\text{Max}(M\alpha_i)) > (\pi/2M)$ is in all cases, and therefore, the stability condition is established. □

Corollary 2. *Consider Theorem 4 under the control law (16). If*

$$\gamma < \frac{-1}{\text{Min}(h_{ii})}, \tag{24}$$

then the agents never follow the leader.

Remark 2. The case $\alpha \neq \beta$ and α_i are not necessarily equal to each other; initially, using controller (7), the fractional order of the follower system is equal to the order of the leader system; then, to consensus of the systems, we use the stability of Theorem 4 and select γ from equation (15).

4. Numerical Example

In this section, some illustrative examples are presented to verify the efficiency of the proposed leader-following consensus approach. The first example considers the case when fractional orders α, β in the leader-following system are not equal, but $\forall i \in \{1, 2, \ldots, N\}, \alpha_i$ are equal and the second one considers the case when fractional orders α, β in the leader-following system are equal, but α_i are not necessarily equal to each other. The third example is considered $\alpha \neq \beta$ and α_i are not necessarily equal to each other, which are all considered under the undirected graph.

Example 1. Consider a multiagent of chaotic different fractional-order consisting of a leader and three agents, and in order to facilitate the solution of our examples, without loss of generality, we assume that $v_0 = (x_0, y_0, z_0)$ and $v_i = (x_i, y_i, z_i), i = 1, 2, \ldots, N$, for all examples in this section. They are the state variables of the leader and state variables of the agents satisfying

$$\begin{cases} D^{\alpha_1} x_0 = \sigma(y_0 - x_0), \\[2mm] D^{\alpha_2} y_0 = \rho x_0 - x_0 z_0 - y_0, \\[2mm] D^{\alpha_3} z_0 = x_0 y_0 - b z_0, \end{cases} \tag{25}$$

$$\begin{cases} D^{\beta_1} x_i = a_2\left(y_i + \dfrac{x_i - 2x_i^3}{7}\right), \\[3mm] D^{\beta_2} y_i = x_i - y_i + z_i, \\[3mm] D^{\beta_3} z_i = -b_2 y_i, \end{cases} \tag{26}$$

where $\sigma = 10, \rho = 28, b = 8/3$ and $a_2 = 12.75, b_2 = 100/7$.

Assume the Lorenz system (25) is the leader system (see [26]) and the Chua system (26) is the agent systems (see [28]). Also, suppose the topology is described as in Figure 1. For convenience, let $w_{ij} = 1 (d_i = 1)$ if $w_{ij} > 0 (d_i > 0)$ and $w_{ij} = 0 (d_i = 0)$, otherwise. Thus, the Laplacian L and matrix D are as follows:

$$L = \begin{pmatrix} 2 & -1 & -1 \\ -1 & 2 & -1 \\ -1 & -1 & 2 \end{pmatrix},$$

$$D = \begin{pmatrix} 1 & 0 & 0 \\ 0 & 1 & 0 \\ 0 & 0 & 0 \end{pmatrix}. \tag{27}$$

A straightforward calculation shows the largest eigenvalue of $H = L + D$ is $\lambda_{\text{Max}} = 4$. In simulation, we choose $\alpha_i = 0.99$ and $\beta_i = 0.9$, the initial conditions of leader system as $(1, 0, -0.5)$ and the initial conditions of agents system as $(-1, 1, 0), (-0.5, 1.5, 1), (4, 1, -1)$. Under the control law (7), the fractional order of the follower system is equal to the order of the leader system; now, according to (8), by choosing $\gamma = -0.1$, we can see that three agents follow the leader. The consensus errors are shown in Figure 2.

Now, if we increase the feedback control gain γ from -0.1 to 0.75 in the above example, it is expected that the consensus speed will increase; in other words, the time to
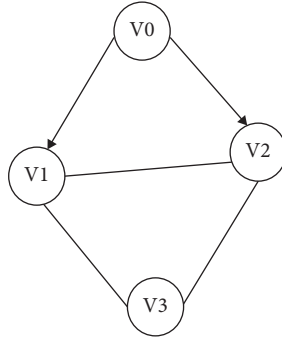
FIGURE 1: The topology of the leader-following multiagent system under the undirected graph.

(a)

(b)

(c)
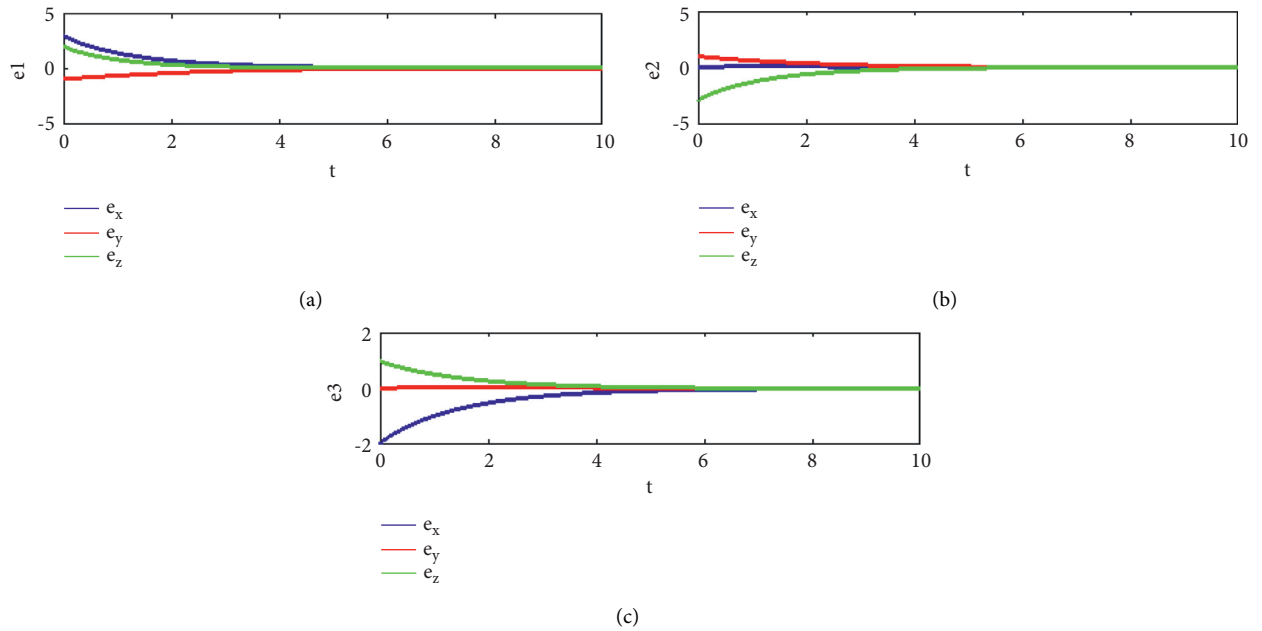
FIGURE 2: The error trajectories of leader and agents with $\gamma = -0.1$ in Example 1. (a) The error trajectories of v0 and v1. (b) The error trajectories of v0 and v2. (c) The error trajectories of v0 and v3.

reach the zero error will decrease, which we see in Figure 3. Time to zero error is reduced from above 5 seconds to below 2 seconds. Table 1 also shows the average time to zero of the variables error with increasing γ.

Also, according eigenvalues of H are $\{0.5858, 3.4142, 4\}$ in the above example; if we suppose $\gamma < -(1/\lambda_{\min})$, for example $\gamma = -0.3$, we will see that the followers do not follow the leader, which is shown in Figure 4. And this example is presented as a proof of Corollary 1.

Example 2. Consider a multiagent of chaotic fractional-order consisting of a leader and three agents. They are the state variables of the leader and state variables of the agents satisfying

$$\begin{cases} D^{\alpha_1} x_0 = a_1 (y_0 - x_0), \\ D^{\alpha_2} y_0 = -x_0 z_0 + c_1 y_0, \\ D^{\alpha_3} z_0 = x_0 y_0 - b_1 z_0, \end{cases} \quad (28)$$

$$\begin{cases} D^{\beta_1} x_i = a_2 (y_i - x_i), \\ D^{\beta_2} y_i = d_2 x_i - x_i z_i + c_2 y_i, \\ D^{\beta_3} z_i = x_i y_i - b_2 z_i, \end{cases} \quad (29)$$

where $a_1 = 36, b_1 = 3,$ and $c_1 = 20$ and $a_2 = 35, b_2 = 3, c_2 = 12,$ and $d_2 = 7.$

Assume the Lü system (28) is the leader system (see [29]) and the Chen system (29) is the agent system (see [30]). Also, suppose the topology is described as in Figure 5. Hence, the Laplacian L and matrix D are as follows:

(a)

(b)

(c)
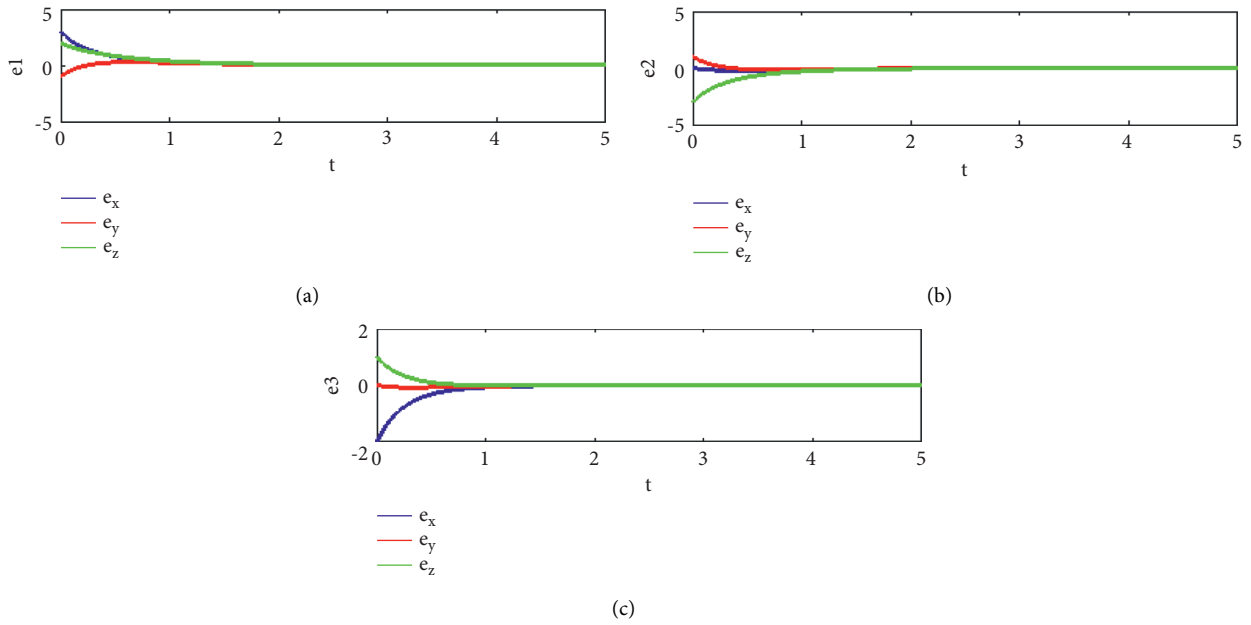
FIGURE 3: The error trajectories of leader and agents with $\gamma = 0.75$ in Example 1. (a) The error trajectories of v0 and v1. (b) The error trajectories of v0 and v2. (c) The error trajectories of v0 and v3.

TABLE 1: Average time to zero of the variables' error with increasing γ in Example 1.

γ	−0.1	0.5	0.75	1	3
T	10.3	2.5	1.8	1.4	1

(a)

(b)

(c)
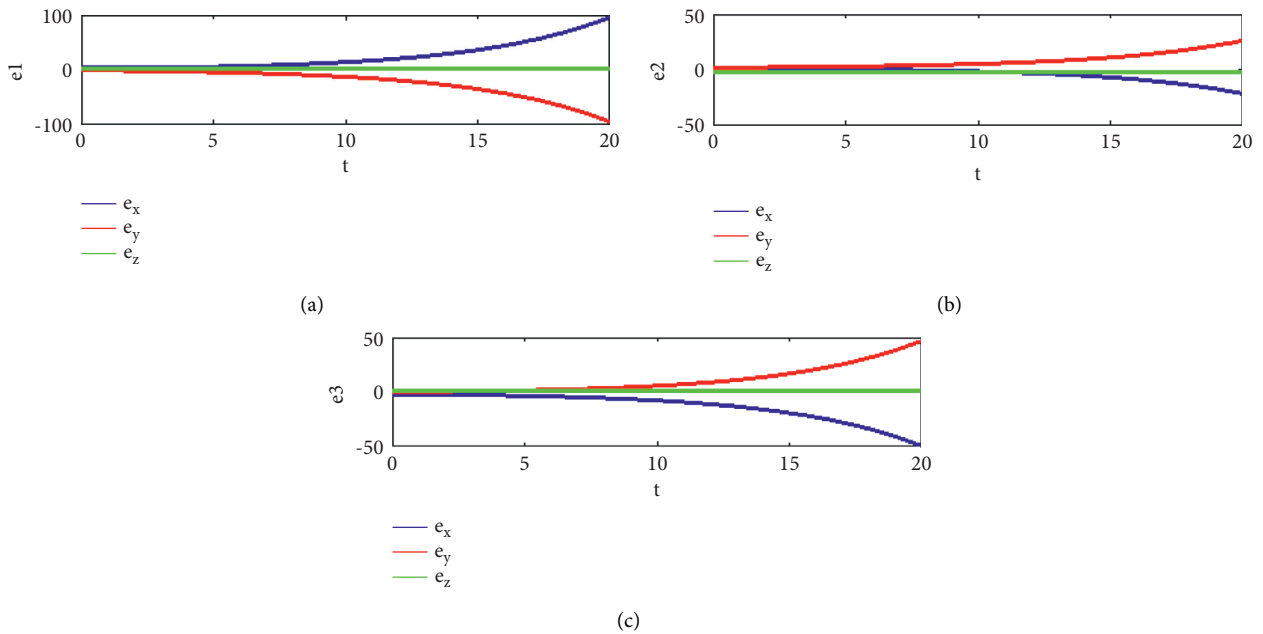
FIGURE 4: The error trajectories of leader and agents with $\gamma = -0.3$ in Example 1. (a) The error trajectories of v0 and v1. (b) The error trajectories of v0 and v2. (c) The error trajectories of v0 and v3.
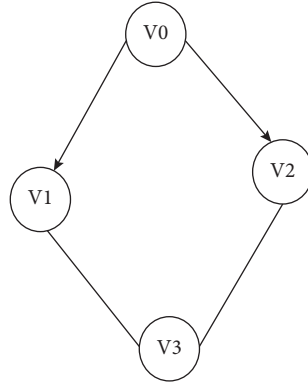
FIGURE 5: The topology of the leader-following multiagent system under the undirected graph.

(a)

(b)

(c)
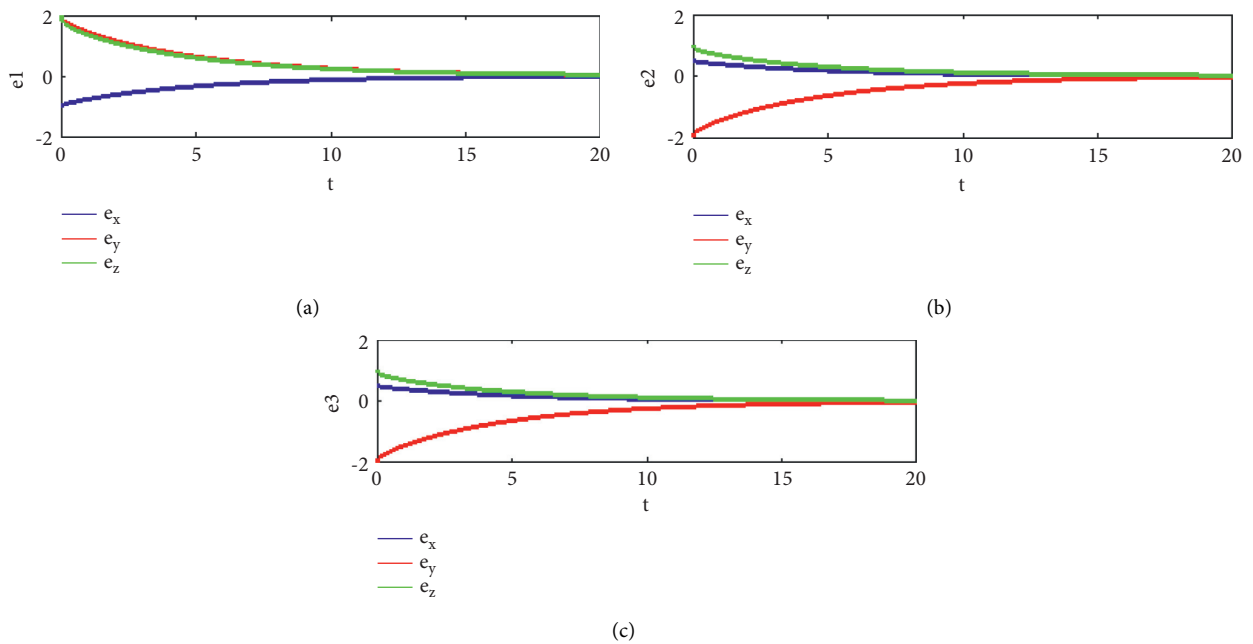
FIGURE 6: The error trajectories of leader and agents with $\gamma = -0.4$ in Example 2. (a) The error trajectories of v0 and v1. (b) The error trajectories of v0 and v2. (c) The error trajectories of v0 and v3.

TABLE 2: Average time to zero of the variables' error with increasing γ in Example 2.

γ	−0.4	−0.1	0.5	1	3
t	22	7.8	3.1	2	0.8

$$L = \begin{pmatrix} 1 & 0 & -1 \\ 0 & 1 & -1 \\ -1 & -1 & 2 \end{pmatrix},$$
$$D = \begin{pmatrix} 1 & 0 & 0 \\ 0 & 1 & 0 \\ 0 & 0 & 0 \end{pmatrix}. \qquad (30)$$

In simulation, we choose $\alpha = \beta = (0.99, 0.98, 0.97)$ and the initial conditions of leader system as $(0.5, 2, 1)$ and the initial conditions of agents syttem as $(-2, 1, 1)$, $(-0.5, 1.5, -3)$, $(4, 0, 1.5)$. Under the control law (16) and

according to equation (17), by choosing $\gamma = -0.4$, consensus occurs in the leader-following system. The consensus errors are shown in Figure 6.

We can see in Table 2 the average time to zero of the variables error with increasing γ in Example 2.

Example 3. Consider Example 1, except that the orders of the leader and follower systems are $\alpha = (0.99, 0.98, 0.97)$ and $\beta_i = 0.96$, respectively. Now, using controller (7), we equalize the orders of the two systems, and then, according to equation (17), we choose $\gamma = 0.5$. The consensus errors are provided in Figure 7.
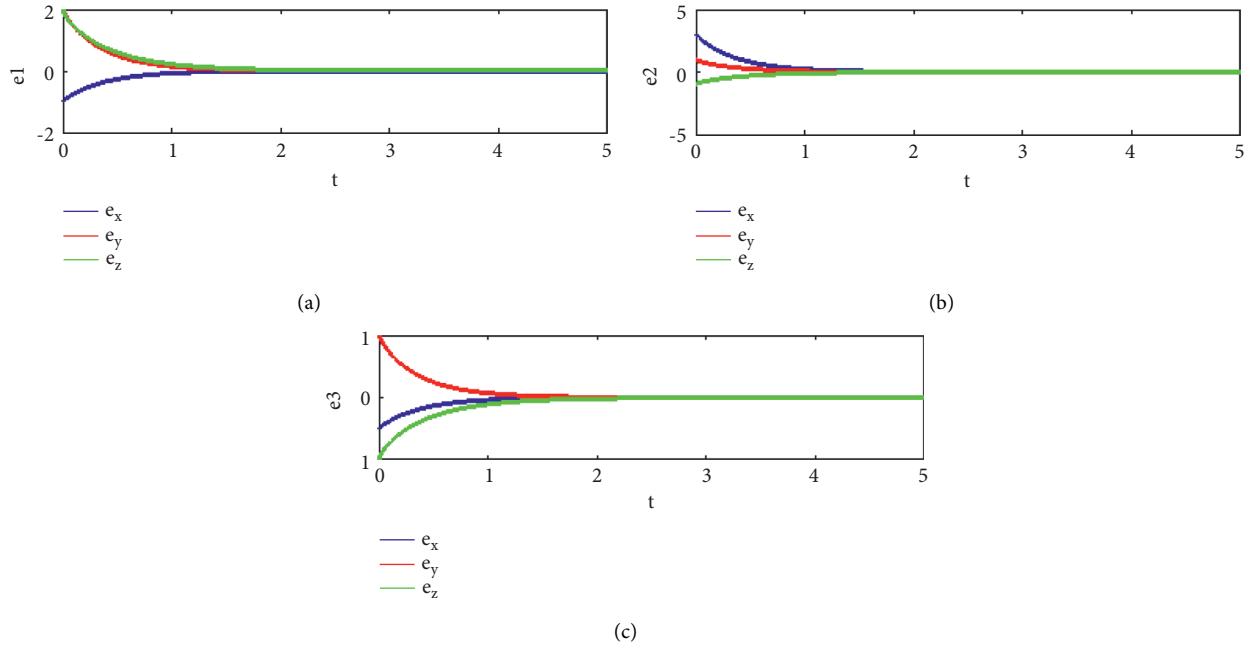
FIGURE 7: The error trajectories of leader and agents with $\gamma = 0.5$ in Example 3. (a) The error trajectories of v0 and v1. (b) The error trajectories of v0 and v2. (c) The error trajectories of v0 and v3.

TABLE 3: Average time to zero of the variables' error with increasing γ in Example 3.

γ	−0.1	0.5	0.75	1	3
t	8.6	2	1.7	1.3	0.7

Table 3 shows the average time to zero of the variables' error with increasing γ in Example 3.

5. Conclusion

In the present paper, we study the consensus of different fractional-order systems with adaptive protocols via an undirected fixed interaction graph. Therefore, using the stability theorems of the fractional order system as well as the concepts of information exchange between graph vertices and corresponding matrices, several types of nonlinear adaptive controllers have been designed to suit the problem conditions. As mentioned in the study, these controllers were designed in such a way that, after applying the controller, the fractional order of all agents of the incommensurate leader-following multiagent system is equal to the fractional order of the leader system so that the two systems can be matched. It should be noted that, in the design of the controllers, the feedback rate coefficient was used and the effective range for the desired coefficient was considered. Future research includes the study of adaptive consensus for fractional time-delayed multiagent systems and or time-varying communication constraints. We can also expand on the condition of consensus in a limited time. Finally, examples and numerical results show that using the appropriate interest rate, the consensus of multiagent systems is guaranteed.

Data Availability

The data used to support the findings of the study are provided within the article.

Conflicts of Interest

The authors declare that they have no conflicts of interest.

References

[1] M. Wooldridge, *An Introduction to Multiagent Systems*, John Wiley & Sons, Hoboken, NJ, USA, 2009.

[2] C. G. Cassandras and W. Li, "Sensor networks and cooperative control," *European Journal of Control*, vol. 11, no. 4-5, pp. 436–463, 2005.

[3] R. Olfati-Saber, "Flocking for multi-agent dynamic systems: algorithms and theory," *IEEE Transactions on Automatic Control*, vol. 51, no. 3, pp. 401–420, 2006.

[4] Z.-w. Hu, J.-h. Liang, L. Chen, and B. Wu, "A hierarchical architecture for formation control of multi-UAV," *Procedia Engineering*, vol. 29, pp. 3846–3851, 2012.

[5] J. Ghommam, M. S. Mahmoud, and M. Saad, "Robust cooperative control for a group of mobile robots with quantized information exchange," *Journal of the Franklin Institute*, vol. 350, no. 8, pp. 2291–2321, 2013.

[6] W. Liu, S. Zhou, Y. Qi, and X. Wu, "Leaderless consensus of multi-agent systems with lipschitz nonlinear dynamics and switching topologies," *Neurocomputing*, vol. 173, pp. 1322–1329, 2016.

[7] F. Chen, Z. Chen, L. Xiang, Z. Liu, and Z. Yuan, "Reaching a consensus via pinning control," *Automatica*, vol. 45, no. 5, pp. 1215–1220, 2009.

[8] Y. Liu and Y. Jia, "Adaptive leader-following consensus control of multi-agent systems using model reference adaptive

control approach," *IET Control Theory & Applications*, vol. 6, no. 13, pp. 2002–2008, 2012.

[9] B. Liu, W. Lu, and T. Chen, "Pinning consensus in networks of multiagents via a single impulsive controller," *IEEE Transactions on Neural Networks and Learning Systems*, vol. 24, no. 7, pp. 1141–1149, 2013.

[10] Y. Qian, X. Wu, J. Lü, and J.-A. Lu, "Second-order consensus of multi-agent systems with nonlinear dynamics via impulsive control," *Neurocomputing*, vol. 125, pp. 142–147, 2014.

[11] Y. Liu and Y. Jia, "Consensus problem of high-order multi-agent systems with external disturbances: an H_∞ analysis approach," *International Journal of Robust and Nonlinear Control*, vol. 20, no. 14, pp. 1579–1593, 2010.

[12] I. Podlubny, "Fractional differential equations," *Mathematicsin Science and Engineering,* vol. 198, Academic Press, San Diego, CA, USA, 1999.

[13] A. A. Kilbas, H. M. Srivastava, and J. J. Trujillo, *Theory and Applications of Fractional Differential Equations*, Elsevier Science Inc., New York, NY, USA, 2006.

[14] C. A. Monje, Y. Q. Chen, B. M. Vinagre, D. Xue, and V. Feliu-Batlle, *Fractional-order Systems and Controls: Fundamentals and Applications*, Springer Science & Business Media, Berlin, Germany, 2010.

[15] Y. Kozlovsky, I. Cohen, I. Golding, and E. Ben-Jacob, "Lubricating bacteria model for branching growth of bacterial colonies," *Physical Review E*, vol. 59, no. 6, pp. 7025–7035, 1999.

[16] Y. Cao, Y. Li, W. Ren, and Y. Q. Chen, "Distributed coordination of networked fractional-order systems," *IEEE Transactions on Systems, Man, and Cybernetics, Part B (Cybernetics)*, vol. 40, no. 2, pp. 362–370, 2009.

[17] Y. Cao, Y. Li, W. Ren, and Y. Q. Chen, "Distributed coordination algorithms for multiple fractional-order systems," in *Proceedings of the 2008 47th IEEE Conference on Decision and Control*, pp. 2920–2925, IEEE, Cancun, Mexico, December 2008.

[18] Y. Cao and W. Ren, "Distributed formation control for fractional-order systems: dynamic interaction and absolute/relative damping," *Systems & Control Letters*, vol. 59, no. 3-4, pp. 233–240, 2010.

[19] W. Sun, Y. Li, C. Li, and Y. Chen, "Convergence speed of a fractional order consensus algorithm over undirected scale-free networks," *Asian Journal of Control*, vol. 13, no. 6, pp. 936–946, 2011.

[20] C. Song and J. Cao, "Consensus of fractional-order linear systems," in *Proceedings of the 2013 9th Asian Control Conference (ASCC)*, pp. 1–4, Istanbul, Turkey, June 2013.

[21] J. Shen and J. Cao, "Necessary and sufficient conditions for consensus of delayed fractional-order systems," *Asian Journal of Control*, vol. 14, no. 6, pp. 1690–1697, 2012.

[22] X. Yin, D. Yue, and S. Hu, "Consensus of fractional-order heterogeneous multi-agent systems," *IET Control Theory & Applications*, vol. 7, no. 2, pp. 314–322, 2013.

[23] D. Hummel, "Formation flight as an energy-saving mechanism," *Israel Journal of Ecology and Evolution*, vol. 41, no. 3, pp. 261–278, 1995.

[24] W. Yu, Y. Li, G. Wen, X. Yu, and J. Cao, "Observer design for tracking consensus in second-order multi-agent systems: fractional order less than two," *IEEE Transactions on Automatic Control*, vol. 62, no. 2, pp. 894–900, 2016.

[25] Z. Yu, H. Jiang, and C. Hu, "Leader-following consensus of fractional-order multi-agent systems under fixed topology," *Neurocomputing*, vol. 149, pp. 613–620, 2015.

[26] Y. Yu, H.-X. Li, S. Wang, and J. Yu, "Dynamic analysis of a fractional-order Lorenz chaotic system," *Chaos, Solitons & Fractals*, vol. 42, no. 2, pp. 1181–1189, 2009.

[27] C. Li and G. Chen, "Chaos and hyperchaos in the fractional-order Rössler equations," *Physica A: Statistical Mechanics and Its Applications*, vol. 341, pp. 55–61, 2004.

[28] J. Hu, S. Chen, and C. Li, "Adaptive control for anti-synchronization of Chua's chaotic system," *Physics Letters A*, vol. 339, no. 6, pp. 455–460, 2005.

[29] J. G. Lu, "Chaotic dynamics of the fractional-order Lü system and its synchronization," *Physics Letters A*, vol. 354, no. 4, pp. 305–311, 2006.

[30] C. Li and G. Chen, "Chaos in the fractional order Chen system and its control," *Chaos, Solitons & Fractals*, vol. 22, no. 3, pp. 549–554, 2004.

[31] S. Ha, H. Liu, and S. Li, "Adaptive fuzzy backstepping control of fractional-order chaotic systems with input saturation," *Journal of Intelligent and Fuzzy Systems*, vol. 37, no. 5, pp. 6513–6525, 2019.

[32] S. Bhalekar and V. Daftardar-Gejji, "Synchronization of different fractional order chaotic systems using active control," *Communications in Nonlinear Science and Numerical Simulation*, vol. 15, no. 11, pp. 3536–3546, 2010.

[33] B. Xin and J. Zhang, "Finite-time stabilizing a fractional-order chaotic financial system with market confidence," *Nonlinear Dynamics*, vol. 79, no. 2, pp. 1399–1409, 2015.

[34] K. Kachia, J. E. Solís-Pérez, and J. F. Gómez-Aguilar, "Chaos in a three-cell population cancer model with variable-order fractional derivative with power, exponential and Mittag-Leffler memories," *Chaos, Solitons & Fractals*, vol. 140, Article ID 110177, 2020.

[35] E. Kaslik and S. Sivasundaram, "Nonlinear dynamics and chaos in fractional-order neural networks," *Neural Networks*, vol. 32, pp. 245–256, 2012.

[36] S. Boyd and S. Sastry, *Adaptive Control: Stability, Convergence, and Robustness*, Prentice Hall, Hoboken, NJ, USA, 1989.

[37] E. E. Mahmoud, "Adaptive anti-lag synchronization of two identical or non-identical hyperchaotic complex nonlinear systems with uncertain parameters," *Journal of the Franklin Institute*, vol. 349, no. 3, pp. 1247–1266, 2012.

[38] W. Deng, C. Li, and J. Lü, "Stability analysis of linear fractional differential system with multiple time delays," *Nonlinear Dynamics*, vol. 48, no. 4, pp. 409–416, 2007.

Research Article

Analysis of Multiterm Initial Value Problems with Caputo–Fabrizio Derivative

Mohammed Al-Refai [iD]¹ and Muhammed Syam [iD]²

¹*Department of Mathematics, Yarmouk University, Irbid, Jordan*
²*Department of Mathematical Sciences, UAE University, Al-Ain, UAE*

Correspondence should be addressed to Mohammed Al-Refai; m_alrefai@yu.edu.jo

In this paper, we discuss the solvability of a class of multiterm initial value problems involving the Caputo–Fabrizio fractional derivative via the Laplace transform. We derive necessary and sufficient conditions to guarantee the existence of solutions to the problem. We also obtain the solutions in closed forms. We present two examples to illustrate the validity of the obtained results.

1. Introduction

Recently, there is great interest to develop new types of fractional derivatives of nonsingular kernel. Motivated by applications, Caputo and Fabrizio were the first to introduce such types of fractional derivatives with nonlocal and nonsingular kernel [1]. The Caputo–Fabrizio derivative is connected with a variety of applications (see [2–6]). Stability analysis of fractional differential equations without inputs was studied in [7], where exponential stability is obtained for the Caputo–Fabrizio derivative. Since their kernels are nonlocal, fractional derivatives preserve memories, and therefore, they have been used to model several (SIR) epidemic models (see [8–14]). Several analytical techniques have been implemented to study various fractional equations with fractional derivatives without singular kernels, such as the Laplace transform, reduction to initial value problems with integer derivatives, maximum principles, and fixed point theorems (see [15–21]), just to mention a few out of

many in the literature. The following definitions are required to state our problem.

Definition 1. A function f is said to be absolutely continuous on $[a, b]$, if there exists a function $f' \in L^1(a, b)$ such that

$$f(t) = f(a) + \int_a^t f'(x)\mathrm{d}x, \quad \forall t \in [a, b]. \quad (1)$$

In the following, we will use the notation $AC([a, b])$ to denote the space of absolutely continuous functions on $[a, b]$.

Definition 2. A function $f: [0, +\infty) \longrightarrow \mathbb{R}$ is said to be of exponential order, if there exists three constants $T, M, C \geq 0$ such that $|f(t)| \leq Ce^{Mt}, \forall t \geq T$.

Then, we define the following space.

Definition 3. The space $\mathcal{M}^1$ is defined by

$$\mathcal{M}^1 = \left\{ f \in L^1_{\text{loc}}: f \text{ is absolutely continuous on } [0, T], \text{ for any } T > 0, \text{ and } f, f' \text{ are of exponential order} \right\}. \quad (2)$$

In this paper, we consider the multiterm fractional initial value problem:

$$\sum_{k=1}^{n} a_k \left({}^{\mathrm{CFC}}D_0^{\alpha_k} y \right)(t) = a_{n+1} y(t) + f(t), \quad t > 0, n \geq 2, \quad (3)$$

$$y(0) = y_0, \qquad (4)$$

where $1 > \alpha_1 > \alpha_2 > \cdots > \alpha_n > 0, a_k > 0, k = 1, \ldots, n$, and $\left({}^{\mathrm{CFC}}D_0^{\alpha} \right)$ is the Caputo–Fabrizio fractional derivative of Caputo sense. Here, we assume that $y, f \in \mathcal{M}^1$, so their Laplace transforms are well defined.

Definition 4 (see [1]). For $0 < \alpha < 1$, $t > 0$ and $f \in \mathcal{M}^1$, the Caputo–Fabrizio fractional derivative of Caputo sense is defined by

$$\left({}^{\mathrm{CFC}}D_0^{\alpha} f \right)(t) = \frac{B(\alpha)}{1 - \alpha} \int_0^t f'(\tau) e^{-(\alpha/(1-\alpha))(t-\tau)} \mathrm{d}\tau, \qquad (5)$$

where $B(\alpha) > 0$ is a normalization function satisfying $B(0) = B(1) = 1$.

For the corresponding fractional integral and more properties of the derivative, we refer the readers to [1, 5, 22–24]. In [15, 17], the fractional initial value problems were transformed to equivalent initial value problems with integer derivatives. However, the technique is not valid for the multiterm initial value problems. The single term of the problem with $n = 1$ was discussed in [23], and the solution of the problem was obtained in a closed form. In this paper, we apply the Laplace transform to analyze the solutions of the fractional initial value problems (3) and (4). This paper is organized as follows: in Section 2, we present some preliminary results about the Caputo–Fabrizio fractional derivative and derive necessary and sufficient conditions to guarantee the existence of solutions to problems (3) and (4). We also obtain the exact solutions in closed forms using the Laplace transform. In Section 3, we present two examples to illustrate the validity of our results. Finally, we close up with some concluding remarks in Section 4.

2. Main Results

We start with the definition and main results concerning the Caputo–Fabrizio derivative. Then, we present necessary and sufficient conditions for the solution of problems (3) and (4). Since $\left({}^{\mathrm{CFC}}D_0^{\alpha} f \right)(t) = (B(\alpha)/(1-\alpha)) f'(t) * e^{-(\alpha/(1-\alpha))t}$, equation (3) can be written as

$$\sum_{k=1}^{n} c_k e^{-\mu_k t} * y'(t) = c_{n+1} y(t) + f(t), \quad t > 0, n \geq 2, \quad (6)$$

where

$$c_k = \frac{B(\alpha_k)}{1 - \alpha_k} a_k,$$

$$\mu_k = \frac{\alpha_k}{1 - \alpha_k}, \quad k = 1, \ldots, n, c_{n+1} = a_{n+1}, \qquad (7)$$

and $*$ denotes to the convolution of two functions.

Remark 1. Let $F(s) = (P_n(s)/Q_m(s))$ where $P_n(s)$ and $Q_m(s)$ are polynomials with degrees n and m, respectively, and are with real coefficients. If $n < m$, then the inverse Laplace transform of $F(s)$ exists and can be evaluated using partial fractions.

Lemma 1. *For $f \in \mathcal{M}^1$, the following hold:*

(1) ${}^{\mathrm{CFC}}D_0^{\alpha}$: $AC([0,T]) \longrightarrow C([0,T])$

(2) $\left({}^{\mathrm{CFC}}D_0^{\alpha} f \right)(0) = 0$

Proof.

(1) For any function $f \in AC([0,T])$, ${}^{\mathrm{CFC}}D_0^{\alpha} f$ is the convolution product of a continuous function and L^1 function, that is continuous

(2) Since for any $f \in AC([0,T])$, ${}^{\mathrm{CFC}}D_0^{\alpha} f$ is continuous; then, ${}^{\mathrm{CFC}}D_0^{\alpha} f(0) = \lim_{t \longrightarrow 0^+} {}^{\mathrm{CFC}}D_0^{\alpha} f(t) = 0$ ☐

Definition 5. Let the space $\mathcal{M}^2$ be defined by

$$\mathcal{M}^2 = \left\{ f \in C^1([0, +\infty)) : f'(0) = f'(0^+) \in \mathbb{R}, f' \in AC([0,T]), \text{for any } T > 0, \text{and } f, f', f'' \text{ are of exponential order} \right\}. \qquad (8)$$

Lemma 2. *The following holds for multiterm fractional initial value problems (3) and (4).*

(1) *If a solution y: $[0, +\infty) \longrightarrow \mathbb{R}$ exists such that $y \in AC([0,T])$ for any $T > 0$, then $c_{n+1} y(0) + f(0) = 0$*

(2) *If $f \in \mathcal{M}^1, c_{n+1} y(0) + f(0) = 0$, and $c_{n+1} \neq \sum_{k=1}^{n} c_k$, then a unique solution $y \in \mathcal{M}^1$ exists*

(3) *If a solution $y \in \mathcal{M}^1$ exists for $y_0 \neq 0$ and $f \in \mathcal{M}^2$, then $c_{n+1} \neq \sum_{k=1}^{n} c_k$*

Proof.

(1) Let $y \in C([0, +\infty))$ be a solution to multiterm fractional initial value problems (3) and (4) with $y \in AC([0,T])$ for any $T > 0$. By Lemma 1, ${}^{\mathrm{CFC}}D_0^{\alpha_k} y(t) = 0$ for any $k = 1, \ldots, n$ Then, from equation (3), one gets

$$c_{n+1} y(0) + f(0) = 0. \qquad (9)$$

(2) Let $y_0 \neq 0$, $f \in \mathcal{M}^1, c_{n+1} y(0) + f(0) = 0$, and $c_{n+1} \neq \sum_{k=1}^{n} c_k$. Then, applying the Laplace transform

to equation (6) and using the convolution result, we have

$$\sum_{k=1}^{n} \frac{c_k}{s + \mu_k} \left[s\mathscr{L}(y)(t) - y_0 \right] = c_{n+1}\mathscr{L}(y)(t) + F(s), \tag{10}$$

where $F(s) = \mathscr{L}(f)(t)$. The above equation yields

$$\mathscr{L}(f)(t)\left(s\sum_{k=1}^{n} \frac{c_k}{s + \mu_k} - c_{n+1} \right) = y_0 \sum_{k=1}^{n} \frac{c_k}{s + \mu_k} + F(s). \tag{11}$$

We have

$$\sum_{k=1}^{n} \frac{c_k}{s + \mu_k} = \frac{c_1}{s + \mu_1} + \frac{c_2}{s + \mu_2} + \cdots + \frac{c_n}{s + \mu_n}$$
$$= \sum_{k=1}^{n} c_k \frac{\prod_{j=1, j\neq k}^{n} (s + \mu_j)}{\prod_{k=1}^{n} (s + \mu_k)} = \frac{Q_{n-1}(s)}{P_n(s)}, \tag{12}$$

where $Q_{n-1}(s) = \sum_{k=1}^{n} c_k \prod_{j=1, j\neq k}^{n} (s + \mu_j)$ and $P_n(s) = \prod_{k=1}^{n} (s + \mu_k)$ are polynomials of degrees $n-1$ and n, respectively. Substituting in equation (11), we have

$$\mathscr{L}(y)\left(s\frac{Q_{n-1}(s)}{P_n(s)} - c_{n+1} \right) = y_0 \frac{Q_{n-1}(s)}{P_n(s)} + F(s), \tag{13}$$

or

$$\mathscr{L}(y)(s) = y_0 \frac{Q_{n-1}(s)}{sQ_{n-1}(s) - c_{n+1}P_n(s)}$$
$$+ \frac{P_n(s)}{sQ_{n-1}(s) - c_{n+1}P_n(s)} F(s). \tag{14}$$

Now, the leading coefficient of the polynomial $Q_{n-1}(s)$ is $\sum_{k=1}^{n} c_k$, and the leading coefficient of the polynomial $P_n(s)$ is 1. If $c_{n+1} \neq \sum_{k=1}^{n} c_k$, then $sQ_{n-1}(s) - c_{n+1}P_n(s)$ is a polynomial of degree n. Let

$$H_1(s) = \frac{Q_{n-1}(s)}{sQ_{n-1}(s) - c_{n+1}P_n(s)},$$
$$H_2(s) = \frac{1}{s} \frac{P_n(s)}{sQ_{n-1}(s) - c_{n+1}P_n(s)}, \tag{15}$$

so that $\mathscr{L}^{-1}(H_1)(s) = h_1(t)$ and $\mathscr{L}^{-1}(H_2)(s) = h_2(t)$ are well defined. Then,

$$\mathscr{L}(y)(t) = y_0 H_1(s) + H_2(s)sF(s)$$
$$= y_0 H_1(s) + H(s)(\mathscr{L}(f')(t) + f(0)). \tag{16}$$

Using the uniqueness result of the inverse Laplace transform, we have

$$y(t) = y_0 h_1(t) + h_2(t) * f'(t) + f(0)h_2(t), \tag{17}$$

which completes the proof.

(3) Let a solution $y \in \mathscr{M}^1$ exists for $y_0 \neq 0$ and $f \in \mathscr{M}^2$. Starting from equation (14), let us define

$$\widetilde{H}_1(s) = y_0 \frac{Q_{n-1}(s)}{sQ_{n-1}(s) - c_{n+1}P_n(s)},$$
$$\widetilde{g}(s) = \frac{P_n(s)}{sQ_{n-1}(s) - c_{n+1}P_n(s)} F(s) \tag{18}$$
$$= \frac{P_n(s)}{s^2(sQ_{n-1}(s) - c_{n+1}P_n(s))} s^2 F(s).$$

Define

$$\widetilde{H}_2(s) = \frac{P_n(s)}{s^2(sQ_{n-1}(s) - c_{n+1}P_n(s))}. \tag{19}$$

$\widetilde{H}_2$ admits an inverse Laplace transform since $sQ_{n-1}(s) - c_{n+1}P_n(s)$ is of degree $n-1$. Moreover, since $f \in \mathscr{M}^2$, also $s^2 F(s)$ admits an inverse Laplace transform, thus also $\widetilde{g}(s)$ (by the convolution rule). One can rewrite equation (14) as

$$\mathscr{L}(y)(s) - \widetilde{g}(s) = \widetilde{H}_1(s). \tag{20}$$

However, since $sQ_{n-1}(s) - c_{n+1}P_n(s)$ is of degree $n-1$ and $y \neq 0$, the right-hand side does not admit an inverse Laplace transform while the left-hand side does, which is a contradiction. □

Lemma 3. *Let $y \in AC([0,T]), T > 0$, be a solution to the multiterm fractional initial value problem (3) with $y(0) = 0$, then $f(0) = 0$.*

Proof. From Lemma 1, since $y_0 = y(0) = 0$, then $f(0) = 0$. □

Remark 2. If $y(0) = f(0) = 0, f \in \mathscr{M}^1$, and $c_{n+1} \neq \sum_{k=1}^{n} c_k$, then a solution $y \in \mathscr{M}^1$ exists by Lemma 2. If $f \in \mathscr{M}^2$, a solution exists even if $c_{n+1} = \sum_{k=1}^{n} c_k$, and it can be evaluated using the Laplace transform in the following manner.

Lemma 4. *Let $y(t)$ be a possible solution to multiterm fractional initial value problems (3) and (4), with $y(0) = f(0) = 0$, $c_{n+1} = \sum_{k=1}^{n} c_k$, and $f \in \mathscr{M}^2$. If $G(s) = s^2\mathscr{L}(f)(t)$ has an inverse Laplace transform, then $y(t) = h_3(t) * \mathscr{L}^{-1}(s^2 F(s))$, where $h_3(t) = \mathscr{L}^{-1}(H_3)(s)$ and H_3 is defined in equation (22).*

Proof. Substituting $y_0 = 0$, in equation (14), we have

$$\mathscr{L}(y)(t) = \frac{P_n(s)}{sQ_{n-1}(s) - c_{n+1}P_n(s)} F(s). \tag{21}$$

Since $c_{n+1} = \sum_{k=1}^{n} c_k$, we have $sQ_{n-1}(s) - c_{n+1}P_n(s)$ is a polynomial of degree $n - 1$. Let

$$H_3(s) = \frac{1}{s^2} \frac{P_n(s)}{sQ_{n-1}(s) - c_{n+1}P_n(s)}, \tag{22}$$

so that $\mathscr{L}^{-1}(H_3)(s) = h_3(t)$ is well defined. Then, equation (14) yields

$$\mathscr{L}(y)(t) = H_3(s)s^2 F(s). \tag{23}$$

If $f \in \mathscr{M}^2$, then $\mathscr{L}(y)(t)$ in equation (23) can be written as

$$\begin{aligned} \mathscr{L}(y)(t) &= H_3(s)\big(\mathscr{L}(f'')(t) + sf(0) + f'(0)\big) \\ &= H_3(s)\big(\mathscr{L}(f'')(t) + f'(0)\big). \end{aligned} \tag{24}$$

Applying the inverse Laplace transform, we have

$$y(t) = h_3 * f''(t) + f'(0)h_3(t). \tag{25}$$

We summarize the obtained results in the following main theorem. □

Theorem 1. *Consider multiterm fractional initial value problems (3) and (4).*

(1) *For $y_0 = 0$, if a solution $y \in AC([0, T]), T > 0$, exists, then $f(0) = 0$*

(2) *If $f \in \mathscr{M}^1, c_{n+1}y(0) + f(0) = 0$, and $c_{n+1} \neq \sum_{k=1}^{n} c_k$, then a solution $y \in \mathscr{M}^1$ exists*

(3) *If $f \in \mathscr{M}^2$ and $y_0 \neq 0$, then a solution $y \in \mathscr{M}^1$ exists if and only if $c_{n+1} = \sum_{k=1}^{n} c_k$*

(4) *If $y_0 = 0, f \in \mathscr{M}^2$, and $f(0) = 0$, then a solution $y \in \mathscr{M}^1$ exists*

3. Illustrative Examples

We discuss two main examples. The first one is a two-term problem where it holds that $c_{n+1} = \sum_{k=1}^{n} c_k$. We show the existence of a solution for a specific case by imposing extra conditions. The second example is a three-term problem where it holds that $c_{n+1} \neq \sum_{k=1}^{n} c_k$. So, the existence of a unique solution is guaranteed. We present the solution in a closed form and discuss several special cases.

Example 1. Consider the two-term fractional initial value problem:

$$\begin{aligned} \big(e^{-\mu_1 t} + e^{-\mu_2 t}\big) * y'(t) &= 2y(t) + f(t), \\ y(0) &= y_0. \end{aligned} \tag{26}$$

Since $c_1 + c_2 = c_3$, then the problem has no solution for $y(0) \neq 0$. For $y(0) = f(0) = 0$ and $s^2 \mathscr{L}(f)(t)$ has Laplace inverse, the problem admits a solution. To verify, let us find the solution given by equation (25). We have

$$Q_1(s) = 2s + \mu_1 + \mu_2,$$

$$P_2(s) = (s + \mu_1)(s + \mu_2),$$

$$\begin{aligned} H_3(s) &= -\frac{1}{s^2} \frac{(s + \mu_1)(s + \mu_2)}{(\mu_1 + \mu_2)s + 2\mu_1\mu_2} \\ &= \frac{R_1}{s} + \frac{R_2}{s^2} + \frac{R_3}{(\mu_1 + \mu_2)s + 2\mu_1\mu_2}, \end{aligned} \tag{27}$$

where

$$R_1 = -\frac{1}{4} \frac{\mu_1 + \mu_2}{\mu_1 \mu_2},$$

$$R_2 = -\frac{1}{2}, \tag{28}$$

$$R_3 = \frac{1}{4} \frac{(\mu_1 - \mu_2)^2}{\mu_1 \mu_2}.$$

Thus,

$$h_3(t) = \mathscr{L}^{-1}(H_3)(s) = R_1 + R_2 t + \frac{R_3}{\mu_1 + \mu_2} e^{-2(\mu_1\mu_2/\mu_1 + \mu_2)t}, \tag{29}$$

and the solution $y(t) = h_3(t) * f''(t) + f'(0)h_3(t)$ is obtained, provided that $f \in \mathscr{M}^2$.

As a special case, let us consider $f(t) = t^2$. Then, $f(0) = 0$, $\mathscr{L}(f)(t) = (2/s^3)$, and $s^2 \mathscr{L}(f)(t) = (2/s)$ have Laplace inverse. Thus,

$$\begin{aligned} y(t) &= h_3(t) * f''(t) + f'(0)h_3(t) = h_3(t) * 2 \\ &= 2 \int_0^t \left(R_1 + R_2 \tau + \frac{R_3}{\mu_1 + \mu_2} e^{-2(\mu_1\mu_2/\mu_1 + \mu_2)\tau} \right) d\tau \\ &= 2R_1 t + R_2 t^2 - \frac{R_3}{\mu_1 \mu_2} \left(e^{-2(\mu_1\mu_2/\mu_1 + \mu_2)} - 1 \right). \end{aligned} \tag{30}$$

For $\mu_1 = (2/3)$ and $\mu_2 = (1/3)$, we have $R_1 = -(9/8), R_2 = -(1/2), R_3 = (1/8)$, and

$$y(t) = \frac{9}{4}t - \frac{1}{2}t^2 - \frac{9}{16} e^{-(4/9)t} + \frac{9}{16}. \tag{31}$$

Example 2. As a second example, we consider the three-term initial value problem:

$$\begin{aligned} \big(e^{-\mu_1 t} + e^{-\mu_2 t} + e^{-\mu_3 t}\big) * y'(t) &= y(t) + f(t), \\ y(0) &= y_0. \end{aligned} \tag{32}$$

Since $c_1 = c_2 = c_3 = c_4 = 1$ and $c_1 + c_2 + c_3 \neq c_4$, the problem has a unique solution given by equation (17) provided that $y(0) + f(0) = 0$. We have

$$Q_2(s) = \sum_{k=1}^{3} c_k \prod_{j=1, j \neq k}^{3} (s + \mu_j) = (s + \mu_2)(s + \mu_3)$$
$$+ (s + \mu_1)(s + \mu_3)$$
$$+ (s + \mu_1)(s + \mu_2), P_3(s)$$
$$= \prod_{k=1}^{3} (s + \mu_k)$$
$$= (s + \mu_1)(s + \mu_2)(s + \mu_3). \tag{33}$$

Let

$$T_3(s) = sQ_2(s) - c_4 P_3(s) = 2s^3 + (\mu_1 + \mu_2 + \mu_3)s^2 - \mu_1 \mu_2 \mu_3, \tag{34}$$

then

$$H_1(s) = \frac{Q_2(s)}{T_3(s)},$$
$$H_2(s) = \frac{1}{s} \frac{P_3(s)}{T_3(s)}, \tag{35}$$

with

$$\mathscr{L}^{-1}(H_1)(s) = h_1(t),$$
$$\mathscr{L}^{-1}(H_2)(s) = h_2(t), \tag{36}$$

and the solution is given by

$$y(t) = y_0 h_1(t) + h_2(t) * f'(t) + f(0)h_2(t). \tag{37}$$

For $f(t) = t$, we have $y(0) = -f(0) = 0$, and thus

$$y(t) = h_2(t) * 1 = \int_0^t h_2(\tau)d\tau. \tag{38}$$

For $f(t) = 1$, we have $y(0) = -f(0) = -1$, and thus

$$y(t) = h_2(t) - h_1(t). \tag{39}$$

As a specific case, if we consider $\mu_1 = (7/5), \mu_2 = (1/2),$ and $\mu_3 = (1/3),$ we have

$$Q_2(s) = 3s^2 + \frac{67}{15}s + \frac{4}{3},$$

$$P_3(s) = s^3 + \frac{67}{30}s^2 + \frac{4}{3}s + \frac{7}{30},$$

$$T_3(s) = 2s^3 + \frac{67}{30}s^2 - \frac{7}{30},$$

$$H_1(s) = \frac{Q_2(s)}{P_3(s)} = \frac{90s^2 + 134s + 40}{60s^3 + 67s^2 - 7} = \frac{A_0}{s+1} + \frac{A_1}{s + \Delta_1} + \frac{A_2}{s + \Delta_2},$$

$$H_2(s) = \frac{P_3(s)}{sT_3(s)} = \frac{30s^3 + 67s^2 + 40s + 7}{s(s+1)(s + \Delta_1)(s + \Delta_2)} = -\frac{1}{s} + H_1(s), \tag{40}$$

where $\Delta_1 = (7 + \sqrt{1729})/120, \Delta_2 = (7 - \sqrt{1729})/120, A_0 = -(2/23), A_1 = (73\sqrt{1729} - 3113)/92\sqrt{1729}, A_2 =$ $(73\sqrt{1729} + 3113)/92\sqrt{1729},$ $h_1(t) = A_0 e^{-t} + A_1 e^{-\Delta_1 t} + A_2 e^{-\Delta_2 t},$ and $h_2(t) = h_1(t) - 1.$

For $f(t) = t,$ we have $y(t) = \int_0^t h_2(\tau)d\tau = (A_0 + (A_1/\Delta_1) + (A_2/\Delta_2)) - t - A_0 e^{-t} - (A_1/\Delta_1)e^{-\Delta_1 t} - (A_2/\Delta_2)e^{-\Delta_2 t}.$

4. Concluding Remarks

We obtained the solutions of a class of multiterm fractional initial value problems in closed forms using the Laplace transform. We have also discussed several necessary and sufficient conditions to guarantee the existence of solutions to the problem. Whether the results are extendable to wider classes of multiterm initial value problems or systems of fractional equations is left for future work.

Data Availability

The data used to support the findings of this study are included within the article.

Conflicts of Interest

The authors declare that there are no conflicts of interest.

Authors' Contributions

The first author has initiated the idea and obtained the analytical results. The second author did the numerical examples, shared the discussion, and approved the final draft of the manuscript.

References

[1] M. Caputo and M. Fabrizio, "A new definition of fractional derivative without singular kernel," *Progress in Fractional Differentiation and Applications*, vol. 1, pp. 73–85, 2015.

[2] B. S. T. Alkahtani and A. Atangana, "Controlling the wave movement on the surface of shallow water with the Caputo-Fabrizio derivative with fractional order," *Chaos, Solitons & Fractals*, vol. 89, pp. 539–546, 2016.

[3] A. Atangana and J. J. Nieto, "Numerical solution for the model of RLC circuit via the fractional derivative without singular kernel," *Advances in Mechanical Engineering*, vol. 7, pp. 1–7, 2015.

[4] A. Atangana, "On the new fractional derivative and application to nonlinear Fisher's reaction-diffusion equation," *Applied Mathematics and Computation*, vol. 273, pp. 948–956, 2016.

[5] M. Caputo and M. Fabrizio, "Applications of new time and spatial fractional derivatives with exponential kernels," *Progress in Fractional Differentiation and Applications*, vol. 2, no. 1, pp. 1–11, 2016.

[6] M. Caputo and M. Fabrizio, "Deformations in elasto-plastic media with memory: the inverse problem," *Progress in Fractional Differentiation and Applications*, vol. 4, no. 1, pp. 5–14, 2018.

[7] N. Sene, "Stability analysis of the fractional differential equations with the Caputo-Fabrizio fractional derivative," *Journal of Fractional Calculus and Applications*, vol. 1, pp. 160–172, 2020.

[8] O. A. Arqub and A. El-Ajou, "Solution of the fractional epidemic model by homotopy analysis method," *Journal of King Saud University Science*, vol. 25, no. 1, pp. 73–81, 2013.

[9] B. Acay, E. Bas, and T. Abdeljawad, "Fractional economic models based on market equilibrium in the frame of different type kernels," *Chaos, Solitons & Fractals*, vol. 130, Article ID 109438, 2020.

[10] Z. Chen, K. Liu, X. Liu, and Y. Lou, "Modelling epidemics with fractional-dose vaccination in response to limited vaccine supply," *Journal of Theoretical Biology*, vol. 486, Article ID 110085, 2020.

[11] M. Khan and A. Atangana, "Modeling the dynamics of novel coronavirus (2019-nCov) with fractional derivative," *Alexandria Engineering Journal*, vol. 4, no. 59, pp. 2379–2389, 2020.

[12] H. Kheiri and M. Jafari, "Fractional optimal control of an HIV/AIDS epidemic model with random testing and contact tracing," *Journal of Applied Mathematics and Computing*, vol. 60, no. 1-2, pp. 387–411, 2019.

[13] D. Kumar and J. Singh, "New aspects of fractional epidemiological model for computer viruses with mittag–leffler law," in *Mathematical Modelling in Health, Social and Applied Sciences. Forum for Interdisciplinary Mathematics*, H. Dutta, Ed., Springer, Singapore, 2020.

[14] N. Sene, "SIR epidemic model with Mittag-Leffler fractional derivative," *Chaos, Solitons & Fractals*, vol. 137, Article ID 109833, 2020.

[15] M. Al-Refai, "Reduction of order formula and fundamental set of solutions for linear fractional differential equations," *Applied Mathematics Letters*, vol. 82, pp. 8–13, 2018.

[16] M. Al-Refai and K. Pal, "A maximum principle for a fractional boundary value problem with convection term and applications," *Mathematical Modeling and Analysis*, vol. 24, no. 1, pp. 62–71, 2019.

[17] M. Al-Refai and K. Pal, "New aspects of Caputo-Fabrizio fractional derivative," *Progress in Fractional Differentiation and Applications*, vol. 5, no. 2, pp. 157–166, 2019.

[18] E. Karimov and S. Pirnafasov, "Higher order multi-term time-fractional partial differential equations involving Caputo-Fabrizio derivative," *The Electronic Journal of Differential Equations*, vol. 243, pp. 1–11, 2017.

[19] H. Marasi, A. Joujehi, and H. Aydi, "An Extension of the Picard theorem to fractional differential equations with a Caputo-Fabrizio derivative," *Journal of Function Spaces*, vol. 2021, Article ID 6624861, 6 pages, 2021.

[20] N. Sene, "Stokes' first problem for heated flat plate with Atangana-Baleanu fractional derivative," *Chaos, Solitons & Fractals*, vol. 117, pp. 68–75, 2018.

[21] A. Shaikh, A. Tassaddiq, K. S. Nisar, and D. Baleanu, "Analysis of differential equations involving Caputo-Fabrizio fractional operator and its applications to reaction-diffusion equations," *Advances in Difference Equations*, vol. 2019, no. 1, Article ID 178, 2019.

[22] T. Abdeljawad and D. Baleanu, "On fractional derivatives with exponential kernel and their discrete versions," *Reports on Mathematical Physics*, vol. 80, no. 1, pp. 11–27, 2017.

[23] J. Losada and J. Nieto, "Properties of a new fractional diffusion equations with fractional derivative of non-singular kernel," *Progress in Fractional Differentiation and Applications*, vol. 1, no. 2, pp. 87–92, 2015.

[24] M. Al-Refai, "Proper inverse operators of fractional derivatives with nonsingular kernels," *Rendiconti del Circolo Matematico di Palermo Series 2*, vol. 2021, 2021.

Research Article

A Fractional Epidemiological Model for Bone Remodeling Process

Muath Awadalla ![ID],[1] **Yves Yannick Yameni Noupoue** ![ID],[2] **and Kinda Abuasbeh** ![ID][1]

[1]*Department of Mathematics and Statistics, College of Science, King Faisal University, Hafuf, Al Ahsa 31982, Saudi Arabia*
[2]*Institute of Statistics, Biostatistics and Actuarial Sciences (ISBA), Universite Catholique de Louvain (UCLouvain), Louvain-la-Neuve 1348, Belgium*

Correspondence should be addressed to Kinda Abuasbeh; kabuasbeh@kfu.edu.sa

This article focuses on modeling bone formation process using a fractional differential approach, named bones remodeling process. The first goal of the work is to investigate existence and uniqueness of the proposed fractional differential model. The next goal is to investigate how similar is the proposed approach to the method based on system classical differential equations. The dynamical system of equations used is built upon three main parameters. These are chemical substances, namely, calcitonin secretion, osteoclastic and osteoblastic, which are involved in the bone's formation process. We implement some numerical simulations to graphically show the impact of an arbitrary fractional order of derivative. We finally obtained that modeling bone formation process using fractional differential equations yielded comparable results with those obtained through a system of classical differential equations. Flexibility in the choice of the fractional order of derivative is an advantage as it helps in selecting the best fractional order of derivative.

1. Introduction

Modeling natural phenomena through differential equation has long been used by scientists. In the early days, differential equations with integer order of derivative were commonly used. Then several fractional order derivatives have been implemented. In earlier days of fractional differential equations, researchers mainly focused on theoretical concepts, investigating existence and uniqueness of solution of built models. A sample of such theoretical works is found in [1–5]. In general, researchers build models based on fractional differential by analogy to the approach that would be used in the case of classical differential [6–8]. Hence, in many cases, authors will try to compare models' performances from both approaches. Despite analogies that might exist between classical and fractional models upon a given problem, both models might not have common properties. For instance, the Carleman embedding technique [9] applicable in the studies of classical differential equations does not hold for the fractional differential equations for instance. Beside theoretical study of fractional differential

equations, a lot have been done by researchers concerning possible application to real life phenomena. One can mention a nonexhaustive field of study with examples for which fractional differential has been successfully performed. In biology, modeling dynamics in human tissues was proposed in [10]. Alcohol can be dangerous when its concentration in high human blood exceeds a certain threshold. In [11], a fractional-based model of alcohol level in blood was proposed.

Following the aims to prove the use of fractional differential equations, we decided to investigate how efficient it will be in modeling bone formation process. Before going into details, we will provide an overview of human bone formation process. Human bone formation and development are a complex process that starts from when a fetus is 3 months old and ends during teenage years, 13–18 years old. However, bone formation never ends in practice. Indeed, bones are living tissue made up of protein, calcium, and other minerals, as well as water. In this regard, bones' tissue constantly renews itself, by breaking down older tissue and replacing it with new tissue. This process is called "bone

remodeling process." In literature, "bone formation" and "bone remodeling" refer often to the same process. There exit various cells or/and chemicals which are at the base of remodeling process. Three chemicals to which we will pay attention include the level of calcitonin above the basal level in the blood, the number of active osteoclasts at time t, and the number of active osteoblasts at time t.

In this work, we build a system of fractional differential equations to modeling bone formation, which we call the bone remodeling process. Detailed information on the biological and chemical processes involved in the study as well as the chemical elements involved in bone formation are found in [12–17] and references therein. Therefore, we provided no or a very shallow biological and chemical description of the phenomenon. We rather focus on building a system of fractional differential equations of the model in which a classical differential equation counterpart is found in [12]. Moreover, we proved the existence and uniqueness of the built model. Lastly, we exhibited the solution of the built system using four numerical approaches of solving nonlinear differential equations, namely, the generalized Euler's method (GEM), the Grünwald–Letnikov method or power series expansion (GL or PSE), the Caputo–Fabrizio method (CF), and the Atangana–Baleanu fractional derivative in Caputo sense (ABC). Modeling approach that consists of performing an experiment on the same data set with different techniques, including the proposed one, then to compare their performance using an error-metric function is not used in this work. Indeed, in the setting of this work, there is no comprehensive way to compare performances of the proposed method with those of existing methods.

2. Preliminaries

Fundamental definitions, terminologies, and notations commonly used in fractional calculus are provided in this section.

Definition 1. Given a function h: $[0, +\infty) \longrightarrow \mathbb{R}$, its Riemann–Liouville fractional integral of order $q > 0$ is defined as

$$\left({}_{\mathrm{RL}}I_{0^+}^q h\right)(t) = \frac{1}{\Gamma(q)} \int_0^t (t-s)^{q-1} h(s) \mathrm{d}s, \qquad (1)$$

with the provision that the right-hand side of the integral is point wise defined on $(0, +\infty)$ and Γ representing the usual gamma function $\Gamma(v) = \int_0^\infty e^{-t} t^{v-1} \mathrm{d}t, \forall v > 0$.

Definition 2. Given a function h: $[0, +\infty) \longrightarrow \mathbb{R}$, its Riemann–Liouville fractional derivative of order $q > 0$ is defined by

$$\left({}_{\mathrm{RL}}D_{0^+}^q h\right)(t) = \frac{1}{\Gamma(n-q)} \left(\frac{\mathrm{d}^n}{\mathrm{d}t^n}\right) \int_0^t (t-s)^{n-q-1} h(s) \mathrm{d}s, \qquad (2)$$

where $n - 1 \leq q < n, n \in \mathbb{N}$.

Definition 3. Considering a function h: $[0, +\infty) \longrightarrow \mathbb{R}$, its Caputo derivative of order $q > 0$ is defined as

$$\left({}_C D_{0^+}^q h\right)(t) = \begin{cases} \displaystyle\int_0^t \frac{(t-s)^{n-q-1} h^{(n)}(s)}{\Gamma(n-q)} \mathrm{d}s, & n-1 < q < n \in \mathbb{R}, \\ \\ h^{(n)}(t), & q \in \mathbb{N}, \end{cases} \qquad (3)$$

where $n = [q] + 1$, $[q]$ is the integer part of q.

Definition 4. Let g be a continuous function and $n = (t - a/h)$, then the Grünwald–Letnikov (GL) fractional derivative of g is given by

$$\left({}_{\mathrm{GL}}D_{a^+}^q g\right)(t) = \lim_{h \longrightarrow 0} \frac{1}{h^q} \sum_{j=0}^{[(t-a)/h]} (-1)^j \binom{q}{j} g(t - jh), \qquad (4)$$

where

$$\binom{q}{j} = \frac{q!}{j!(q-j)!} = \frac{\Gamma(q+1)}{\Gamma(j+1)\Gamma(q-j+1)},$$

$$\binom{q}{0} = 1. \qquad (5)$$

Definition 5. Let $g \in H^1(a, b), b > a$ and $q \in [0, 1]$, then the new Caputo version of fractional derivative is defined as

$$\left({}_{\mathrm{CF}}D_0^q g\right)(t) = \frac{M(q)}{(1-q)} \int_a^t g'(s) \exp\left[-\frac{q}{1-q}(t-s)\right] \mathrm{d}s, \qquad (6)$$

where $M(q)$ is the normalization function with $M(0) = M(1) = 1$. If $g \notin H^1[a, b]$, then the new derivative called Caputo–Fabrizio fractional derivative can be defined as

$$\left({}_{\mathrm{CF}}D_0^q g\right)(t) = \frac{M(q)}{(1-q)} \int_0^t g'(s) \exp\left[-\frac{q}{1-q}(t-s)\right] \mathrm{d}s. \qquad (7)$$

Definition 6. Let $g \in H^1(a, b), b > a$ and $q \in [0, 1]$. Then, the Atangana–Baleanu operator in the Caputo sense (ABC derivative) is defined as

$$\left({}_{ABC}D_0^q g\right)(t) = \frac{B(q)}{(1-q)} \int_a^t g'(s) E_q\left[-\frac{q}{1-q}(t-s)^q\right] \mathrm{d}s, \qquad (8)$$

where $B(q)$ is the normalization function with $B(0) = B(1) = 1$.

3. Numerical Techniques of Solving Nonlinear Differential Equations

We discussed in this section some general numerical methods that are often used for computing numerical solution to nonlinear fractional differential equations. These methods are applied on the fractional model built in sequel.

3.1. The Generalized Euler's Method (GEM).

The GEM is discussed in this subsection. This method was first introduced by Odibat and Momani [18]. The method is derived from the well-known Euler's method of solving classical differential equations. Consider the fractional order nonlinear differential equation defined by

$$\left({}_{C}D_{0^+}^{q}\right)(t) = g(t, x(t)), \quad x(0) = 0, \tag{9}$$

where the fractional order of derivative $q \in (0, 1]$ and $t > 0$. Moreover, let us assume that the following functions $x(t)$, ${}_{C}D_{0^+}^{q}x(t)$ and ${}_{C}D_{0^+}^{2q}x(t)$ are continuous on the closed interval $[0, T]$. In order to compute the numerical solution to the problem defined by equation (9) over the interval $[0, T]$, a discretization of $[0, T]$ into k subintervals $[t_j, t_{j+1}]$ of equal width $h = T/k$ is required. The set of points $\{t_j, x(t_j)\}$ is also used in the approximation process. The GEM approximate solution is defined by

$$x(t_{j+1}) = x(t_j) + \frac{h^q}{\Gamma(q+1)} g(t_j, x(t_j)), \quad j = 0, 1, \ldots, k-1, \tag{10}$$

where the node $t_j = jh, j = 1, 2, \ldots, k$.

3.2. The Grünwald–Letnikov Method GL or PSE.

Grünwald provided a numerical approach of solving nonlinear differential equation. This approach is discussed in detail in [19].

Definition 7. The explicit fractional numerical approximation formula of qth derivative at the points kh, ($k = 1, 2, \ldots$) in the Grünwald–Letnikov sense has the following form [19]:

$$_{(k-L_m/h)}\left({}_{GL}D_{t_k}^{q}g\right)(t) \approx \frac{1}{h^q} \sum_{j=0}^{k} (-1)^j \binom{q}{j} g(t_{k-j}), \tag{11}$$

where L_m is the memory length; $t_k = kh$; the time-space step of iteration is h and $(-1)^j \binom{q}{j}$ are referred to as binomial coefficients. For computational issue, the binomial coefficients are usually denoted by $c_j^{(q)}, (j = 0, 1, \ldots)$ and computed as follows: $\begin{cases} c_0^{(q)} = 1 \\ c_j^{(q)} = (1 - (1 + q/j))c_{j-1}^{(q)} \end{cases}$.

Consider a nonlinear fractional differential equation, where the fractional derivative is taken in the Grünwald–Letnikov sense, with initial condition, defined by

$$\left({}_{GL}D_{a^+}^{q}u\right)(t) = g(u(t), t). \tag{12}$$

The numerical solution to the problem stated by equation (12) is given by

$$u(t_k) = g(u(t_k), t_k)h^q - \sum_{j=1}^{k} c_j^{(q)} u(t_{k-j}). \tag{13}$$

3.3. The Caputo–Fabrizio Method (CF).

Consider a nonlinear fractional differential equation with initial condition, where the fractional derivative is taken in the Caputo–Fabrizio sense, defined by

$$\left({}_{CF}D_0^{q}u\right)(t) = g(t, u(t)), \quad u(0) = u_0. \tag{14}$$

The numerical solution to the problem defined by equation (14) is built based on the Adam–Bashforth method as (see [20, 21])

$$u_{n+1} = u_n + \left(\frac{1-q}{M(q)} + \frac{3qh}{2M(q)}\right)g(t_n, u_n) \\ + \left(\frac{1-q}{M(q)} + \frac{qh}{2M(q)}\right)g(t_{n-1}, u_{n-1}). \tag{15}$$

3.4. Atangana–Baleanu Fractional Derivative in Caputo Sense (ABC).

Let us consider the following fractional differential equation:

$$\left({}_{ABC}D_0^{q}u\right)(t) = g(t, u(t)), \quad u(0) = u_0. \tag{16}$$

The numerical solution to the problem defined by equation (16) is built based on the Adam–Bashforth method as (see [20, 21])

$$u_{n+1} = u_n + \left(\frac{1-q}{ABC(q)} + \frac{q}{ABC(q)h}\left[\frac{2ht_{n+1}^q}{q} - \frac{2ht_{n+1}^{q+1}}{q+1}\right] - \frac{q}{ABC(q)\Gamma(h)h}\left[\frac{2ht_{n+1}^q}{q} - \frac{2ht_{n+1}^{q+1}}{q+1}\right]\right)g(t_n, u_n) \\ + \left(\frac{q-1}{ABC(q)} - \frac{q}{ABC(q)\Gamma(h)h}\left[\frac{ht_{n+1}^q}{q} - \frac{ht_{n+1}^{q+1}}{q+1} + \frac{t_{q+1}}{ABC(q)\Gamma(h)h}\right]\right)g(t_{n-1}, u_{n-1}). \tag{17}$$

4. Bone Remodeling Process

In this section, the bone remodeling process is discussed. Before the fractional model, we recall the classical differential equations model described in [12]. The system is made of three nonlinear differential equations

$$\frac{dx}{dt} = \left(\frac{c_1 + c_2 y}{m_1 + y}\right) - d_1 x,$$

$$\frac{dy}{dt} = \left(c_3 - \frac{c_4 x}{m_2 + x^2}\right) yz - d_2 y, \qquad (18)$$

$$\frac{dz}{dt} = \left(\frac{c_5 + c_6 x}{m_3 + x}\right) z - d_3 z,$$

where

$x(t)$: the level of CT above the basal level in the blood,

$y(t)$: the number of active osteoclasts at time t,

$z(t)$: the number of active osteoblasts at time t.

$$(19)$$

The system given by equation (18) is converted into a fractional differential system by introducing the Caputo–Fabrizio fractional derivative as follows:

$$_{0}^{CF}D_t^q x = \left(\frac{c_1 + c_2 y}{m_1 + y}\right) - d_1 x,$$

$$_{0}^{CF}D_t^q y = \left(c_3 - \frac{c_4 x}{m_2 + x^2}\right) yz - d_2 y, \qquad (20)$$

$$_{0}^{CF}D_t^q z = \left(\frac{c_5 + c_6 x}{m_3 + x}\right) z - d_3 z.$$

Alongside with the initial conditions,

$$\begin{aligned} x(0) &= x_0, \\ y(0) &= y_0, \qquad (21) \\ z(0) &= z_0. \end{aligned}$$

Let us assume that the three variables involved in the process are such that $T = X + Y + Z$, let Ψ be the Banach space of continuous functions defined on the interval J endowed with the norm $\|(x, y, z)\| = \|x\| + \|y\| + \|z\|$, where $\|x\| = \sup\{|x(t)|, t \in J\}$, $\|y\| = \sup\{|y(t)|, t \in J\}$, $\|z\| = \sup\{|z(t)|, t \in J\}$. Particularly, $\Psi = C(J) \times C(J)$, where $C(J)$ is the Banach space of continuous functions defined on J.

4.1. Existence and Uniqueness of the System of Bone Remodeling Process of Fractional Order. The existence and uniqueness of a solution for the system of fractional differential equations defined by equation (20) are investigated in this section through the fixed-point theory.

It follows from the application of the fractional integral operator introduced by Nieto and Losada [22], to equation (20), that

$$x(t) - x(0) = {}_{0}^{CF}I_t^q \left[\left(\frac{c_1 + c_2 y}{m_1 + y}\right) - d_1 x\right],$$

$$y(t) - y(0) = {}_{0}^{CF}I_t^q \left[\left(c_3 - \frac{c_4 x}{m_2 + x^2}\right) yz - d_2 y\right], \qquad (22)$$

$$z(t) - z(0) = {}_{0}^{CF}I_t^q \left[\left(\frac{c_5 + c_6 x}{m_3 + x}\right) z - d_3 z\right].$$

It follows from equation (22) that

$$x(t) - x(0) = \frac{2(1-q)}{(2-q)M(q)}\left[\left(\frac{c_1 + c_2 y(t)}{m_1 + y(t)}\right) - d_1 x(t)\right] + \frac{2q}{(2-q)M(q)} \int_0^t \left[\left(\frac{c_1 + c_2 y(s)}{m_1 + y(s)}\right) - d_1 x(s)\right] ds,$$

$$\begin{aligned} y(t) - y(0) = \;&\frac{2(1-q)}{(2-q)M(q)}\left[\left(c_3 - \frac{c_4 x(t)}{m_2 + x^2(t)}\right) y(t) z(t) - d_2 y(t)\right] \\ &+ \frac{2q}{(2-q)M(q)} \int_0^t \left[\left(c_3 - \frac{c_4 x(s)}{m_2 + x^2(s)}\right) y(s) z(s) - d_2 y(s)\right] ds, \end{aligned} \qquad (23)$$

$$\begin{aligned} z(t) - z(0) = \;&\frac{2(1-q)}{(2-q)M(q)}\left[\left(\frac{c_5 + c_6 x(t)}{m_3 + x(t)}\right) z(t) - d_3 z(t)\right] \\ &+ \frac{2q}{(2-q)M(q)} \int_0^t \left[\left(\frac{c_5 + c_6 x(s)}{m_3 + x(s)}\right) z(s) - d_3 z(s)\right] ds. \end{aligned}$$

Let us denote for convenience,

$$Q_1(t, x) = \left(\frac{c_1 + c_2 y(t)}{m_1 + y(t)}\right) - d_1 x(t),$$

$$Q_2(t, y) = \left(c_3 - \frac{c_4 x(t)}{m_2 + x^2(t)}\right) y(t) z(t) - d_2 y(t),$$

$$Q_3(t, z) = \left(\frac{c_5 + c_6 x(t)}{m_3 + x(t)}\right) z(t) - d_3 z(t),$$

$$\mu_1 = |d_1|,$$ (24)

$$\mu_2 = \left\|\left(c_3 - \frac{c_4 x}{m_2 + x^2}\right) z - d_2\right\|,$$

$$\mu_3 = \left\|\left(\frac{c_5 + c_6 x}{m_3 + x}\right) - d_3\right\|,$$

provided that the functions x, y, and z are bounded as assumed above.

Theorem 1. *The kernel Q_1 satisfies the Lipschitz condition and contraction, if the following inequality holds:*

$$0 \le \mu_1 < 1.$$ (25)

Proof. Let x and x_1 be two functions, then

$$\|Q_1(t, x) - Q_1(t, x_1)\| = \left\|\left(\left(\frac{c_1 + c_2 y(t)}{m_1 + y(t)}\right) - d_1 x(t)\right) \right.$$

$$\left. - \left(\left(\frac{c_1 + c_2 y(t)}{m_1 + y(t)}\right) - d_1 x_1(t)\right)\right\|$$

$$\le \mu_1 \|x - x_1\|.$$ (26)

Hence, Lipschitz condition satisfied for Q_1 and if additionally $0 \le \mu_1 < 1$, then it is also contraction. □

Theorem 2. *The kernel Q_2 satisfies the Lipschitz condition and contraction, if the following inequality holds:*

$$0 \le \mu_2 < 1.$$ (27)

Theorem 3. *The kernel Q_3 satisfies the Lipschitz condition and contraction, if the following inequality holds:*

$$0 \le \mu_3 < 1.$$ (28)

Remark 1. Theorems 2 and 3 are proved in a similar approach to what is used in the proof of Theorem 1.

Using the notations introduced above, the system given by equation (23) is written in a simple form as follows:

$$x(t) = x(0) + \frac{2(1-q)}{(2-q)M(q)} Q_1(t, x) + \frac{2q}{(2-q)M(q)} \int_0^t Q_1(s, x) ds,$$

$$y(t) = y(0) + \frac{2(1-q)}{(2-q)M(q)} Q_2(t, y) + \frac{2q}{(2-q)M(q)} \int_0^t Q_2(s, y) ds,$$

$$z(t) = z(0) + \frac{2(1-q)}{(2-q)M(q)} Q_3(t, z) + \frac{2q}{(2-q)M(q)} \int_0^t Q_3(s, z) ds.$$ (29)

Let us consider the following system of recursive formula derived from equation (29):

$$x_n(t) = \frac{2(1-q)}{(2-q)M(q)} Q_1(t, x_{n-1}) + \frac{2q}{(2-q)M(q)} \int_0^t Q_1(s, x_{n-1}) ds,$$

$$y_n(t) = \frac{2(1-q)}{(2-q)M(q)} Q_2(t, y_{n-1}) + \frac{2q}{(2-q)M(q)} \int_0^t Q_2(s, y_{n-1}) ds,$$

$$z_n(t) = \frac{2(1-q)}{(2-q)M(q)} Q_3(t, z_{n-1}) + \frac{2q}{(2-q)M(q)} \int_0^t Q_3(s, z_{n-1}) ds.$$ (30)

The difference between two consecutive terms of each of the equation from the system above can be written as follows:

$$_x\phi_n(t) = x_n(t) - x_{n-1}(t) = \frac{2(1-q)}{(2-q)M(q)} (Q_1(t, x_{n-1}) - Q_1(t, x_{n-2}))$$

$$+ \frac{2q}{(2-q)M(q)} \int_0^t (Q_1(s, x_{n-1}) - Q_1(s, x_{n-2})) ds,$$

$$_y\phi_n(t) = y_n(t) - y_{n-1}(t) = \frac{2(1-q)}{(2-q)M(q)} (Q_2(t, y_{n-1}) - Q_2(t, y_{n-2}))$$

$$+ \frac{2q}{(2-q)M(q)} \int_0^t (Q_2(s, y_{n-1}) - Q_2(s, y_{n-2})) ds,$$

$$_z\phi_n = z_n(t) - z_{n-1}(t) = \frac{2(1-q)}{(2-q)M(q)} (Q_3(t, z_{n-1}) - Q_3(t, z_{n-2}))$$

$$+ \frac{2q}{(2-q)M(q)} \int_0^t (Q_3(s, z_{n-1}) - Q_3(s, z_{n-2})) ds.$$ (31)

It follows from equations (30) and (31) that

$$x_n(t) = \sum_{i=1}^{n} {}_x\phi_i(t),$$

$$y_n(t) = \sum_{i=1}^{n} {}_y\phi_i(t), \qquad (32)$$

$$z_n(t) = \sum_{i=1}^{n} {}_z\phi_i(t).$$

Moreover, considering the first equation of the system defined by equation (31), we have the relation

$$\left\| {}_x\phi_n(t) \right\| = \left\| x_n(t) - x_{n-1}(t) \right\| \le \frac{2(1-q)}{(2-q)M(q)} \left\| Q_1(t, x_{n-1}) - Q_1(t, x_{n-2}) \right\|$$

$$+ \frac{2q}{(2-q)M(q)} \left\| \int_0^t (Q_1(s, x_{n-1}) - Q_1(s, x_{n-2})) \mathrm{d}s \right\|. \qquad (33)$$

Since Q_1 fulfills the Lipschitz condition, it follows from equation (33) that

$$\left\| {}_x\phi_n(t) \right\| \le \frac{2(1-q)}{(2-q)M(q)} \mu_1 \left\| {}_x\phi_{n-1}(t) \right\|$$

$$+ \frac{2q}{(2-q)M(q)} \mu_1 \int_0^t \left\| {}_x\phi_{n-1}(s) \right\| \mathrm{d}s. \qquad (34)$$

Similarly, it follows that

$$\left\| {}_y\phi_n(t) \right\| \le \frac{2(1-q)}{(2-q)M(q)} \mu_2 \left\| {}_y\phi_{n-1}(t) \right\|$$

$$+ \frac{2q}{(2-q)M(q)} \mu_2 \int_0^t \left\| {}_y\phi_{n-1}(s) \right\| \mathrm{d}s, \qquad (35)$$

$$\left\| {}_z\phi_n(t) \right\| \le \frac{2(1-q)}{(2-q)M(q)} \mu_3 \left\| {}_z\phi_{n-1}(t) \right\|$$

$$+ \frac{2q}{(2-q)M(q)} \mu_3 \int_0^t \left\| {}_z\phi_{n-1}(s) \right\| \mathrm{d}s. \qquad (36)$$

Theorem 4. *The system of fractional differential equations for bone remodeling process equation (20) has an exact coupled solution, if there is t_0 such that*

$$\frac{2(1-q)}{(2-q)M(q)} \mu_1 + \frac{2q}{(2-q)M(q)} \mu_1 t_0 < 1. \qquad (37)$$

Proof. The following conditions hold on functions x, y, and z, $\|x\| \le M_1 < \infty$, $\|y\| \le M_2 < \infty$, and $\|z\| \le M_3 < \infty$; moreover, we have proven that the kernels satisfied the Lipschitz condition, hence on consideration of equations (34)–(36) and by using the recursive method, we can derive the following nonrecursive formulae:

$$\left\| {}_x\phi_n(t) \right\| \le \left\| x_n(0) \right\| \left[\frac{2(1-q)}{(2-q)M(q)} \mu_1 + + \frac{2q}{(2-q)M(q)} \mu_1 t \right]^n,$$

$$\left\| {}_y\phi_n(t) \right\| \le \left\| y_n(0) \right\| \left[\frac{2(1-q)}{(2-q)M(q)} \mu_2 + + \frac{2q}{(2-q)M(q)} \mu_2 t \right]^n,$$

$$\left\| {}_z\phi_n(t) \right\| \le \left\| z_n(0) \right\| \left[\frac{2(1-q)}{(2-q)M(q)} \mu_3 + + \frac{2q}{(2-q)M(q)} \mu_3 t \right]^n. \qquad (38)$$

The system given by equation (39) stands as the solution of equation (20). Moreover, each equation of this system is continuous. Hence, the existence and continuity are proven. Now, let us prove that equation (39) is a solution of the fractional system equation (20). Let us assume that

$$x(t) - x(0) = x_n(t) - {}_xT_n(t),$$

$$y(t) - y(0) = y_n(t) - {}_yT_n(t), \qquad (39)$$

$$z(t) - z(0) = z_n(t) - {}_zT_n(t).$$

It follows from the assumption that

$$\left\| {}_xT_n(t) \right\| = \left\| \frac{2(1-q)}{(2-q)M(q)} (Q_1(t, x) - Q_1(t, x_{n-1})) + \frac{2q}{(2-q)M(q)} \int_0^t (Q_1(s, x) - Q_1(s, x_{n-1})) \mathrm{d}s \right\|$$

$$\le \frac{2(1-q)}{(2-q)M(q)} \left\| Q_1(t, x) - Q_1(t, x_{n-1}) \right\| + \frac{2q}{(2-q)M(q)} \int_0^t \left\| Q_1(s, x) - Q_1(s, x_{n-1}) \right\| \mathrm{d}s \qquad (40)$$

$$\le \frac{2(1-q)}{(2-q)M(q)} \mu_1 \left\| x - x_{n-1} \right\| + \frac{2q}{(2-q)M(q)} \mu_1 \left\| x - x_{n-1} \right\| t.$$

Applying the process recursively yields

$$\left\| {}_x T_n(t) \right\| \leq \left(\frac{2(1-q)}{(2-q)M(q)} + \frac{2q}{(2-q)M(q)} t \right)^{n+1} \mu_1^{n+1} a. \tag{41}$$

At $t = t_0$, we have

$$\left\| {}_x T_n(t) \right\| \leq \left(\frac{2(1-q)}{(2-q)M(q)} + \frac{2q}{(2-q)M(q)} t_0 \right)^{n+1} \mu_1^{n+1} a. \tag{42}$$

At the limit case when n approaches infinity, it follows from equation (42) that $\left\| {}_x T_n(t) \right\| \longrightarrow 0$.

Similarly, we can prove that $\left\| {}_y T_n(t) \right\| \longrightarrow 0$ and $\left\| {}_z T_n(t) \right\| \longrightarrow 0$. This proves the existence of a solution of equation (20), which furthermore is equation (38).

Let us now prove the uniqueness of a system of solution of system equation (20). Let us assume there exists another set of solution to the system equation (20); let us denote this by $x_1(t)$, $y_1(t)$, and $z_1(t)$, then

$$x(t) - x_1(t) = \frac{2(1-q)}{(2-q)M(q)} \left(Q_1(t,x) - Q_1(t,x_1) \right)$$

$$+ \frac{2q}{(2-q)M(q)} \int_0^t \left(Q_1(s,x) - Q_1(s,x_1) \right) ds. \tag{43}$$

Applying the norm on equation (43), it follows that

$$\left\| x(t) - x_1(t) \right\| \leq \frac{2(1-q)}{(2-q)M(q)} \mu_1 \left\| x(t) - x_1(t) \right\|$$

$$+ \frac{2q}{(2-q)M(q)} \mu_1 t \left\| x(t) - x_1(t) \right\|. \tag{44}$$

Consequently,

$$\left\| x(t) - x_1(t) \right\| \left(1 - \frac{2(1-q)}{(2-q)M(q)} \mu_1 - \frac{2q}{(2-q)M(q)} \mu_1 t \right) \leq 0. \tag{45}$$

□

Theorem 5. *The system of equation (20) has a unique solution if the following condition holds:*

$$\left(1 - \frac{2(1-q)}{(2-q)M(q)} \mu_1 - \frac{2q}{(2-q)M(q)} \mu_1 t \right) > 0. \tag{46}$$

Proof. If the above condition holds, then

$$\left\| x(t) - x_1(t) \right\| \left(1 - \frac{2(1-q)}{(2-q)M(q)} \mu_1 - \frac{2q}{(2-q)M(q)} \mu_1 t \right) \leq 0, \tag{47}$$

implying that

$$\left\| x(t) - x_1(t) \right\| = 0, \quad \text{thus } x(t) = x_1(t). \tag{48}$$

Similarly, we can prove that $y(t) = y_1(t)$ and $z(t) = z_1(t)$. □

5. Experimental Studies and Numerical Simulations

In this section, we performed the numerical study of the solution of the systems of classical differential equation (18) of the bone formation process alongside the solution of the fractional differential equation (20) that we introduced for the same process. Computation and plotting are all done using mathematical software called MATLAB. The values of initials parameters and constants appearing in the equations are often determined experimentally by a biologist. For convenience, we used in our simulations the values retrieved from [12]. The initial conditions of the problem are defined as $x_0 = 1$, $y_0 = 5$, and $z_0 = 5$.

The constants are $a_1 = 0.1; a_2 = 0.5; a_3 = 0.4; a_4 = 0.7;$ $a_5 = 0.7; a_6 = 0.085; k_1 = 3; k_2 = 5;$ $k_3 = 2; b_1 = 0.1; b_2 = 0.2;$ and $b_3 = 0.2$.

5.1. Classical Model. In this section, solution to the problem defined by equation (18) is discussed. First order derivative equations are used in the system. Recall that the model has four variables, namely x, y, z, and t, where x, y, and z are the three chemicals involved in the process, respectively, the variation over time of the level of CT above the basal level in the blood; the number of active osteoclasts at a given time t; and the number of active osteoblasts at a given time t. The parameter t represents the time involved in the bone's formation process. 4-D representation would be appropriate tool to simultaneously visualize the behavior of x, y, and z with respect to t. However, only 1-D, 2-D, and 3-D representations are efficient for representation. In this regard, we choose a 2-D representation to show the variation of each of the substances x, y, and z, involved in the process as a function of time t. Figures 1(a)–1(c) represent the variation of each of the elements x, y, and z over time, whereas Figure 1(d) shows a joint and simultaneous variation of x and z.

Figures 1(a)–1(d) represent the dynamic of chemicals involved in bone formation process. Figures 1(a)–1(c), respectively, represent the variation over time of the level of CT above the basal level in the blood; the number of active osteoclasts at a given time t; and the number of active osteoblasts at a given time t. One can observe from Figures 1(a)–1(c) that chemical production decreases over time for all the three chemicals involved in the process. Moreover, the variation in chemical production shows a sinusoidal shape reflecting the high fluctuation in the process. The level of CT above basal level fluctuates on either side of the value 2.5 and tends to converge toward 2.5 over time. The number of active osteoclasts decreases very quickly and tends to 0 with time. Finally, the number of active osteoblasts fluctuates and tends to 1 with time. Figure 1(d) aims to investigate if there exists a correlation between any two of the chemicals produced in the process. Without loss of generality, correlation between variation over time of the level of CT above the basal level in the blood and the number of active osteoblasts at time t is investigated. The outcome of the investigation is that there is not a correlation in the way the produced chemical evolved over time.

(a)

(b)

(c)

(d)

Figure 1: (a)–(d)) Dynamic of chemicals involved in bone formation process obtained through classical differential equations.

5.2. Letnikov Fractional Model. Likewise the classical model case, we use a 2-D visualization to display the variation over time of the level of CT above the basal level in the blood; the number of active osteoclasts at a given time t; and the number of active osteoblasts at a given time t (namely, *x, y,* and *z,* respectively). A numerical approach based of the fractional Letnikov model is used to produce variation graphs, which are shown in sequel. The initial parameters and constants are same with those used in the previous section for the classical approach, except the fractional order of derivative, which we selected as $q = 0.95$ in this study. Figures 2(a)–2(c) represent the variation of each of the elements *x, y,* and *z* over time, whereas Figure 2(d) shows a joint and simultaneous variation of *x* and *z*.

Figures 2(a)–2(d) represent the dynamic of chemicals involved in bone formation process. Figures 2(a)–2(c), respectively, represent the variation over time of the level of CT above the basal level in the blood; the number of active osteoclasts at a given time t; and the number of active

osteoblasts at a given time t obtained from Letnikov fractional differential model. One can observe from Figures 2(a)–2(c) that chemical production decreases over time for all the three chemicals involved in the process. Moreover, the variation in chemical production shows a sinusoidal shape reflecting the high fluctuation in the process. The level of CT above basal level fluctuates on either side of the value 2.5 and tends to converge toward 2.5 over time. The number of active osteoclasts decreases very quickly and converges to a small but nonzero value over time. Finally, the number of active osteoblasts fluctuates and tends to 1 with time. Figure 1(d) aims to investigate if there exists a correlation between any two of the chemicals produced in the process. Without loss of generality, correlation between variation over time of the level of CT above the basal level in the blood and the number of active osteoblasts at time t is investigated. The outcome of the investigation is that there is not a correlation in the way the produced chemical evolved over time.
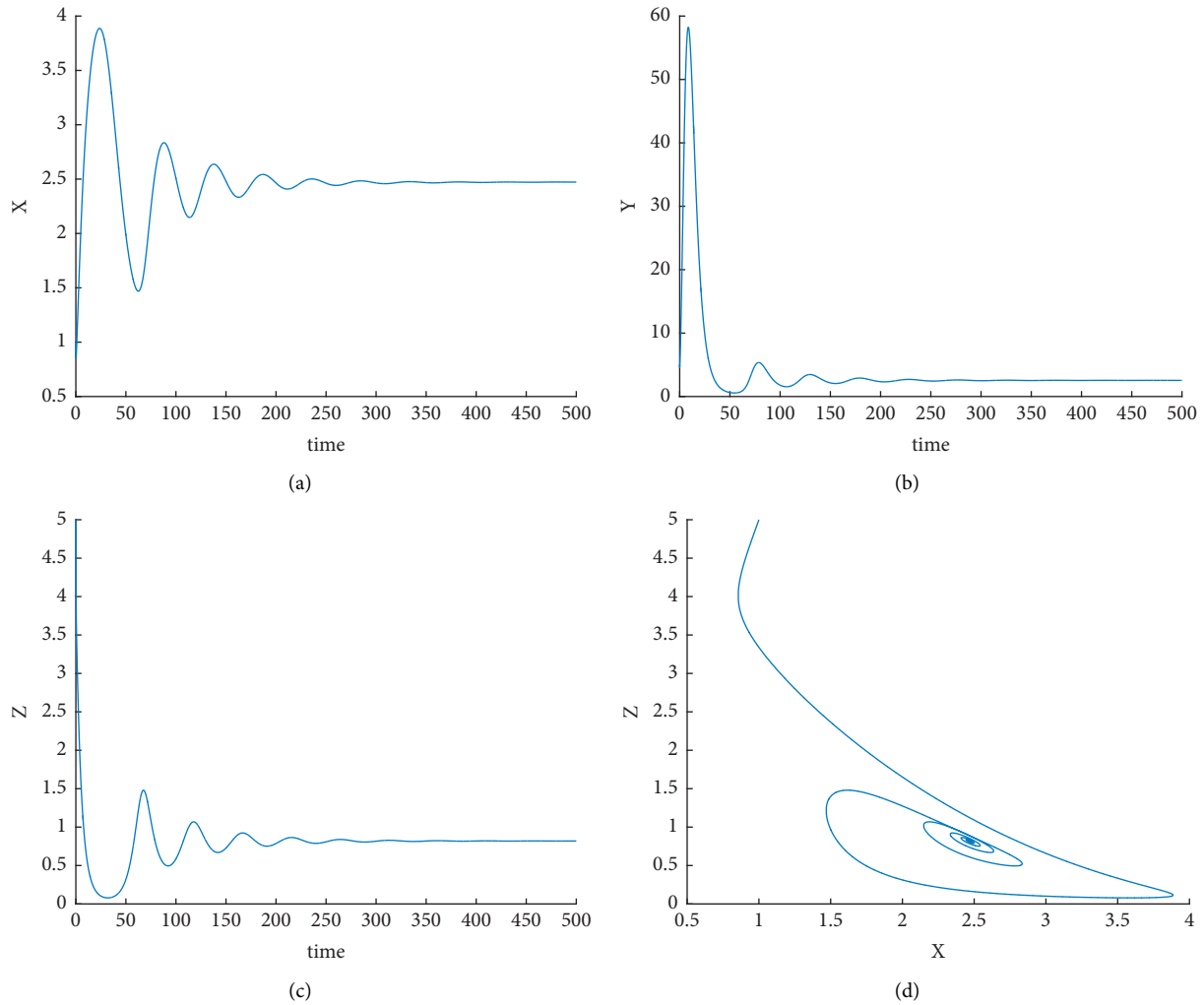
FIGURE 2: (a)–(d)) Dynamic of chemicals involved in bone formation process obtained through fractional model of bone remodeling process by Letnikov.

Figures 2(a)–2(c) have the same sinusoidal shape as their counterpart from classical model. They also decrease over time. However, maximum (respectively minimum) value of the graph in classical model is larger (respectively smaller) than those obtained in the Letnikov model. Figures 1(d) and 2(d) have same shape; they both show same trend.

5.3. Caputo–Fabrizio Fractional Model.
In this section, numerical solution based on Caputo–Fabrizio fractional model is discussed. The initial parameters and constants are like those used in Section 5.3. Figures 3(a)–3(c) represent the variation over time of the level of CT above the basal level in the blood; the number of active osteoclasts at a given time t; and the number of active osteoblasts at a given time t (namely, x, y, and z), whereas Figure 3(d) is a joint and simultaneous variation of the variation over time of the level of CT above the basal level in the blood and the number of active osteoblasts at a given time t.

Figures 3(a)–3(c) represent the dynamic of chemicals involved in bone formation process. Figures 3(a)–3(c),

respectively, represent the variation over time of the level of CT above the basal level in the blood; the number of active osteoclasts at a given time t; and the number of active osteoblasts at a given time t. It is shown from Figures 3(a)–3(c) that chemical production decreases over time for all the three chemicals involved in the process. Moreover, the variation in chemical production shows a sinusoidal shape reflecting the high fluctuation in the process. The level of CT above basal level fluctuates on either side of the value 2.5 and tends to converge toward 2.5 over time. The number of active osteoclasts decreases very quickly and tends to 0 with time. Finally, the number of active osteoblasts fluctuates and tends to 1 with time. Figure 3(d) aims to investigate if there exists a correlation between any two of the chemicals produced in the process. Without loss of generality, correlation between variation over time of the level of CT above the basal level in the blood and the number of active osteoblasts at time t is investigated. The outcome of the investigation is that there is not a correlation in the way the produced chemical evolved over time.
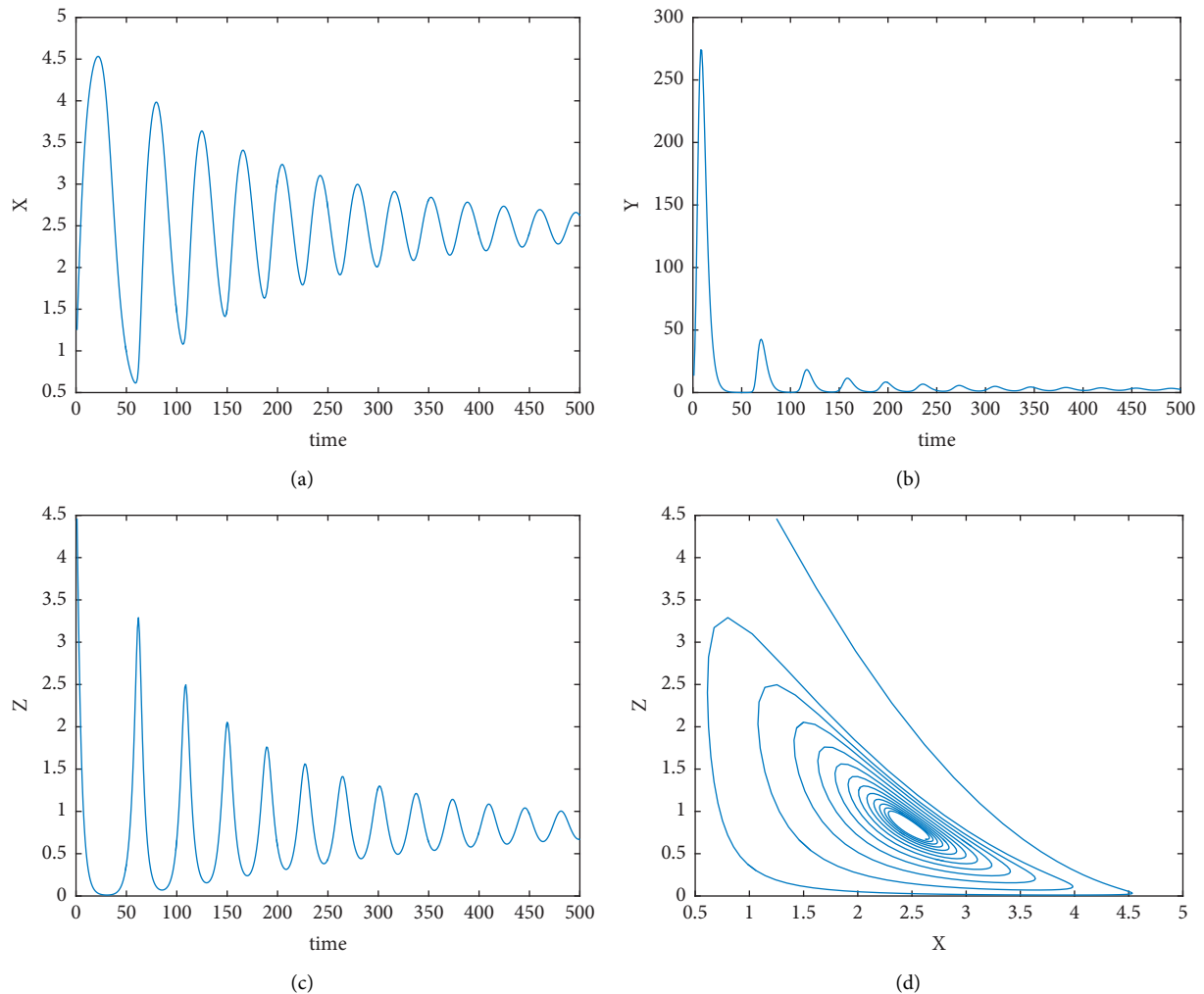
FIGURE 3: (a)–(d)) Dynamic of chemicals involved in bone formation process obtained through fractional model of bone remodeling process by Caputo and Fabrizio.

6. Conclusion and Comments

The goal of this paper was to build a system of differential equations for bone formation process based on various fractional differential equations. Indeed, Letnikov and Caputo–Fabrizio fractional derivatives were used alongside classical differential equation method for comparison purposes. The work does not follow traditional quantitative modeling approach in which historical data exist, various models including a proposed model are used to fit the data; and their error rates are compared to pick the best model. We put all these models together rather to investigate if the proposed fractional differential equations-based models are effective. In the course of the work, we proved existence and uniqueness of the proposed system of differential equations; moreover, we studied the solution of the system using numerical approaches. From the numerical simulation of the classical model and those from the proposed fractional model, one can observe similarity in both approaches. This consolidates the results obtained in the theoretical part of the work. As a matter of fact, one can conclude that fractional differential equation is effective in modeling bone formation process. In further study, we will investigate advantages and disadvantages of using such method over classical approach.

Data Availability

No datasets were used or analyzed during the current study.

Conflicts of Interest

The authors declare that they have no conflicts of interest.

Authors' Contributions

Each of the authors, M.A, Y.Y.Y, and KA, contributed to each part of this work equally and read and approved the final version of the manuscript.

Acknowledgments

References

[1] N. I. Mahmudov, M. Awadalla, and K. Abuassba, "Nonlinear sequential fractional differential equations with nonlocal boundary conditions," *Advances in Difference Equations*, vol. 2017, no. 1, p. 319, 2017.

[2] N. I. Mahmudov, M. Awadalla, and K. Abuassba, "Hadamard and caputo-hadamard FDE's with three point integral boundary conditions," *Nonlinear Analysis and Differential Equations*, vol. 5, no. 6, pp. 271–282, 2017, www.m-hikari.com https://doi.org/10.12988/nade.2017.7916.

[3] C. Li and S. Sarwar, "Existence and contiuation of solution for Caputo type fractional differential equations," *The Electronic Journal of Differential Equations*, vol. 2016, pp. 1–14, 2016.

[4] A. Babakhani and V. Daftardar-Gejji, "Existence of positive solutions of nonlinear fractional differential equations," *Journal of Mathematical Analysis and Applications*, vol. 278, no. 2, pp. 434–442, 2003.

[5] X. Zhang, X. Zhang, Z. Liu, W. Ding, H. Cao, and T. Shu, "On the general solution of impulsive systems with hadamard fractional derivatives," *Mathematical Problems in Engineering*, vol. 2016, Article ID 2814310, 12 pages, 2016.

[6] M. Awadalla and Y. Y. Yameni, "Modeling exponential growth and exponential decay real phenomena by ψ-caputo fractional derivative," *Journal of Advances in Mathematics and Computer Science*, vol. 28, 2018.

[7] R. Almeida, N. R. O. Bastos, and M. T. T. Monteiro, "Modeling some real phenomena by fractional differential equations," *Mathematical Methods in the Applied Sciences*, vol. 39, no. 16, pp. 4846–4855, 2015.

[8] I. Area, H. Batarfi, J. Losada, J. J. Nieto, W. Shammakh, and Á. Torres, "On a fractional order Ebola epidemic model," *Advances in Difference Equations*, vol. 2015, no. 1, p. 278, 2015.

[9] K. Kowalski and W. H. Steeb, *Nonlinear Dynamical Systems and Carleman Linearization*, World Scientific, Singapore, 1991.

[10] R. L. Magin, "Fractional calculus models of complex dynamics in biological tissues," *Computers & Mathematics with Applications*, vol. 59, no. 5, pp. 1586–1593, 2010.

[11] M. M. Khader and K. M. Saad, "Numerical treatment for studying the blood ethanol concentration systems with different forms of fractional derivatives," *International Journal of Modern Physics C*, vol. 31, no. 3, p. 2050044, 2020.

[12] C. Rattanakul and S. Rattanamongkonkul, "Effect of calcitonin on bone formation and resorption: mathematical modeling approach," *System*, vol. 3, no. 4, p. 2, 2011.

[13] R. S. Cotran: Cellular Injury and Cellular Death. Pathologic Basis of Disease.

[14] M. Kroll, "Parathyroid hormone temporal effects on bone formation and resorption," *Bulletin of Mathematical Biology*, vol. 62, no. 1, pp. 163–188, 2000.

[15] R. A. Lobo, J. Kelsey, and R. Marcus, *Menopause: Biology and Pathobiology*, Academic Press, Cambridge, MA, USA, 2000.

[16] R. T. Turner, B. L. Riggs, and T. C. Spelsberg, "Skeletal effects of estrogen*," *Endocrine Reviews*, vol. 15, no. 3, pp. 275–300, 1994.

[17] E. H. Holt and H. Peery, *Basic Medical Endocrinology*, Academic Press, Cambridge, MA, USA, 2010.

[18] Z. M. Odibat and S. Momani, "An algorithm for the numerical solution of differential equations of fractional order," *Journal of Applied Mathematics & Informatics*, vol. 26, no. 1_2, pp. 15–27, 2008.

[19] I. Petráš, *Fractional-order Nonlinear Systems: Modeling, Analysis and Simulation*, Springer Science & Business Media, Berlin, Germany, 2011.

[20] A. Atangana and K. M. Owolabi, "New numerical approach for fractional differential equations," *Mathematical Modelling of Natural Phenomena*, vol. 13, no. 1, p. 3, 2018.

[21] N. R. Bastos, "Calculus of variations involving Caputo-Fabrizio fractional differentiation," *Statistics*, vol. 2310, p. 5070, 2018.

[22] J. Losada and J. J. Nieto, "Properties of a new fractional derivative without singular kernel," *Progress in Fractional Differentiation and Applications*, vol. 1, no. 2, pp. 87–92, 2015.

Research Article

On Semianalytical Study of Fractional-Order Kawahara Partial Differential Equation with the Homotopy Perturbation Method

Muhammad Sinan [iD],[1,2] **Kamal Shah** [iD],[3] **Zareen A. Khan** [iD],[4] **Qasem Al-Mdallal** [iD],[5] **and Fathalla Rihan** [iD][5]

[1]*School of Mathematical Sciences, University of Electronic Science and Technology of China, Chengdu 611731, China*
[2]*Department of Mathematics and Statistics, University of Swat, Swat, Khyber Pakhtunkhwa, Pakistan*
[3]*Department of Mathematics, University of Malakand, Chakdara Dir (L) 18000, Khyber Pakhtunkhwa, Pakistan*
[4]*College of Science, Mathematical Sciences, Princess Nourah Bint Abdulrahman University, Riyadh, Saudi Arabia*
[5]*Department of Mathematical Sciences, UAE University, P.O. Box 15551, Al-Ain, UAE*

Correspondence should be addressed to Fathalla Rihan; frihan@uaeu.ac.ae

In this study, we investigate the semianalytic solution of the fifth-order Kawahara partial differential equation (KPDE) with the approach of fractional-order derivative. We use Caputo-type derivative to investigate the said problem by using the homotopy perturbation method (HPM) for the required solution. We obtain the solution in the form of infinite series. We next triggered different parametric effects (such as x, t, and so on) on the structure of the solitary wave propagation, demonstrating that the breadth and amplitude of the solitary wave potential may alter when these parameters are changed. We have demonstrated that He's approach is highly effective and powerful for the solution of such a higher-order nonlinear partial differential equation through our calculations and simulations. We may apply our method to an additional complicated problem, particularly on the applied side, such as astrophysics, plasma physics, and quantum mechanics, to perform complex theoretical computation. Graphical presentation of few terms approximate solutions are given at different fractional orders.

1. Introduction

PDEs have important applications in physics, engineering, and other applied sciences. They can describe different phenomena and processes of real-world problems. One of the important KPDE arises in the theory of magnetoacoustic and shallow-water waves. Furthermore, it arises in the theory of shallow-water waves with surface tension and magnetoacoustic waves in plasmas. Therefore, several analytical and numerical methods have been established in literature to investigate the prosed problems of PDEs. For instance, [1] authors have used the comparison method for the solution of the famous Kawahara equation. In the same line, a procedure was developed in [2] for the exact solution of the said problem. Also, authors [3] have computed the solution of the Kawahara equation by using symbolic

computation. In this study, we apply a semianalytic HPM to solve the fifth-order KPDEs. As in the last several decades' investigation, traveling-waves solutions for nonlinear equations played an important role in the study of the nonlinear physical phenomenon [4]. The mentioned method provides an efficient approach to solve a nonlinear problem. The KPDE was first suggested by Kawahara [5] in 1972. Since these nonlinear equations need to be solved by using some approximate methods, researchers have solved several nonlinear problems by using HPM. This method was first proposed by He [6] and has been applied in [7] for the solution of differential equations and integral equations in both linear and nonlinear cases. The said method is a combination of topological homotopy and traditional perturbation methods. The advantage of this method is to provide an analytic approximate solution in applied sciences

with a capacious range, and in this method, a small parameter is not necessary for an equation. This method is also applied to the system of the nonlinear system of equations as in [8] for the analytic approximate solution for the model of rabies transmission dynamics.

Because of the popularity of fractional calculus and applications in many fields of science and engineering [9], fluid mechanics [10], some more frequent applications in a diverse area of science by using fraction calculus have been investigated in [11, 12]. The mentioned derivative extends order from integer to any real or complex number which provides a detailed explanation to physical problems. Fractional derivatives can produce a complete spectrum of the geometry which includes its integer counterpart as a special case. Motivated from the aforesaid work, we extend the given KPDE [13].

$$\frac{\partial u}{\partial t} + \rho u \frac{\partial u}{\partial x} + \sigma \frac{\partial^3 u}{\partial x^3} - \gamma \frac{\partial^5 u}{\partial x^5} = 0, \tag{1}$$

$$u(x, 0) = g(x),$$

where g is a continuous function, while $\rho, \sigma,$ and γ are the nonzero arbitrary constants to fractional order as

$$\frac{\partial^\alpha u}{\partial t^\alpha} + \rho u \frac{\partial^\beta u}{\partial x^\beta} + \sigma \frac{\partial^\kappa u}{\partial x^\kappa} - \gamma \frac{\partial^\delta u}{\partial x^\delta} = 0, \quad 0 < \alpha \le 1, \tag{2}$$

$$u(x, 0) = g(x), \tag{3}$$

while $0 < \beta \le 1$, $2 < \kappa \le 3$, $4 < \delta \le 5$, and $g: R \longrightarrow R$ is continuous function.

For the demonstration of our problem, we testified the example given by Albert [14] as

$$\frac{\partial^\alpha u}{\partial t^\alpha} + \rho u \frac{\partial^\beta u}{\partial x^\beta} + \sigma \frac{\partial^\kappa u}{\partial x^\kappa} - \gamma \frac{\partial^\delta u}{\partial x^\delta} = 0, \tag{4}$$

with the initial condition

$$u(x, 0) = \frac{105}{169} \text{sech}^4 \left(\frac{x}{2\sqrt{13}} \right), \tag{5}$$

by using fractional derivative in Caputo sense. We also present the solutions graphically and then, at the end, provide conclusion and discussion.

2. Preliminaries and Notations

Here, we recall some preliminaries and notations from [15].

Definition 1. Caputo fractional-order derivative of a function ϕ on the interval $[0, \infty)$ is defined as

$$^c D_{0+}^\alpha \phi(t) = \frac{1}{\Gamma(n - \alpha)} \int_0^t (t - s)^{n - \alpha - 1} \frac{d^n}{ds^n} \phi(s) ds, \tag{6}$$

where $n = [\alpha] + 1$ and $[\alpha]$ represent the integral part of α.

Definition 2. If $\alpha > 0$, the Caputo fractional integral is defined as

$$I^\alpha \phi(t) = \frac{1}{\Gamma(\alpha)} \int_0^t (t - s)^{\alpha - 1} \phi(s) ds, \tag{7}$$

where $\alpha \in (0, \infty)$.

Lemma 1. *The following result holds:*

$$I^n \left[C D_{0+}^n \phi(t) \right] = \phi(t) + a_0 + a_1 t + a_2 t^2 + \cdots + a_{n-1} t^{n-1}, \tag{8}$$

for arbitrary $a_i \in R$, $i = 0, 1, 2, 3, \ldots, n - 1$, where $n = [\eta] + 1$ and $[\eta]$ represent the integral part of η.

3. A General Algorithm about HPM

Consider a general type problem given by

$$A(\mu) - f(r) = 0, \quad r \in \Omega, \tag{9}$$

with boundary condition as

$$\beta \left(\mu, \frac{\partial \mu}{\partial n} \right) = 0, r \in \Gamma, \tag{10}$$

where A is a general differential operator, β is a boundary operator, $f(r)$ is a known analytic function, and Γ is the boundary of the domain Ω. The operator A is divided into linear part L and nonlinear part N. Therefore, (9) can be written as

$$L(\mu) + N(u) - f(r) = 0. \tag{11}$$

By HPM, we can construct a homotopy as

$$v(r, p): \Omega \times [0, 1] \longrightarrow R, \tag{12}$$

satisfying

$$H(v, p) = (1 - p)[L(v) - L(\mu)] + p[A(v - f(r))] = 0, \tag{13}$$

which is also equivalent to

$$H(v, p) = L(v) - L(\mu_0) + pL(v_0) + p[N(v) - f(r)] = 0, \tag{14}$$

where $p \in [0; 1]$ is an embedding parameter, and μ_0 is the initial approximation of the given equation that satisfies the boundary conditions; we have

$$H(v, 0) = L(v) - L(\mu_0) = 0,$$
$$H(v, 1) = A(v) - f(r) = 0. \tag{15}$$

Keeping these points, we construct the required solution to equation (11) as

$$v = v_0 + p^1 v_1 + p^2 v_2 + p^3 v_3 + \cdots. \tag{16}$$

Furthermore, by taking limit as $p \longrightarrow 1$ in the approximation equation (16), one has

$$\lim_{p \longrightarrow 1} v = \lim_{p \longrightarrow 1} v_0 + p^1 v_1 + p^2 v_2 + p^3 v_3 + \cdots, \tag{17}$$

which yields

$$v = v_0 + v_1 + v_2 + v_3 + \cdots. \tag{18}$$

Equation (18) represents the semianalytic solution of the problem equation (9).

4. Approximate Solution to Considered Problem

Here, in view of HPM as discussed in previous section, we proceed as

$$H(u, p) = \frac{\partial^\alpha u}{\partial t^\alpha} - \frac{\partial^\alpha}{\partial t^\alpha} g(x) + p \frac{\partial^\alpha}{\partial t^\alpha} g(x) + p \left[\alpha u \frac{\partial^\beta u}{\partial x^\beta} + \sigma \frac{\partial^\kappa u}{\partial x^\kappa} - \gamma \frac{\partial^\delta u}{\partial x^\delta} \right] = 0. \tag{19}$$

We assume the solution of equation (2) as follows:

$$u(x, t) = \sum_{i=0}^{\infty} p^i u_i(x, t). \tag{20}$$

Now, using equation (20) in (19) and comparing the coefficients of p^i, for $i = 0, 1, 2, 3, \ldots$, we have

$$p^0 := \frac{\partial^\alpha u_0}{\partial t^\alpha} - \frac{\partial^\alpha}{\partial t^\alpha} g(x) = 0,$$

$$p^1 := \frac{\partial^\alpha u_1}{\partial t^\alpha} + \rho u_0 \frac{\partial^\beta}{\partial x^\beta} u_0 + \sigma \frac{\partial^\kappa}{\partial x^\kappa} u_0 - \gamma \frac{\partial^\delta}{\partial x^\delta} u_0 = 0,$$

$$p^2 := \frac{\partial^\alpha u_2}{\partial t^\alpha} + \rho u_1 \frac{\partial^\beta}{\partial x^\beta} u_1 + \sigma \frac{\partial^\kappa}{\partial x^\kappa} u_1 - \gamma \frac{\partial^\delta}{\partial x^\delta} u_1 = 0,$$

$$p^3 := \frac{\partial^\alpha u_3}{\partial t^\alpha} + \rho u_2 \frac{\partial^\beta}{\partial x^\beta} u_2 + \sigma \frac{\partial^\kappa}{\partial x^\kappa} u_2 - \gamma \frac{\partial^\delta}{\partial x^\delta} u_2 = 0,$$

$$p^4 := \frac{\partial^\alpha u_4}{\partial t^\alpha} + \rho u_3 \frac{\partial^\beta}{\partial x^\beta} u_3 + \sigma \frac{\partial^\kappa}{\partial x^\kappa} u_3 - \gamma \frac{\partial^\delta}{\partial x^\delta} u_3 = 0,$$

$$\vdots$$

$$\tag{21}$$

From system equation (21), we get

Zeroth-order problem

Consider zeroth-order problem as

$$\frac{\partial^\alpha u_0}{\partial t^\alpha} = \frac{\partial^\alpha g(x)}{\partial t^\alpha}. \tag{22}$$

Which yields

$$u_0 = g(x). \tag{23}$$

First-order problem

$$\frac{\partial^\alpha u_1}{\partial t^\alpha} == \frac{\partial^\alpha g(x)}{\partial t^\alpha} + \gamma \frac{\partial^\delta}{\partial x^\delta} u_0 - \rho u_0 \frac{\partial^\beta}{\partial x^\beta} u_0 - \sigma \frac{\partial^\kappa}{\partial x^\kappa} u_0,$$

$$u_1 = \left(\gamma \frac{\partial^\delta}{\partial x^\delta} u_0 - \rho u_0 \frac{\partial^\beta}{\partial x^\beta} u_0 - \sigma \frac{\partial^\kappa}{\partial x^\kappa} u_0 \right) \frac{t^\alpha}{\Gamma(\alpha + 1)}. \tag{24}$$

Second-order problem

$$\frac{\partial^\alpha u_2}{\partial t^\alpha} = \frac{\gamma t^\alpha}{\Gamma(\alpha + 1)} \frac{\partial^\delta}{\partial x^\delta} \xi - \frac{\rho \xi t^{2\alpha}}{\Gamma(\alpha + 1)^2} \frac{\partial^\beta}{\partial x^\beta} \xi - \frac{\sigma t^\alpha}{\Gamma(\alpha + 1)} \frac{\partial^\kappa}{\partial x^\kappa} \xi,$$

$$u_2 = \frac{\gamma t^{2\alpha}}{\Gamma(\alpha + 2)} \frac{\partial^\delta}{\partial x^\delta} \xi - \frac{\rho \xi t^{3\alpha}}{\Gamma(\alpha + 2)^2 \Gamma(\alpha + 3)} \frac{\partial^\beta}{\partial x^\beta} \xi - \frac{\sigma t^{2\alpha}}{\Gamma(\alpha + 2)} \frac{\partial^\kappa}{\partial x^\kappa} \xi. \tag{25}$$

Where

$$\xi = \gamma \frac{\partial^{\delta}}{\partial x^{\delta}} u_0 - \rho u_0 \frac{\partial^{\beta}}{\partial x^{\beta}} u_0 - \sigma \frac{\partial^{\kappa}}{\partial x^{\kappa}} u_0. \qquad (26)$$

Third-order problem

$$
\begin{aligned}
u_3 = {} & \gamma \frac{\partial^{\delta}}{\partial x^{\delta}} \left(\frac{\gamma t^{3\alpha}}{\Gamma(\alpha+3)} \frac{\partial^{\delta}}{\partial x^{\delta}} \xi - \frac{\rho \xi t^{4\alpha}}{\Gamma(\alpha+1)^2 \Gamma(\alpha+4)} \frac{\partial^{\beta}}{\partial x^{\beta}} \xi - \frac{\sigma t^{3\alpha}}{\Gamma(\alpha+3)} \frac{\partial^{\kappa}}{\partial x^{\kappa}} \xi \right) \\
& - \alpha \left(\frac{\gamma t^{2\alpha}}{\Gamma(\alpha+2)} \frac{\partial^{\delta}}{\partial x^{\delta}} \xi - \frac{\rho \xi t^{3\alpha}}{\Gamma(\alpha+1)^2 \Gamma(\alpha+3)} \frac{\partial^{\beta}}{\partial x^{\beta}} \xi - \frac{\sigma t^{2\alpha}}{\Gamma(\alpha+2)} \frac{\partial^{\kappa}}{\partial x^{\kappa}} \xi \right) \\
& \times \frac{\partial^{\beta}}{\partial x^{\beta}} \left(\frac{\gamma t^{3\alpha}}{\Gamma(\alpha+3)} \frac{\partial^{\delta}}{\partial x^{\delta}} \xi - \frac{\rho \xi t^{4\alpha}}{\Gamma(\alpha+1)^2 \Gamma(\alpha+4)} \frac{\partial^{\beta}}{\partial x^{\beta}} \xi - \frac{\sigma t^{3\alpha}}{\Gamma(\alpha+3)} \frac{\partial^{\kappa}}{\partial x^{\kappa}} \xi \right) \\
& - \beta \frac{\partial^{\kappa}}{\partial x^{\kappa}} \left(\frac{\gamma t^{3\alpha}}{\Gamma(\alpha+3)} \frac{\partial^{\delta}}{\partial x^{\delta}} \xi - \frac{\rho \xi t^{4\alpha}}{\Gamma(\alpha+1)^2 \Gamma(\alpha+4)} \frac{\partial^{\beta}}{\partial x^{\beta}} \xi - \frac{\sigma t^{3\alpha}}{\Gamma(\alpha+3)} \frac{\partial^{\kappa}}{\partial x^{\kappa}} \xi \right).
\end{aligned}
\qquad (27)
$$

In the same way, one has

Now, taking the limit as $p \longrightarrow 1$ in equation (20), we get

$$u(x,t) = \sum_{i=0}^{\infty} u_i(x,t). \qquad (28)$$

Next, equations (23)–(28) imply that

$$
\begin{aligned}
u(x,t) = {} & g(x) + \left(\gamma \frac{\partial^{\delta}}{\partial x^{\delta}} u_0 - \rho u_0 \frac{\partial^{\beta}}{\partial x^{\beta}} u_0 - \sigma \frac{\partial^{\kappa}}{\partial x^{\kappa}} u_0 \right) \frac{t^{\alpha}}{\Gamma(\alpha+1)} \\
& + \frac{\gamma t^{2\alpha}}{\Gamma(\alpha+2)} \frac{\partial^{\delta}}{\partial x^{\delta}} \xi - \frac{\rho \xi t^{3\alpha}}{\Gamma(\alpha+1)^2 \Gamma(\alpha+3)} \frac{\partial^{\beta}}{\partial x^{\beta}} \xi - \frac{\sigma t^{2\alpha}}{\Gamma(\alpha+2)} \frac{\partial^{\kappa}}{\partial x^{\kappa}} \xi \\
& + \gamma \frac{\partial^{\delta}}{\partial x^{\delta}} \left(\frac{\gamma t^{3\alpha}}{\Gamma(\alpha+3)} \frac{\partial^{\delta}}{\partial x^{\delta}} \xi - \frac{\rho \xi t^{4\alpha}}{\Gamma(\alpha+1)^2 \Gamma(\alpha+4)} \frac{\partial^{\beta}}{\partial x^{\beta}} \xi - \frac{\sigma t^{3\alpha}}{\Gamma(\alpha+3)} \frac{\partial^{\kappa}}{\partial x^{\kappa}} \xi \right) \\
& - \alpha \left(\frac{\gamma t^{2\alpha}}{\Gamma(\alpha+2)} \frac{\partial^{\delta}}{\partial x^{\delta}} \xi - \frac{\rho \xi t^{3\alpha}}{\Gamma(\alpha+1)^2 \Gamma(\alpha+3)} \frac{\partial^{\beta}}{\partial x^{\beta}} \xi - \frac{\sigma t^{2\alpha}}{\Gamma(\alpha+2)} \frac{\partial^{\kappa}}{\partial x^{\kappa}} \xi \right) \\
& \times \frac{\partial^{\beta}}{\partial x^{\beta}} \left(\frac{\gamma t^{3\alpha}}{\Gamma(\alpha+3)} \frac{\partial^{\delta}}{\partial x^{\delta}} \xi - \frac{\rho \xi t^{4\alpha}}{\Gamma(\alpha+1)^2 \Gamma(\alpha+4)} \frac{\partial^{\beta}}{\partial x^{\beta}} \xi - \frac{\sigma t^{3\alpha}}{\Gamma(\alpha+3)} \frac{\partial^{\kappa}}{\partial x^{\kappa}} \xi \right) \\
& - \beta \frac{\partial^{\kappa}}{\partial x^{\kappa}} \left(\frac{\gamma t^{3\alpha}}{\Gamma(\alpha+3)} \frac{\partial^{\delta}}{\partial x^{\delta}} \xi - \frac{\rho \xi t^{4\alpha}}{\Gamma(\alpha+1)^2 \Gamma(\alpha+4)} \frac{\partial^{\beta}}{\partial x^{\beta}} \xi - \frac{\sigma t^{3\alpha}}{\Gamma(\alpha+3)} \frac{\partial^{\kappa}}{\partial x^{\kappa}} \xi \right) + \cdots,
\end{aligned}
\qquad (29)
$$

where

$$\xi = \gamma \frac{\partial^{\delta}}{\partial x^{\delta}} u_0 - \rho u_0 \frac{\partial^{\beta}}{\partial x^{\beta}} u_0 - \sigma \frac{\partial^{\kappa}}{\partial x^{\kappa}} \xi. \qquad (30)$$

Hence, (29) is a required solution of the fractional-order KPDE.

4.1. *Fractional Temporal Numerical Example.* Consider the fractional-order KPDE given by

$$\frac{\partial^{\alpha} u}{\partial t^{\alpha}} + u \frac{\partial^{\beta} u}{\partial x^{\beta}} + \frac{\partial^{\kappa} u}{\partial x^{\kappa}} - \frac{\partial^{\delta} u}{\partial x^{\delta}} = 0, \ 0 < \alpha \le 1, \ 0 < \beta \le 1, \ 2 < \kappa \le 3, \ 4 < \delta \le 5, \tag{31}$$

with initial condition

$$u(x, 0) = \frac{105}{169} \sec h^4 \left(\frac{x}{2\sqrt{13}} \right). \tag{32}$$

Using HPM, equation (21) yields that

$$H(u, p) := \frac{\partial^{\alpha}}{\partial t^{\alpha}} u - \frac{105}{169} \frac{\partial^{\alpha}}{\partial t^{\alpha}} \sec h^4 \left(\frac{x}{2\sqrt{13}} \right) + \frac{105}{169} p \left[\frac{\partial^{\alpha}}{\partial t^{\alpha}} \sec h^4 \left(\frac{x}{2\sqrt{13}} \right) \right]$$

$$+ p \left[u \frac{\partial^{\beta}}{\partial x^{\beta}} u + \frac{\partial^{\kappa}}{\partial x^{\kappa}} u - \frac{\partial^{\delta}}{\partial x^{\delta}} u \right]. \tag{33}$$

Using equations (20) and (33), we get the following comparison with respect to p:

$$p^0 := \frac{\partial^{\alpha}}{\partial t^{\alpha}} u_0 - \frac{105}{169} \frac{\partial^{\alpha}}{\partial t^{\alpha}} \sec h^4 \left(\frac{x}{2\sqrt{13}} \right) = 0,$$

$$p^1 := \frac{\partial^{\alpha}}{\partial t^{\alpha}} u_1 + \left(\frac{105}{169} \right)^2 \sec h^4 \left(\frac{x}{2\sqrt{13}} \right) \frac{\partial^{\beta}}{\partial x^{\beta}} \sec h^4 \left(\frac{x}{2\sqrt{13}} \right). \tag{34}$$

$$+ \frac{105}{169} \frac{\partial^{\kappa}}{\partial x^{\kappa}} \sec h^4 \left(\frac{x}{2\sqrt{13}} \right) - \frac{105}{169} \frac{\partial^{\delta}}{\partial x^{\delta}} \sec h^4 \left(\frac{x}{2\sqrt{13}} \right) = 0. \tag{35}$$

$$\vdots$$

Zeroth-order problem

From equation (34), we get the zeroth-order problem or $u(x, 0)$:

$$u_0 = \frac{105}{169} \sec h^4 \left(\frac{x}{2\sqrt{13}} \right), \text{ if } u(x, 0) = \frac{105}{169} \sec h^4 \left(\frac{x}{2\sqrt{13}} \right). \tag{36}$$

First-order problem

From equation (35),

$$u_1(x, t) = \frac{11025 t^{\alpha}}{28561 \Gamma(\alpha + 1)} \sec h^4 \left(\frac{x}{2\sqrt{13}} \right) \frac{\partial}{\partial x} \sec h^4 \left(\frac{x}{2\sqrt{13}} \right) + \frac{105 t^{\alpha}}{169 \Gamma(\alpha + 1)} \frac{\partial^3}{\partial x^3} \sec h^4 \left(\frac{x}{2\sqrt{13}} \right)$$

$$- \frac{105 t^{\alpha}}{169 \Gamma(\alpha + 1)} \frac{\partial^5}{\partial x^5} \sec h^4 \left(\frac{x}{2\sqrt{13}} \right) = 0, \tag{37}$$

which gives

$$u_1(x,t) = -\frac{22050\sqrt{13}t^\alpha}{371293\Gamma(\alpha+1)}\sec h^4\left(\frac{x}{2\sqrt{13}}\right)\sec h\left(\frac{x\sqrt{13}}{26}\right)^4\tanh\left(\frac{x\sqrt{13}}{26}\right) + \frac{735\sqrt{13}t^\alpha}{28561\Gamma(\alpha+1)}\sec h\left(\frac{x\sqrt{13}}{26}\right)^4$$

$$\times\tanh\left(\frac{x\sqrt{13}}{26}\right)\left(1-\tanh\left(\frac{x\sqrt{13}}{26}\right)^2\right) - \frac{840\sqrt{13}t^\alpha}{28561\Gamma(\alpha+1)}\sec h\left(\frac{x\sqrt{13}}{26}\right)^4\tanh\left(\frac{x\sqrt{13}}{26}\right)^3$$

$$+\frac{13755\sqrt{13}t^\alpha}{371293\Gamma(\alpha+1)}\sec h\left(\frac{x\sqrt{13}}{26}\right)^4\tanh\left(\frac{x\sqrt{13}}{26}\right)^3\left(1-\tanh\left(\frac{x\sqrt{13}}{26}\right)^2\right) - \frac{3360\sqrt{13}t^\alpha}{371293\Gamma(\alpha+1)}\sec h\left(\frac{x\sqrt{13}}{26}\right)^4$$

$$\times\tanh\left(\frac{x\sqrt{13}}{26}\right)^5 - \frac{4935\sqrt{13}t^\alpha}{371293\Gamma(\alpha+1)}\sec h\left(\frac{x\sqrt{13}}{26}\right)^4\tanh\left(\frac{x\sqrt{13}}{26}\right)\left(1-\tanh\left(\frac{x\sqrt{13}}{26}\right)^2\right)^2.$$

(38)

If we use $p \longrightarrow 1$, then solution of equation (31) implies that

$$u(x,t) = u_0 + u_1(x,t) + u_2(x,t) + \cdots u(x,t) = \frac{105}{169}\sec h^4\left(\frac{x}{2\sqrt{13}}\right)$$

$$-\frac{22050\sqrt{13}t^\alpha}{371293\Gamma(\alpha+1)}\sec h^4\left(\frac{x}{2\sqrt{13}}\right)\sec h\left(\frac{x\sqrt{13}}{26}\right)^4\tanh\left(\frac{x\sqrt{13}}{26}\right)$$

$$+\frac{735\sqrt{13}t^\alpha}{28561\Gamma(\alpha+1)}\sec h\left(\frac{x\sqrt{13}}{26}\right)^4\tanh\left(\frac{x\sqrt{13}}{26}\right)\left(1-\tanh\left(\frac{x\sqrt{13}}{26}\right)^2\right) - \frac{840\sqrt{13}t^\alpha}{28561\Gamma(\alpha+1)}$$

$$\times\sec h\left(\frac{x\sqrt{13}}{26}\right)^4\tanh\left(\frac{x\sqrt{13}}{26}\right)^3 + \frac{13755\sqrt{13}t^\alpha}{371293\Gamma(\alpha+1)}\sec h\left(\frac{x\sqrt{13}}{26}\right)^4\tanh\left(\frac{x\sqrt{13}}{26}\right)^3\left(1-\tanh\left(\frac{x\sqrt{13}}{26}\right)^2\right)$$

(39)

$$-\frac{3360\sqrt{13}t^\alpha}{371293\Gamma(\alpha+1)}\sec h\left(\frac{x\sqrt{13}}{26}\right)^4\tanh\left(\frac{x\sqrt{13}}{26}\right)^5 - \frac{4935\sqrt{13}t^\alpha}{371293\Gamma(\alpha+1)}\sec h\left(\frac{x\sqrt{13}}{26}\right)^4\tanh\left(\frac{x\sqrt{13}}{26}\right)$$

$$\times\left(1-\tanh\left(\frac{x\sqrt{13}}{26}\right)^2\right)^2 + \cdots.$$

In Figures 1–4, we present graphical presentation of solutions.

5. Fractional Spatial Numerical Solution

Consider the equation with orders $0 < \beta \le 1$, $2 < \kappa \le 3$, $4 < \delta \le 5$ for fractional spatial numerical solution, that is,

$$\frac{\partial^\alpha u}{\partial t^\alpha} + u\frac{\partial^\beta u}{\partial x^\beta} + \frac{\partial^\kappa u}{\partial x^\kappa} - \frac{\partial^\delta u}{\partial x^\delta} = 0, \quad 0 < \alpha \le 1. \quad (40)$$

In this equation, for the fractional spatial solution, we only consider the first fractional derivative with order β for the sake of eliminating long calculations. Therefore, the first-order problem is turn out to be as follows.

First-order problem
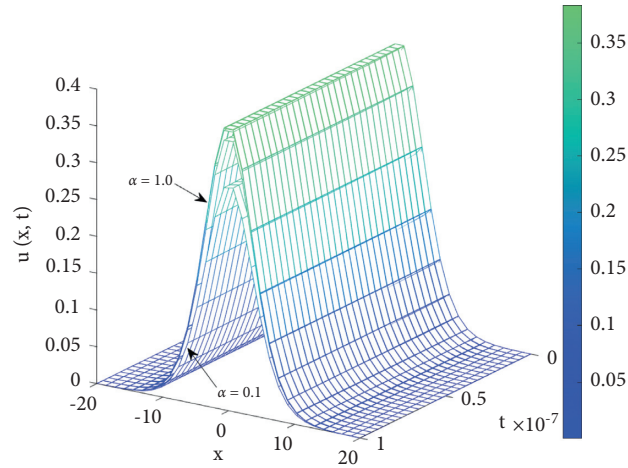
FIGURE 1: 3D fractional temporal numerical solution $u(x, t)$ for order $\alpha \in (0, 1]$, $\kappa = 4$, and $\delta = 5$.

$$u_1(x, t) = \frac{11025t^\alpha}{28561\Gamma(\alpha + 1)} \sec h^4\left(\frac{x}{2\sqrt{13}}\right) \frac{\partial^\beta}{\partial x^\beta} \sec h^4\left(\frac{x}{2\sqrt{13}}\right) + \frac{105t^\alpha}{169\Gamma(\alpha + 1)} \frac{\partial^3}{\partial x^3} \sec h^4\left(\frac{x}{2\sqrt{13}}\right)$$

$$- \frac{105t^\alpha}{169\Gamma(\alpha + 1)} \frac{\partial^5}{\partial x^5} \sec h^4\left(\frac{x}{2\sqrt{13}}\right) = 0,$$

(41)

implies that

$$u_1(x, t) = \frac{105t^\alpha}{169\Gamma(\alpha + 1)} \sec h^4\left(\frac{x}{2\sqrt{13}}\right)\left(\frac{5.93227042 \times 10^{-10}}{\Gamma(2 - \beta)}x^{(1-\beta)} + \frac{0.04779241642}{\Gamma(3 - \beta)}x^{(2-\beta)}\right.$$

$$\left. + \frac{1.104877850 \times 10^{-6}}{\Gamma(4 - \beta)}x^{(3-\beta)}\right) + \frac{735\sqrt{13}t^\alpha}{28561\Gamma(\alpha + 1)} \sec h\left(\frac{x\sqrt{13}}{26}\right)^4 \tanh\left(\frac{x\sqrt{13}}{26}\right)$$

$$\times \left(1 - \tanh\left(\frac{x\sqrt{13}}{26}\right)^2\right) - \frac{840\sqrt{13}t^\alpha}{28561\Gamma(\alpha + 1)} \sec h\left(\frac{x\sqrt{13}}{26}\right)^4 \tanh\left(\frac{x\sqrt{13}}{26}\right)^3$$

$$+ \frac{13755\sqrt{13}t^\alpha}{371293\Gamma(\alpha + 1)} \sec h\left(\frac{x\sqrt{13}}{26}\right)^4 \tanh\left(\frac{x\sqrt{13}}{26}\right)^3\left(1 - \tanh\left(\frac{x\sqrt{13}}{26}\right)^2\right)$$

$$- \frac{3360\sqrt{13}t^\alpha}{371293\Gamma(\alpha + 1)} \sec h\left(\frac{x\sqrt{13}}{26}\right)^4 \tanh\left(\frac{x\sqrt{13}}{26}\right)^5 - \frac{4935\sqrt{13}t^\alpha}{371293\Gamma(\alpha + 1)} \sec h\left(\frac{x\sqrt{13}}{26}\right)^4$$

$$\times \tanh\left(\frac{x\sqrt{13}}{26}\right)\left(1 - \tanh\left(\frac{x\sqrt{13}}{26}\right)^2\right)^2.$$

(42)

Hence, the solution at $p \longrightarrow 1$ becomes
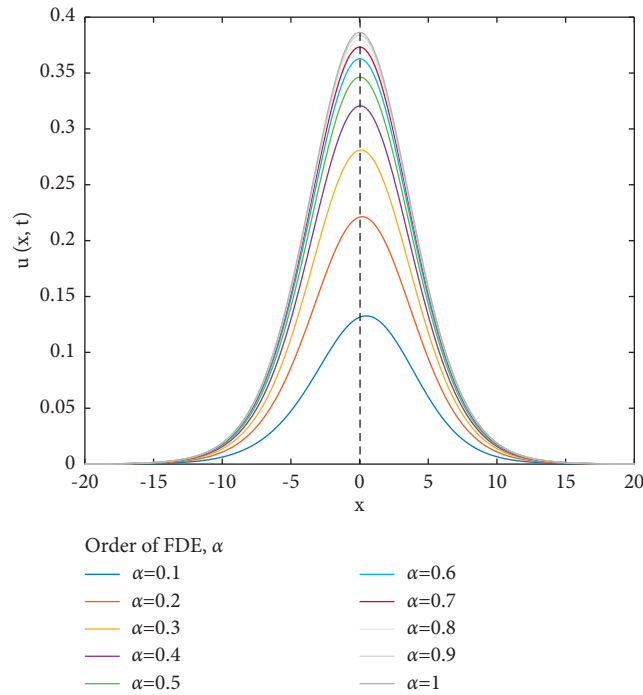
FIGURE 2: 2D fractional temporal numerical solution $u(x)$ for order $t = 0.01$, $\kappa = 4$, and $\delta = 5$.

$$u(x, t) = \sum_{i=0}^{\infty} u_i(x, t), \qquad (43)$$

which implies that

$$u(x, t) = u_0 + u_1(x, t) + u_2(x, t) + \cdots$$

$$u(x, t) = \frac{105}{169} \sec h^4\left(\frac{x}{2\sqrt{13}}\right) + \frac{105 t^\alpha}{169 \Gamma(\alpha + 1)} \sec h^4\left(\frac{x}{2\sqrt{13}}\right) \left(\frac{5.93227042 \times 10^{-10}}{\Gamma(2 - \beta)} x^{(1-\beta)}\right)$$

$$+ \frac{105 t^\alpha}{169 \Gamma(\alpha + 1)} \sec h^4\left(\frac{x}{2\sqrt{13}}\right) \left(\frac{0.04779241642}{\Gamma(3 - \beta)} x^{(2-\beta)} + \frac{1.104877850 \times 10^{-6}}{\Gamma(4 - \beta)} x^{(3-\beta)}\right)$$

$$+ \frac{735\sqrt{13} t^\alpha}{28561 \Gamma(\alpha + 1)} \sec h\left(\frac{x\sqrt{13}}{26}\right)^4 \tanh\left(\frac{x\sqrt{13}}{26}\right) \left(1 - \tanh\left(\frac{x\sqrt{13}}{26}\right)^2\right) - \frac{840\sqrt{13} t^\alpha}{28561 \Gamma(\alpha + 1)}$$

$$\times \sec h\left(\frac{x\sqrt{13}}{26}\right)^4 \tanh\left(\frac{x\sqrt{13}}{26}\right)^3 + \frac{13755\sqrt{13} t^\alpha}{371293 \Gamma(\alpha + 1)} \sec h\left(\frac{x\sqrt{13}}{26}\right)^4 \tanh\left(\frac{x\sqrt{13}}{26}\right)^3$$

$$\times \left(1 - \tanh\left(\frac{x\sqrt{13}}{26}\right)^2\right) - \frac{3360\sqrt{13} t^\alpha}{371293 \Gamma(\alpha + 1)} \sec h\left(\frac{x\sqrt{13}}{26}\right)^4 \tanh\left(\frac{x\sqrt{13}}{26}\right)^5$$

$$- \frac{4935\sqrt{13} t^\alpha}{371293 \Gamma(\alpha + 1)} \sec h\left(\frac{x\sqrt{13}}{26}\right)^4 \tanh\left(\frac{x\sqrt{13}}{26}\right) \left(1 - \tanh\left(\frac{x\sqrt{13}}{26}\right)^2\right)^2 + \cdots.$$

$$(44)$$

6. Results and Discussion

In Figure 1, we have plotted the temporal solution of the fractional-order Kawahara partial differential equation against position x and time t based on equation (35), for different fractional-order α, the plot shows that with α amplitude of the solitary wave potential increases while its width squeeze in size slightly. In Figure 2, we have the
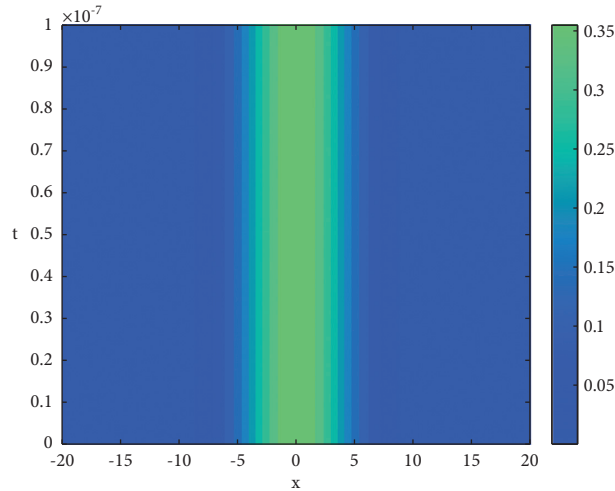
FIGURE 3: Contour of fractional temporal numerical solution $u(x)$ for order $\alpha = 0.6$, $\kappa = 4$, and $\delta = 5$.

Variations in time, t

—— $t=0$	—— $t=2.5$
—— $t=0.5$	—— $t=3$
—— $t=1$	—— $t=3.5$
—— $t=1.5$	—— $t=4$
—— $t=2$	—— $t=4.5$
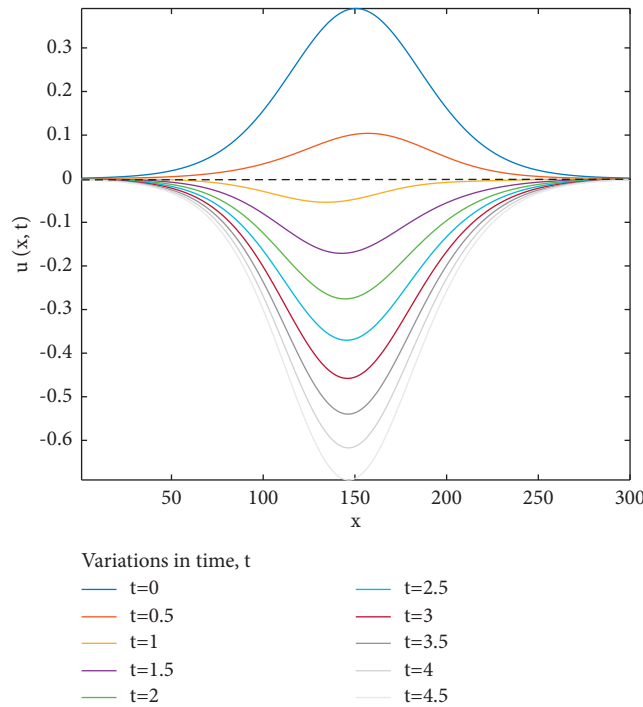
FIGURE 4: 2D fractional temporal numerical solution $u(x)$ for order $\alpha = 0.6$, $\kappa = 4$, and $\delta = 5$.

comparison of the solitary wave temporal solution $u(x)$ against x for $t = 0.01$ and with different fractional-order α; this simulation shows a more clear picture of amplitude and dispersion variation with α. Figure 3 is the contour plot of solitary wave propagation against x and t for order $\alpha = 0.6$. In Figure 4, the plot is among solitary wave propagation $u(x, t)$ against x and for different time t, which shows a very interesting situation of the solitary waves structure; while at the smaller time, we found a compressive type of solitary wave, but when we take the time t greater than 0.6, then we observe the refractive type of the solitary wave and that

waves increase its amplitude with time t and also its dispersion property.

In Figure 5, we have the 3D spatial numerical solution $u(x, t)$ of solitary wave propagation against x and t for differential spatial-order β based on equation (40); the simulation shows us that with spatial-order fluctuation, amplitude of the solitary wave change slightly, but the width of the solitary wave change dramatically in greater steps; likewise in Figure 6, we have shown the 2D cross-sectional wave of Figure 5 that demonstrates the amplitude and width of the solitary wave clearly with spatial-order β for $t = 0.01$.
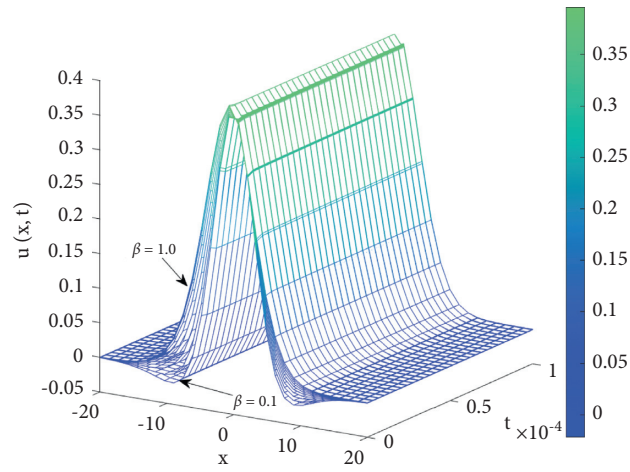
FIGURE 5: 3D fractional spatial numerical solution $u(x, t)$ at order $\beta \in (0, 1]$, $\kappa = 3$, $\delta = 5$.

Order of FDE, β

— $\beta = 0.1$ — $\beta = 0.6$
— $\beta = 0.2$ — $\beta = 0.7$
— $\beta = 0.3$ — $\beta = 0.8$
— $\beta = 0.4$ — $\beta = 0.9$
— $\beta = 0.5$ — $\beta = 1$
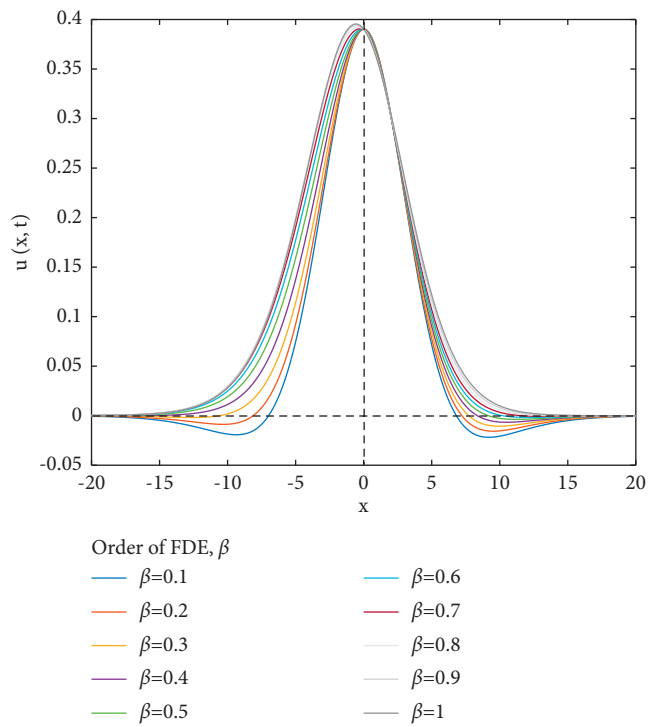
FIGURE 6: 2D fractional spatial numerical solution $u(x)$ at orders $\alpha = 0.9$, $\beta = 1$, $\kappa = 3$, $\delta = 5$, and time $t = 0.01$.
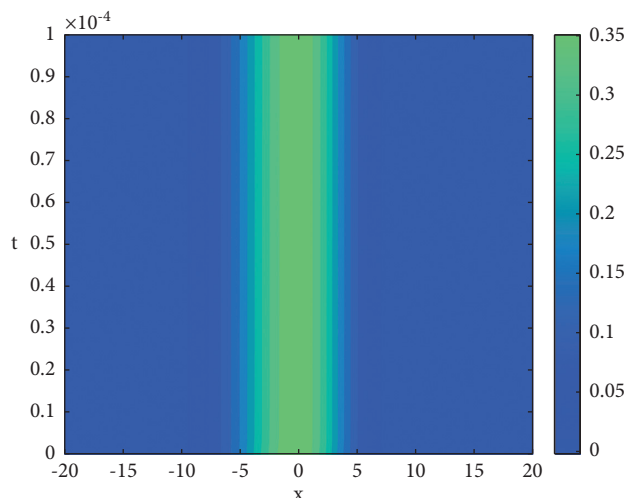
FIGURE 7: Contour of fractional spatial numerical solution $u(x, t)$ at orders $\alpha = \beta = 0.6$, $\kappa = 3$, $\delta = 5$.

Figure 7 is the contour plot of solitary wave spatial solution against x and t.

7. Conclusion

Upon the use of the homotopy perturbation method (HPM), we have investigated the Kawahara fractional-order partial differential equation of fifth-order under fractional order. By using Caputo derivative of fractional order separately on temporal and spatial bases, obtained the semianalytical solution for the Kawahara frictional-order differential equation. We have then stimulated various parametric effects (such as x, t, α, and β) on the structure of the solitary wave propagation that demonstrates that the width, as well as the amplitude of the solitary wave potential clearly, can change with the change of these parameters. We have shown through our calculation and simulation that He's technique is very useful and power full for the solution of such a higher-order nonlinear partial differential equation. We can extend our calculation to other complex problems especially to the applied side such as astrophysics, plasma physics, and quantum mechanics to solve a complex theoretical calculation by that technique.

Data Availability

The data used to support the findings of this study are included within the article.

Conflicts of Interest

The authors declare that they have no conflicts of interest.

Acknowledgments

References

[1] D. Kaya and K. Al-Khaled, "A numerical comparison of a Kawahara equation," *Physics Letters A*, vol. 363, no. 5-6, pp. 433–439, 2007.

[2] A. Dascioglu and S.Ç. Ünal, "New exact solutions for the space-time fractional Kawahara equation," *Applied Mathematical Modelling*, vol. 89, pp. 952–959, 2021.

[3] T. Özis and I. Aslan, "Application of the G'/G-expansion method to Kawahara type equations using symbolic computation," *Applied Mathematics and Computation*, vol. 216, no. 8, pp. 2360–2365, 2010.

[4] K. Muhammet, "Approximate analytic solutions of the modified Kawahara equation with homotopy analysis method," *Advances in Difference Equations*, vol. 2012, p. 178, 2012.

[5] T. Kawahara, "Oscillatory solitary waves in dispersive media," *Journal of the Physical Society of Japan*, vol. 33, no. 1, pp. 260–264, 1972.

[6] J.-H. He, "Homotopy perturbation technique," *Computer Methods in Applied Mechanics and Engineering*, vol. 178, no. 3-4, pp. 257–262, 1999.

[7] J.-H. He, "Comparison of homotopy perturbation method and homotopy analysis method," *Applied Mathematics and Computation*, vol. 156, no. 2, pp. 527–539, 2004.

[8] M. Sinan, "Analytic approximate solution of Rabies transmission dynamics using Homotopy perturbation method," *Matrix Science Mathematic*, vol. 4, no. 1, pp. 01–05, 2020.

[9] K. Oldham and J. Spanier, *The Fractional Calculus Theory and Applications of Differentiation and Integration to Arbitrary Order*, Academic Press, New York, NY, USA, 1974.

[10] K. S. Miller and B. Ross: An Introduction to the Fractional Calculus and Fractional Differential Equations.

[11] I. Podlubny, *Fractional Differential Equations*, Academic Press, San Diego, CA, USA, 1998.

[12] L. Debnath, "Recent applications of fractional calculus to science and engineering," *International Journal of Mathematics and Mathematical Sciences*, vol. 2003, pp. 753601–30, 2003.

[13] J. Lu, "Analytical approach to Kawahara equation using variational iteration method and homotopy perturbation method," *Topological Methods in Nonlinear Analysis*, vol. 31, no. 2, pp. 287–293, 2018.

[14] M. Stefan, "Traveling wave solutions to Kawahara and related equations," *Differential Equations and Dynamical Systems*, vol. 27, no. 1-3, pp. 19–37, 2019.

[15] A. Ali, M. Y. Khan, M. Sinan et al., "Theoretical and numerical analysis of novel COVID-19 via fractional order mathematical model," *Results in Physics*, vol. 20, p. 103676, 2021.

Research Article

Research on Population Development Trend in Huizhou of China Forecast Based on Optimal Weighted Combination Method and Fractional Grey Model

Dewang Li [iD],[1] **Jianbao Chen** [iD],[2] **and Meilan Qiu** [iD][1]

[1]*School of Mathematics and Statistics, Huizhou University, Huizhou 516007, China*
[2]*School of Mathematics and Statistics, Fujian Normal University, Fuzhou 350117, China*

Correspondence should be addressed to Jianbao Chen; jbchen@fjnu.edu.cn

In this paper, the optimal weighted combination model and fractional grey model are constructed. The coefficients of the optimal weighted combination model are determined by minimizing the sum of squares of resists of each model. On the other hand, the optimal conformable fractional order and dynamic background value coefficient are determined by the quantum inspired evolutionary algorithm (QIEA). Taking the resident population from 2008 to 2018 as the research object, the optimal weighted combination model and fractional grey model were used to study the estimated and predicted values. The results are compared and analyzed. The results show that the fractional grey model is better than the optimal weighted combination model in the estimation of the values. The optimal weighted combination model is better than the fractional grey model in predicting. Meanwhile, the fractional grey model is found to be very suitable for the data values that are large, and the changes between the data are relatively small. The research results expand the application of the fractional grey model and have important implications for the policy implementation activities of Huizhou government according to the population growth trend in Huizhou.

1. Introduction

With the massive urbanization of the population, population development is still an important issue in China. The current situation of population development is that the proportion of the population with young children is gradually decreasing, and the proportion of the elderly is gradually increasing [1]. Population scale is one of the main indicators of regional economic development, and the population problem is also the basic problem that people pay most attention to. Professor Zeng [2] has analyzed the past, present, and future of demography. Therefore, China has implemented a new birth policy. From the implementation of the "two-child" birth policy in 2013 to the implementation of the "two-child comprehensive" birth policy in 2015, new changes have taken place in population development. Before 2000, the foundation of population and Family Planning in Huizhou was not very good. Huizhou's population

reproduction is "high birth rate, low death rate, and high natural population growth rate." The birth rate and natural growth rate show a characteristic fluctuation trend. In 1979, the birth rate was as high as 26.68 per thousand, the death rate remained stable at around 5 per thousand, and the population grew rapidly [3]. In recent years, population development has become a new research hotspot.

The mathematical method of population forecast set the advantage of the statistical method and demography method [4]. In the seventeenth century, there were studies on population prediction abroad, and a series of population prediction methods were summarized. Fitting the population development trend, we can forecast the future population scale development trend according to the geometric progression growth. For example the retardation growth model sets the maximum population carrying capacity under certain environmental conditions. When the population growth reaches the limit, the population growth

rate is zero. The Leslie model uses the difference equation matrix to discuss the law of population change under the condition of stable development. One is to use statistical methods to build regression models and time series models for population forecasting. The other is the population prediction method, which uses birth, death, and migration data to explore population trends. For example, the cohort factor method sets parameters such as death, birth, and migration and structural change according to the input parameters of population size. Others are the BP neural network method which simulates the biological neural dynamic principle to predict the population with high precision.

In domestic population studies, professor Zha [5] proposed population projections with three possibilities. In the population prediction method, based on cybernetics, Professor Song et al. [6] introduced the birth rate, death rate, fertility rate, and other indicators to construct the population control partial differential equation of population prediction. In the short term forecast, Professor Deng [7] established a grey system to be used in population forecasting. He regarded the population system as a grey system based on model uncertainty and model mathematics, which could obtain more accurate prediction results without too much basic data.

Some Chinese scholars have explored the improvement methods based on the domestic and foreign population prediction models. Chen [8] established the progressive population development model of children's subclass age and made a new attempt to predict population based on demographic structure factors. Hao and Wang constructed a grey dynamic model of China's population development trend and verified the practicability of the grey model [9]. Zhai et al. [10] studied the application of the queuing factor method in population prediction software PADIS-INT and considered that the software has the characteristics of multiple functions, convenient input of parameters, strong applicability, and detailed results, which can be used for more detailed population prediction. Wang [11] derived the problem of progressive fertility parameters in the progressive child population prediction model in detail and proved the practicality of the progressive child population prediction model in population prediction. Wang [11] deduced in detail the problem of the progressive fertility parameters in the progressive child population prediction model and proved the practicability of the progressive child population prediction model in population prediction. To sum up, most of the literature is about the population situation of a country, a province, or a region, while there are few studies on the population development trend of second- and third-tier cities. The combined model can make up for the shortcomings of the single model and can absorb the advantages of the single model. Compared with single model, it has higher precision and predictive value and has higher precision. As far as we know, few scholars use the fractional grey model to study the population situation of prefecture-level cities. Based on this, this paper develops the research and obtains good results. The results of the fractional grey model and the optimal weighted combination model are compared and analyzed. At the same time, this research process is also the attempt to examine the seventh national Population Census Data and statistical yearbook data in Huizhou.

2. The Optimal Weighted Combination Model

To extract the most available information, various models are combined to improve the reliability of the prediction. The combination forecasting method is to combine different forecasting submodels into one model. Compared with the single forecasting model, the combined forecasting model is more specific, detailed, comprehensive, and scientific, which can reduce the influence of some random factors on the single forecasting model [12]. The most important part of combinatorial forecasting method is to obtain the coefficient of each submodel, that is, the combination weight coefficient. The estimation of weight coefficient includes optimal weight method, variance-covariance method, recursive variance method, and positive weight synthesis method. In this paper, the optimal weighting method is used. The optimal weighting method is realized by minimizing the total error of the combined prediction in a certain time. The objective function constructed according to a given criterion is minimized under a series of constraints to obtain the weight coefficient [13]. The construction of the objective function depends on the selection of error statistics and the type of minimization criteria.

Suppose $\{y_t\}(t = 1, 2, \ldots, n)$ for the original data sequence, the original data sequence is first built, and the individual m models are predicted, and the predicted value is $\{\hat{y}_{it}\}$, $i = 1, 2, \ldots, m$ and $t = 1, 2, \ldots, n$. And then, the individual m models are combined to calculate combined $K = (k_1, k_1, \ldots, k_m)^T$ combined to calculate combined . The model is the optimal weighted combination model when the statistical error of the model is the minimum, that is, $Q = \sum_{i=1}^{m} e_{it}^2$ the minimum [14]:

$$\begin{cases} \min & Q, \\ \text{s.t.} & \sum_{i=1}^{m} k_i = 1, \end{cases} \tag{1}$$

where Q is the objective function constructed by the model and s.t. is the constraint premise of the objective function. Turn it into a mathematical programming problem as follows:

$$\begin{cases} \min & Q = \sum_{i=1}^{m} e_{it}^2 = e^T e = K^T E K, \\ \text{s.t.} & \sum_{i=1}^{m} k_i = R^T K = 1. \end{cases} \tag{2}$$

In the formula, $R = [\ 1, \ 1, \ \ldots, \ 1\ ]^T$ is the matrix of $n \times 1$ and E is the matrix of estimated error information. Using the Lagrange multiplier formula, from

$$\frac{\partial}{\partial K}\left(K^T E K - 2\lambda\left(R^T K - 1\right)\right) = 0, \tag{3}$$

we obtain

$$EK - \lambda R = 0,$$
$$K = \lambda E^{-1} R. \tag{4}$$

At the same time, from

$$\frac{\mathrm{d}}{\mathrm{d}\lambda}\left(K^T E K - 2\lambda\left(R^T K - 1\right)\right) = 0, \tag{5}$$

we obtain

$$R^T K = 1,$$
$$R^T \lambda E^{-1} R = 1, \tag{6}$$
$$\lambda = \frac{1}{R^T E^{-1} R}.$$

Combining (4) and (6), the optimal weighted vector is solved:

$$K_0 = \frac{E^{-1} R}{R^T E^{-1} R}. \tag{7}$$

The minimum value of the objective function is as follows:

$$Q_0 = K_0^T E K_0 = \frac{1}{R^T E^{-1} R}. \tag{8}$$

3. The Fractional Grey Model

3.1. FGM (1, 1) Mode. The fractional grey model is firstly propounded by Wu et al. [15]; the results showed that compared with the traditional grey model, this model greatly improves the prediction accuracy. Zeng et al. proposed a self-adaptive intelligence grey prediction model with fractional accumulation [16]. Ma et al. proposed a novel definition of conformable fractional accumulation which is more feasible and simple compared with the traditional fractional grey model [17]. Wu et al. further perfected the definition of conformable fractional accumulation and successfully utilized it to predict carbon dioxide emissions of BRICS [18]. Wu et al. utilized a novel fractional nonlinear grey Bernoulli model to forecast short-term renewable energy consumption [19]. Ma et al. proposed a fractional delay grey model based on the grey system optimization algorithm and applied it to the prediction of natural gas consumption in Chongqing [20]. Wu et al. [18] applied the univariate inhomogeneous grey model to study the CO_2 emissions of BRICS countries without considering external factors. Under several error metrics, one can see that the grey forecasting model can provide excellent results for the five countries. Based on the definition of the conformable fractional derivative, Ma et al. [17] proposed conformable fractional accumulation and difference. Then, a novel conformable fractional grey model is proposed based on the fractional accumulation and difference, and the brute force method is introduced to optimize its fractional order.

Fractional grey models are divided into fractional accumulation and derivative grey models. The fractional accumulation generating operator (FAGO) can reflect the characteristics of new information priority and is a generalization of integer accumulation generation [15]. FAGO is extended from a GM (1, 1) to grey Bernoulli [21]. The new information priority principle is embodied in the FAGO grey Bernoulli model [22]. To solve the prediction problem with memory characteristics, based on the memory principle, Mao [23] proposed to improve the integral differential equation into a fractional differential equation and established a univariable fractional derivative grey prediction model. Kang [24] extended it to a Caputo-type multivariate fractional grey prediction model. Although some achievements have been made in grey prediction models, they all use first-order differential equations [25, 26] or constant fractional differential equations [23, 27].

Based on this theoretical knowledge, this paper expands a novel conformable fractional grey model and the optimal weighted combination model to estimate and predict the population of Huizhou of China. The main novelties of this paper can be outlined as follows. Firstly, the fractional grey model and the optimal weighted combination model are compared and analyzed in research of Huizhou's population. Secondly, the optimal conformable fractional order and dynamic background value coefficient are determined by Quantum Inspired Evolutionary Algorithm (QIEA) [28]. In order to verify the effectiveness of the two new models, the two models were compared with GM (1, 1) model, regression model, and growth model. Finally, the optimal weighted combination model and the fractional grey model are applied to predict the population of Huizhou of China from 2019 to 2021.

3.2. Modeling Process of FGM (1, 1).
(1) Construct an additive sequence of order r: Write the original nonnegative data as the original order column $U^{(0)} = \left\{u^{(0)}(1), u^{(0)}(2), \ldots, u^{(0)}(n)\right\}$. After calculation, the $r$order accumulation sequence $U^{(r)} = \left\{u^{(r)}(1), u^{(r)}(2), \ldots, u^{(r)}(n)\right\}$ is obtained where $u^{(k)}(r) = \sum_{i=1}^{k} C_{k-i+r-1}^{k-i} u^{(0)}(i)$, $C_{r-1}^0 = 1, C_k^{K+1} = 0, k = 0, 1, \ldots, n-1$,

$$C_{k-i+r-1}^{k-i} = \frac{(k-i+r-1)(k-i+r-2), \ldots, (r+1)r}{(k-i)!}. \tag{9}$$

(2) Set up the differential equation and solve it: Set up the whitening differential equation as follows:

$$\frac{\mathrm{d}x^{(r)}(t)}{\mathrm{d}t} + ax^{(r)}(t) = b. \tag{10}$$

Suppose $s^{(r)}(t) = 0.5[u^{(r)}(t) + u^{(r)}(t-1)]$, $w^{(r)}(k) = [u^{(r)}(t) - u^{(r)}(t-1)]$ $(t = 2, 3, \ldots, n)$. Then,

$$B = \begin{bmatrix} -s^{(r)}(2) & 1 \\ -s^{(r)}(3) & 1 \\ \vdots & \vdots \\ -s^{(r)}(n) & 1 \end{bmatrix},$$

$$D = \begin{bmatrix} w^{(r)}(2) \\ w^{(r)}(3) \\ \vdots \\ w^{(r)}(n) \end{bmatrix}. \tag{11}$$

Use the least square method to obtain the numerical solution of the parameters as follows:

$$\begin{bmatrix} \widehat{a} \\ \widehat{b} \end{bmatrix} = \left(B^T B \right)^{-1} B^T D. \tag{12}$$

The formal solution of equation (6) is

$$\widehat{u}^{(r)}(t+1) = \left(u^{(0)}(1) - \frac{\widehat{b}}{\widehat{a}} \right) e^{-\widehat{a}t} + \frac{\widehat{b}}{\widehat{a}}. \tag{13}$$

(3) Accumulation and subtraction of r-order sequence: Change $U^{(r)} = \left\{ \widehat{u}^{(r)}(1), \widehat{u}^{(r)}(2), \ldots, \widehat{u}^{(r)}(n), \ldots \right\}$ is accumulated for order 1-r and then accumulated and subtracted for order 1, which is

$$\alpha^{(r)}U^{(0)} = \left\{ \alpha^{(1)}\widehat{u}^{(1-r)}(1), \alpha^{(1)}\widehat{u}^{(1-r)}(2), \ldots, \right.$$
$$\left. \alpha^{(1)}\widehat{u}^{(1-r)}(n), \alpha^{(1)}\widehat{u}^{(1-r)}(n+1), \ldots \right\}. \tag{14}$$

Calculate the fitted value $\widehat{u}^{(0)}(1), \widehat{u}^{(0)}(2), \ldots, \widehat{u}^{(0)}(n)$ and the predicted value $\widehat{u}^{(0)}(n+1), \widehat{u}^{(0)}(n+2), \ldots$.

(4) Evaluation model: The mean absolute percentage error (MAPE) was used to evaluate the model:

$$\text{MAPE} = \frac{1}{n} \sum_{t=1}^{n} \left| \frac{(\widehat{u}_t - u_t)}{u_t} \right|. \tag{15}$$

(5) The optimal order r is selected to get the predicted sequence as follows:

$$\widehat{u}^{(0)}(n), \widehat{u}^{(0)}(n+1), \ldots, \widehat{u}^{(0)}(n+m). \tag{16}$$

(6) Error test: Perform residual test or correlation test or calibration error probability test for $\widehat{u}^{(0)}(1), \widehat{u}^{(0)}(2), \ldots, \widehat{u}^{(0)}(n)$, judge the fitting effect of the model according to the test result, and qualitatively analyze the prediction accuracy of the model; if the fitting accuracy is not ideal, the cumulative order can be adjusted r, that is, return to (1) until the accuracy reaches the ideal state.

4. Empirical Analysis of the Optimal Weighted Combination Model and FGM

4.1. Linear Regression Model. Since population prediction has certain assumptions and stable population theory is an important prerequisite, choosing a specific linear function or curve function to fit the historical data of population development has a certain impact on short-term population prediction, and the basic data required are less and easy to obtain. The data in this paper are from the statistical yearbook of Huizhou. The permanent resident population data of Huizhou from 2008 to 2018 are selected. The linear regression model is fitted, and SPSS is used for correlation analysis. The R^2 is 0.769, so the fitting error is not large.

The linear regression equation is as follows:

$$y = 432.41 + 5.21x. \tag{17}$$

The fitting Figure 1 is drawn. See Table 1 for the estimated values in 2008–2018.

4.2. GM (1, 1). On the basis of the fuzzy uncertainty in fuzzy mathematics, the population system is regarded as a grey system and its future development is predicted. The GM model was proposed by Professor Deng [7]. This paper selects the permanent population data of Huizhou from 2008 to 2018 to build an estimated model. Python software was used for modeling and testing. The posterior difference ratio of this model is 0.37535, which meets the requirement of level 2 accuracy (qualified), and the predicted result is in good fitting degree with the actual situation. The population development of Huizhou from 2019 to 2021 shows a linear trend of growth, which is consistent with the stable mortality rate and recently improved fertility rate of Huizhou. It shows the release of fertility potential energy in recent years due to the influence of policies and economy, and the population growth trend is shown in Figure 1. The estimated value of 2008–2018 is shown in Table 1.

4.3. Growth Model. The permanent resident population from 2008 to 2018 was selected from the data block, and the population growth estimation model was established. The model considered the needs of the block growth model based on the previous population growth rate to estimate the regional maximum population capacity and population growth rate, and then sample data were selected to fit the population development trend of Huizhou. In this paper, the growth model is established by using MATLAB software. The modeling steps are as follows:

(1) Establish a function file and import the growth function:

$$y = e^{\beta_0 + \beta_1 x}. \tag{18}$$

(2) Import population data.

(3) Select the least square method and fit function in MATLAB; then, the parameter estimation can be completed and the growth model can be obtained.

(4) The regression model is as follows:

$$y = e^{6.07 + 0.011x}. \tag{19}$$

From 2008 to 2018, Huizhou's population growth rate has been on the rise. The overall population shows an
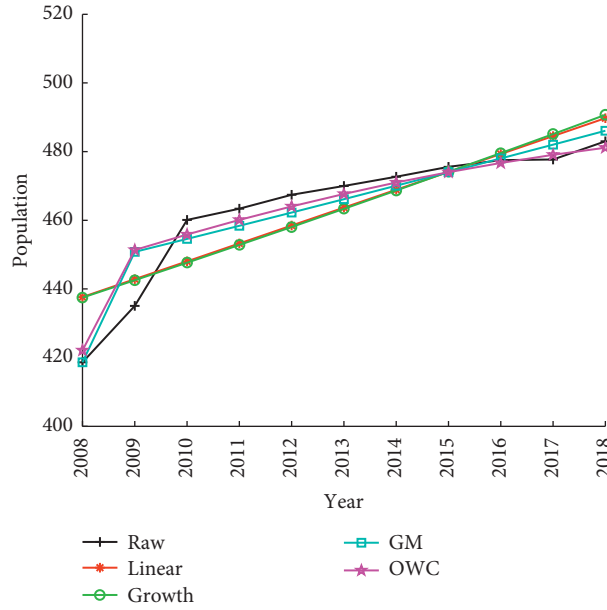
Figure 1: Huizhou population estimated results of various models.

Table 1: Estimated results of Huizhou population with various models, units: 10,000.

Year	Raw	Linear	Growth	GM	OWC	FGM	ARIMA	Logistic
2008	418.65	437.62	437.47	418.65	422.08	418.65	436.45	437.49
2009	435.08	442.83	442.53	450.79	451.32	436.79	432.32	442.75
2010	460.11	448.04	447.64	454.58	455.85	452.83	455.92	448.02
2011	463.36	453.25	452.81	458.40	460.09	462.62	472.40	453.28
2012	467.40	458.46	458.04	462.25	464.03	468.99	465.16	458.53
2013	470.00	463.67	463.33	466.14	467.66	473.19	464.59	463.77
2014	472.66	468.88	468.68	470.06	470.98	475.91	462.18	469.01
2015	475.55	474.09	474.09	474.01	473.99	477.55	470.63	474.23
2016	477.50	479.30	479.57	478.00	476.69	478.37	477.42	479.44
2017	477.70	484.51	485.10	482.02	479.06	478.54	484.94	484.64
2018	483.00	489.72	490.71	486.07	481.11	478.20	489.18	489.83
MAPE		1.70%	1.76%	1.03%	0.81%	0.56%	1.40%	1.69%

increasing trend, and the fertility potential energy is still in the release period. By 2021, the population growth tends to 5.0471 million. Draw the fitting Figure 1 is drawn. See Table 1 for the estimated values in 2008–2018.

4.4. Application of Optimal Weighted Combination (OWC) Model

(1) Construct the optimal weighted combination model:

$$
\begin{cases}
\min Q = \sum_{i=1}^{m} e_{it}^2 = e^T e = K^T E K \\
s.t. \sum_{i=1}^{m} k_i = R^T K = 1
\end{cases}
\tag{20}
$$

(2) Select an error statistic, i.e., fitting error, and calculate the error information matrix.

(3) According to the predicted and actual values of the above three submodels, the fitting error and the prediction error information matrix are calculated:

$$
E = \begin{bmatrix}
\sum_{t=1}^{n} e_{1t}^2 & \sum_{t=1}^{n} e_{1t} e_{2t} & \sum_{t=1}^{n} e_{1t} e_{3t} \\
\sum_{t=1}^{n} e_{2t} e_{1t} & \sum_{t=1}^{n} e_{2t}^2 & \sum_{t=1}^{n} e_{2t} e_{3t} \\
\sum_{t=1}^{n} e_{3t} e_{1t} & \sum_{t=1}^{n} e_{3t} e_{2t} & \sum_{t=1}^{n} e_{3t}^2
\end{bmatrix}
$$

$$
= \begin{bmatrix}
898.96 & 921.14 & 372.01 \\
921.14 & 945.40 & 381.45 \\
372.01 & 381.45 & 380.74
\end{bmatrix}.
\tag{21}
$$

(4) Calculate the weight of the model:

According to the Lagrange multiplier method, the weight coefficient is solved as follows:

$$K_0 = \frac{E^{-1}R}{R^T E^{-1} R} = \begin{bmatrix} 5.65 & 0.86 & -5.51 \end{bmatrix}^T. \quad (22)$$

Therefore, in the optimal weighted combination model, the weight coefficients of each combination are as follows: the linear regression model is 5.65, the grey prediction model is 0.86, and the growth model is −5.51. Therefore, the final prediction model is

$$Q_0 = 5.65\widehat{y}_1 + 0.86\widehat{y}_2 - 5.51\widehat{y}_3. \quad (23)$$

The prediction results are shown in Table 1.

4.5. FGM.
Construct the original sequence of population data in Huizhou from 2008 to 2018 (unit: ten thousand) $U^{(0)}$ = {418.65, 435.08, 460.11, 463.36, 467.40, 470.00, 472.66, 475.55, 477.50, 477.70, 483}. 0.9 order accumulation sequence is

$$U^{(0.9)} = \{418.65, 811.86, 1209.62, 1595.46, 1974.77, 2348.33, 2717.72, 3084.17, 3447.44, 3806.39, 4166.76\}. \quad (24)$$

Use the least square method to calculate the unknown parameters $\widehat{a}$ and $\widehat{b}$:

$$\begin{bmatrix} \widehat{a} \\ \widehat{b} \end{bmatrix} = (B^T B)^{-1} B^T D = \begin{pmatrix} 0.01743 \\ 402.16 \end{pmatrix}, \quad (25)$$

where

$$B^T = -\begin{bmatrix} 615.25 & 1010.74 & 1402.54 & 1785.12 & 2161.55 & 2533.03 & 2900.95 & 3265.81 & 3626.92 & 3986.58 \\ -1 & -1 & -1 & -1 & -1 & -1 & -1 & -1 & -1 & -1 \end{bmatrix},$$
$$D^T = \begin{bmatrix} 393.21 & 397.76 & 385.83 & 379.30 & 373.55 & 369.39 & 366.45 & 363.26 & 358.95 & 360.36 \end{bmatrix}. \quad (26)$$

Obtain the response function between time periods:

$$\widehat{u}^{(0.9)}(t+1) = \left(418.65 - \frac{40216}{1.1743}\right)e^{-0.01743t} + \frac{40216}{1.1743}. \quad (27)$$

The fitting value of order 0.9 additive sequence is

$$\widehat{U}^{(0.9)} = \left\{\widehat{u}^{(0.9)}(1), \widehat{u}^{(0.9)}(2), \ldots, \widehat{u}^{(0.9)}(11)\right\},$$
$$= 10^3 \times \{0.4187, 1.0651, 1.6384, 2.2019, 2.7556, 3.2997, 3.8344, 4.3599, 4.8763, 5.3838, 5.8826\}. \quad (28)$$

Restore order list as follows:

$$\widehat{U}^{(1)} = \left\{\widehat{u}^{(0.9)(0.1)}(1), \widehat{u}^{(0.9)(0.1)}(2), \ldots, \widehat{u}^{(0.9)(0.1)}(10), \widehat{u}^{(0.9)(0.1)}(11),$$
$$= \{418.65, 855.44, 1308.27, 1770.89, 2239.88, 2713.07, 3188.98, 3666.53, 5101.81, 5580.01\}. \quad (29)$$

The simulated value of Huizhou population is

$$\widehat{U}^{(0)} = \left\{\widehat{u}^{(0)}(1), \widehat{u}^{(0)}(2), \ldots, \widehat{u}^{(0)}(10), \widehat{u}^{(0)}(11),$$
$$= \{418.65, 436.79, 452.83, 462.62, 468.99, 473.19, 475.91, 477.55, 478.37, 478.54, 478.20\}. \quad (30)$$

Taking the minimum average absolute percentage error value of the FGM (1, 1) model as the object function and using the particle swarm optimization algorithm, the prediction effect of the FGM (1, 1) model is the best when the order r is 0.9, and the prediction result is more accurate. Python software is used to complete the above estimation and simulation. The estimated values with fractional grey model are shown in Figure 2.

As can be seen from Figure 1, the optimal weighted combination model balances the characteristics of higher predicted value of the growth model, strong linear trend and rapid growth of the regression model's forecast curve, and the GM (1, 1) model has a high degree of agreement with the prediction curve of the optimal weighted combination method. The estimated curves of the optimal weighted combination model are closer to the truth than those of the three submodels. It can be seen from Figure 1 that the truth estimation of the optimal weighted combination model is better than the modification of the three submodels. The value of MAPE in Table 1 can also draw OWC superior to its submodels. The optimal weighted group method predicts that the permanent population of Huizhou will continue to grow and maintain a stable growth from 2019 to 2021. It can be seen that the population scale development trend of Huizhou in the next decade is as follows: under the influence of the national fertility policy reform, the fertility level of Huizhou has been improved, and the permanent resident population of Huizhou will gradually rise in the next decade. By 2021, the total population of Huizhou will reach 5029000, with an average annual growth of 1.49% and an average annual growth of 72633. The predicted population values for 2019–2021 are shown in Table 2. Figure 2 shows that FGM estimates the raw data better than OWC. Most points on the FGM curve are closer to the true value than those on the OWC curve. These can be indirectly reflected from the values of MAE and RMSE in Table 2. Figure 2 shows that the fractional grey model has a better fitting effect on the truth value than that of the optimal combination model.

From Table 1, we also get MAPE = 0.56% of the fractional cumulative grey model, which is smaller than that of the other three methods. The MAPE value of model OWC is smaller than that of its three submodels. At the same time, the MAPE value of OWC is smaller than that of ARIMA model and logistic model.

4.6. Model Test. Seen the values of MAPE from Table 1, the optimal weighted combination model is superior to each submodel. However, the estimation result of the fractional grey prediction model is better than that of the optimal weighted combination model. To further compare the estimated results of these two models, we apply the mean absolute error and root mean square error to measure them.

Mean absolute error (MAE) is as follows:

$$\text{MAE} = \frac{1}{N} \sum_{t=1}^{n} |(\hat{y}_t - y_t)|. \tag{31}$$

Root mean square error (RMSE) is as follows:
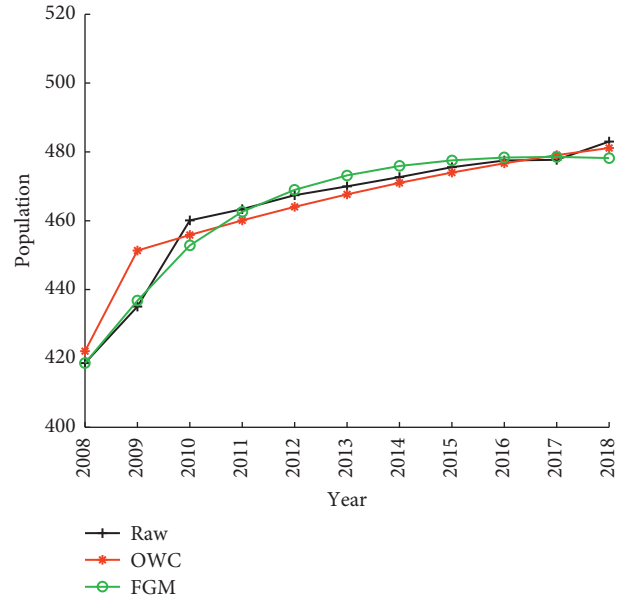
FIGURE 2: Comparison graph of Huizhou population development trend estimated by the optimal weighted group model and the fractional grey model.

TABLE 2: Test results of the prediction model.

Year	OWC	FGM	ARIMA	Logistic
2019	497.42	477.43	499.21	494.99
2020	500.31	476.31	512.83	500.14
2021	502.90	474.90	520.77	505.27
MAE	4.1334	2.3882	6.7958	7.6208
RMSE	5.9247	3.1369	8.2047	8.8579

$$\text{RMSE} = \sqrt{\frac{1}{N} \sum_{t=1}^{n} (\hat{y}_t - y_t)^2}, \tag{32}$$

where N is the total number of years, y_t is the real value, and $\hat{y}_t$ is the estimated value.

Table 2 shows that the MAE of the OWC model is 4.1334, and the MAPE is 5.9247, and the MAE of FGM is 2.3882, and RMSE is 3.1369. We add ARIMA and logistic to estimate and forecast the original data and find that MAE and RMSE values of these two methods are larger than those of OWC and FGM. The results show that the prediction effect of the optimal weighted combination model is obviously poor than that of the fractional grey model. However, when it comes to predicting trends, the optimal weighting combination is clearly stronger than that of the fractional grey model. The population of Huizhou has been increasing steadily in recent years. From the perspective of stability, when the sample size is small, the fractional grey model is relatively stable.

5. Conclusions and Suggestions

The present situation of population development in Huizhou city is analyzed qualitatively and quantitatively. Then, we

adopted a series of mathematical methods, i.e., the fractional grey model, the optimal weighted combination method, the linear regression model, the growth model, and the GM (1, 1) prediction model, combined with MATLAB and Python to forecast the population development trend of Huizhou and analyzed the predicted results. We can obtain that the total population development trend of Huizhou is increasing year by year from 2019 to 2021. It will break through 5 million population marks around the end of 2021. In the estimation and prediction of Huizhou population, the optimal combination model and the fractional grey model have their advantages. In the next decade, the population of Huizhou will increase steadily, the population growth rate will be slower over time, but there will be no downward trend. According to the above conclusions, we proposed the following two suggestions: on the one hand, we will continue to implement the national three-child policy, increase subsidies for family planning, and raise the fertility level; on the other hand, measures should be taken to combine family care with social care to ensure that the elderly can rely on others for retirement and support.

In this paper, we combine the optimal weighted combination method and the fractional grey model to implement the prediction of the total population development trend of Huizhou in three years and analyze the results in depth. The forecast results show that the total population of Huizhou city will increase year by year from 2019 to 2021, and the labor supply is relatively sufficient in a demographic dividend period. However, it will soon enter a small and aging population, which is not conducive to this sustainable development. Therefore, we must pay attention to the population planning of Huizhou and turn the population advantage into the capital advantage in a period of demographic dividend. At the same time, we will raise the fertility rate and improve the old-age security system. Our future work is to study the population of Huizhou with the novel conformable fractional nonhomogeneous grey model and nonhomogenous discrete grey model with fractional-order accumulation.

Data Availability

The data used to support the findings of this study are included within the article.

Conflicts of Interest

The authors declare that they have no conflicts of interest.

Acknowledgments

References

[1] X. M. Ni, X. X. Shen, S. Hung, and J. Y. Zhang, "The convergence trend of the age structure and the aging population in China," *Journal of Applied Sport Management*, vol. 39, no. 2, pp. 191–205, 2020.

[2] Y. Zeng, "Past, present and future of demography," *Population Research*, vol. 33, no. 5, pp. 8–22, 2009.

[3] M. .Z. Luo, C. H. Gan, X. W. Huang, and W. L. Zhou, "Shift from government paradigm to governance paradigm: a case analysis of the comprehensive reform in family planning in Huizhou," *South China Population*, vol. 26, no. 2, pp. 13–19, 2011.

[4] J. Song, "Inheritance and evolution of demographic methods: and on the development of demography in China," *Population & Economics*, vol. 1, pp. 1–14, 2020.

[5] R. C. Zha, "Several basic problems of population prediction," *Population Research*, vol. 2, pp. 25–32, 1980.

[6] J. Song, J. Y. Yu, and D. Y. Kong, "Population control theory," *China Soft Science*, vol. 1, pp. 1–7, 1989.

[7] J. L. Deng, "Gray control system," *Journal of Central China Institute of Technology*, vol. 3, pp. 9–18, 1982.

[8] Y. H. Chen, "Child age progressive population development model," *China Population Science*, vol. 6, pp. 29–34, 1994.

[9] Y. H. Hao and X. M. Wang, "The dynamic model of gray system and its application to population forecasting," *Mathematics in Practice and Theory*, vol. 5, pp. 813–820, 2002.

[10] Z. W. Zhai, L. Li, J. J. Chen, and W. Chen, "Applications of population projection in the PADIS-INT: comparative study on MORTPAK," *Spectrum and PADIS-INT, Population Research*, vol. 41, no. 6, pp. 84–97, 2017.

[11] G. Z. Wang, "China's population forecast methods and future population policies," *Financial Minds*, vol. 3, no. 3, pp. 112–138, 2018.

[12] Y. Shang and Y. M. Ding, "Evaluation and analysis of optimal combination forecasting methods," *Statistics & Decisions*, vol. 17, pp. 122-123, 2005.

[13] K. Y. Mao, *Determination and Application of Weight in Combination Forecasting*, pp. 9–16, Chengdu University of Technology, Sichuan, China, 2007.

[14] X. W. Tang, "Optimal combination forecasting method and its application," *Journal of Applied Sport Management*, vol. 1, pp. 31–35, 1992.

[15] L. Wu, S. Liu, L. Yao, S. Yan, and D. Liu, "Grey system model with the fractional order accumulation," *Communications in Nonlinear Science and Numerical Simulation*, vol. 18, no. 7, pp. 1775–1785, 2013.

[16] B. Zeng and S. Liu, "A self-adaptive intelligence gray prediction model with the optimal fractional order accumulating operator and its application," *Mathematical Methods in the Applied Sciences*, vol. 40, no. 18, pp. 7843–7857, 2017.

[17] X. Ma, W. Wu, B. Zeng, Y. Wang, and X. Wu, "The conformable fractional grey system model," *ISA Transactions*, vol. 96, pp. 255–271, 2020.

[18] W. Wu, X. Ma, Y. Zhang, W Li, and Y Wang, "A novel conformable fractional non-homogeneous grey model for forecasting carbon dioxide emissions of BRICS countries," *The Science of the Total Environment*, vol. 707, Article ID 135447, 2020.

[19] W. Wu, X. Ma, B. Zeng, Y. Wang, and W. Cai, "Forecasting short-term renewable energy consumption of China using a novel fractional nonlinear grey Bernoulli model," *Renewable Energy*, vol. 140, pp. 70–87, 2019.

[20] X. Ma, X. Mei, W. Wu, X. Wu, and B. Zeng, "A novel fractional time delayed grey model with Grey Wolf Optimizer and its applications in forecasting the natural gas and coal consumption in Chongqing China," *Energy*, vol. 178, pp. 487–507, 2019.

[21] Q. Xiao, M. Shan, M. Gao, X. Xiao, and M. Goh, "Parameter optimization for nonlinear grey Bernoulli model on biomass energy consumption prediction," *Applied Soft Computing*, vol. 95, Article ID 106538, 2020.

[22] Y. Zhang, S. Mao, and Y. Kang, "A clean energy forecasting model based on artificial intelligence and fractional derivative grey Bernoulli models," *Grey Systems: Theory and Application (ahead-of-print)*, vol. 11, no. 4, pp. 571–595, 2021.

[23] S. H. Mao, M. Y. Gao, X. P. Xiao, and M. Zhu, "A novel fractional grey system model and its application," *Applied Mathematical Modelling*, vol. 40, no. 7-8, pp. 5063–5076, 2016.

[24] Y. X. Kang, S. .H. Mao, and Y. H. Zhang, "Fractional derivative multivariable grey model for nonstationary sequence and its application," *Journal of Systems Engineering and Electronics*, vol. 31, no. 5, pp. 1011–1020, 2020.

[25] H. Duan, X. Xiao, J. Long, and Y. Liu, "Tensor alternating least squares grey model and its application to short-term traffic flows," *Applied Soft Computing*, vol. 89, Article ID 106145, 2020.

[26] S. Mao, M. Zhu, X. Wang, and X. Xiao, "Grey-Lotka-Volterra model for the competition and cooperation between third-party online payment systems and online banking in China," *Applied Soft Computing*, vol. 95, Article ID 106501, 2020.

[27] Y. Zhang, S. Mao, Y. Kang, and J. Wen, "Fractal derivative fractional grey Riccati model and its application," *Chaos, Solitons & Fractals*, vol. 145, Article ID 110778, 2021.

[28] K. Kuk-Hyun Han and J. Jong-Hwan Kim, "Quantum-inspired evolutionary algorithm for a class of combinatorial optimization," *IEEE Transactions on Evolutionary Computation*, vol. 6, no. 6, pp. 580–593, 2002.

Research Article

On a Memristor-Based Hyperchaotic Circuit in the Context of Nonlocal and Nonsingular Kernel Fractional Operator

Shahram Rezapour [ID],[1,2] **Chernet Tuge Deressa** [ID],[3] **and Sina Etemad** [ID][1]

[1]*Department of Mathematics, Azarbaijan Shahid Madani University, Tabriz, Iran*
[2]*Department of Medical Research, China Medical University Hospital, China Medical University, Taichung, Taiwan*
[3]*College of Natural Sciences, Department of Mathematics, Jimma University, Jimma, Ethiopia*

Correspondence should be addressed to Chernet Tuge Deressa; chernet.deressa@ju.edu.et

Memristor is a nonlinear and memory element that has a future of replacing resistors for nonlinear circuit computation. It exhibits complex properties such as chaos and hyperchaos. A five-dimensional memristor-based circuit in the context of a nonlocal and nonsingular fractional derivative is considered for analysis. The Banach fixed point theorem and contraction principle are utilized to verify the existence and uniqueness of the solution of the five-dimensional system. A numerical method developed by Toufik and Atangana is used to get approximate solutions of the system. Local stability analysis is examined using the Matignon fractional-order stability criteria, and it is shown that the trivial equilibrium point is unstable. The Lyapunov exponents for different fractional orders exposed that the nature of the five-dimensional fractional-order system is hyperchaotic. Bifurcation diagrams are obtained by varying the fractional order and two of the parameters in the model. It is shown using phase-space portraits and time-series orbit figures that the system is sensitive to derivative order change, parameter change, and small initial condition change. Master-slave synchronization of the hyperchaotic system was established, the error analysis was made, and the simulation results of the synchronized systems revealed a strong correlation among themselves.

1. Introduction

In the last decade, fractional differential equations started gaining much attention in modeling several real-world problems in different areas including in mathematical epidemiology, physics, engineering, and many others. Fractional-order operators are either with singular kernels such as the Caputo derivative and the Reimann–Liouville fractional derivatives or with nonsingular kernels such as the Caputo–Fabrizio and Atangana–Baleanu fractional derivatives [1–4].

One of the differences between integer- and fractional-order derivatives is that the integer-order derivative describes local properties of a certain dynamic system, whereas the fractional-order derivative representation of a dynamic system involves the whole space of the process [5]. That is, applying fractional derivative orders in modeling real-world

problems is essential for describing the hereditary specifications and effectiveness of the memory as essential aspects of different mechanisms in the problem [6, 7].

The recent increase in the study of different dynamical systems using fractional-order derivatives is attributed to the fact that most of the dynamic systems associated with complex systems are found to be nonlocal involving long memory in time and intrinsically fractional derivative operators can describe such systems more accurately than the integer derivatives [8]. In other words, important features of many physical systems are best described or exposed by using fractional-order operators.

There are different studies conducted using fractional derivatives for diverse types of systems pertinenet to different problems. For instance, stability analysis of fractional differential equations with unknown parameters was considered using the D-decomposition method by Koksal [9].

Time- and frequency-domain response of the RLC circuit with fractional-order derivative was investigated in [10]. Telegraph equation used for the power transmission line with a nonlocal boundary value problem was deliberated with a different type of finite difference numerical schemes in [11].

Chaos theory has attracted many researchers and has applications in the fields of encryption and secure of communication [12], modeling financial systems, representing circuit diagrams, and many others [13, 14].

Nowadays, there are many pieces of literature dedicated to the analysis of chaotic systems using fractional derivative operators. This includes chaotic systems of Chua's electrical circuits and memristor-based circuit systems. Some of the literature are reviewed as follows.

Sene applied the Caputo fractional derivative operator in detecting the chaotic behavior of different 3D and 4D chaotic systems. He used Lyapunov exponent and bifurcation diagrams to identify the nature of the chaos and impact of parameter variation for the different chaotic models investigated [15–18]. Different chaotic systems including Chua's electric circuit and several other chaotic systems were analyzed using fractional derivative order mathematical models by Petráš [19]. Bifurcation and chaotic behaviors in fractional-order simplified Lorenz system using Adams–Bashforth–Moulton predictor-corrector scheme were considered in [20]. Atangana–Baleanu fractional derivative operators were used for modeling and analysis of different chaotic and hyperchaotic systems, and solutions were approximated using a two-step Adams–Bashforth numerical scheme in [21].

It was in 1971 that circuit theorist Chua proposed memristor as a missing two-terminal nonlinear electrical component. The three basic components of a circuit are resistor, capacitor, and inductor. Memristor known for its memory effect and nonlinear characteristics is the fourth circuit component. Memristor relates magnetic flux and electric charge linkage in which case it is called a charge-controlled electric model ($\phi = \phi(q)$) or it models a relationship between charges and flux ($q = q(\phi)$) in which case it is called a flux-controlled model [12, 22].

At present, there are several studies conducted on memristor-based chaotic circuits using both integer and fractional-order derivatives. In [23], a conformal fractional-order simplest memristor-based chaotic circuit was investigated based on conformable Adomian decomposition method, Lyapunov exponent, bifurcation diagram, and Poincaré' sections. Buscarino et al. introduced a chaotic circuit based on a realistic model of the HP memristor, and numerical results showed a generation of chaotic attractors [22]. A novel 5D chaotic system with flux-controlled memristor and integer-order derivative, extracted from Wang's 4D hyperchaotic system, was proposed by Wang et al. [24]. A memristor-based chaotic circuit modified by replacing the nonlinear resistor in Chua's circuit with a flux-controlled memristor was analyzed in [12].

This research aims to study the memory effect properties and detection of chaos in a five-dimensional memristor-based system. Accordingly, an integer model

memristor-based circuit is represented by Atangana–Baleanu fractional derivatives in the Caputo sense (ABC), and the existence and uniqueness of solution of the ABC fractional model are analyzed based on Banach fixed point theorem for contraction principle. From the different concepts of fractional-order operators introduced above, the purpose of choosing the ABC fractional derivative is due to the fact that it possesses nonlocal kernels and of course it allows the inclusion of traditional initial conditions in the formulation of a mathematical model. Numerical approximation of the ABC fractional model is made using the newly developed numerical approximation for fractional derivative developed by Toufik and Atangana in [25]. Local stability of the fractional model representation is accomplished using the Matignon stability criterion. The existence and nature of chaos in the fractional model are investigated using Lyapunov exponents. A bifurcation diagram for different fractional derivatives and parameter variation is given. Several phase portraits are depicted as a verification for the impact of different parameter values and different fractional derivative orders. The impact of initial conditions on the solution trajectory of the system is also investigated using simulation of the trajectories of the system for different initial conditions. Lastly, master-slave synchronization of the system is performed accompanied by the corresponding error analysis and simulation of several cases of the synchronized system. All the phase portraits and solution trajectories in this work were obtained from the numerical scheme of Toufik and Atangana adapted for the memristor chaotic model considered in this work. A computing software application called Matlab 2019a is used for the simulation of different results.

A Matlab code for Lyapunov exponents and bifurcation diagram of fractional-order systems called Danca algorithm [26] is used to quantify the chaos by calculating Lyapunov exponents and obtaining bifurcation diagrams for different fractional orders and different parameter values of the model. Some of the evidence for the originality of this work includes the application of Atangana–Baleanu fractional operator to the memristor-based system considered in this study, application of the newly developed numerical approximation by Toufik and Atangana for the fractional-order systems, obtaining the phase portraits of the system from the numerical scheme, and performing synchronization of the five-dimensional system using the numerical approximation.

The remaining part of this paper is arranged as follows. In Section 2, the memristor-based circuit model considered in this study is described in the context of integer derivative. Section 3 is devoted to the fractional derivative representation of the memristor-based systems following some recapping of preliminary concepts and definitions of Atangana–Baleanu fractional derivatives. The existence and uniqueness of the solution for the fractional derivative representation of the model are portrayed in Section 4 of the paper. The numerical scheme applied to get all the phase portraits and approximate time-series solution of the memristor-based system are developed in Section 5. Section 6 is concerned with the local stability analysis of the

fractional model followed by Lyapunov exponents, bifurcation diagrams with different fractional orders, and parameter variation in Section 7. Investigation of the impact of small change in the initial conditions on the dynamics of the system is considered in Section 8 followed by synchronization of the hyperchaotic system in Section 9. Finally, in Section 10, conclusions are given followed by list of references.

2. Mathematical Model Description of Memristor-Based Circuit

Wang et al. [27] developed a new four-dimensional hyperchaotic circuit system using an improved modularized design and proposed implementation of the circuit. The hyperchaotic circuit system mentioned in [24] is described under an integer-order system of differential equations. Later on, Wang et al. [24] proposed a five-dimensional flux-controlled memristor-based circuit system and demonstrated that the system exhibits hyperchaotic character under an integer-order system of differential equations. The five-dimensional nondimensionalized flux-controlled memristor-based circuit developed by Wang et al. is described using integer-order differential as given in the following equation:

$$
\begin{aligned}
\frac{\mathrm{d}x}{\mathrm{d}t} &= \beta_1 (y - x) + 4yz - 0.02x(t)W(u), \\[4pt]
\frac{\mathrm{d}y}{\mathrm{d}t} &= -x + 16y - xz + w, \\[4pt]
\frac{\mathrm{d}z}{\mathrm{d}t} &= -\beta_2 z + xy - xu - yw, \\[4pt]
\frac{\mathrm{d}w}{\mathrm{d}t} &= -10y + 0.15xz - 0.3zu, \\[4pt]
\frac{\mathrm{d}u}{\mathrm{d}t} &= -x,
\end{aligned}
\tag{1}
$$

where the memductance used in this study is

$$
W(u) = a + 3bu^2, \quad a > 0, b > 0. \tag{2}
$$

In this study, motivated by the contribution of Wang et al. [24] in developing the five-dimensional memristor-based circuit, we analyzed system (1) under ABC fractional derivatives.

3. Fractional Derivative Representation of the Model

In this section, we recall the definitions and basic properties of nonsingular and nonlocal Atangana–Baleanu fractional derivative of Caputo type (ABC) used for our analysis of the circuit.

Definition 1. Let $f \in C^1(a,b), a < b$, and let $q \in [0,1]$. The AB fractional derivative of order q is defined as [7, 28, 29]

$$
{}^{\mathrm{ABC}}_{a}D^q_t f(t) = \frac{F(q)}{1-q} \int_a^t \frac{\mathrm{d}f}{\mathrm{d}k} E_q\left[-\frac{q}{1-q}(t-k)^q \right] \mathrm{d}k, \tag{3}
$$

where $F(q) = 1 - q - q/\Gamma(q)$ and the Mittag-Leffler function is

$$
E_q[z] = \sum_{\beta=0}^{\infty} \frac{z^\beta}{\Gamma(1 + q\beta)}, \quad q, z \in \mathbb{C}, \Re(q) > 0. \tag{4}
$$

Definition 2. The Atangana–Baleanu (AB) fractional integral of the function $f \in C^1(a,b), a < b$, is given by [7, 28, 29]

$$
{}^{\mathrm{AB}}_{a}I^q_t f(t) = \frac{1-q}{F(q)} f(t) + \frac{q}{F(q)\Gamma(q)} \int_a^t f(k)(t-k)^{q-1} \mathrm{d}k. \tag{5}
$$

Lemma 1. *The AB fractional derivative and AB fractional integral of $f \in C^1(a,b), a < b$, fulfill [30]*

$$
{}^{\mathrm{AB}}_{a}I^q_t \left({}^{\mathrm{ABC}}_{a}D^q_t f(t) \right) = f(t) - f(a). \tag{6}
$$

Lemma 2. *For $f, g \in C^1(a,b), b > a$, the AB fractional derivative in the Caputo sense satisfies the Lipschitz condition [29]:*

$$
\left\| {}^{\mathrm{AB}}_{a}D^q_t f(t) - {}^{\mathrm{AB}}_{a}D^q_t g(t) \right\| \le \Lambda \| f(t) - g(t) \|. \tag{7}
$$

Now we continue with the reformulation of (1) in terms of ABC fractional derivatives.

Lemma 3. *Let $G(t) \in H^1(a,b)$. Then, ${}^{\mathrm{ABC}}_{0}D^q_t(f(t)) = G(t), f(0) = G_0$, admits one solution given by*

$$
f(t) = G_0 + \frac{1-q}{F(q)} G(t) + \frac{q}{F(q)\Gamma(q)} \int_0^t (t-k)^{q-1} G(k) \mathrm{d}k. \tag{8}
$$

We can describe the result in Lemma 3 in the form of the Banach fixed theorem point as follows. We begin by defining a Banach space

$$
X = \{ x \in C(J, \mathbb{R}), J = [0,1] \}, \tag{9}
$$

with a norm defined as $\|x\|_x = \mathrm{Sup}_{t \in J} |x(t)|$.

Now define the operators $M_1, M_2, M_3, M_4, M_5 : X \longrightarrow X$ by

$$M_1 x(t) = x_0 + \frac{1-q}{F(q)} \left(\beta_1 (y(t) - x(t)) + 4y(t)z(t) - 0.02x(t)W(u(t)) \right)$$

$$+ \frac{q}{F(q)\Gamma(q)} \int_0^t (t-k)^{q-1} \left(\beta_1 (y - x) + 4yz - 0.02x(t)W(u(k)) \right) \mathrm{d}k, \tag{10}$$

$$M_2 y(t) = y_0 + \frac{1-q}{F(q)} \left(-x(t) + 16y(t) - x(t)z(t) + w(t) \right)$$

$$+ \frac{q}{F(q)\Gamma(q)} \int_0^t (t-k)^{\alpha-1} \left(-x(k) + 16y(k) - x(k)z(k) + w(k) \right) \mathrm{d}k, \tag{11}$$

$$M_3 z(t) = z_0 + \frac{1-q}{F(q)} \left(-\beta_2 z(t) + x(t)y(t) - x(t)u(t) - y(t)w(t) \right)$$

$$+ \frac{q}{F(q)\Gamma(q)} \int_0^t (t-k)^{q-1} \left(-\beta_2 z(k) + x(k)y(k) - x(k)u(k) - y(k)w(k) \right) \mathrm{d}k, \tag{12}$$

$$M_4 w(t) = w_0 + \frac{1-q}{F(q)} \left(-10y(t) + 0.15x(t)z(t) - 0.3z(t)u(t) \right)$$

$$+ \frac{q}{F(q)\Gamma(q)} \int_0^t (t-k)^{q-1} \left(-10y(k) + 0.15x(k)z(k) - 0.3z(k)u(k) \right) \mathrm{d}k, \tag{13}$$

$$M_5 u(t) = z_0 + \frac{1-q}{F(q)} \left(-x(t) \right) + \frac{q}{F(q)\Gamma(q)} \int_0^t (t-k)^{q-1} \left(-x(k) \right) \mathrm{d}k. \tag{14}$$

We are now ready to describe the dynamic equation for the memristor-based chaotic circuit given in (1) using ABC fractional derivative:

$$\begin{aligned}
{}_0^{\mathrm{ABC}}D_t^q x(t) &= \beta_1 (y - x) + 4yz - 0.02x(t)W(u), \\
{}_0^{\mathrm{ABC}}D_t^q y(t) &= -x + 16y - xz + w, \\
{}_0^{\mathrm{ABC}}D_t^q z(t) &= -\beta_2 z + xy - xu - yw, \\
{}_0^{\mathrm{ABC}}D_t^q w(t) &= -10y + 0.15xz - 0.3zu, \\
{}_0^{\mathrm{ABC}}D_t^q u(t) &= -x.
\end{aligned} \tag{15}$$

The initial condition is given as $(x(0), y(0), z(0), w(0), u(0)) = (x_0, y_0, z_0, w_0, u_0)$ and $W(u) = a + 3bu^2$.

4. Existence Theory on the Model

Here, the existence and uniqueness of the solution for the ABC model given in (15) are shown using Banach fixed point theorem for contraction mapping. The following two theorems are worth recalling before proceeding further.

Theorem 1. *Let Π be any nonempty closed subset of a Banach space X. Then, any contraction $M: \Pi \longrightarrow \Pi$ has a unique fixed point [31, 32].*

Theorem 2. *Assume that x, y, z, w, u are continuous functions satisfying the following conditions:*

(C1) There exist constants $k_1, k_2, k_3, k_4, k_5 > 0$ such that $|x(t)| < k_1, |y(t)| < k_2, |z(t)| < k_3, |w(t)| < k_4, |u(t)| < k_5$.

(C2) $(\Gamma(q)(1-q) + 1)(\beta_1 + 0.02|W|) < F(q)\Gamma(q)$, $16(1-q)\Gamma(q) + 16 < F(q)\Gamma(q)$, and $(\Gamma(q)(1-q) + 1)\beta_2 < F(q)\Gamma(q)$; then, the ABC fractional derivative system given by (15) has a unique solution in the region X.

Proof. Let us show that the operator M_1 defined in (10) is well defined in the sense that $M_1 x(t) \in \mathfrak{I}_r$ and ${}_0^{\mathrm{ABC}}D_t^q M_1 x(t)$ is continuous on $J = [0, 1]$, where

$$\mathfrak{I}_r = \{ B \in X, \|B\| \leq r, r \geq 0 \}, \tag{16}$$

for $(\beta_1 (k_2 + k_1) + 4k_2 k_3 + 0.02k_1 (a + 3bk_5^2))(\|x_0\|_X \ F(q)\Gamma(q) + \Gamma(q)(1-q) + 1)/F(q)\Gamma(q) < r$.

Now for any $x \in \mathfrak{I}_r$ and from (10), we have

$$
\begin{aligned}
\|M_1 x\| &= \|x_0\|_X + \frac{1-q}{F(q)} \sup_{t \in J} \left(\beta_1 \left(y(t) - x(t)\right) + 4y(t)z(t) - 0.02x(t)W(u(t))\right) \\
&\quad + \frac{q}{F(q)\Gamma(q)} \sup_{t \in J} \int_0^t (t-k)^{q-1} \left(\beta_1 (y-x) + 4yz - 0.02x(t)W(u(k))\right) \mathrm{d}k \\
&\leq \|x_0\| + \left(\left|\beta_1 (k_2 - k_1) + 4k_2 k_3 - 0.02 k_1 \left(a + 3bk_5^2\right)\right|\right) \left(\frac{1-q}{F(q)} + \frac{q}{F(q)\Gamma(q)} \sup_{t \in J} \int_0^t (t-k)^{q-1} \mathrm{d}k\right) \\
&\leq \left(\frac{\|x_0\| F(q)\Gamma(q) + \Gamma(q)(1-q) + 1}{F(q)\Gamma(q)}\right) \left(\beta_1 (k_2 + k_1) + 4k_2 k_3 + 0.02 k_1 \left(a + 3bk_5^2\right)\right) < r.
\end{aligned}
\tag{17}
$$

Consequently, we have $M_1 x(t) \in \mathfrak{I}_r$.

To show continuous differentiability on $J = [0,1]$ we proceed from ${}_0^{\mathrm{ABC}}D_t^q M_1 x(t) = {}_0^{\mathrm{ABC}}D_{t0}^{q\mathrm{AB}}I_t^q \ (\beta_1 (y-x) + 4yz - 0.02x(t)W(u))\beta_1 (y-x) + 4yz - 0.02x(t)W(u)$ which is continuous on $J = [0,1]$, and then we conclude that ${}_0^{\mathrm{ABC}}D_t^q M_1 x(t)$ is continuous on J; as a result, $M_1 \mathfrak{I}_r \subset \mathfrak{I}_r$.

To show that the operator M_1 has a fixed point based on Theorem 1, it is enough to show that M_1 is a contraction mapping. Indeed, let $x_1, x_2 \in X, t \in J$, and it is not difficult to show that

$$
\|M_1 x_1 - M_1 x_2\|_X \leq \frac{(\Gamma(q)(1-q) + 1)}{F(q)\Gamma(q)} \left(\beta_1 + 0.02 \|W(u)\|_X\right) \|x_2 - x_1\|_X \leq H \|x_2 - x_1\|_X,
\tag{18}
$$

where $H = (\Gamma(q)(1-q) + 1)(\beta_1 + 0.02\|W(u)\|_X)/F(q)\Gamma(q)$. Since $H < 1$ by hypothesis of Theorem 2, we conclude that M_1 is a contraction mapping.

To show that the remaining operators M_2, M_3, M_4, and M_4 are contraction mappings, we proceed in the same manner.

Let us show that the operator M_2 defined in (14) is well defined in the sense that $M_2 y(t) \in \mathfrak{I}'$ and ${}_0^{\mathrm{ABC}}D_t^q M_2 y(t)$ is continuous on $J = [0,1]$, where

$$
\mathfrak{I}'_r = \{B \in X, \|B\| \leq r', r' \geq 0\},
\tag{19}
$$

for $r' > (k_1 + 16k_2 + k_1 k_3 + k_4)(\|y_0\|_X F(q)\Gamma(q) + \Gamma(q)(1-q) + 1)/F(q)\Gamma(q)$.

Now for any $y \in \mathfrak{I}'_r$ and from (11), we have

$$
\begin{aligned}
\|M_2 y(t)\|_x &= \|y_0\|_X + \frac{1-q}{F(q)} \sup_{t \in J} \left(-x(t) + 16y(t) - x(t)z(t) + w(t)\right) \\
&\quad + \frac{q}{F(q)\Gamma(q)} \sup_{t \in J} \int_0^t (t-k)^{q-1} \left(-x(k) + 16y(k) - x(k)z(k) + w(k)\right) \mathrm{d}k \\
&\leq \frac{(k_1 + 16k_2 + k_1 k_3 + k_4)\left(\|y_0\|_X F(q)\Gamma(q) + \Gamma(q)(1-q) + 1\right)}{F(q)\Gamma(q)} \leq r\prime.
\end{aligned}
\tag{20}
$$

Consequently, we have $M_2 y(t) \in \mathfrak{I}'_r$. To show continuous differentiability on $J = [0,1]$, we proceed from ${}_0^{\mathrm{ABC}}D_t^q M_2 y(t) = {}_0^{\mathrm{ABC}}D_{t0}^{q\mathrm{AB}}I_t^q (-x + 16y - xz + w) = -x + 16y - xz + w$ which is continuous on $J = [0,1]$, and we

conclude that ${}_0^{\mathrm{ABC}}D_t^q M_2 y(t)$ is continuous on J; as a result, ${}_0^{\mathrm{ABC}}D_t^q M_2 y(t)$.

To show that the operator M_2 has a fixed point, we apply Theorem 1. Following the theorem, it is sufficient to show

that M_2 is a contraction mapping. Indeed, let $y_1, y_2 \in X, t \in J$. Then,

$$\left\|M_2 y_2 - M_2 y_1\right\|_X \le \frac{1-q}{F(q)} 16 \left\|y_2 - y_1\right\| + \frac{q16\left\|y_2 - y_1\right\|}{F(q)\Gamma(q)} \sup_{t \in J} \int_0^t (t-k)^{q-1} \mathrm{d}k$$

$$\le \frac{16(1-q)\Gamma(q) + 16}{F(q)\Gamma(q)} \left\|y_2 - y_1\right\| \le H' \left\|y_2 - y_1\right\|_X, \tag{21}$$

where $H' = (16(1-q)\Gamma(q) + 16)/F(q)\Gamma(q)$. Since $H' < 1$, we conclude that M_2 is a contraction mapping.

Let us show that the operator M_3 defined in (12) is well defined in the sense that $_0^{ABC}D_t^q M_2 y(t) = _0^{ABC}D_{t0}^{qAB}I_t^q(-x + 16y - xz + w)$ and $_0^{ABC}D_t^q M_3 z(t)$ is continuous on $J = [0, 1]$, where

$$\mathfrak{I}_{r''}'' = \{u \in X, \|u\| \le r'', r'' \ge 0\}, \tag{22}$$

for $r'' > (\beta_2 k_3 + k_1 k_2 + k_1 k_5 + k_2 k_4)(\|z_0\|F(q)\Gamma(q) + \Gamma(q)(1-q) + 1)/F(q)\Gamma(q)$.

Now for any $z \in \mathfrak{I}_{r''}''$ and from (12), we have

$$\left\|M_3 z(t)\right\|_X = \left\|z_0\right\|_X + \frac{1-q}{F(q)} \sup_{t \in J} \left(-\beta_2 z(t) + x(t)y(t) - x(t)u(t) - y(t)w(t)\right)$$

$$+ \frac{q}{F(q)\Gamma(q)} \sup_{t \in J} \int_0^t (t-k)^{q-1} \left(-\beta_2 z(k) + x(k)y(k) - x(k)u(k) - y(k)w(k)\right)\mathrm{d}k$$

$$\le \left\|z_0\right\|_X + \frac{1-q}{F(q)} \left|-\beta_2 k_3 + k_1 k_2 - k_1 k_5 - k_2 k_4\right| + \frac{q}{F(q)\Gamma(q)} \left|-\beta_2 k_3 + k_1 k_2 - k_1 k_5 - k_2 k_4\right| \sup_{t \in J} \int_0^t (t-k)^{q-1} \mathrm{d}k$$

$$\le \frac{(\beta_2 k_3 + k_1 k_2 + k_1 k_5 + k_2 k_4)\left(\left\|z_0\right\|_X F(q)\Gamma(q) + \Gamma(q)(1-q) + 1\right)}{F(q)\Gamma(q)} < r''. \tag{23}$$

Consequently, we have $M_3 z(t) \in \mathfrak{I}_{r''}''$. To show continuous differentiability on $J = [0, 1]$, we proceed from $_0^{ABC}D_t^q M_3 z(t) = _0^{ABC}D_{t0}^{qAB}I_t^q(-\beta_2 z + xy - xu - yw) = -\beta_2 z + xy - xu - yw$ which is continuous on $J = [0, 1]$, and we conclude that $_0^{ABC}D_t^q M_3 z(t)$ is continuous on J; as a result, $M_3 \mathfrak{I}_{r''}'' \subset \mathfrak{I}_{r''}''$.

To show that the operator M_3 has a fixed point, we apply Theorem 1. Following the theorem, it is sufficient to show that M_3 is a contraction mapping. Indeed, let $z_1, z_2 \in X, t \in J$. Then,

$$\left\|M_3 z_1 - M_3 z_2\right\|_X \le \frac{1-q}{F(q)} \left(\beta_2 \left\|z_2 - z_1\right\|_X\right) + \frac{q}{F(q)\Gamma(q)} \beta_2 \left\|z_2 - z_1\right\|_X \sup_{t \in J} \int_0^t (t-k)^{q-1} \mathrm{d}k$$

$$\le \frac{(\Gamma(q)(1-q) + 1)\beta_2}{F(q)\Gamma(q)} \left\|z_2 - z_1\right\|_X \le H'' \left\|z_2 - z_1\right\|_X, \tag{24}$$

where $H'' = (\Gamma(q)(1-q) + 1)\beta_2/F(q)\Gamma(q)$. Since by hypothesis $H'' < 1$, we conclude that M_3 is a contraction mapping.

We have then proved that the operators $M_1, M_2,$ and M_3 are well defined and are contraction mappings. The case for the operators M_4 and M_5 follows immediately. Hence, by

the Banach fixed point theorem, system (17) has a unique solution in X. $\square$

5. Numerical Solutions

In this part, the numerical scheme applied to get the phase portrait of the dynamic system (15) is introduced. In the context of chaotic or hyperchaotic fractional differential equations, the use of analytical methods such as the Sudumu transform method, the Laplace transform method, the homotopy analysis method, and the homotopy perturbation method cannot easily be applied because of the nonlinearities of the system [13]. This leads to the need for using numerical methods to approximate the solutions of systems of fractional differential equations. Some of the numerical methods that can be applied for this case include Adams–Bashforth and Toufik–Atangana numerical schemes [8]. Both of these methods are based on Lagrange interpolation polynomials. In this study, the newly developed numerical approximation for fractional derivatives by Toufik and Atangana is employed. The numerical scheme is particularly developed for approximation of Atangana–Baleanu fractional derivative considered in this study, and it is proved to be convergent, stable, and consistent [8].

For convenience, let us write (15) in the following form:

$$
\begin{aligned}
{}_0^{ABC}D_t^q x &= N_1(t, x, y, z, w, u), \\
{}_0^{ABC}D_t^q y &= N_2(t, x, y, z, w, u), \\
{}_0^{ABC}D_t^q z &= N_3(t, x, y, z, w, u), \\
{}_0^{ABC}D_t^q w &= N_4(t, x, y, z, w, u), \\
{}_0^{ABC}D_t^q u &= N_5(t, x, y, z, w, u),
\end{aligned}
\tag{25}
$$

where

$$
\begin{aligned}
N_1(t, x, y, z, w, u) &= \beta_1(y - x) + 4yz - 0.02x(t)W(u), \\
N_2(t, x, y, z, w, u) &= -x + 16y - xz + w, \\
N_3(t, x, y, z, w, u) &= -\beta_2 z + xy - xu - yw, \\
N_4(t, x, y, z, w, u) &= -10y + 0.15xz - 0.3zu, \\
N_5(t, x, y, z, w, u) &= -x.
\end{aligned}
\tag{26}
$$

Now from Lemma 3 and the first equation of (25), we have

$$
\begin{aligned}
{}_0^{ABC}D_t^q x(t) &= N_1(t, x(t), y(t), z(t), \phi(t)), \\
x(0) &= x_0.
\end{aligned}
\tag{27}
$$

The solution for (27) is given as follows:

$$
\begin{aligned}
x(t) &= x_0 + \frac{1-q}{F(q)}N_1(t, x(t)) \\
&\quad + \frac{q}{F(q)\Gamma(q)} \int_0^t N_1(k, x(k))(t-k)^{q-1}\,dk.
\end{aligned}
\tag{28}
$$

Applying Lagrange's interpolation polynomial on $[t_k, t_{k+1}]$ to equality $N_1(s, x(s), y(s), z(s), \phi(s)) = \beta_1(y - x) + 4yz - 0.02x(t)W(u)$ leads to

$$
x_k \approx \frac{1}{h}\left[(s - t_{k-1})N_1(t_k, x(t_k), y(t_k)) - (s - t_k)N_1(t_{k-1}, x(t_{k-1}), y(t_{k-1}))\right],
\tag{29}
$$

where $h = t_k - t_{k-1}$.

Substituting (28) into (29), we obtain

$$
\begin{aligned}
x(t_{n+1}) &= x_0 + \frac{1-q}{F(q)}N_1(t_k, x(t_k), y(t_k)) \\
&\quad + \frac{q}{F(q)\Gamma(q)}\sum_{j=1}^{n}\left(\frac{N_1(t_j, x(t_j), y(t_j))}{h}\Upsilon_{j-1} - \frac{N_1(t_{j-1}, x(t_{j-1}), y(t_{j-1}))}{h}\Upsilon_j\right),
\end{aligned}
\tag{30}
$$

where

$$
\Upsilon_{j-1} = \int_{t_j}^{t_{j+1}} (s - t_{j-1})(t_{n+1} - s)^{q-1} ds = -\frac{1}{q} \left[(t_{j+1} - t_{j-1})(t_{n+1} - t_{j+1})^q - (t_j - t_{j-1})(t_{n+1} - t_j)^q \right]
$$

$$
- \frac{1}{q(q+1)} \left[(t_{n+1} - t_{j+1})^{q+1} (t_{n+1} - t_{j+1})^q - (t_{n+1} - t_j)^{q+1} \right], \tag{31}
$$

$$
\Upsilon_j = \int_{t_j}^{t_{j+1}} (y - t_{j-1})(t_{n+1} - s)^{q-1} ds = -\frac{1}{q} \left[(t_{j+1} - t_{j-1})(t_{n+1} - t_{j+1})^q \right]
$$

$$
- \frac{1}{q(q+1)} \left[(t_{n+1} - t_{j+1})^{q+1} - (t_{n+1} - t_j)^{q+1} \right]. \tag{32}
$$

Substituting $t_j = jh$ in (31) and (32) results in

$$
\Upsilon_{j-1} = \frac{h^{q+1}}{q(q+1)} \left[(n+1-j)^q (n-j+2+q) - (n-j)^q (n-j+2+2q) \right], \tag{33}
$$

$$
\Upsilon_j = \frac{h^{q+1}}{q(q+1)} \left[(n+1-j)^{q+1} - (n-j)^q (n-j+1+q) \right]. \tag{34}
$$

The expression (30) can be expressed in terms of (31) and (34) as shown in the following equation:

$$
x(t_{n+1}) = x_0 + \frac{1-q}{F(q)} N_1(t_n, x(t_n), y(t_n))
$$

$$
+ \frac{q}{F(q)\Gamma(q)} \sum_{j=1}^{n} \left(\left(\frac{N_1(t_j, x(t_j), y(t_j))}{\Gamma(q+2)} \right) \times h^q \left[(n+1-j)^q (n-j+2+q) - (n-j)q(n-j+2+2q) \right] \right. \tag{35}
$$

$$
\left. - \left(\frac{N_1(t_{j-1}, x(t_{j-1}), y(t_{j-1}))}{\Gamma(q+2)} \right) \times h^q \left[(n+1-j)^{q+1} - (n-j)^q (n-j+1+q) \right] \right).
$$

Similarly, we get the following equations for the rest of the state variables:

$$
y\left(t_{n+1}\right) = y_0 + \frac{1-q}{F(q)} N_2\left(t_n, x\left(t_n\right), y\left(t_n\right), z\left(t_n\right)\right)
$$

$$
+ \frac{q}{F(q)\Gamma(q)} \sum_{j=1}^{n} \left(\frac{N_2\left(t_j, x\left(t_j\right), y\left(t_j\right), z\left(t_j\right)\right)}{\Gamma(q+2)} \times h^q \left[(n+1-j)^q (n-j+2+q) - (n-j)^q (n-j+2+2q) \right] \right.
$$

$$
\left. - \frac{N_2\left(t_{j-1}, x\left(t_{j-1}\right), y\left(t_{j-1}\right), z\left(t_{j-1}\right)\right)}{\Gamma(q+2)} \times h^q \left[(n+1-j)^{q+1} - (n-j)^q (n-j+1+q) \right] \right),
$$
(36)

$$
z\left(t_{n+1}\right) = z_0 + \frac{1-q}{F(q)} N_3\left(t_n, y\left(t_n\right), z\left(t_n\right)\right)
$$

$$
+ \frac{q}{F(q)\Gamma(q)} \sum_{j=1}^{n} \left(\frac{N_3\left(t_j, y\left(t_j\right), z\left(t_j\right)\right)}{\Gamma(q+2)} \times h^q \left[(n+1-j)^q (n-j+2+q) - (n-j)^q (n-j+2+2q) \right] \right.
$$

$$
\left. - \frac{N_3\left(t_{j-1}, y\left(t_{j-1}\right), z\left(t_{j-1}\right)\right)}{\Gamma(q+2)} \times h^q \left[(n+1-j)^{q+1} - (n-j)^q (n-j+1+q) \right] \right),
$$
(37)

$$
w\left(t_{n+1}\right) = w_0 + \frac{1-q}{F(q)} N_4\left(t_n, y\left(t_n\right), z\left(t_n\right)\right)
$$

$$
+ \frac{q}{F(q)\Gamma(q)} \sum_{j=1}^{n} \left(\frac{N_4\left(t_j, y\left(t_j\right), z\left(t_j\right)\right)}{\Gamma(q+2)} \times h^q \left[(n+1-j)^q (n-j+2+q) - (n-j)^q (n-j+2+2q) \right] \right.
$$

$$
\left. - \frac{N_4\left(t_{j-1}, y\left(t_{j-1}\right), z\left(t_{j-1}\right)\right)}{\Gamma(q+2)} \times h^q \left[(n+1-j)^{q+1} - (n-j)^q (n-j+1+q) \right] \right),
$$
(38)

$$
u\left(t_{n+1}\right) = u_0 + \frac{1-q}{F(q)} N_5\left(t_n, y\left(t_n\right), z\left(t_n\right)\right)
$$

$$
+ \frac{q}{F(q)\Gamma(q)} \sum_{j=1}^{n} \left(\frac{N_5\left(t_j, y\left(t_j\right), z\left(t_j\right)\right)}{\Gamma(q+2)} \times h^q \left[(n+1-j)^q (n-j+2+q) - (n-j)^q (n-j+2+2q) \right] \right.
$$

$$
\left. - \frac{N_5\left(t_{j-1}, y\left(t_{j-1}\right), z\left(t_{j-1}\right)\right)}{\Gamma(q+2)} \times h^q \left[(n+1-j)^{q+1} - (n-j)^q (n-j+1+q) \right] \right).
$$
(39)

6. Local Stability Analysis

In this section of the study, the local stability analysis of the fractional model represented in (25) is performed. It is known that the equilibrium points of chaotic systems are not generally stable. Some of the standard methods of stability analysis in fractional calculus are the Matignon criterion and the Laplace transform methods. In this work, the Matignon method is used for its simplicity and is most commonly used in the literature for the same purpose [1, 7, 13, 17].

The Matignon criterion is given by

$$
|\arg \lambda(J)| > \frac{q\pi}{2} 2,
$$
(40)

where J represents the Jacobian matrix, $\lambda(J)$ is the set of the eigenvalues of J, and q is the fractional-order derivative. In the context of fractional derivative, an equilibrium point of (25) is said to be locally stable provided that the Matignon criterion (40) is satisfied for each of the eigenvalues of the Jacobian matrix.

To determine if the equilibrium points of (25) are stable or not, we proceed as follows:

(i) The equilibrium points: the equilibrium points of (25) are given as $(0, 0, 0, 0, 0)$, and line equilibrium is given by $\{\alpha(0, 0, 0, 0, 1): \alpha \in \mathbb{R}\}$.

(ii) The Jacobian matrix: in this study, analysis is made regarding the trivial equilibrium point for simplicity. The parameter values used, unless otherwise mentioned, are set as $a = 0.1, b = 0.01$, $\beta_1 = 30$, and $\beta_2 = 8$. Thus, the Jacobian matrix of (25) evaluated at the trivial equilibrium point is given by

$$J_o = \begin{pmatrix} -\beta_1 - 0.002 & \beta_1 & 0 & 0 & 0 \\ -1 & 16 & 0 & 1 & 0 \\ 0 & 0 & -\beta_2 & 0 & 0 \\ 0 & -10 & 0 & 0 & 0 \\ -1 & 0 & 0 & 0 & 0 \end{pmatrix}. \qquad (41)$$

The eigenvalues of the Jacobian matrix J are given by $\lambda_1 = 0$, $\lambda_2 = -29.3453$, $\lambda_4 = 0.6981$, $\lambda_4 = 0.6981$, and $\lambda_5 = -8.0000$. To check the local stability of the trivial equilibrium point, using the Matignon criteria, we need to verify if all the eigenvalues satisfy condition (40). Indeed, $|\arg(\lambda_{1,3,4})| = 0 > q\pi/2$ which is not possible since $q \in (0, 1)$. $|\arg(\lambda_{2,5})| = 3.1416 = \pi > q\pi/2$ is true for all $q \in (0, 1)$. It can then be concluded that the equilibrium point $E_{eqpts} = (0, 0, 0)$ is locally unstable for the parameter values considered.

Furthermore, since one of the eigenvalues of the Jacobian matrix is with positive real part, it can be inferred that system (25) satisfies the necessary condition for showing the double scroll attractor [19].

7. Lyapunov Exponents, Bifurcation, and Chaos with Different Fractional Orders of q and Different Parameter Values

In this section, the level of chaos in system (25) is quantified using the Lyapunov exponent method. Bifurcation diagrams of the system (25) related to the fractional derivative order q and three of the parameters in the model named, β_1, β_2, and β_3, are depicted.

A Matlab code for Lyapunov exponents of fractional-order systems named the Danca algorithm [26] is used to quantify the chaos by calculating Lyapunov exponents for different fractional orders of model (25). The initial conditions used in this part of the work are given by $(0.11, 0.11, 0.11, 0.11)$. The parameter values used are similar to the ones used above for calculating the Jacobian matrix. The corresponding Lyapunov exponents (LEs) for different fractional orders $q = 0.94, 0.96, 0.98, 1.00$ are shown in Table 1.

It is then possible to conclude that the 5D system considered in this study is dissipative since the sum of the LEs in each column of Table 1 is negative and the system exhibits a hyperchaotic behavior since there are at least two positive LEs in each column of the table and the largest LE is positive. Moreover, Kaplan–Yorke dimension coresponding to the fractional derivatives considered in Table 1can be calculated. For instance, the dimension of two of the fractional orders is given as follows.

For $q = 0.99$,

$$\dim(\text{LE}) = 4 + \frac{15.3837 + 0.7298 + 0.005 - 8.4128}{|-30.6645|} = 4.2511. \qquad (42)$$

For $q = 0.98$,

$$\dim(\text{LE}) = 4 + \frac{16.1855 + 0.7676 + 0.005 - 8.8488}{|-32.1742|} = 4.2520. \qquad (43)$$

7.1. Bifurcations due to Variation of the Fractional Order q. For obtaining bifurcation diagrams due to the variation of the fractional order q, the values of all the parameters are kept fixed and the order of the fractional derivative q is varied in the interval $(0.8, 1)$ with an increment of 0.001. The other parameter values used in this simulation are $a = 0.1, b = 0.01, \beta_1 = 30$, and $\beta_2 = 8$, and the initial condition is $(0.11, 0.11, 0.11, 0.11, 0.11)$. The bifurcation diagram is shown in Figure 1.

As shown in Figure 1, when $q \in (0.8, 1)$, the system is hyperchaotic. As a verification of the observation, the phase portraits corresponding to $q = 0.98$ and $q = 0.99$ using the numerical approximations for fractional-order systems indicated by equations (35)–(39) are shown in Figures 2 and 3, respectively. In both Figures 2 and 3, the dependence of the hyperchaotic system on the fractional derivative is observable as the two figures are seen to be different from each other for a fractional order difference of 0.01. If we consider the trajectories in Figure 3, the orbit due to $q = 0.98$ converged in less than 13.5 seconds which is not the case for $q = 0.99$. That means different fractional derivative orders generate reasonably different dynamics of the system (25).

7.2. Bifurcations due to Variation of the Parameter β_1. The values of the parameters used are $a = 0.1, b = 0.01$, and $\beta_2 = 8$, the fractional derivative order is $q = 0.99$, and the initial condition is $(0.11, 0.11, 0.11, 0.11, 0.11)$. The value of the parameter β_1 is made to vary in the interval $(29.5, 30.5)$ with an increment of 0.001. The bifurcation diagram is shown in Figure 4. It can be observed from the diagram that system (25) exhibits significant hyperchaos throughout the interval under consideration. In support of this conclusion, some of the phase portraits of hyperchaotic system (25) are depicted in Figure 5 projected on different planes.

It can be inferred from Figures 5(a)–5(d) that the orbits seem to overlap initially, but as time increases, their divergence from each other increases. That is, as time goes, the orbit due to $\beta_1 = 30.5$ showed more contraction than the trajectory due to $\beta_1 = 30$; this is because of the sum of all the

TABLE 1: LEs corresponding to different fractional orders of model (25) for a simulation time of 300 s.

q	0.94	0.96	0.98	0.99	1
LE1	19.8323	17.9163	16.1855	15.3837	14.6215
LE2	0.9387	0.8490	0.7676	0.7298	0.6938
LE3	0.0050	0.0050	0.0050	0.0050	0.0050
LE4	−10.7674	−9.7560	−8.8353	−8.4066	−7.9978
LE5	−38.8609	−35.3857	−32.1742	−30.6645	−29.2172
Sum of all LEs	−28.8523	−26.3714	−24.0496	−22.9526	−21.8497

FIGURE 1: Bifurcation diagram for variation of the fractional derivative order q in the interval (0.8, 1).

Lyapunov exponents (LEs) of the respective parameter values considered in this case. The sum of LEs for $\beta_1 = 30$ is −22.9526 (the LEs are shown in Table 1), the sum of LEs for $\beta_1 = 30.5$ is −23.4693 (LEs are 15.3796, 0.7298, 0.0051, −8.4066, and −31.1772), and the sum of LEs for $\beta_1 = 30.25$ is −23.2106 (LEs are 15.3817, 0.7298, 0.0051, −8.4066, and −30.9209). Since the system under investigation is dissipative, the contraction rate of volumes due to $\beta_1 = 30.5$ is stronger than the contraction rate of volumes due to $\beta_1 = 30$ which is inferred from the magnitude of the sum of all LEs for the corresponding parameter values.
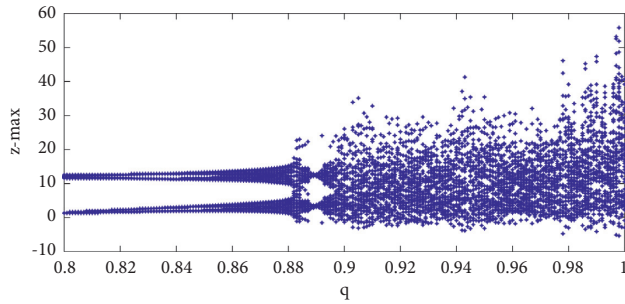
7.3. Bifurcations due to Variation of the Parameter β_2. The values of the parameters used are $a = 0.1, b = 0.01$, and $\beta_2 = 8$, the fractional derivative order is $q = 0.99$, and the initial condition is (0.11, 0.11, 0.11, 0.11, 0.11). The value of the parameter β_2 is made to vary in the interval [7, 8.5] with an increment of 0.001. The bifurcation diagram is shown in Figure 6. It can be observed from the diagram that system (25) exhibits significant hyperchaos throughout the interval under consideration. In support of this conclusion, some of the phase portraits of the hyperchaotic system (25) are depicted in Figure 7 projected on different planes and some of the time-series trajectories are depicted in Figure 8.

It can be inferred from Figures 7(a)–7(c) that the orbits seem to overlap initially, but as time increases, their divergence from each other increases. That is, as time goes, the orbit due to $\beta_1 = 30.5$ showed more contraction than the trajectory due to $\beta_1 = 30$, as can be observed from the sum of all LEs of the respective parameter values considered in this case. The sum of LEs for $\beta_2 = 8$ is −22.9526 (the LEs are shown in Table 1) and the sum of LEs for $\beta_2 = 7.5$ is −22.4277 (LEs are 15.3837, 0.7298, −7.8817, 0.0050, and −30.6645). Since the system under investigation is dissipative, the contraction rate of volumes due to $\beta_2 = 8$ is stronger

than the contraction rate of volumes due to $\beta_1 = 7.5$ which is inferred by the magnitude of the sum of all LEs corresponding to the parameter values.

The trajectories in Figure 8 seem to overlap for the first few seconds and then begin diverging from each other; the divergence increases with time.

8. Impact of Initial Condition

In this section, the impact of different initial conditions on the dynamics of the system (25) is addressed. It is well known that one of the properties of chaotic systems is sensitivity to initial conditions, and thus it seems relevant to verify the impact of applying different initial conditions on the phase-space and time-series solutions of system (25). Accordingly, the parameter values and derivative order used are $a = 0.1, b = 0.01, \beta_1 = 30, \beta_2 = 8$, and $q = 0.99$. In Figure 9, some of the phase portraits of hyperchaotic system (25) are depicted corresponding to initial conditions (0.11,0.11,0.11,0.11.0.11) by varying initial coordinates of $u(0) = 0.5, and\ 1.0$is made to run for 5 seconds with a time step of $h = 0.001$. The simulation result is shown in Figure 9.

As can be observed from the figures, hyperchaotic system (25) is sensitive to changes in initial conditions. As the variation in the initial condition increases, the dynamics of the system become different from each other at least for this example.

As can be observed from Figures 9 and 10, a small difference of the initial condition generates a significantly observable change in the dynamics of system (25).

9. Synchronization of the Hyperchaotic Model

Synchronization between two chaotic systems is one of the most interesting phenomena in the study of dynamic systems. Synchronization is an occurrence in which two or more chaotic/hyperchaotic systems express a strong correlation among themselves. It is very interesting to see that two hyperchaotic systems, being highly sensitive to initial conditions and exponential divergence of nearby orbits, get synchronized starting from two different initial conditions. Pecora and Caroll [33, 34] in 1990 showed for the first time the possibility of synchronizing two chaotic systems starting from two different initial conditions. Pecora and Caroll used a technique called replacement synchronization. Chaotic synchronization has a range of applications including securing communications based on phase synchronization and controlling insulin production by beta cells. In this
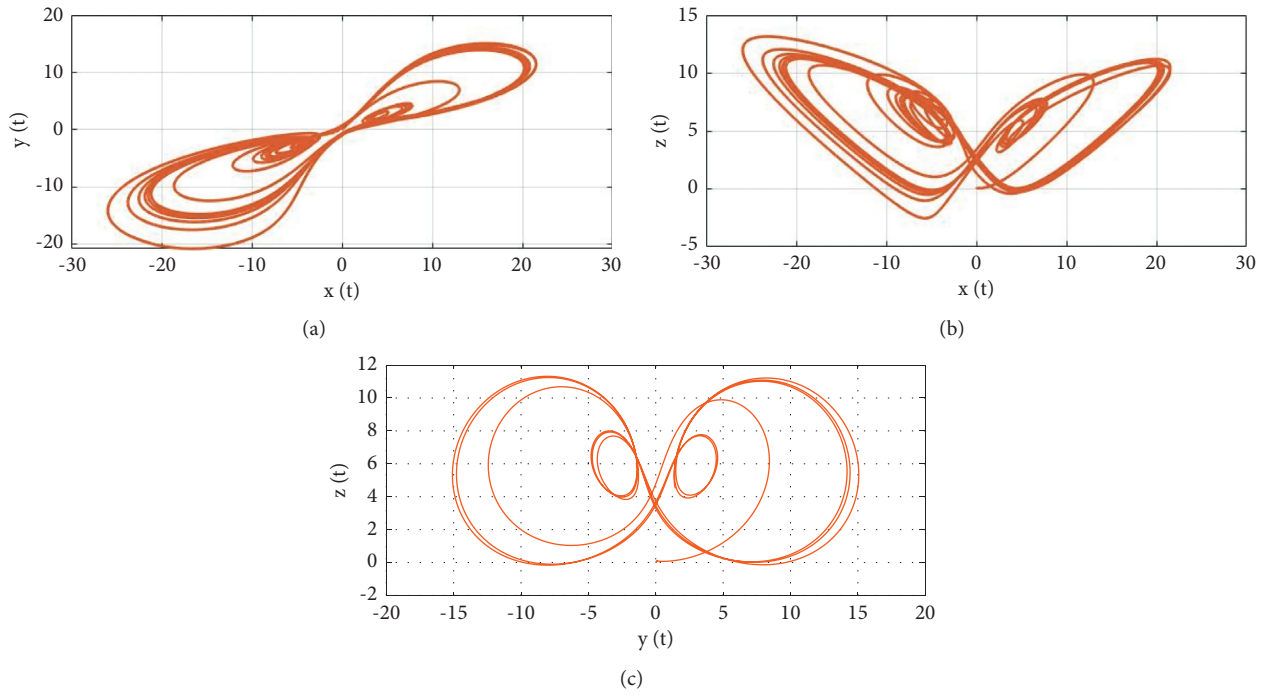
FIGURE 2: Phase portraits of system (25) for derivative order of $q = 0.98$ projected on different planes. (a) x-y plane. (b) x-z plane. (c) y-z plane.
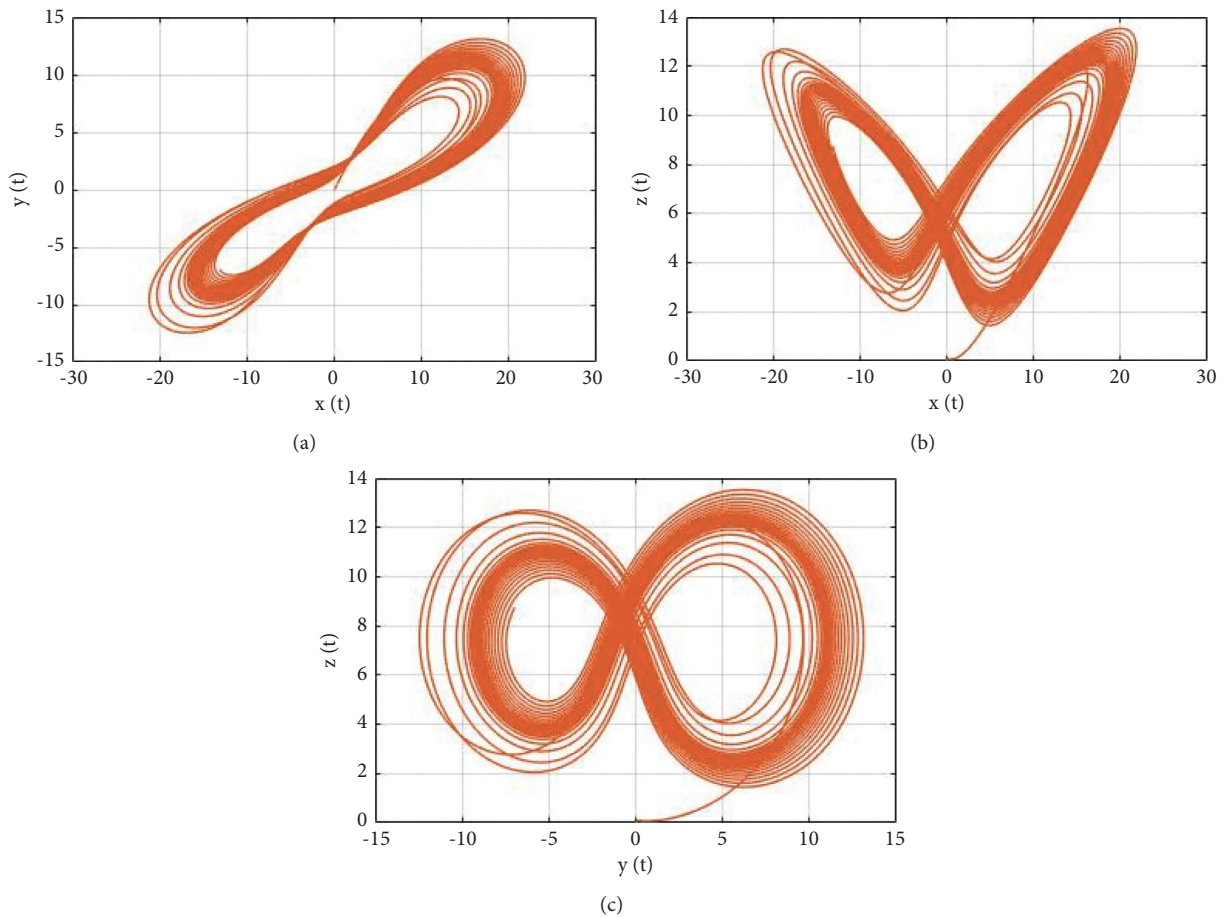
FIGURE 3: Phase portraits of system (25) for derivative order of $q = 0.99$ projected on different planes. (a) x-y plane. (b) x-z plane. (c) y-z plane.
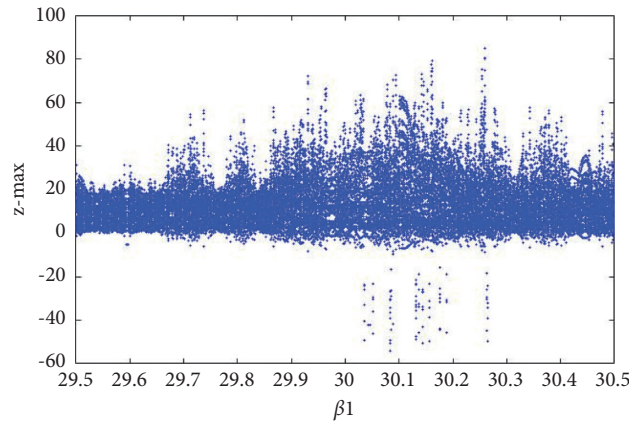
FIGURE 4: Bifurcation diagram for variation of the parameter β_1 in the interval (29.5, 30.5).

(a)

(b)

(c)

(d)
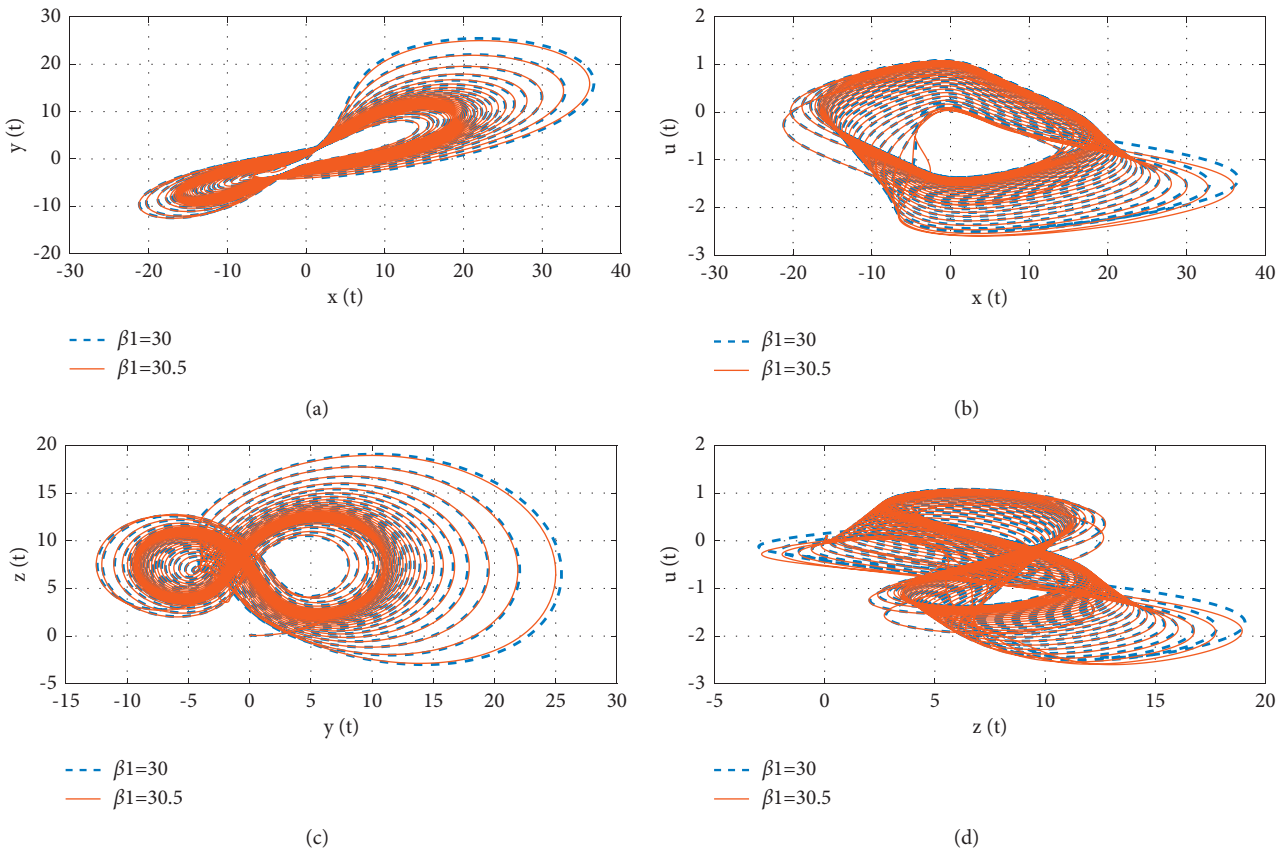
FIGURE 5: Phase portraits of the system (25) for different values the parameter β_1. (a) x-y plane. (b) x-u plane. (c) y-z plane. (d) z-u plane.

study, we applied the master-slave synchronization technique. That is, we considered two identical copies of system (25) and related them with a coupling function. We considered different initial conditions for the coupled systems, showed that the error dynamics are asymptotically stable,

and portrayed some of the simulation results. The coupling function is added to the slave system to make it respond to the master system.

Now the master hyperchaotic fractional model is given by
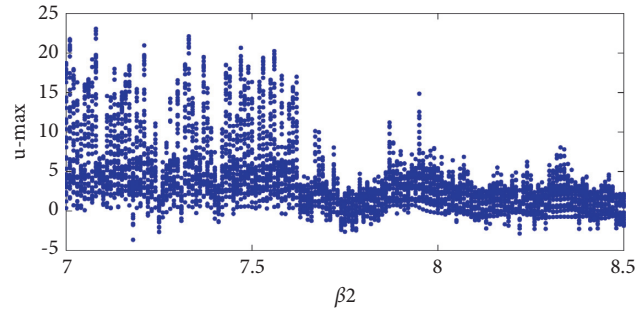
FIGURE 6: Bifurcation diagram system (25) for the parameter β_2 in the interval [7, 8.5].

(a)

(b)

(c)
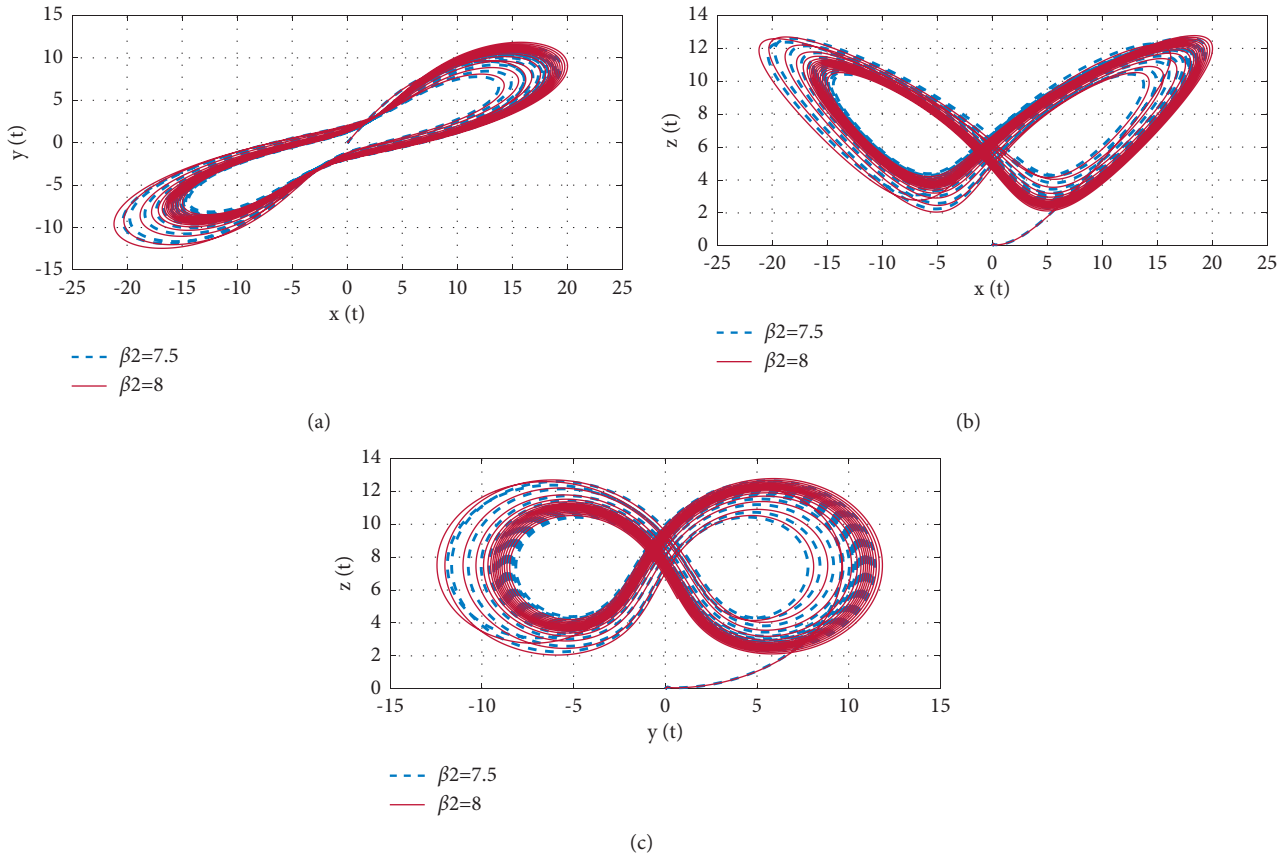
FIGURE 7: Phase portraits of the system (25) for different values parameter of β_2. (a) x-y plane. (b) x-z plane. (c) y-z plane.

(a)

(b)
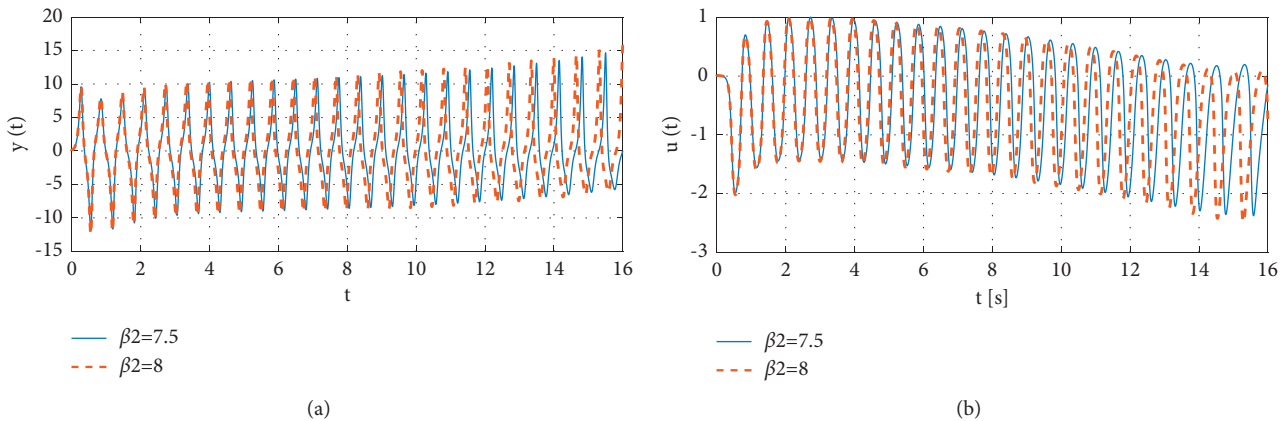
FIGURE 8: Time series solutions of the state variables $y(t)$ and $u(t)$ of system (25) for different parameter values of β_2.

(a)

(b)
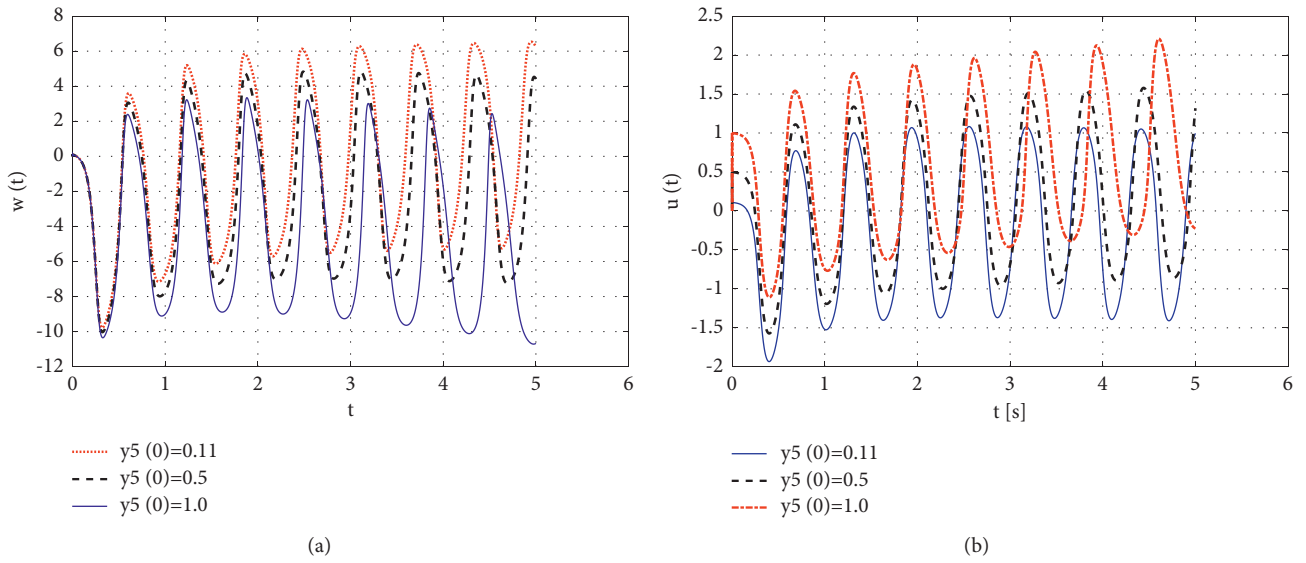
FIGURE 9: Some of the time series orbits of the system (25) due to small changes in the initial conditions.

(a)

(b)
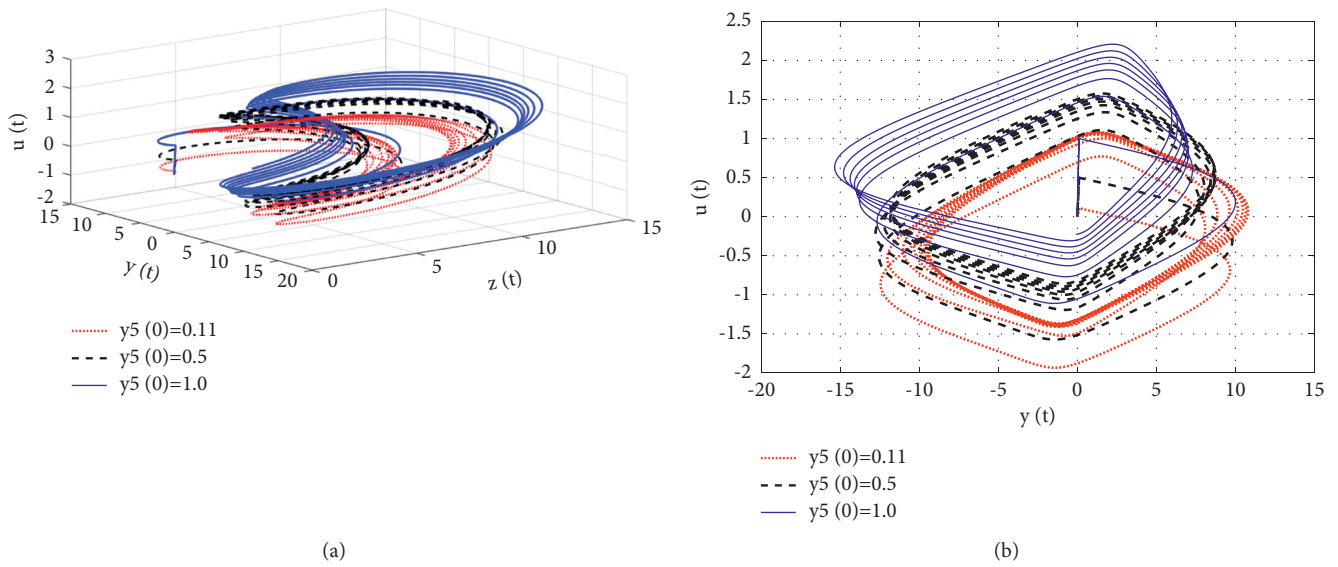
FIGURE 10: Some of the Phase portraits of the system (25) due to small changes in the initial condition. (a) z-y-u space. (b) y-u plane.

$$
{}_{0}^{\text{ABC}}D_{t}^{q}x(t) = 30(y - x) + 4yz - \left(0.002x + 0.0006xu^{2}\right),
$$

$$
{}_{0}^{\text{ABC}}D_{t}^{q}y(t) = -x + 16y - xz + w,
$$

$$
{}_{0}^{\text{ABC}}D_{t}^{q}z(t) = -8z + xy - xu - yw, \tag{44}
$$

$$
{}_{0}^{\text{ABC}}D_{t}^{q}w(t) = -10y + 0.15xz - 0.3zu,
$$

$$
{}_{0}^{\text{ABC}}D_{t}^{q}u(t) = -x.
$$

Let the slave model be given by

$$
\begin{cases}
{}^{ABC}_0 D_t^q x_s(t) = 30\left(y_s - x_s\right) + 4y_s z_s - \left(0.002x_s + 0.0006x_s u_s^2\right) + c_1, \\
{}^{ABC}_0 D_t^q y_s(t) = -x_s + 16y_s - x_s z_s + w_s + c_2, \\
{}^{ABC}_0 D_t^q z_s(t) = -8z_s + y_s x_s - x_s u_s - y_s w_s + c_3, \; {}^{ABC}_0 D_t^q w_s(t) = -10y_s + 0.15x_s z_s - 0.3u_s z_s + c_4, \; {}^{ABC}_0 D_t^q u_s(t) = -x_s + c_5.
\end{cases}
\tag{45}
$$

Define the error terms by

$$
e_1 = x_s - x, e_2 = y_s - y, e_3 = z_s - z, e_4 = w_s - w, e_5 = u_s - u.
\tag{46}
$$

The error dynamics are then given by

$$
\begin{cases}
{}^{ABC}_0 D_t^q e_1(t) = \beta_1 e_2 - \beta_1 e_1 + 4\left(e_3\left(e_2 + y\right) + e_2 z\right) - 0.002e_1 + 0.0006\left(-e_1 e_5^2 + 2e_1 e_5 u - u^2 e_1 - xe_5^2 + 2e_5 ux\right) + c_1, \\
{}^{ABC}_0 D_t^q e_2(t) = -e_1 + 16e_2 + \left(-e_1 e_3 - e_1 z - xe_3\right) + e_4 + c_2, \\
{}^{ABC}_0 D_t^q e_3(t) = -\beta_2 e_3 + \left(e_1 e_2 + e_1 y + xe_2\right) + \left(-e_1 e_5 - e_1 u - xe_5\right) + \left(-e_2 e_4 - e_4 y - e_2 w\right) + c_3, \\
{}^{ABC}_0 D_t^q e_4(t) = -10e_2 + 0.15\left(e_1 e_3 + e_1 z + xe_3\right) + 0.3\left(-e_5 e_4 - e_5 z - ue_4\right) + c_4, \\
{}^{ABC}_0 D_t^q e_5(t) = -e_1 + c_5.
\end{cases}
\tag{47}
$$

The vector $(c_1, c_2, c_3, c_4, c_s)^T$ is chosen as

$$
\begin{pmatrix} c_1 \\ c_2 \\ c_3 \\ c_4 \\ c_5 \end{pmatrix} = -\begin{pmatrix} \beta_1 e_2 - \beta_1 e_1 + 4\left(e_3\left(e_2 + y\right) + e_2 z\right) - 0.002e_1 + 0.0006\left(-e_1 e_5^2 + 2e_1 e_5 u - u^2 e_1 - xe_5^2 + 2e_5 ux\right), \\ -e_1 + 16e_2 + \left(-e_1 e_3 - e_1 z - xe_3\right), \\ -\beta_2 e_3 + \left(e_1 e_2 + e_1 y + xe_2\right) + \left(-e_1 e_5 - e_1 u - xe_5\right) + \left(-e_2 e_4 - e_4 y - e_2 w\right), \\ -10e_2 + 0.15\left(e_1 e_3 + e_1 z + xe_3\right) + 0.3\left(-e_5 e_4 - e_5 z - ue_4\right), \\ -e_1, \end{pmatrix} + H.\zeta,
\tag{48}
$$
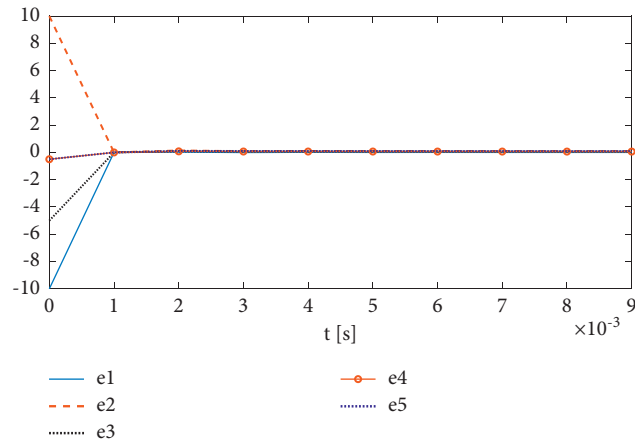
Figure 11: Error dynamics of the synchronization process.
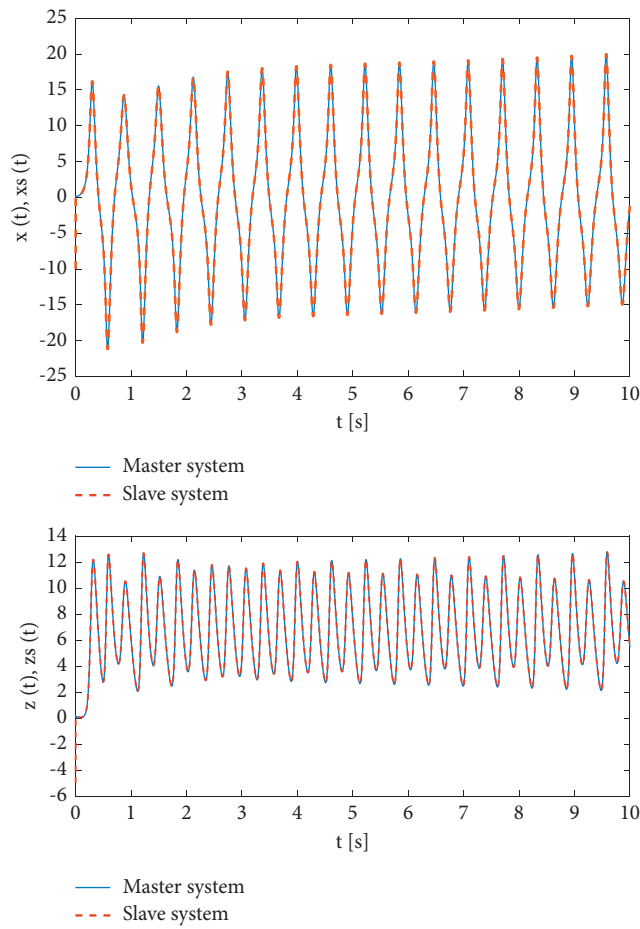
Figure 12: Some of the time series graphs of synchronized orbits.
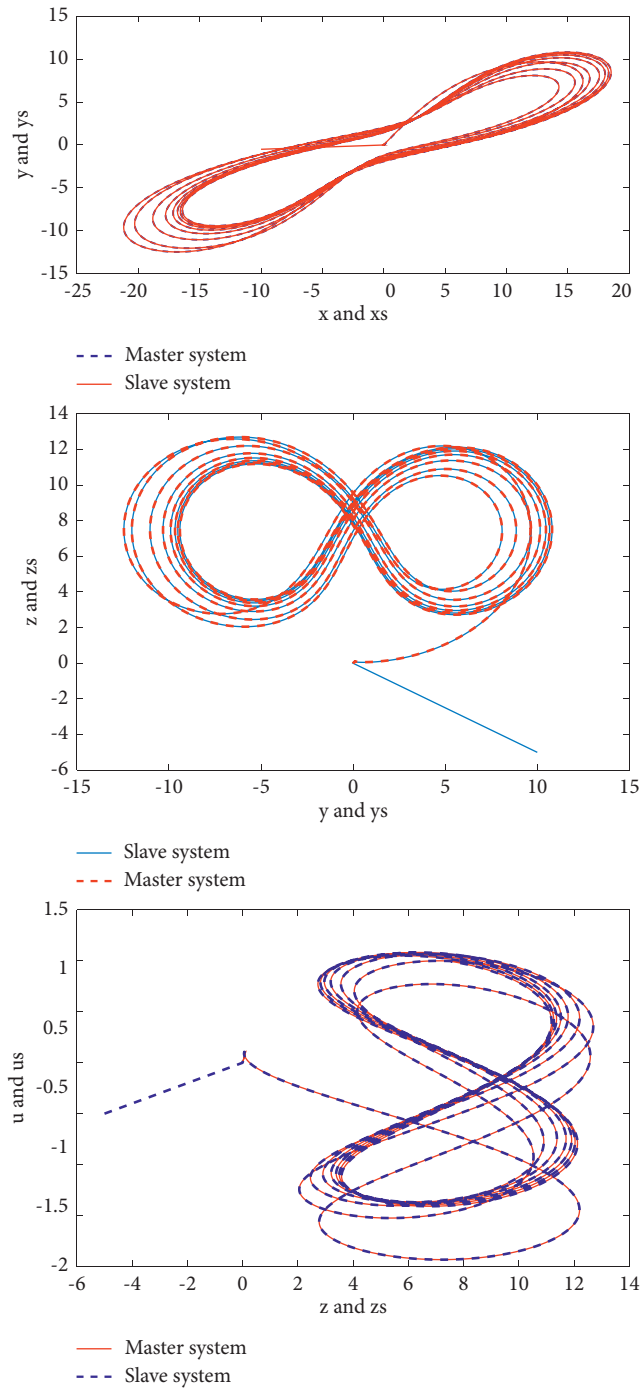
Figure 13: Some of the synchronized phase spaces projected to different planes.
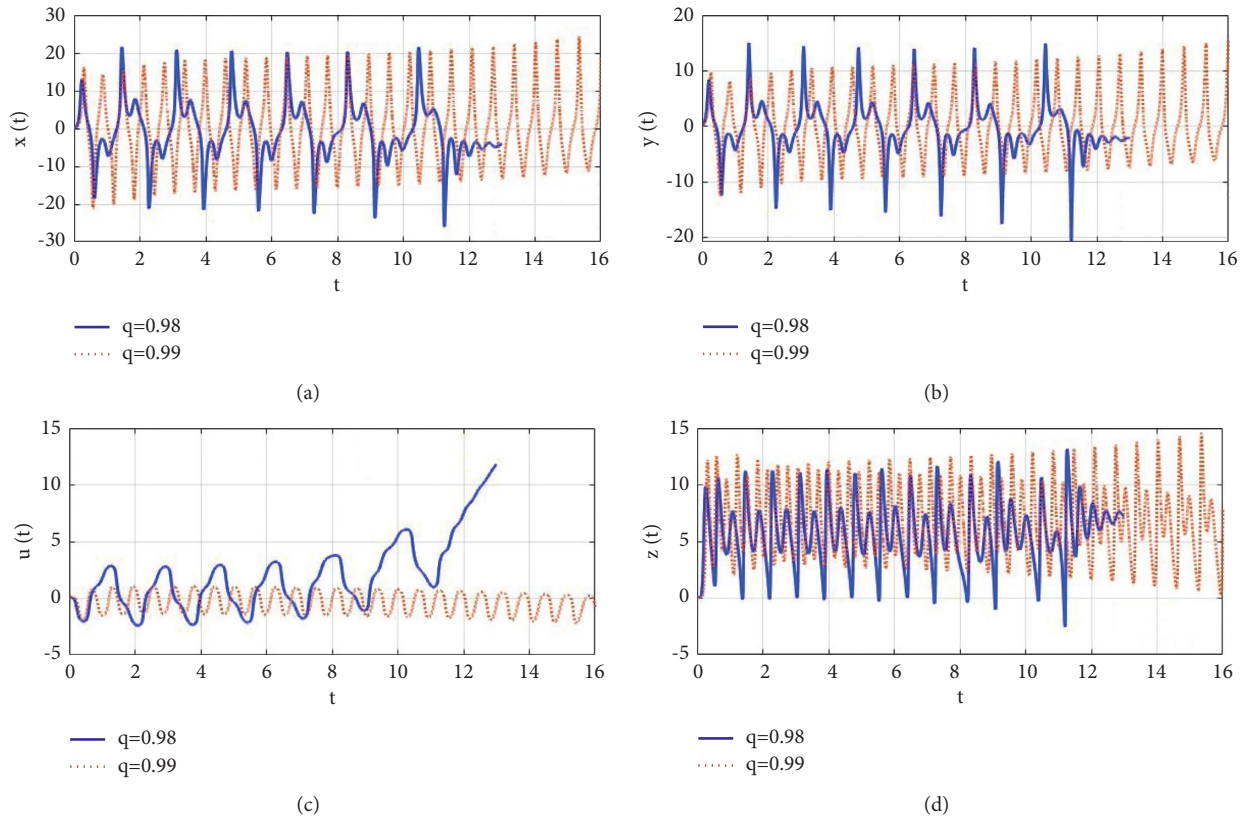
FIGURE 14: Some of the time series orbits of the system (25) due to different fractional-order derivatives.

where

$$
H.\zeta = \begin{pmatrix} -30 & -14.5 & 0 & 0 & 0.5 \\ -14.5 & -21 & 0 & 4.5 & 0 \\ 0 & 0 & -13 & 0 & 0 \\ 0 & 4.5 & 0 & -5 & 0 \\ 0.5 & 0 & 0 & 0 & -5 \end{pmatrix} \begin{pmatrix} e_1 \\ e_2 \\ e_3 \\ e_4 \\ e_5 \end{pmatrix}. \tag{49}
$$

The choice of the matrix H is arbitrary except that all of its eigenvalues must satisfy the Matignon criteria of stability (40).

Then, the error dynamics become

$$
\begin{pmatrix} {}^{ABC}_{0}D^{q}_{t}e_{10} & {}^{ABC}D^{q}_{t}e_{20} & {}^{ABC}D^{q}_{t}e_{30} & {}^{ABC}D^{q}_{t}e_{40} & {}^{ABC}D^{q}_{t}e_{5} \end{pmatrix} = \begin{pmatrix} -30 & -14.5 & 0 & 0 & 0.5 \\ -14.5 & -21 & 0 & 4.5 & 0 \\ 0 & 0 & -13 & 0 & 0 \\ 0 & 4.5 & 0 & -5 & 0 \\ 0.5 & 0 & 0 & 0 & -5 \end{pmatrix} \begin{pmatrix} e_1 \\ e_2 \\ e_3 \\ e_4 \\ e_5 \end{pmatrix}. \tag{50}
$$

The eigenvalues of matrix H are -40.8876, -13.0000, -12.1143, -4.9900, and -3.0081, and all the eigenvalues satisfy Matignon criteria, and thus the error dynamics are asymptotically stable.

Now the slave system is given by

$$
\begin{aligned}
{}_{0}^{\mathrm{ABC}}D_t^q x_s(t) &= 44.5y - 0.002x + 4yz - 0.5u - 0.0006xu^2 - 30x_s - 14.5y_s + 0.5u_s, \\
{}_{0}^{\mathrm{ABC}}D_t^q y_s(t) &= 13.5x + 37y - xz - 3.5w - 14.5x_s - 21y_s + 4.5w_s, \\
{}_{0}^{\mathrm{ABC}}D_t^q z_s(t) &= 7z + xy - xu - yw - 13z_s, \\
{}_{0}^{\mathrm{ABC}}D_t^q w_s(t) &= 5w + 0.15xz - 14.5y - 0.3zu + 4.5y_s - 5w_s, \\
{}_{0}^{\mathrm{ABC}}D_t^q u_s(t) &= -1.5x + 5u + 0.5x_s - 5u_s.
\end{aligned}
\tag{51}
$$

The numerical simulation that verified a strong correlation between the master and the slave system in the form of phase space, time-series orbits, and the error dynamics are depicted in Figures 11–13. The numerical approximation for fractional order system (25) given in equations (35)–(39) is adapted to simulate each of the error dynamics (50), the master system (44), and slave system (51). The simulation results are shown in Figures 11–13. The parameter values and derivative order used are $a = 0.1, b = 0.01, \beta_1 = 30, \beta_2 = 8$, and $q = 0.99$. The initial condition used for master systems is (0.11, 0.11, 0.11, 0.11, 0.11), and it is (−10, 10, −5, −0.5, −0.5) for the slave system. The error graphs indicate fast synchronization of the slave and master systems.

10. Conclusion

In this study, a 5-dimensional memristor-based hyperchaotic circuit in the context of the fractional operator was considered and different qualitative and quantitative analyses are made: numerical approximation of the solution, bifurcation diagrams, Lyapunov exponents for different fractional orders, and parameter values are used to investigate the nature of the solution and chaotic system. The system is found to be hyperchaotic. Sensitivity to initial conditions and sensitivity to parameter value changes were found to cause a significant effect on the dynamics of the system. Furthermore, in the course of making several simulation results on the dynamics of the system, the hyperchaotic system is sensitive to almost any change made in the system including time scale increment change used in the study. The sensitivity of the system to fractional derivative order is very strong in the sense that the simulation results for $q = 0.98$ and 0.99 are significantly different (see Figures 2, 3, and 14). This is perhaps related to the contraction rate of volumes due to the different fractional-order derivatives. The magnitude of the sum of all the LEs corresponding to different fractional-order derivatives decreases as the order of the derivative increases for the case of the hyperchaotic system considered in this study (see Table 1). This requires further investigation. Synchronization of the system is also established and exhibited a strong agreement. The dependence of synchronization on the fractional derivative orders and variation of parameters needs further investigation.

Data Availability

No datasets were generated or analyzed during the current study.

Conflicts of Interest

The authors declare that they have no conflicts of interest.

Authors' Contributions

The authors declare that the study was realized in collaboration with equal responsibility. All authors read and approved the final manuscript.

Acknowledgments

References

[1] N. Sene, "Generalized Mittag-Leffler input stability of the fractional-order electrical circuits," *IEEE Open Journal of Circuits and Systems*, vol. 1, pp. 233–242, 2020.

[2] H. Mohammadi, S. Kumar, S. Rezapour, and S. Etemad, "A theoretical study of the Caputo-Fabrizio fractional modeling for hearing loss due to Mumps virus with optimal control," *Chaos, Solitons & Fractals*, vol. 144, Article ID 110668, 2021.

[3] D. Baleanu, A. jajarmi, H. Mohammadi, and S. Rezapour, "A new study on the mathematical modelling of human liver with Caputo-Fabrizio fractional derivative," *Chaos, Solitons & Fractals*, vol. 134, Article ID 109705, 2020.

[4] D. Baleanu, S. Etemad, and S. Rezapour, "A hybrid Caputo fractional modeling for thermostat with hybrid boundary value conditions," *Boundary Value Problems*, vol. 2020, no. 1, Article ID 64, 2020.

[5] T. Li and Y. Wang, "Stability of a class of fractional-order nonlinear systems," *Discrete Dynamics in Nature and Society*, vol. 2014, Article ID 724270, 2014.

[6] H. Khan, J. F. Gómez-Aguilar, A. Alkhazzan, and A. Khan, "A fractional order HIV-TB coinfection model with nonsingular Mittag-Leffler Law," *Mathematical Methods in the Applied Sciences*, vol. 43, no. 6, pp. 3786–3806, 2020.

[7] C. T. Deressa and G. F. Duressa, "Analysis of Atangana-Baleanu fractional-order SEAIR epidemic model with optimal

control," *Advances in Difference Equations*, vol. 2021, Article ID 174, 25 pages, 2021.

[8] A. H. Assi, *Engineering Education and Research Using MATLAB*, Intech Open, London, UK, 2011.

[9] M. E. Koksal, "Stability analysis of fractional differential equations with unknown parameters," *NAMC*, vol. 24, no. 2, pp. 224–240, 2019, https://www.journals.vu.lt/nonlinear-analysis/article/view/12899.

[10] M. Emir Koksal, "Time and frequency responses of non-integer order RLC circuits," *AIMS Mathematics*, vol. 4, no. 1, pp. 64–78, 2019.

[11] M. E. Koksal, M. Senol, and A. K. Unver, "Numerical simulation of power transmission lines," *Chinese Journal of Physics*, vol. 59, pp. 507–524, 2019.

[12] Y. Li, X. Huang, and M. Guo, "The generation, analysis, and circuit implementation of a new memristor based chaotic system," *Mathematical Problems in Engineering*, vol. 2013, Article ID 398306, 2013.

[13] A. Atangana and K. M. Owolabi, "New numerical approach for fractional differential equations," *Mathematical Modelling of Natural Phenomena*, vol. 13, no. 1, pp. 1–21, 2018.

[14] N. Sene, "Study of a fractional-order chaotic system represented by the Caputo operator," *Complexity*, vol. 2021, Article ID 5534872, 2021.

[15] N. Sene, "Analysis of a fractional-order chaotic system in the context of the Caputo fractional derivative via bifurcation and Lyapunov exponents," *Journal of King Saud University Science*, vol. 33, no. 1, Article ID 101275, 2021.

[16] N. Sene, "Introduction to the fractional-order chaotic system under fractional operator in Caputo sense," *Alexandria Engineering Journal*, vol. 60, no. 4, pp. 3997–4014, 2021.

[17] N. Sene, "Qualitative analysis of class of fractional-order chaotic system via bifurcation and Lyapunov exponent notions," *Journal of Mathematics*, vol. 2021, Article ID 5548569, 2021.

[18] N. Sene, "Mathematical views of the fractional Chua's electrical circuit described by the Caputo-Liouville derivative," *Revista Mexicana de Física*, vol. 67, no. 1, pp. 91–99, 2021.

[19] I. Petras, *Fractional-order Nonlinear Systems: Modeling, Analysis and Simulation*, Springer-Verlag, Berlin, Heidelberg, 2011.

[20] K. Sun, X. Wang, and J. C. Sprott, "Bifurcations and chaos in fractional-order simplified Lorenz system," *International Journal of Bifurcation and chaos*, vol. 20, no. 4, pp. 1209–1219, 2010.

[21] K. M. Owolabi and A. Atangana, "On the formulation of Adams-Bashforth scheme with Atangana-Baleanu- Caputo fractional derivative to model chaotic problems," *Chaos (Woodbury, N.Y.)*, vol. 29, no. 2, Article ID 023111, 2019.

[22] A. Buscarino, L. Fortuna, M. Frasca, and L. V. Gambuzza, "A chaotic circuit based on Hewlett-Packard memristor," *Chaos (Woodbury, N.Y.)*, vol. 22, Article ID 023136, 2012.

[23] J. Ruan, K. Sun, J. Mou, S. He, and L. Zhang, "Fractional-order simplest memristor-based chaotic circuit with new derivative," *The European Physical Journal Plus*, vol. 133, Article ID 3, 2018.

[24] R. Wang, M. Li, Z. Gao, and H. Sun, "A new memristor-based 5D chaotic system and circuit implementation," *Complexity*, vol. 2018, Article ID 6069401, 2018.

[25] M. Toufik and A. Atangana, "New numerical approximation of fractional derivative with non-local and nonsingular kernel: application to chaotic models," *The European Physical Journal Plus*, vol. 132, no. 10, p. 444, 2017.

[26] M. F. Danca and N. Kuznetsov, "Matlab code for Lyapunov exponents of fractional-order systems," *International Journal of Bifurcation and Chaos*, vol. 28, no. 05, Article ID 1850067, 2018.

[27] W. Rui, S. Hui, W. Jie-Zhi, W. Lu, and W. Yan-Chao, "Applications of modularized circuit designs in a new hyperchaotic system circuit implementation," *Chinese Physics B*, vol. 24, no. 2, Article ID 020501, 2015.

[28] A. Atangana and S. İğret Araz, "New numerical method for ordinary differential equations: Newton polynomial," *Journal of Computational and Applied Mathematics*, vol. 372, Article ID 112622, 2020.

[29] A. Atangana and D. Baleanu, "New fractional derivatives with nonlocal and non-singular kernel: theory and application to heat transfer model," *Thermal Science*, vol. 20, no. 2, pp. 763–769, 2016.

[30] T. Abdeljawad and D. Baleanu, "Integration by parts and its applications of a new nonlocal fractional derivative with Mittag-Leffler nonsingular kernel," *Journal of Nonlinear Sciences and Applications*, vol. 10, no. 03, pp. 1098–1107, 2017.

[31] N. Sene and A. Ndiaye, "On class of fractional-order chaotic or hyperchaotic systems in the context of the Caputo fractional-order derivative," *Journal of Mathematics*, vol. 2020, Article ID 8815377, 2020.

[32] A. Granas and J. Dugundji, "Elementary fixed point theorems," in *Fixed Point Theory*Springer, New York, NY, USA, 2003.

[33] L. M. Pecora and T. L. Carroll, "Synchronization in chaotic systems," *Physical Review Letters*, vol. 64, no. 8, pp. 821–824, 1990.

[34] S. H. Strogatz, *Nonlinear Dynamics and Chaos (With Applications to Physics, Biology, Chemistry, and Engineering)*, p. 498, Addison-Wesley, Reading, MA, USA, 1994.

Research Article

Nonfragile Synchronization of Semi-Markovian Jumping Neural Networks with Time Delays via Sampled-Data Control and Application to Chaotic Systems

K. Sivaranjani [ID],[1] **M. Sivakumar** [ID],[2] **S. Dharani** [ID],[3] **K. Loganathan** [ID],[4]
and Ngawang Ngmgyel [ID][5]

[1]*Department of Mathematics, Karunya Institute of Technology and Sciences, Coimbatore 641 114, Tamilnadu, India*
[2]*Department of Mathematics, PSG College of Technology, Coimbatore 641 004, Tamilnadu, India*
[3]*Department of Mathematics, Bannari Amman Institute of Technology and Sciences, Erode 638 401, Tamilnadu, India*
[4]*Department of Mathematics and Statistics, Manipal University Jaipur, Jaipur, Rajasthan, India*
[5]*Jigme Namgyel Engineering College, Royal University of Bhutan, Dewathang, Thimphu, Bhutan*

Correspondence should be addressed to K. Loganathan; loganathankaruppusamy304@gmail.com and Ngawang Ngmgyel;
ngawangnamgyel@jnec.edu.bt

This study discusses the synchronization problem for delayed neural networks with semi-Markovian jumping parameters. With the support of Jenson's inequality and Writinger-based integral inequality, a suitable Lyapunov–Krasovskii functional was constructed, and a synchronization criterion for the considered system was derived in the form of LMIs. In order to cope with system uncertainties, the nonfragile controller was taken into account. Also, sampled-data controller is used to improve the effectiveness of the bandwidth usage. In order to achieve the benefits of both control techniques, the nonfragile sampled-data controller was considered for synchronization of semi-Markovian jumping neural networks and to assure that the error system is asymptotically stable. At last, numerical simulations are exhibited to validate the proposed technique.

1. Introduction

Due to their effective implementation in cryptography, image analysis, associative memory, model identification, and so on, more attention has been given to different neural network (NN) models over the past centuries [1–4]. In latest years, the stability assessment of the constructed networks has appeared as a significant study subject due to the dynamic nature of these applications. In many of the engineering and neural systems, the communication transmission in a network is frequently interrupted by some exterior factors, which may direct to adverse dynamic behaviors such as oscillation and instability, and there arises time-delay. In addition to the fact that time delays in NNs are unavoidable, the literature has explored the stability assessment of delayed NNs well [5–8]. For example,

synchronization problem for coupled inertial networks with reaction diffusion terms and time-varying delays via pinning sampled-data control has been considered in [5]. Finite time synchronization of drive response networks with discontinuous nodes and noise distribution has been analyzed in [9]. H_∞ filtering problem for fuzzy stochastic NNs with mixed time-delays has been investigated in [10].

In the actual application, since the system's state equation tends to have some randomness, a linear time-invariant system cannot generally describe such systems. The Markov jump system, however, can describe such dynamic systems accurately, which has led to extensive research by scholars [11, 12]. Since the jump time of a Markov chain is exponentially distributed, Markovian jumping parameters have severe limitations in applications. A semi-Markovian process is a continuous stochastic process whose sojourn

time fits a variety of probability distributions, such as the Weibull and Gaussian distributions. As a result of the relaxed conditions on the probability distributions, semi-Markovian jumping parameters are more general than Markovian jumping parameters in modelling realistic systems. Semi-MJSs have a fixed matrix of transition probabilities and a matrix of sojourn time probability density functions, while Markovian jumping systems (MJSs) have constant transition rates. This means that the transition rates in S-MJSs are time-varying. Due to these advantages, researchers paid their attention towards semi-Markovian jumping systems [13–16]. Recently, in [17], stochastic synchronization problem for semi-Markovian jumping Lure's system with packet dropouts subject to multiple sampling periods has been discussed. In [18], network-based nonlinear semi-Markovian jump systems with randomly occurring parameter uncertainties and transmission delay have been taken into account. Event-triggered synchronization problem for semi-Markovian jumping complex dynamical networks with a reliable control technique has been investigated in [19].

To stabilize the NNs, there are many control techniques such as impulsive control [20, 21], feedback control [22], sampled-data control [23–25], intermittent control [26, 27], and so on. It should be noted that the sampled-data control will improve the efficacy of the use of bandwidth by radically deducing the amount of information transmitted. Analog signal processing techniques are frequently replaced by digital signal processing techniques to achieve improved efficiency, reliability, and precision, in addition to the hasty developments in discrete measurement and intelligent instruments. Sampled-data control systems are continuous-time systems operated by a digital controller, and they are usually made up of continuous-time plants to be controlled, a discrete-time controller to control them, and an ideal sampler and ZOH to transform continuous-time signals into discrete-time signals and vice versa. The sampled-data systems are hybrid in nature because they operate in the continuous-time domain with both continuous-time and discrete-time signals. One of the discrete controllers, the sampled-data control system, allows control signals to adjust only at discrete sampling, resulting in a significant reduction in communication traffic and energy savings. As a result, sampled-data controllers have received a lot of attention in recent decades, with related findings published in the literature [28, 29].

Practically, the designed controller should be able to tolerate some uncertainties in its coefficients because uncertainty cannot be avoided for many reasons, such as the inherent imprecision in analog systems and additional parameter tuning in the final implementation of the controller. Due to this fact, the nonfragile controller has been studied by

many researchers [30–32]. Nonfragile synchronization for chaotic time-delay neural networks with semi-Markovian jump parameters has been discussed in [32]. Synchronization stability criteria for delay-coupled fractional-order complex Cohen–Grossberg neural networks under parameter uncertainties are discussed in [33].

By the impact of the preceding facts, this manuscript discusses the synchronization problem for SMJNN with hybrid control strategy. At first, synchronization analysis has been performed to consider SMJNNs with recently introduced integral inequality techniques and proposed control strategy. Later, the synchronization criteria for SMJNNs have been explored with the nonfragile control technique. Finally, in numerical simulations, chaotic NNs are considered to verify the designed control technique.

The main contributions and features of this study are presented as follows:

(i) Distinguished from the previous works, this article aims to study the synchronization issue for SMJNNs with time delays by using nonfragile sampled-data control

(ii) Moreover, in an aim to enjoy the benefits of the nonfragile control technique and sampled-data control technique, the nonfragile sampled-data control which has the features of both control techniques has been adopted for achieving synchronization

(iii) By utilizing novel integral inequalities and designed controller, synchronization criteria have been given in the form of LMIs. The resulting LMIs are solved with the help of Matlab LMI toolbox.

(iv) Finally, numerical simulations are presented to validate the correctness of the proposed control technique

2. Problem Formulation

Let $\{\beta(t), t \geq 0\}$ be a discrete-state continuous-time semi-Markov process and assume the values in the finite set $= \{1, 2, \ldots, N\}$ are given by

$$\Pr\{\beta(t+l) = j \mid \beta(t) = i\} = \begin{cases} \alpha_{ij}(l)l + o(l) & i \neq j \\ 1 + \alpha_{ii}(l)l + o(l) & i = j \end{cases},$$

(1)

where $\Delta = \alpha_{ij}(l)$ denotes the transition probability matrix, $\lim_{l \to 0}(o(l)/l) = 0$, and $\alpha_{ij}(l) \geq 0$, for $i \neq j$, is the transition rate from mode i at time t to mode j at time $t + l$, and $\alpha_{ii}(l) = \sum_{j \in S, j \neq i} \alpha_{ij}(l)$.

Consider the SMJ-delayed neural networks:

$$\dot{\zeta}(t) = -D(\beta(t))\zeta(t) + A(\beta(t))f(\zeta(t)) + B(\beta(t))f(\zeta(t - \varrho(t))) + J(t),$$

(2)

where $\zeta(t) = (\zeta_1(t), \zeta_2(t), \ldots, \zeta_n(t))$ represents the state vector. $f(x(t)) = (f_1(x(t)), \ldots, f_n(x(t)))$ stands for neuron activation function and $\tau(t)$ is the time-varying delay with

$0 \le \varrho(t) \le \varrho$. $D = \text{diag}\{d_1, d_2, \ldots, d_n\}$ with $d_i > 0$. A and B are connection and delayed connection weight matrices. The external input is denoted by $J(t)$. The slave system is described as

$$\dot{\xi}(t) = -D(\beta(t))\xi(t) + A(\beta(t))f(\xi(t)) + B(\beta(t))f(\xi(t - \varrho(t))) + J(t) + u(t), \tag{3}$$

where $u(t) \in R^n$ is the control input. By letting the error as $\psi(t) = \zeta(t) - \xi(t)$, the error system is

$$\dot{\psi}(t) = -D(\beta(t))\psi(t) + A(\beta(t))f(\psi(t)) + B(\beta(t))f(\psi(t - \varrho(t))) + u(t). \tag{4}$$

Consider the nonfragile sampled-data control as

$$u_i(t) = (K + \Delta K(t))\psi(t_k) = \overline{K}\psi(t_k), \tag{5}$$

where K is the gain matrix to be designed, and t_k denotes the sampling instant and satisfies $0 = t_0 < t_1 < \cdots < t_k < \cdots < \lim_{k \to \infty} t_k$. $\Delta K(t)$ stands for the controller gain fluctuations. It takes the form

$$\Delta K(t) = MF(t)N, \tag{6}$$

where $F^T(t)F(t) \le I$. Using the input-delay approach $t - t_k = \sigma(t)$, $t_k \le t < t_{k+1}$, and $0 < \sigma(t) < \sigma$, then the controller becomes

$$u_i(t) = \overline{K}\psi(t - \sigma(t)). \tag{7}$$

Then, (4) can be written as

$$\dot{\psi}(t) = -D(\beta(t))\psi(t) + A(\beta(t))f(\psi(t)) + B(\beta(t))f(\psi(t - \varrho(t))) + \overline{K}\psi(t - \sigma(t)). \tag{8}$$

Lemma 1 (see [34]). *For any two scalars $v_2 \ge v_1 > 0$, constant matrix $H \in \mathbb{R}^{n \times n}$, $H = H^T > 0$, such that the integrations concerned are well defined:*

$$-(v_2 - v_1)\int_{t-v_2}^{t-v_1} \xi^T(s)H\xi(s)ds \le -\left(\int_{t-v_2}^{t} \xi(s)ds\right)^T H\left(\int_{t}^{t-v_1} \xi(s)ds\right). \tag{9}$$

Lemma 2 (see [35]). *For any matrix $E \in \mathbb{R}^{n \times m}$, $E = E^T > 0$, differentiable function θ from $[a, b] \longrightarrow \mathbb{R}^n$, the succeeding inequality holds:*

$$\int_a^b \dot{z}^T(s)E\dot{z}(s)ds \ge \frac{\vartheta^T\left[\Upsilon_1^T E\Upsilon_1 + \pi^2\Upsilon_2^T E\Upsilon_2\right]\vartheta}{b - a}, \tag{10}$$

where $\vartheta = [z^T(b) z^T(a) \int_a^b ((z^T(s))/(b-a))ds]^T$, $\Upsilon_1 = [I - I0]$, and $\Upsilon_2 = [(I/2)(I/2) - I]$.

Lemma 3 (see [36]). *Let $S = S^T$, U and V be the real constant matrices of appropriate dimensions $S + UF(t)V + V^T F^T(t)U^T < 0$ for F, satisfying $F^T(t)F(t) = I$ if and only if there exists a scalar $\varepsilon > 0$, such that $S + \varepsilon^{-1}UU^T + \varepsilon V^T V < 0$.*

Assumption 1. Each activation function $f_i(\cdot)$ is continuous and bounded and there exist constants F_i^- and F_i^+ such that

$$F_i^- \le \frac{f_i(k_1) - f_i(k_2)}{k_1 - k_2} \le F_i^+, \quad i = 1, 2, \ldots, n, \tag{11}$$

where $k_1, k_2 \in R$ and $k_1 \ne k_2$.

3. Nonfragile Sampled-Data Synchronization

This section derives some sufficient conditions for the synchronization of considered system (8), which can be seen through the subsequent theorem.

Theorem 1. *The system (8) is asymptotically synchronized, if there exist matrices $\mathfrak{P} > 0, \mathfrak{Q}_1 > 0, \mathfrak{Q}_2 > 0, \mathfrak{R}_1 > 0, \mathfrak{R}_2 > 0, \mathfrak{Z}_1 > 0, \mathfrak{Z}_2 > 0$ and matrices S, L, G, for a given scalar γ, such that the following LMI holds:*

$$\Upsilon(\delta) < 0, \tag{12}$$

where

$$\Upsilon_{1,1} = 2\mathfrak{P} + \mathfrak{Q}_1 + \mathfrak{Q}_3 + \tau_1^2 \mathfrak{R}_1 + \varrho \mathfrak{R}_2 + \frac{\varrho^2}{4}\mathfrak{T}_1 + \mathfrak{Z}_1$$

$$- 2GD_i - \left(\mathfrak{Z}_2 + \frac{\pi^2}{4}\mathfrak{Z}_2\right)$$

$$- \left(\mathfrak{R}_1 + \frac{\pi^2}{4}\mathfrak{R}_1\right) - F_1\Lambda_{1i} + \sum_{j=1}^{N} \alpha_{ij}(\delta)\mathfrak{P}_j,$$

$$\Upsilon_{1,2} = GA_i + F_2\Lambda_{1i},$$

$$\Upsilon_{1,3} = GB_i,$$

$$\Upsilon_{1,4} = G\overline{K} + \mathfrak{Z}_2 - \frac{\pi^2}{4}\mathfrak{Z}_2,$$

$$\Upsilon_{1,5} = \mathfrak{R}_1 - \frac{\pi^2}{4}\mathfrak{R}_1,$$

$$\Upsilon_{1,7} = -G + \mathfrak{P}_i,$$

$$\Upsilon_{1,9} = \frac{\pi^2}{4}\frac{1}{\varrho}\mathfrak{R}_1,$$

$$\Upsilon_{1,12} = -\frac{\pi^2}{2}\mathfrak{Z}_2,$$

$$\Upsilon_{2,2} = -\Lambda_{1i} + \mathfrak{Q}_2,$$

$$\Upsilon_{2,5} = F_2\widetilde{\Lambda}_{2i},$$

$$\Upsilon_{2,7} = GA_i,$$

$$\Upsilon_{3,3} = (1 - \mu)\mathfrak{Q}_2,$$

$$\Upsilon_{3,7} = \gamma GB_i,$$

$$\Upsilon_{4,4} = 2\left(-\mathfrak{Z}_2 - \frac{\pi^2}{4}\mathfrak{Z}_2\right),$$

$$\Upsilon_{4,7} = G\overline{K},$$

$$\Upsilon_{5,5} = -\mathfrak{Q}_1 - 2\left(\mathfrak{R}_1 + \frac{\pi^2}{4}\mathfrak{R}_1\right)$$

$$\Upsilon_{5,6} = \mathfrak{R}_1 - \frac{\pi^2}{4}\mathfrak{R}_1,$$

$$\Upsilon_{5,7} = \gamma GB_i,$$

$$\Upsilon_{5,8} = \frac{\pi^2}{4}\mathfrak{R}_1,$$

$$\Upsilon_{5,9} = \frac{\pi^2}{2}\mathfrak{R}_1,$$

$$\Upsilon_{6,6} = -\mathfrak{Q}_3 - \left(\mathfrak{Z}^2 + \frac{\pi^2}{4}\mathfrak{Z}_2\right),$$

$$\Upsilon_{7,7} = \tau^2 \mathfrak{R}_1 + \eta^2 \mathfrak{Z}_2 - 2\gamma G,$$

$$\Upsilon_{8,8} = -\pi^2 \mathfrak{R}_1,$$

$$\Upsilon_{9,9} = -\pi^2 \mathfrak{R}_1,$$

$$\Upsilon_{10,10} = -\mathfrak{Z}_1 - \mathfrak{Z}_2 - \frac{\pi^2}{4}\mathfrak{Z}_2,$$

$$\Upsilon_{10,11} = \frac{\pi^2}{2}\mathfrak{Z}_2,$$

$$\Upsilon_{11,11} = -\pi^2 \mathfrak{Z}_2,$$

$$\Upsilon_{12,12} = -\pi^2 \mathfrak{Z}_2,$$

$$\Upsilon_{13,13} = -\mathfrak{T}_1.$$

$$(13)$$

Proof. Consider the following Lyapunov–Krasovskii functional:

$$\mathfrak{V}(t) = \sum_{i=1}^{5} \mathfrak{V}_i(t), \tag{14}$$

where

$$\mathfrak{B}_1(t) = \psi^T(t)\mathfrak{P}_i\psi(t),$$

$$\mathfrak{B}_2(t) = \int_{t-\varrho(t)}^{t} \psi^T(s)\mathfrak{Q}_1\psi(s)ds + \int_{t-\varrho(t)}^{t} g^T(\psi(s))\mathfrak{Q}_2 g(\psi(s))ds$$

$$+ \int_{t-\varrho}^{t} \psi^T(s)\mathfrak{Q}_3\psi(s)ds,$$

$$\mathfrak{B}_3(t) = \varrho \int_{-\varrho}^{0} \int_{t+\theta}^{t} \dot{\psi}^T(s)\mathfrak{R}_1\dot{\psi}(s)dsd\theta + \int_{-\varrho}^{0} \int_{t+\theta}^{t} \psi^T(s)\mathfrak{R}_2\psi(s)dsd\theta,$$

$$\mathfrak{B}_4(t) = \frac{\varrho}{2} \int_{-\varrho}^{0} \int_{\theta}^{0} \int_{t+\lambda}^{t} \psi^T(s)\mathfrak{T}_1\psi(s)dsd\lambda d\theta,$$

$$\mathfrak{B}_5(t) = \int_{t-\sigma_m}^{t} \psi^T(s)\mathfrak{Z}_1\psi(s)ds + \sigma_m \int_{-\sigma_m}^{0} \int_{t+\theta}^{t} \dot{\psi}^T(s)\mathfrak{Z}_2\dot{\psi}(s)dsd\theta. \tag{15}$$

Calculating the time-derivative of (14) along (8) gives

$$\mathfrak{LB}_1(t) = -2\psi^T(t)\mathfrak{P}_i\psi(t) + \xi^T(t)\sum_{j=1}^{N} \pi_{ij}(\delta)\mathfrak{P}_j\psi(t),$$

$$\mathfrak{LB}_2(t) = \psi^T(t)Q_1\psi(t) - (1-\mu)\psi^T(t-\varrho(t))\mathfrak{Q}_1\psi(t-\varrho(t)) + g^T(\psi(t))\mathfrak{Q}_2 g(\psi(t))$$

$$- (1-\mu)g^T(t-\tau(t))\mathfrak{Q}_2 g(t-\varrho(t)) + \psi^T(t)\mathfrak{Q}_3\psi(t) - \psi^T(t-\varrho)\mathfrak{Q}_3\psi(t-\varrho),$$

$$\mathfrak{LB}_3(t) = \varrho^2\dot{\psi}^T(t)\mathfrak{R}_1\dot{\psi}(t) - \varrho \int_{t-\varrho}^{t} \dot{\psi}^T(s)\mathfrak{R}_1\dot{\psi}(s)ds + \varrho\psi^T(t)\mathfrak{R}_2\psi(t)$$

$$- \int_{t-\varrho}^{t} \psi^T(s)\mathfrak{R}_2\psi(s)ds, \tag{17}$$

$$\mathfrak{LB}_4(t) = \frac{\varrho^4}{4}\psi^T(t)\mathfrak{T}_1\psi(t) - \int_{-\varrho}^{0} \int_{t+\theta}^{t} \psi^T(s)dsd\theta\mathfrak{T}_1 \int_{-\varrho}^{0} \int_{t+\theta}^{t} \psi(s)dsd\theta, \tag{18}$$

$$\mathfrak{LB}_5(t) = \psi^T(s)\mathfrak{Z}_1\psi(s) - \psi^T(t-\sigma_m)\mathfrak{Z}_1\psi(t-\sigma_m) + \sigma_m^2\dot{\psi}^T(t)\mathfrak{Z}_2\dot{\psi}(t)$$

$$- \sigma_m \int_{t-\sigma_M}^{t} \dot{\psi}^T(s)\mathfrak{Z}_2\dot{\psi}(s)ds. \tag{19}$$

From Lemma 1, it follows from equation (19) that

$$-\int_{t-\varrho}^{t} \psi^T(s)\mathfrak{R}_2\psi(s)ds \leq -\frac{1}{\varrho}\begin{bmatrix} \int_{t-\varrho}^{t-\varrho(t)} \psi(s)ds \\ \int_{t-\varrho(t)}^{t} \psi(s)ds \end{bmatrix}^T \begin{bmatrix} \mathfrak{R}_2 & 0 \\ 0 & \mathfrak{R}_2 \end{bmatrix} \begin{bmatrix} \int_{t-\varrho}^{t-\varrho(t)} \psi(s)ds \\ \int_{t-\varrho(t)}^{t} \psi(s)ds \end{bmatrix}. \tag{20}$$

From Lemma 2, (19) becomes

$$-\sigma_m \int_{t-\sigma_m}^{t-\sigma(t)} \dot{\psi}^T(s)\mathfrak{Z}_2\dot{\psi}(s)\mathrm{d}s \leq -\begin{bmatrix} \psi(t-\sigma(t)) \\ \psi(t-\sigma) \\ \dfrac{1}{\sigma}\displaystyle\int_{t-\sigma}^{t-\sigma(t)}\psi(s)\mathrm{d}s \end{bmatrix}^T$$

$$\times \begin{bmatrix} \mathfrak{Z}_2 + \dfrac{\pi^2}{4}\mathfrak{Z}_2 & -Z_2 + \dfrac{\pi^2}{4}\mathfrak{Z}_2 & \dfrac{\pi^2}{4}\mathfrak{Z}_2 \\[2mm] -\mathfrak{Z}_2 + \dfrac{\pi^2}{4}\mathfrak{Z}_2 & Z_2 + \dfrac{\pi^2}{4}\mathfrak{Z}_2 & \dfrac{\pi^2}{2}\mathfrak{Z}_2 \\[2mm] -\dfrac{\pi^2}{4}\mathfrak{Z}_2 & -\dfrac{\pi^2}{4}\mathfrak{Z}_2 & \pi^2\mathfrak{Z}_2 \end{bmatrix}\begin{bmatrix} \psi(t-\sigma(t)) \\ \psi(t-\sigma) \\ \dfrac{1}{\sigma}\displaystyle\int_{t-\sigma}^{t-\sigma(t)}\psi(s)\mathrm{d}s \end{bmatrix} \tag{21}$$

and

$$-\sigma_m \int_{t-\sigma(t)}^{t} \dot{\psi}^T(s)\mathfrak{Z}_2\dot{\psi}(s)\mathrm{d}s \leq \begin{bmatrix} \psi(t) \\ \psi(t-\sigma(t)) \\ \dfrac{1}{\sigma}\displaystyle\int_{t-\sigma(t)}^{t}\psi(s)\mathrm{d}s \end{bmatrix}^T$$

$$\times \begin{bmatrix} \mathfrak{Z}_2 + \dfrac{\pi^2}{4}\mathfrak{Z}_2 & -\mathfrak{Z}_2 + \dfrac{\pi^2}{4}\mathfrak{Z}_2 & -\dfrac{\pi^2}{4}\mathfrak{Z}_2 \\[2mm] -\mathfrak{Z}_2 + \dfrac{\pi^2}{4}\mathfrak{Z}_2 & \mathfrak{Z}_2 + \dfrac{\pi^2}{4}\mathfrak{Z}_2 & \dfrac{\pi^2}{2}\mathfrak{Z}_2 \\[2mm] -\dfrac{\pi^2}{4}\mathfrak{Z}_2 & -\dfrac{\pi^2}{4}\mathfrak{Z}_2 & \pi^2\mathfrak{Z}_2 \end{bmatrix}\begin{bmatrix} \psi(t) \\ \psi(t-\sigma(t)) \\ \dfrac{1}{\sigma}\displaystyle\int_{t-\sigma(t)}^{t}\psi(s)\mathrm{d}s \end{bmatrix}. \tag{22}$$

From (17), we have

$$\int_{t-\varrho}^{t-\varrho(t)} \dot{\psi}^T(s)\mathfrak{R}_1\dot{\psi}(s)ds \geq \frac{1}{\varrho} \begin{bmatrix} \psi(t-\varrho(t)) \\ \psi(t-\varrho) \\ \frac{1}{\varrho}\int_{t-\varrho(t)}^{t-\varrho(t)}\psi(s)ds \end{bmatrix}^T$$

$$\times \begin{bmatrix} \mathfrak{R}_1 + \frac{\pi^2}{4}\mathfrak{R}_1 & -\mathfrak{R}_1 + \frac{\pi^2}{4}\mathfrak{R}_1 & -\frac{\pi^2}{4}\mathfrak{R}_1 \\ -\mathfrak{R}_1 + \frac{\pi^2}{4}\mathfrak{R}_1 & \mathfrak{R}_1 + \frac{\pi^2}{4}\mathfrak{R}_1 & \frac{\pi^2}{2}\mathfrak{R}_1 \\ -\frac{\pi^2}{4}\mathfrak{R}_1 & -\frac{\pi^2}{4}\mathfrak{R}_1 & \pi^2\mathfrak{R}_1 \end{bmatrix} \begin{bmatrix} \psi(t-\varrho(t)) \\ \psi(t-\varrho) \\ \frac{1}{\varrho}\int_{t-\varrho(t)}^{t-\varrho(t)}\psi(s)ds \end{bmatrix}, \tag{23}$$

and

$$\int_{t-\varrho(t)}^{t} \dot{\psi}^T(s)\mathfrak{R}_1\dot{\psi}(s)ds \geq \frac{1}{\varrho} \begin{bmatrix} \psi(t) \\ \psi(t-\varrho(t)) \\ \frac{1}{\varrho}\int_{t-\varrho(t)}^{t-\varrho(t)}\psi(s)ds \end{bmatrix}^T$$

$$\times \begin{bmatrix} \mathfrak{R}_1 + \frac{\pi^2}{4}\mathfrak{R}_1 & -\mathfrak{R}_1 + \frac{\pi^2}{4}\mathfrak{R}_1 & -\frac{\pi^2}{4}\mathfrak{R}_1 \\ -\mathfrak{R}_1 + \frac{\pi^2}{4}\mathfrak{R}_1 & \mathfrak{R}_1 + \frac{\pi^2}{4}\mathfrak{R}_1 & \frac{\pi^2}{2}\mathfrak{R}_1 \\ -\frac{\pi^2}{4}\mathfrak{R}_1 & -\frac{\pi^2}{4}\mathfrak{R}_1 & \pi^2\mathfrak{R}_1 \end{bmatrix} \begin{bmatrix} \psi(t) \\ \psi(t-\varrho(t)) \\ \frac{1}{\varrho}\int_{t-\varrho(t)}^{t-\varrho(t)}\psi(s)ds \end{bmatrix}. \tag{24}$$

By Assumption 1, for diagonal matrices Λ_{1i} and $\Lambda_2 i$,

$$0 \leq -\psi^T(t)\mathfrak{F}_1\Lambda_{1i}\psi(t) + \psi^T(t)\mathfrak{F}_2\Lambda_{1i}g(\psi(t)) + g^T(\psi(t))\mathfrak{F}_2\widetilde{\Lambda}_{1i}\psi(t) \\ - g^T(\psi(t))\widetilde{\Lambda}_{1i}g(\psi(t)), \tag{25}$$

$$0 \leq -\psi^T(t-\tau(t))\mathfrak{F}_1\Lambda_{2i}\psi(t-\tau(t)) + \psi^T(t-\tau(t))\mathfrak{F}_2\widetilde{\Lambda}_{2i}g(\psi(t-\varrho(t))) \\ + g(\psi(t-\varrho(t)))\mathfrak{F}_2\widetilde{\Lambda}_{2i}\psi(t-\varrho(t)) - g^T(\psi(t-\varrho(t)))\widetilde{\Lambda}_{2i}g(\psi(t-\varrho(t))). \tag{26}$$

For any matrix G, we have

$$0 = 2\left[\psi^T(t)G + \dot{\psi}^T(t)G\right]\left[-\dot{\psi}(t) - D(\beta(t))\psi(t) + A(\beta(t))f(\psi(t))\right.$$
$$\left. + B(\beta(t))f(\psi(t - \varrho(t))) + \overline{K}\psi(t - \sigma(t))\right]. \tag{27}$$

From equations (15)–(27), we have

$$E\{LV(t)\} \leq \chi^T(t)\Upsilon\chi(t) < 0, \tag{28}$$

where

$$\chi(t) = [\psi(t)\ g(\psi(t))\ g(\psi(t - \varrho(t)))\ \psi(t - \sigma(t))\ \psi(t - \varrho(t))\ \psi(t - \varrho)\ \dot{\psi}(t)$$

$$\int_{t-\varrho}^{t-\varrho(t)}\psi(s)ds\ \int_{t-\varrho(t)}^{t}\psi(s)ds\ \psi(t - \sigma)\ \frac{1}{\sigma}\int_{t-\sigma}^{t-\sigma(t)}\psi(s)ds\ \frac{1}{\sigma}\int_{t-\sigma(t)}^{t}\psi(s)ds \tag{29}$$

$$\int_{-\varrho}^{0}\int_{t+\theta}^{t}\psi(s)dsd\theta\Bigg],$$

and the elements of the matrix Υ are given in the statement of theorem.

Based on the above theorem, now we are in a position to design the gain matrix of the derived controller. □

Theorem 2. *The system (8) is asymptotically synchronized, if there exist matrices* $\mathfrak{P} > 0, \mathfrak{Q}_1 > 0, \mathfrak{Q}_2 > 0, \mathfrak{R}_1 > 0,$ $\mathfrak{R}_2 > 0, \mathfrak{Z}_1 > 0, \mathfrak{Z}_2 > 0$ *and matrices* $S, L, G,$ *for a given scalar* $\gamma,$ *such that the following LMI holds:*

$$\begin{bmatrix} \Upsilon(\delta) & \mathfrak{U}_1 & \varepsilon\mathfrak{B}_1 & \mathfrak{U}_2 & \varepsilon\mathfrak{B}_2 \\ * & -\epsilon_1 I & 0 & 0 & 0 \\ * & * & -\epsilon_1 I & 0 & 0 \\ * & * & * & -\epsilon_2 I & 0 \\ * & * & * & * & -\epsilon_2 I \end{bmatrix} < 0, \tag{30}$$

where

$$\Upsilon_{1,1} = 2\mathfrak{P} + \mathfrak{Q}_1 + \mathfrak{Q}_3 + \tau_1^2\mathfrak{R}_1 + \varrho\mathfrak{R}_2 + \frac{\varrho^2}{4}\mathfrak{T}_1 + \mathfrak{Z}_1$$

$$- 2GD_i - \left(\mathfrak{Z}_2 + \frac{\pi^2}{4}\mathfrak{Z}_2\right)$$

$$- \left(\mathfrak{R}_1 + \frac{\pi^2}{4}\mathfrak{R}_1\right) - F_1\Lambda_{1i} + \sum_{j=1}^{N}\pi_{ij}(\delta)\mathfrak{P}_j,$$

$$\Upsilon_{1,2} = GA_i + F_2\Lambda_{1i},$$

$$\Upsilon_{1,3} = GB_i,$$

$$\Upsilon_{1,4} = GK + \mathfrak{Z}_2 - \frac{\pi^2}{4}\mathfrak{Z}_2,$$

$$\Upsilon_{1,5} = \mathfrak{R}_1 - \frac{\pi^2}{4}\mathfrak{R}_1,$$

$$\Upsilon_{1,7} = -G + \mathfrak{P}_i,$$

$$\Upsilon_{1,9} = \frac{\pi^2}{4}\frac{1}{\varrho}\mathfrak{R}_1,$$

$$\Upsilon_{1,12} = -\frac{\pi^2}{2}\mathfrak{Z}_2,$$

$$\Upsilon_{2,2} = -\Lambda_{1i} + \mathfrak{Q}_2,$$

$$\Upsilon_{2,5} = F_2\widetilde{\Lambda}_{2i},$$

$$\Upsilon_{2,7} = GA_i,$$

$$\Upsilon_{3,3} = (1 - \mu)\mathfrak{Q}_2,$$

$$\Upsilon_{3,7} = \gamma GB_i,$$

$$\Upsilon_{4,4} = 2\left(-\mathfrak{Z}_2 - \frac{\pi^2}{4}\mathfrak{Z}_2\right),$$

$$\Upsilon_{4,7} = GK,$$

$$\Upsilon_{5,5} = -\mathfrak{Q}_1 - 2\left(\mathfrak{R}_1 + \frac{\pi^2}{4}\mathfrak{R}_1\right),$$

$$\Upsilon_{5,6} = \mathfrak{R}_1 - \frac{\pi^2}{4}\mathfrak{R}_1,$$

$$\Upsilon_{5,7} = \gamma GB_i,$$

$$\Upsilon_{5,8} = \frac{\pi^2}{4}\mathfrak{R}_1,$$

$$\Upsilon_{5,9} = \frac{\pi^2}{2}\mathfrak{R}_1,$$

$$\Upsilon_{6,6} = -\mathfrak{Q}_3 - \left(\mathfrak{Z}^2 + \frac{\pi^2}{4}\mathfrak{Z}_2\right),$$

$$\Upsilon_{7,7} = \tau^2\mathfrak{R}_1 + \eta^2\mathfrak{Z}_2 - 2\gamma G,$$

$$\Upsilon\Upsilon_{8,8} = -\pi^2\mathfrak{R}_1,$$

$$\Upsilon_{9,9} = -\pi^2 \mathfrak{R}_1,$$

$$\Upsilon_{10,10} = -\mathfrak{Z}_1 - \mathfrak{Z}_2 - \frac{\pi^2}{4}\mathfrak{Z}_2,$$

$$\Upsilon_{10,11} = \frac{\pi^2}{2}\mathfrak{Z}_2,$$

$$\Upsilon_{11,11} = -\pi^2 \mathfrak{Z}_2, \qquad (31)$$

$$\Upsilon_{12,12} = -\pi^2 \mathfrak{Z}_2,$$

$$\Upsilon_{13,13} = -\mathfrak{T}_1.$$

Moreover, the desired gain matrices are computed by $K = LG^{-1}$.

Proof. By making use of $\Delta K(t) = \mathfrak{U}F(t)\mathfrak{B}$, LMI in (12) can be written as

$$\Upsilon_{(i,j),\overline{w}} + \mathfrak{U}_1 F(t)\mathfrak{B}_1 + \mathfrak{B}_1^T F(t)\mathfrak{U}_1^T + \mathfrak{U}_2 F(t)\mathfrak{B}_2 + \mathfrak{B}_2^T F(t)\mathfrak{U}_2, \qquad (32)$$

where

$$\mathfrak{U}_1 = \left[\underbrace{0\cdots 0}_{3} \; G\mathfrak{U} \; \underbrace{0\cdots 0}_{9}\right],$$

$$\mathfrak{U}_2 = \left[\underbrace{0\cdots 0}_{3} \; G\mathfrak{U} \; \underbrace{0\cdots 0}_{9}\right],$$

$$\mathfrak{B}_1 = \left[\mathfrak{B} \; \underbrace{0\cdots 0}_{12}\right], \qquad (33)$$

$$\mathfrak{B}_2 = \left[\underbrace{0\cdots 0}_{6} \; \mathfrak{B} \; \underbrace{0\cdots 0}_{6}\right].$$

From Lemma 3, we have

$$\Upsilon_{(i,j),\overline{w}} + \varsigma_1^{-1}\mathfrak{U}_1\mathfrak{U}_1^T + \varsigma_1\mathfrak{B}_1^T\mathfrak{B}_1 + \varsigma_2^{-1}\mathfrak{U}_2\mathfrak{U}_2^T + \varsigma_2\mathfrak{B}_2^T\mathfrak{B}_2. \qquad (34)$$

Thus, one can get

$$\begin{bmatrix} \Upsilon_{(i,j),\overline{w}} & \mathfrak{U}_1 & \varsigma_1\mathfrak{B}_1 & \mathfrak{U}_2 & \varsigma_2\mathfrak{B}_2 \\ * & -\varsigma_1 I & 0 & 0 & 0 \\ * & * & -\varsigma_1 I & 0 & 0 \\ * & * & * & -\varsigma_2 I & 0 \\ * & * & * & * & -\varsigma_2 I \end{bmatrix}, \quad i = 1, 2, \ldots, s. \qquad (35)$$

Theorem 3. *The system (8) is asymptotically synchronized, if there exist matrices* $\mathfrak{P} > 0, \mathfrak{Q}_1 > 0, \mathfrak{Q}_2 > 0, \mathfrak{R}_1 > 0, \mathfrak{R}_2 > 0,$ $\mathfrak{Z}_1 > 0, \mathfrak{Z}_2 > 0$ *and matrices* $S, L, G,$ *for a given scalar* $\gamma,$ *such that the following LMI holds:*

$$\begin{bmatrix} \Upsilon(\delta) & M_1 & \varsigma_1 N_1 & M_2 & \varsigma_2 N_2 \\ * & -\varsigma_1 I & 0 & 0 & 0 \\ * & * & -\varsigma_1 I & 0 & 0 \\ * & * & * & -\varsigma_2 I & 0 \\ * & * & * & * & -\varsigma_2 I \end{bmatrix} < 0, \qquad (36)$$

where

$$\Upsilon_{1,1} = 2\mathfrak{P} + \mathfrak{Q}_1 + \mathfrak{Q}_3 + \tau_1^2\mathfrak{R}_1 + \varrho\mathfrak{R}_2 + \frac{\varrho^2}{4}\mathfrak{T}_1 + \mathfrak{Z}_1$$

$$- 2GD_i - \left(\mathfrak{Z}_2 + \frac{\pi^2}{4}\mathfrak{Z}_2\right)$$

$$- \left(\mathfrak{R}_1 + \frac{\pi^2}{4}\mathfrak{R}_1\right) - F_1\Lambda_{1i} + \sum_{j=1}^{N}\pi_{ij}(\delta)\mathfrak{P}_j,$$

$$\Upsilon_{1,2} = GA_i + F_2\Lambda_{1i},$$

$$\Upsilon_{1,3} = GB_i,$$

$$\Upsilon_{1,4} = GK + \mathfrak{Z}_2 - \frac{\pi^2}{4}\mathfrak{Z}_2,$$

$$\Upsilon_{1,5} = \mathfrak{R}_1 - \frac{\pi^2}{4}\mathfrak{R}_1,$$

$$\Upsilon_{1,7} = -G + \mathfrak{P}_i,$$

$$\Upsilon_{1,9} = \frac{\pi^2}{4}\frac{1}{\varrho}\mathfrak{R}_1,$$

$$\Upsilon_{1,12} = -\frac{\pi^2}{2}\mathfrak{Z}_2,$$

$$\Upsilon_{2,2} = -\Lambda_{1i} + \mathfrak{Q}_2,$$

$$\Upsilon_{2,5} = F_2\widetilde{\Lambda}_{2i},$$

$$\Upsilon_{2,7} = GA_i,$$

$$\Upsilon_{3,3} = (1 - \mu)\mathfrak{Q}_2,$$

$$\Upsilon_{3,7} = \gamma GB_i,$$

$$\Upsilon_{4,4} = 2\left(-\mathfrak{Z}_2 - \frac{\pi^2}{4}\mathfrak{Z}_2\right),$$

$$\Upsilon_{4,7} = GK,$$

$$\Upsilon_{5,5} = -\mathfrak{Q}_1 - 2\left(\mathfrak{R}_1 + \frac{\pi^2}{4}\mathfrak{R}_1\right),$$

$$\Upsilon_{5,6} = \mathfrak{R}_1 - \frac{\pi^2}{4}\mathfrak{R}_1,$$

$$\Upsilon_{5,7} = \gamma GB_i,$$

$$\Upsilon_{5,8} = \frac{\pi^2}{4}\mathfrak{R}_1,$$

$$\Upsilon_{5,9} = \frac{\pi^2}{2}\mathfrak{R}_1,$$

$$\Upsilon_{6,6} = -\mathfrak{Q}_3 - \left(\mathfrak{Z}^2 + \frac{\pi^2}{4}\mathfrak{Z}_2\right),$$

$$\Upsilon_{7,7} = \tau^2 \mathfrak{R}_1 + \eta^2 \mathfrak{Z}_2 - 2\gamma G,$$

$$\Upsilon_{8,8} = -\pi^2 \mathfrak{R}_1,$$

$$\Upsilon_{9,9} = -\pi^2 \mathfrak{R}_1,$$

$$\Upsilon_{10,10} = -\mathfrak{Z}_1 - \mathfrak{Z}_2 - \frac{\pi^2}{4}\mathfrak{Z}_2, \qquad (37)$$

$$\Upsilon_{10,11} = \frac{\pi^2}{2}\mathfrak{Z}_2,$$

$$\Upsilon_{11,11} = -\pi^2 \mathfrak{Z}_2,$$

$$\Upsilon_{12,12} = -\pi^2 \mathfrak{Z}_2,$$

$$\Upsilon_{13,13} = -\mathfrak{T}_1.$$

Moreover, the desired gain matrices are given by $K = LG^{-1}.$

Let us assume $\Delta K(t) = 0$; then, the controller in (7) will reduce to the form of sampled-data control. Then, the above theorem can be rewritten.

Theorem 4. *The system (8) is asymptotically synchronized, if there exist matrices* $\mathfrak{P} > 0, \mathfrak{Q}_1 > 0, \mathfrak{Q}_2 > 0, \mathfrak{R}_1 > 0, \mathfrak{R}_2 > 0, \mathfrak{Z}_1 > 0, \mathfrak{Z}_2 > 0$ *and matrices* S, L, G, *for a given scalar* γ, *such that the following LMI holds:*

$$\Upsilon(\delta) < 0, \qquad (38)$$

where

$$\Upsilon_{1,1} = 2\mathfrak{P} + \mathfrak{Q}_1 + \mathfrak{Q}_3 + \tau_1^2 \mathfrak{R}_1 + \varrho \mathfrak{R}_2 + \frac{\varrho^2}{4}\mathfrak{T}_1 + \mathfrak{Z}_1$$

$$- 2G\,D - \left(\mathfrak{Z}_2 + \frac{\pi^2}{4}\mathfrak{Z}_2\right)$$

$$- \left(\mathfrak{R}_1 + \frac{\pi^2}{4}\mathfrak{R}_1\right) - F_1 \Lambda_{1i} + \sum_{j=1}^{N} \pi_{ij}(\delta)\mathfrak{P}_j,$$

$$\Upsilon_{1,2} = GA + F_2 \Lambda_{1i},$$

$$\Upsilon_{1,3} = GB,$$

$$\Upsilon_{1,4} = GK + \mathfrak{Z}_2 - \frac{\pi^2}{4}\mathfrak{Z}_2,$$

$$\Upsilon_{1,5} = \mathfrak{R}_1 - \frac{\pi^2}{4}\mathfrak{R}_1,$$

$$\Upsilon_{1,7} = -G + \mathfrak{P},$$

$$\Upsilon_{1,9} = \frac{\pi^2}{4}\frac{1}{\varrho}\mathfrak{R}_1,$$

$$\Upsilon_{1,12} = -\frac{\pi^2}{2}\mathfrak{Z}_2,$$

$$\Upsilon_{2,2} = -\Lambda_{1i} + \mathfrak{Q}_2,$$

$$\Upsilon_{2,5} = F_2 \tilde{\Lambda}_{2i},$$

$$\Upsilon_{2,7} = GA,$$

$$\Upsilon_{3,3} = (1 - \mu)\mathfrak{Q}_2,$$

$$\Upsilon_{3,7} = \gamma GB,$$

$$\Upsilon_{4,4} = 2\left(-\mathfrak{Z}_2 - \frac{\pi^2}{4}\mathfrak{Z}_2\right),$$

$$\Upsilon_{4,7} = GK,$$

$$\Upsilon_{5,5} = -\mathfrak{Q}_1 - 2\left(\mathfrak{R}_1 + \frac{\pi^2}{4}\mathfrak{R}_1\right),$$

$$\Upsilon_{5,6} = \mathfrak{R}_1 - \frac{\pi^2}{4}\mathfrak{R}_1,$$

$$\Upsilon_{5,7} = \gamma GB, \qquad (39)$$

$$\Upsilon_{5,8} = \frac{\pi^2}{4}\mathfrak{R}_1,$$

$$\Upsilon_{5,9} = \frac{\pi^2}{2}\mathfrak{R}_1,$$

$$\Upsilon_{6,6} = -\mathfrak{Q}_3 - \left(\mathfrak{Z}^2 + \frac{\pi^2}{4}\mathfrak{Z}_2\right),$$

$$\Upsilon_{7,7} = \tau^2 \mathfrak{R}_1 + \eta^2 \mathfrak{Z}_2 - 2\gamma G,$$

$$\Upsilon_{8,8} = -\pi^2 \mathfrak{R}_1,$$

$$\Upsilon_{9,9} = -\pi^2 \mathfrak{R}_1,$$

$$\Upsilon_{10,10} = -\mathfrak{Z}_1 - \mathfrak{Z}_2 - \frac{\pi^2}{4}\mathfrak{Z}_2,$$

$$\Upsilon_{10,11} = \frac{\pi^2}{2}\mathfrak{Z}_2,$$

$$\Upsilon_{11,11} = -\pi^2 \mathfrak{Z}_2,$$

$$\Upsilon_{12,12} = -\pi^2 \mathfrak{Z}_2,$$

$$\Upsilon_{13,13} = -\mathfrak{T}_1.$$

Along with, the controller gain matrices are defined as $G = KL^{-1}.$

Remark 1. In the literature, one can find many control methods for achieving synchronization of neural networks such as pinning control, feedback control, adaptive control, impulsive control, and sampled-data control. Different from

the previous literature, in this work, we employed the novel control technique, namely, nonfragile sampled-data control which includes the benefits of both control techniques for synchronization of SMJNNs. Moreover, switching topology or jump connection often arises in a network due to link failures or new development. In Markovian jumping systems, the jump time is exponentially distributed and also irrelevant to sojourn time which leads some restrictions in the utilization of the network. Thus, semi-Markovian jumping parameters which generalizes Markovian jumping parameters are also taken into account. This shows the novelty of the work.

Remark 2. It is worth noting that fractional calculus has a nearly identical background to traditional calculus. Its applications in physics and engineering, on the other hand, are a relatively new source of interest. Fractional-order models would be more suitable for describing memory and inherited properties of different materials than conventional integer-order models. Many known structures that exhibit fractional dynamics have been found to be useful in interdisciplinary fields such as viscoelasticity, dielectric polarization, electromagnetic waves, and complex system quantum evolution. Due to this reason, fractional-order system has been one of the most promising research topics in recent times. In our future work, the qualitative behaviors of fractional-order systems will be considered.

4. Numerical Simulation

This section displays two numerical examples to highlight the advantages of the theoretical results.

Example 1. Consider the NNs with

$$
\begin{aligned}
D_1 &= \begin{bmatrix} 1.2 & 0 \\ 0 & 0.7 \end{bmatrix}, \\
D_2 &= \begin{bmatrix} 1.1 & 0 \\ 0 & 0.6 \end{bmatrix}, \\
A_1 &= \begin{bmatrix} -1.2 & -2.3 \\ -2.1 & -1.4 \end{bmatrix}, \\
A_2 &= \begin{bmatrix} 1.5 & -1.14 \\ 5.0 & -2.6 \end{bmatrix}, \\
B_1 &= \begin{bmatrix} 3.2 & -5.3 \\ 3.1 & 4.1 \end{bmatrix}, \\
B_2 &= \begin{bmatrix} 2.1 & -1.2 \\ 5.15 & -1.05 \end{bmatrix}.
\end{aligned}
\tag{40}
$$

The nonlinear activation functions are taken as

$$
f_1(\omega) = f_2(\omega) = \tanh(\omega(t)),
\tag{41}
$$

with $\mathfrak{F}_1^+ = \mathfrak{F}_2^+ = 1$ and $\mathfrak{F}_1^- = \mathfrak{F}_2^- = 0$. Then,

$$
\begin{aligned}
F_1 &= \begin{bmatrix} 0 & 0 \\ 0 & 0 \end{bmatrix}, \\
F_2 &= \begin{bmatrix} 0.5 & 0 \\ 0 & 0.5 \end{bmatrix}.
\end{aligned}
\tag{42}
$$

The transition rates are assumed to be $\alpha_{11}(\delta) \in [2.2, 1.8]$, $\alpha_{22}(\delta) \in [-1.9, -1.5]$. From that, we have $\alpha_{11,1} = -2.2$, $\alpha_{11,2} = -1.8$, $\alpha_{22,1} = -1.9$, and $\alpha_{22,2} = -1.5$.

By resolving the LMIs obtained in Theorem 1 and by using the help of Matlab LMI toolbox with the parameters $\varrho = 0.2$, the gain matrix is attained as

$$
K = 10^{-3} \times \begin{bmatrix} -0.2654 & 0.3954 \\ 0.3608 & 0.2513 \end{bmatrix}.
\tag{43}
$$

Figure 1 displays the chaotic nature of the master system and Figure 2 shows the chaotic behavior of the slave system. By applying the designed nonfragile sampled-data control technique, the phase portraits of the error system are shown in Figure 3.

Example 2. Consider the NNs with

$$
\begin{aligned}
D_1 &= \begin{bmatrix} 1.2 & 0 \\ 0 & 1.8 \end{bmatrix}, \\
D_2 &= \begin{bmatrix} 1 & 0 \\ 0 & 1.5 \end{bmatrix}, \\
A_1 &= \begin{bmatrix} -3.7 + \dfrac{\pi}{4} & 4.1 \\ 3.0 & -4.8 + \dfrac{\pi}{4} \end{bmatrix}, \\
A_2 &= \begin{bmatrix} -3.7 + \dfrac{\pi}{4} & 4.1 \\ 3.0 & -4.8 + \dfrac{\pi}{4} \end{bmatrix}, \\
B_1 &= \begin{bmatrix} -0.1\sqrt{(2)}\ \dfrac{\pi}{4} & -3.6 \\ 1.8 & -3.1\sqrt{(2)}\ \dfrac{\pi}{4} \end{bmatrix}, \\
B_2 &= \begin{bmatrix} -0.1\sqrt{(2)}\ \dfrac{\pi}{4} & -3.6 \\ 1.8 & -3.1\sqrt{(2)}\ \dfrac{\pi}{4} \end{bmatrix}.
\end{aligned}
\tag{44}
$$

The nonlinear activation function and transition rates are taken as in the previous example. From the LMIs in Theorem 4 with the parameters $\varsigma_1 = \varsigma_2 = 0.2$, $\varrho = 0.5$, one can get the gain matrix
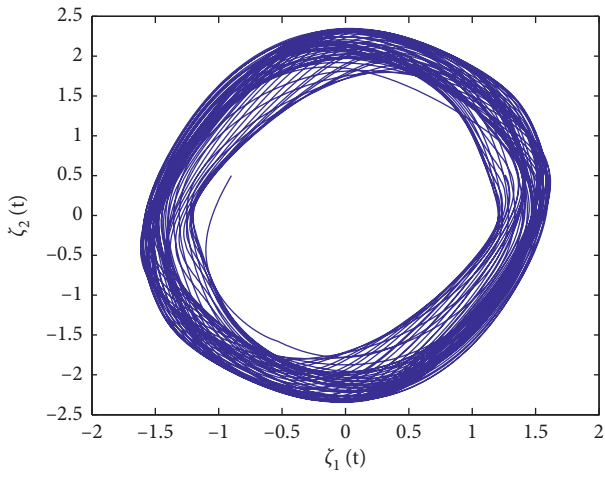
FIGURE 1: Chaotic behavior of the master system.
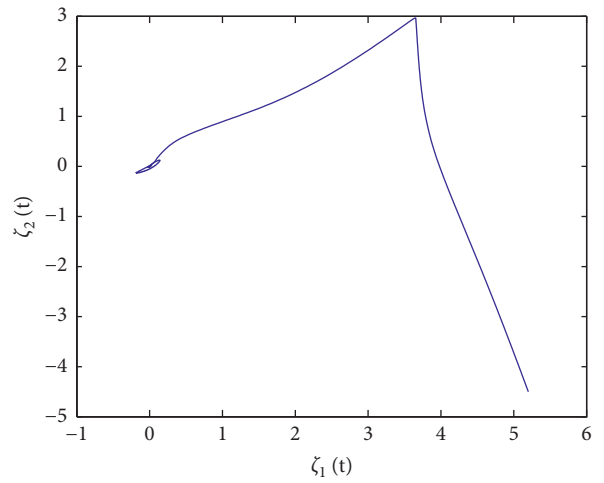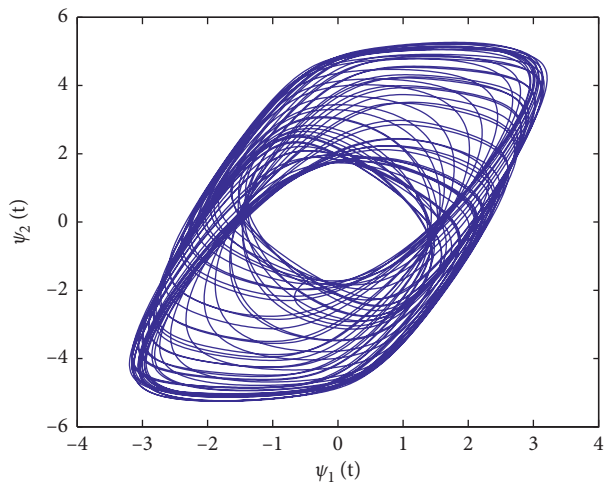

FIGURE 2: Chaotic behavior of slave system.

FIGURE 3: State response of the error system.

FIGURE 4: Chaotic nature of the master system.

FIGURE 5: Chaotic nature of the slave system.
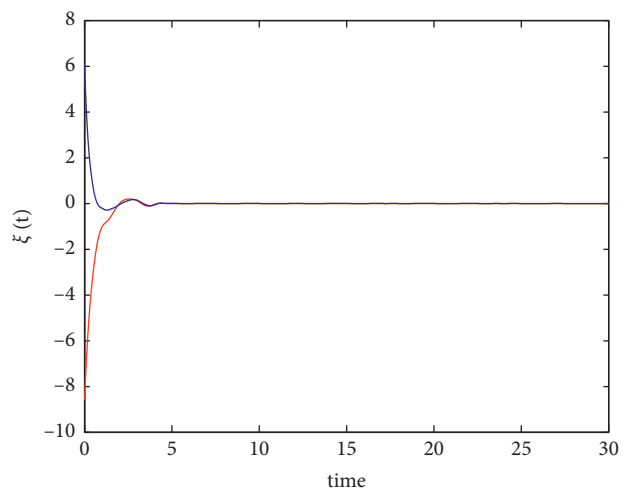
FIGURE 6: State trajectories of the error system.

$$K = \begin{bmatrix} 0.0351 & 0 \\ 0 & 0.0552 \end{bmatrix}. \tag{45}$$

In Figure 4, the chaotic nature of the master system is presented, and Figure 5 shows the chaotic behavior of the slave system. By making use of the nonfragile sampled-data control technique, the state trajectories of the error system are shown in Figure 6.

5. Conclusion

In this work, the synchronization of SMJNNs has been analyzed through the hybrid control technique, namely, nonfragile sampled-data control. Some criteria that ensure the synchronization of investigated SMJNNs with and without uncertainties in the control technique have been derived in the form of LMIs using Lyapunov stability theory and Writinger-based integral inequality approaches. The acquired LMIs are solved with Matlab LMI toolbox. Last, numerical simulations are granted to validate the designed controllers. Quaternion-valued neural network is the generalization of complex-valued neural networks, in which state, connection weight, and activation function are all quaternion numbers. Compared to real-valued NNs and complex-valued NNs, quaternion-valued NNs show significant advantages in multidimensional data processing. Recently, fractional-order quaternion-valued neural networks have gained great attention among the researchers due to its applications in many fields such as attitude control, image processing, computer graphics, prediction of three-dimensional wind processing, and so on. Due to its growing applications, it is important to analyze the qualitative behaviors of the fractional-order quaternion-valued NN. This will be our future work.

Data Availability

The data used to support the findings of this study are available from the corresponding author upon request.

Conflicts of Interest

The authors declare that they have no conflicts of interest.

Authors' Contributions

All authors contributed equally to this work.

References

[1] L. Pan, J. Cao, U. A. Juboori, and M. A. Aty, "Cluster synchronization of stochastic neural networks with delay via pinning impulsive control," *Neurocomputing*, vol. 366, 2019.

[2] S. Ding, Z. Wang, and H. Zhang, "Dissipativity analysis for stochastic memristive neural networks with time-varying delays: a discrete-time case," *IEEE Transactions on Neural Networks and Learning Systems*, vol. 29, no. 3, pp. 618–630, 2018.

[3] W. Xu, S. Zhu, X. Fang, and W. Wang, "Adaptive synchronization of memristor based complex-valued neural networks with time delays," *Neurocomputing*, vol. 364, 2019.

[4] Y. Zhao, X. Li, and P. Duan, "Observer-based sliding mode control for synchronization of delayed chaotic neural networks with unknown disturbance," *Neural Networks*, vol. 117, pp. 268–273, 2019.

[5] S. Dharani, R. Rakkiyappan, and J. H. Park, "Pinning sampled-data synchronization of coupled inertial neural networks with reaction-diffusion terms and time-varying delays," *Neurocomputing*, vol. 227, pp. 101–107, 2017.

[6] D. Huang, M. Jiang, and J. Jian, "Finite-time synchronization of inertial memristive neural networks with time-varying delays via sampled-date control," *Neurocomputing*, vol. 266, pp. 527–539, 2017.

[7] J. Feng, F. E. Alsaadi, and T. Hayat, "Fixed time synchronization of four dimensional energy resource systems with mismatched parameters," *Journal of applied Mathematics and Computing*, vol. 58, pp. 289–304, 2018.

[8] S. Wang, A. Yousefpour, A. Yusuf et al., "Synchronization of a non-equilibrium four-dimensional chaotic system using a disturbance-observer-based adaptive terminal sliding mode control method," *Entropy*, vol. 22, no. 3, p. 271, 2020.

[9] Y. Li, W. Xiao, J. Li, and L. Jiao, "H ∞ filtering for discrete-time fuzzy stochastic neural networks with mixed time-delays," *Journal of applied Mathematics and Computing*, vol. 52, no. 1-2, pp. 1–26, 2016.

[10] N. Li, X. Wu, J. Feng, and Y. Xu, "Fixed-time synchronization in probability of drive-response networks with discontinuous nodes and noise disturbances," *Nonlinear Dynamics*, vol. 97, no. 1, pp. 297–311, 2019.

[11] F. Li, S. Song, J. Zhao, S. Xu, and Z. Zhang, "Synchronization control for Markov jump neural networks subject to HMM observation and partially known detection probabilities," *Applied Mathematics and Computation*, vol. 360, pp. 1–13, 2019.

[12] P. Wang, J. Feng, and H. Su, "Stabilization of stochastic delayed networks with Markovian switching and hybrid nonlinear coupling via aperiodically intermittent control," *Nonlinear analysis: Hybrid Systems*, vol. 32, pp. 115–130, 2019.

[13] J. Wang, S. Ma, and C. Zhang, "Stability analysis and stabilization for nonlinear continuous-time descriptor semi-Markov jump systems," *Applied Mathematics and Computation*, vol. 279, pp. 90–102, 2016.

[14] X. Wu and X. Mu, "Event-triggered control for networked nonlinear semi-Markovian jump systems with randomly occurring uncertainties and transmission delay," *Information Sciences*, vol. 487, pp. 84–96, 2019.

[15] H. Yan, Y. Tian, H. Li, H. Zhang, and Z. Li, "Input-output finite-time mean square stabilization of nonlinear semi-Markovian jump systems," *Automatica*, vol. 104, pp. 82–89, 2019.

[16] Z. Wang and H. Wu, "Global synchronization in fixed time for semi-Markovian switching complex dynamical networks with hybrid couplings and time-varying delays," *Nonlinear Dynamics*, vol. 95, no. 3, pp. 2031–2062, 2019.

[17] Q. Li, X. Liu, Q. Zhu, S. Zhong, and J. Cheng, "Stochastic synchronization of semi-Markovian jump chaotic Lure's systems with packet dropouts subject to multiple sampling periods," *Journal of the Franklin Institute*, 2019.

[18] M. Zhang, P. Shi, L. Ma, J. Cai, and H. Su, "Network-based fuzzy control for nonlinear Markov jump systems subject to quantization and dropout compensation," *Fuzzy Sets and Systems*, vol. 371, pp. 96–109, 2019.

[19] K. Sivaranjani, R. Rakkiyappan, and Y. H. Joo, "Event triggered reliable synchronization of semi-Markovian jumping complex dynamical networks via generalized integral

inequalities," *Journal of the Franklin Institute*, vol. 355, no. 8, pp. 3691–3716, 2018.

[20] Z. Huang, J. Cao, J. Li, and H. Bin, "Quasi-synchronization of neural networks with parameter mismatches and delayed impulsive controller on time scales," *Nonlinear Analysis: Hybrid Systems*, vol. 33, pp. 104–115, 2019.

[21] R. Rakkiyappan and K. Sivaranjani, "Sampled-data synchronization and state estimation for nonlinear singularly perturbed complex networks with time-delays," *Nonlinear Dynamics*, vol. 84, no. 3, pp. 1623–1636, 2016.

[22] Y. Wan, J. Cao, and G. Wen, "Quantized synchronization of chaotic neural networks with scheduled output feedback control," *IEEE transactions on Neural networks and Learning systems*, vol. 28, no. 11, pp. 2638–2647, 2017.

[23] Y. Liu, L. Tong, J. Lou, J. Lu, and J. Cao, "Sampled-data control for the synchronization of boolean control networks," *IEEE Transactions on Cybernetics*, vol. 49, no. 2, pp. 726–732, 2019.

[24] Y. Liu and S. M. Lee, "Sampled-Data Synchronization of Chaotic Lur'e Systems with Stochastic Sampling," *Circuits, Systems, and Signal Processing*, vol. 34, no. 12, pp. 3725–3739, 2015.

[25] Y. Guan, Y. Wu, H. Wu, Y. Li, and S. He, "Synchronization of complex dynamical networks with actuator saturation by using sampled-data control," *Circuits, Systems, and Signal Processing*, vol. 38, no. 12, pp. 5508–5527, 2019.

[26] Q. Tang and J. Jian, "Exponential synchronization of inertial neural networks with mixed time-varying delays via periodically intermittent control," *Neurocomputing*, vol. 338, pp. 181–190, 2019.

[27] Y. Feng, X. Yang, Q. Song, and J. Cao, "Synchronization of memristive neural networks with mixed delays via quantized intermittent control," *Applied Mathematics and Computation*, vol. 339, pp. 874–887, 2018.

[28] Y. Liu, Z. Xuan, Z. Wang, J. Zhou, and Y. Liu, "Sampled-data exponential synchronization of time-delay neural networks subject to random controller gain perturbations," *Applied Mathematics and Computation*, vol. 385, Article ID 125429, 2020.

[29] J. Cheng, J. H. Park, H. R. Karimi, and H. Shen, "A flexible terminal approach to sampled-data exponentially synchronization of markovian neural networks with time-varying delayed signals," *IEEE Transactions on Cybernetics*, vol. 48, pp. 2232–2244, 2018.

[30] R. Rakkiyappan, K. Maheswari, K. Sivaranjani, and Y. H. Joo, "Non-fragile finite-time$l2−l\infty$state estimation for discrete-time neural networks with semi-Markovian switching and random sensor delays based on Abel lemma approach," *Nonlinear Analysis: Hybrid Systems*, vol. 29, pp. 283–302, 2018.

[31] R. Sakthivel, S. Santra, B. Kaviarasan, and K. Venkatanareshbabu, "Dissipative analysis for network-based singular systems with non-fragile controller and event-triggered sampling scheme," *Journal of the Franklin Institute*, vol. 354, no. 12, pp. 4739–4761, 2017.

[32] Y. Zhou, Y. Wang, Q. Kong, J. Zhou, and Z. Wang, "Non-fragile L2−L∞ synchronization for chaotic time-delay neural networks with semi-Markovian jump parameters," *Physica Scripta*, vol. 95, no. 3, Article ID 035215, 2020.

[33] P. Anbalagan, E. Hincal, E. Hincal et al., "Delay-coupled fractional order complex Cohen-Grossberg neural networks under parameter uncertainty: synchronization stability criteria," *AIMS Mathematics*, vol. 6, no. 3, pp. 2844–2873, 2021.

[34] K. Gu, V. L. Kharitonov, and J. Chen, *Stability of Time-Delay Systems*, Birkhauser, Boston, MA, USA, 2003.

[35] A. Seuret and F. Gouaisbaut, "Wirtinger-based integral inequality: application to time-delay systems," *Automatica*, vol. 49, no. 9, pp. 2860–2866, 2013.

[36] S. Boyd, E. L. Ghaoui, E. Feron, and V. Balakrishnan, *Linear Matrix Inequalities in System and Control Theory*, SIAM, Philadelphia, PA, USA, 1994.

Research Article

Multiple Positive Solutions for a Class of Boundary Value Problem of Fractional (p, q)-Difference Equations under (p, q)-Integral Boundary Conditions

Yongyang Liu and Yansheng Liu (iD)

School of Mathematics and Statistics, Shandong Normal University, Jinan 250014, China

Correspondence should be addressed to Yansheng Liu; yanshliu@gmail.com

This paper is mainly concerned with a class of fractional (p, q)-difference equations under (p, q)-integral boundary conditions. Multiple positive solutions are established by using the topological degree theory and Krein–Rutman theorem. Finally, two examples are worked out to illustrate the main results.

1. Introduction

The q-difference operator was first systematically studied by Jackson [1]. Then, q-calculus has been studied extensively. See [2–4] and references therein. q-calculus and q-difference equations have been used by many researchers to solve physical problems such as molecular problems and chemical physics [1, 5–7]. For example, in 1967, Floreanini and Vinet [3] studied the behaviors of hydrogen atoms by using Schrödinger equation and q-calculus. Diaz and Osler [8] investigated the q-field theory.

In the last decades, the theory of quantum calculus based on two-parameter (p, q)-integer has been studied since it can be used efficiently in many fields such as difference equations, Lie group, hypergeometric series, and physical sciences. The (p, q)-calculus was first studied by Chakrabarti and Jagannathan [2] in the field of quantum algebra in 1991. Njionou Sadjang [9] systematically established the basic theory of (p, q)-calculus and some (p, q)-Taylor formula. Milovanovic and Gupta [10] developed the concept of (p, q)-beta and (p, q)-gamma functions. These basic concepts and theories promote the development of

(p, q)-calculus. For detailed results on (p, q)-calculus, please see [9–13] and references therein.

On the contrary, the research of fractional calculus in discrete settings was initiated in [8, 11, 14]. In 2020, Soontharanonl and Sitthiwirattham [15] introduced the fractional (p, q)-calculus, which has been found in a wide range of applications in many fields such as concrete mathematical models of quantum mechanics and fluid mechanics [7, 13, 15].

As we all know, in recent decades, more and more researchers pay much attention to the fractional differential equations and have obtained substantial achievements, we refer the readers to see [16–34] and references therein. Although the results of discrete fractional calculus are similar to those of continuous fractional calculus, the theory of discrete fractional calculus remains much less developed than that of continuous fractional calculus [35, 36]. Therefore, it is very important to develop discrete calculus. In particular, the fractional (p, q)-difference equations involving (p, q)-integral boundary conditions have rarely been studied. In order to make up for this gap, the paper mainly studies the following boundary value problem of fractional

(p, q)-difference equations under (p, q)-integral boundary conditions:

$$\begin{cases} D_{p,q}^\alpha x(t) + f(t, x) = 0, t \in (0, 1), \\ x(0) = D_{p,q} x(0) = 0, D_{p,q} x(1) = \int_0^1 h(t) D_{p,q} x(t) d_{p,q} t, \end{cases} \tag{1}$$

where $2 < \alpha < 3$, $0 < q < p \le 1$, $f \in C([0, 1] \times R^+, R^+)$, and $D_{p,q}^\alpha$ is fractional (p, q)-difference operator.

It should be pointed out that the boundary conditions of BVP equation (1) are more extensive. Furthermore, two parameters in the discrete environment makes the boundary value problem more complex. In order to overcome these difficulties, we constructed a special cone. The existence and multiplicity of the positive solution for the BVP equation (1) are obtained by using the topological degree theory, Krein–Rutman theorem.

This paper is structured as follows. In Section 2, we introduce some definitions of (p, q)-fractional integral and differential operator together with some basic properties and lemmas. The main results are given and proved in Section 3. Finally, in Section 4, two examples are given to show the applicability of our main results.

2. Preliminaries

In this section, we list some basic definitions and lemmas that will be used in this paper. For $0 < q < p \le 1$, we let

$$[k]_{p,q} := \begin{cases} \dfrac{p^k - q^k}{p - q} = p^{k-1} [k] m q_{q/p}, & k \in N, \\ 1, & k = 0. \end{cases} \tag{2}$$

The (p, q)-analogue of the power function $(a - b)_{p,q}^n$ with $n \in N_0 \coloneq 0, 1, 2, \ldots$, is given by

$$(a - b)_{p,q}^0 =: 1, \quad (a - b)_{p,q}^n := \prod_{k=0}^{n-1} (a p^k - b q^k), \quad a, b \in R. \tag{3}$$

For $\alpha \in R$,

$$(a - b)_{p,q}^\alpha := a^\alpha \prod_{i=0}^\infty \left[\frac{1 - (b/a)(q/p)^i}{1 - (b/a)(q/p)^{\alpha+i}} \right], \quad a \ne 0. \tag{4}$$

By [15], we obtain

$$(a - b)_{p,q}^\alpha = p^{(\alpha/2)} (a - b)_{q/p}^\alpha = a^\alpha \prod_{i=0}^\infty \frac{1}{p^\alpha} \left[\frac{1 - b/a (q/p)^i}{1 - b/a (q/p)^{\alpha+i}} \right], \quad a \ne 0. \tag{5}$$

Note that $a_q^\alpha = a_{p,q}^\alpha = a^\alpha$ and $(0)_q^\alpha = (0)_{p,q}^\alpha = 0$ for $\alpha > 0$. The (p, q)-gamma and (p, q)-beta functions are defined by

$$\Gamma_{p,q}(x) := \begin{cases} \dfrac{(p - q)_{p,q}^{x-1}}{(p - q)^{x-1}} = \dfrac{(1 - q/p)_{p,q}^{x-1}}{(1 - q/p)^{x-1}}, & x \in R \smallsetminus \{0, -1, -2, \ldots,\}, \\ [x - 1]_{p,q}!, & x \in N, \end{cases} \tag{6}$$

$$B_{p,q}(x, y) := \int_0^1 t^{x-1} (1 - qt)_{p,q}^{y-1} d_{p,q} t = p^{\frac{1}{2}(y-1)(2x+y-2)} \frac{\Gamma_{p,q}(x) \Gamma_{p,q}(y)}{\Gamma_{p,q}(x + y)},$$

respectively.

Definition 1 (see [15]). For $0 < q < p \le 1$ and $f: [0, T] \longrightarrow R$, we define the (p, q)-difference of f as

$$D_{p,q} f(t) := \frac{f(pt) - f(qt)}{(p - q)(t)}, \quad t \ne 0, \tag{7}$$

where $D_{p,q} f(0) = f'(0)$, provided that f is differentiable at 0.

Definition 2 (see [15]). For $N - 1 < \alpha < N$, $0 < q < p \le 1$, and $f: I_{p,q}^T \longrightarrow R$, the fractional (p, q)-difference is defined by

$$D_{p,q}^\alpha f(t) = \frac{(p - q) t^{N-\alpha}}{p^{\binom{N-\alpha}{2}} \Gamma_{p,q}(N - \alpha)} \sum_{k=0}^\infty \frac{q^k}{p^{k+1}} \left(1 - \left(\frac{q}{p} \right)^{k+1} \right)_{p,q}^{N-\alpha-1} D_{p,q}^N f \left(\frac{q^k}{p^{k+N-\alpha}} t \right), \tag{8}$$

where $I_{p,q}^T = \{(q^k/p^{k+1})T: k \in \mathbb{N}_0\} \bigcup \{0\}$.

Definition 3 (see [15]). Let I be any closed interval of R containing a, b, and 0. Assuming that $f: I \longrightarrow R$ is a given function, we define (p,q)-integral of f from a to b by

$$\int_a^b f(t)d_{p,q}t = \int_0^b f(t)d_{p,q}t - \int_0^a f(t)d_{p,q}t, \qquad (9)$$

where

$$I_{p,q}f(x) = \int_a^x f(t)d_{p,q}t$$

$$= (p-q)x \sum_{k=0}^{\infty} \frac{q^k}{p^{k+1}} f\left(\frac{q^k}{p^{k+1}}x\right), \quad x \in I, \qquad (10)$$

provided that the series converges at $x = a$ and $x = b$. f is called (p,q)-integrable on $[a,b]$.

Definition 4 (see [15]). For $\alpha > 0$, $0 < q < p \le 1$, and $f: [0,T] \longrightarrow R$, the fractional (p,q)-integral is defined by

$$I_{p,q}^\alpha f(t) := \frac{1}{p^{\binom{\alpha}{2}}\Gamma_{p,q}(\alpha)} \int_0^t (t-qs)_{p,q}^{\alpha-1} f\left(\frac{s}{p^{\alpha-1}}\right)d_{p,q}s, \qquad (11)$$

and $(I_{p,q}^0 f)(t) = f(t)$.

Lemma 1 (see [15]). *Let f, g be (p,q)-differentiable. The properties of (p,q)-difference operator are as follows:*

(i) $D_{p,q}[f(t) + g(t)] = D_{p,q}f(t) + D_{p,q}g(t)$

(ii) $D_{p,q}[\alpha f(t)] = \alpha D_{p,q}f(t)$, for $\alpha \in R$

Lemma 2 (see [15]). *For $0 < q < p \le 1$, $\alpha \ge 1$, and $a \in R$, we have*

(i) $D_{p,q}(t-a)_{p,q}^\alpha = [\alpha]_{p,q}(pt-a)_{p,q}^{\alpha-1}$

(ii) $D_{p,q}(a-t)_{p,q}^\alpha = -[\alpha]_{p,q}(a-qt)_{p,q}^{\alpha-1}$

Lemma 3 (see [15]). *For $\alpha, \beta \ge 0$ and $0 < q < p \le 1$, (p,q)-integral and (p,q)-difference operators have the following properties:*

(i) $I_{p,q}^\alpha[I_{p,q}^\beta f(x)] = I_{p,q}^\beta[I_{p,q}^\alpha f(x)] = I_{p,q}^{\alpha+\beta}f(x)$

(ii) $D_{p,q}I_{p,q}f(x) = f(x)$ and $I_{p,q}D_{p,q}f(x) = f(x) - f(0)$

Lemma 4. *Assume $h \ge 0$, $A = 1 - \int_0^1 h(t)t^{\alpha-2}d_{p,q}t > 0$, and $\alpha \in (2,3)$. If $g \in C[0,1]$, then the following boundary value problem,*

$$\begin{cases} D_{p,q}^\alpha x(t) + g(t) = 0, & t \in (0,1), \\ x(0) = D_{p,q}x(0) = 0, & D_{p,q}x(1) = \int_0^1 h(t)D_{p,q}x(t)d_{p,q}t, \end{cases} \qquad (12)$$

has a unique solution

$$x(t) = \int_0^1 G(t,qs)g\left(\frac{s}{p^{\alpha-2}}\right)d_{p,q}s, \qquad (13)$$

where

$$G(t,qs) = G_0(t,qs) + \frac{t^{\alpha-1}}{A}\int_0^1 h(t)G_1(t,qs)d_{p,q}t,$$

$$G_0(t,qs) = \frac{1}{p^{(\alpha-1/2)}\Gamma_{p,q}(\alpha)} \begin{cases} \dfrac{1}{p^{2\alpha-2/\alpha-2}}t^{\alpha-1}(1-qs)^{(\alpha-2)} - (t-qs)^{(\alpha-1)}, & 0 \le s \le t \le 1, \\[3mm] \dfrac{1}{p^{2\alpha-2/\alpha-2}}t^{\alpha-1}(1-qs)^{(\alpha-2)}, & 0 \le t \le s \le 1, \end{cases} \qquad (14)$$

$$G_1(t,qs) = \frac{1}{p^{(\alpha-1/2)}\Gamma_{p,q}(\alpha)} \begin{cases} \dfrac{1}{p^{2\alpha-2/\alpha-2}}t^{\alpha-2}(1-qs)^{(\alpha-2)} - (t-qs)^{(\alpha-2)}, & 0 \le s \le t \le 1; \\[3mm] \dfrac{1}{p^{2\alpha-2/\alpha-2}}t^{\alpha-2}(1-qs)^{(\alpha-2)}, & 0 \le t \le s \le 1. \end{cases}$$

Proof. According to $D_{p,q}^\alpha x(t) = -g(t)$, we have

$$x(t) = C_1 t^{\alpha-1} + C_2 t^{\alpha-2} + C_3 t^{\alpha-3} - I_{p,q}^\alpha g(t). \qquad (15)$$

From $\quad x(0) = D_{p,q}x(0) = 0,\quad$ one can easily obtain $C_2 = C_3 = 0$. Hence,

$$
x(t) = C_1 t^{\alpha-1} - I_{p,q}^{\alpha} g(t),
$$

$$
D_{p,q}x(1) = C_1 \frac{\Gamma_{p,q}(\alpha)}{\Gamma_{p,q}(\alpha-1)} - \frac{1}{p^{(\alpha-1/2)}\Gamma_{p,q}(\alpha-1)} \int_0^1 (1-qs)^{(\alpha-2)} g\left(\frac{s}{p^{\alpha-2}}\right) d_{p,q}s
$$

$$
= \int_0^1 h(t) D_{p,q}x(t) d_{p,q}t \tag{16}
$$

$$
= \int_0^1 h(t)\left[C_1 \frac{\Gamma_{p,q}(\alpha)}{\Gamma_{p,q}(\alpha-1)} t^{\alpha-2} \right.
$$

$$
\left. - \frac{1}{p^{(\alpha-1/2)}\Gamma_{p,q}(\alpha-1)} \int_0^t (t-qs)^{(\alpha-2)} g\left(\frac{s}{p^{\alpha-2}}\right) d_{p,q}s \right] d_{p,q}t.
$$

Based on the hypothesis in Lemma 4, we can deduce that

$$
C_1 = \frac{1}{Ap^{(\alpha-1/2)}\Gamma_{p,q}(\alpha)} \int_0^1 (1-qs)^{(\alpha-2)} g\left(\frac{s}{p^{\alpha-2}}\right) d_{p,q}s - \frac{1}{Ap^{(\alpha-1/2)}\Gamma_{p,q}(\alpha)} \int_0^1 h(t) d_{p,q}t \int_0^t (t-qs)^{(\alpha-2)} g\left(\frac{s}{p^{\alpha-2}}\right) d_{p,q}s. \tag{17}
$$

Thus,

$$
x(t) = C_1 t^{\alpha-1} - I_{p,q}^{\alpha} g(t)
$$

$$
= \frac{1}{Ap^{(\alpha-1/2)}\Gamma_{p,q}(\alpha)} \int_0^1 t(1-qs)^{(\alpha-2)} g\left(\frac{s}{p^{\alpha-2}}\right) d_{p,q}s
$$

$$
- \frac{1}{Ap^{(\alpha-1/2)}\Gamma_{p,q}(\alpha)} \int_0^1 h(t) d_{p,q}t \int_0^t t^{\alpha-1}(t-qs)^{(\alpha-2)} g\left(\frac{s}{p^{\alpha-2}}\right) d_{p,q}s
$$

$$
- \frac{1}{p^{(\alpha/2)}\Gamma_{p,q}(\alpha)} \int_0^t (t-qs)^{(\alpha-1)} g\left(\frac{s}{p^{\alpha-1}}\right) d_{p,q}s
$$

$$
= \frac{1}{Ap^{(\alpha-1/2)}\Gamma_{p,q}(\alpha)} \int_0^1 t^{\alpha-2}(1-qs)^{(\alpha-2)} g\left(\frac{s}{p^{\alpha-2}}\right) d_{p,q}s
$$

$$
- \frac{1}{Ap^{(\alpha-1/2)}\Gamma_{p,q}(\alpha)} \int_0^1 h(t) d_{p,q}t.
$$

$$
- \frac{1}{p^{(\alpha-1/2)}\Gamma_{p,q}(\alpha)} \int_0^t \frac{1}{p^{2\alpha-2/\alpha-2}}(t-qs)^{(\alpha-1)} g\left(\frac{s}{p^{\alpha-2}}\right) d_{p,q}s + \frac{1}{p^{(\alpha-1/2)}\Gamma_{p,q}(\alpha)} \int_0^1 \frac{t^{\alpha-1}}{p^{2\alpha-2/\alpha-2}}(1-qs)^{(\alpha-1)} g\left(\frac{s}{p^{\alpha-2}}\right) d_{p,q}s \tag{18}
$$

$$
- \frac{1}{p^{(\alpha-1/2)}\Gamma_{p,q}(\alpha)} \int_0^1 \frac{t^{\alpha-1}}{p^{2\alpha-2/\alpha-2}}(1-qs)^{(\alpha-1)} g\left(\frac{s}{p^{\alpha-2}}\right) d_{p,q}s
$$

$$
= \int_0^1 G_0\left(\frac{s}{p^{\alpha-2}}\right) d_{p,q}s + \frac{t^{\alpha-1}}{Ap^{(\alpha-1/2)}\Gamma_{p,q}(\alpha)} \int_0^1 h(t) t^{\alpha-2} d_{p,q}t \int_0^1 \frac{1}{p^{2\alpha-2/\alpha-2}}(1-qs)^{(\alpha-2)} g\left(\frac{s}{p^{\alpha-1}}\right) d_{p,q}s
$$

$$
- \frac{t^{\alpha-1}}{Ap^{(\alpha-1/2)}\Gamma_{p,q}(\alpha)} \int_0^1 h(t) d_{p,q}t \int_0^t \frac{1}{p^{2\alpha-2/\alpha-2}}(t-qs)^{(\alpha-2)} g\left(\frac{s}{p^{\alpha-2}}\right) d_{p,q}s
$$

$$
= \frac{t^{\alpha-1}}{Ap^{(\alpha-1/2)}\Gamma_{p,q}(\alpha)} \int_0^1 \left[\int_0^1 \frac{1}{p^{2\alpha-2/\alpha-2}} h(t) t^{\alpha-2}(1-qs)^{(\alpha-2)} d_{p,q}t - \int_s^1 \frac{1}{p^{2\alpha-2/\alpha-2}} h(t)(t-qs)^{(\alpha-2)} d_{p,q}t \right] g\left(\frac{s}{p^{\alpha-2}}\right) d_{p,q}s
$$

$$
= \int_0^1 G_0(t,qs) g\left(\frac{s}{p^{\alpha-2}}\right) d_{p,q}s + \frac{t^{\alpha-1}}{A} \int_0^1 \int_0^1 G_1(t,qs) g\left(\frac{s}{p^{\alpha-2}}\right) d_{p,q}s
$$

$$
= \int_0^1 G(t,qs) g\left(\frac{s}{p^{\alpha-2}}\right) d_{p,q}s.
$$

This completes the proof. □

Lemma 5. *The functions* $G_i \, (i = 0, 1)$ *have the following properties:*

(1) $G_i(t, qs) \geq 0$, *for* $t, s \in [0, 1]$

(2) $t^{\alpha-1} G_0(1, qs) \leq G_0(t, qs) \leq G_0(1, qs)$, *for* $t, s \in [0, 1]$

Proof

(1) On the one hand, for $0 \leq s \leq t \leq 1$, we know

$$G_0(t, qs) = \frac{1}{p^{(\alpha-1/2)} \Gamma_{p,q}(\alpha)} \left[\frac{1}{p^{2\alpha-2/\alpha-2}} t^{\alpha-1} (1-qs)^{(\alpha-2)} - (t-qs)^{(\alpha-1)} \right]. \tag{19}$$

Thus, for $t \neq 0$, it is easy to see that

$$
\begin{aligned}
G_0(t, qs) &= \frac{1}{p^{(\alpha-1/2)} \Gamma_{p,q}(\alpha)} \left[\frac{1}{p^{2\alpha-2/\alpha-2}} t^{\alpha-1} (1-qs)^{(\alpha-2)} - (t-qs)^{(\alpha-1)} \right] \\
&= \frac{1}{p^{(\alpha-1/2)} \Gamma_{p,q}(\alpha)} \left[\frac{1}{p^{2\alpha-2/\alpha-2}} t^{\alpha-1} (1-qs)^{(\alpha-2)} - t^{\alpha-1} \left(1 - q\frac{s}{t}\right)^{(\alpha-1)} \right] \\
&\geq \frac{t^{\alpha-1}}{p^{(\alpha-1/2)} \Gamma_{p,q}(\alpha)} \left[(1-qs)^{(\alpha-2)} - (1-qs)^{(\alpha-1)} \right] \\
&\geq 0.
\end{aligned}
\tag{20}
$$

Similarly, for $0 \leq s \leq t \leq 1$, we know

$$G_1(t, qs) = \frac{1}{p^{(\alpha-1/2)} \Gamma_{p,q}(\alpha)} \left[\frac{1}{p^{2\alpha-2/\alpha-2}} t^{\alpha-2} (1-qs)^{(\alpha-2)} - (t-qs)^{(\alpha-2)} \right]. \tag{21}$$

Thus, for $t \neq 0$, it is also easy to see that

$$
\begin{aligned}
G_1(t, qs) &= \frac{1}{p^{(\alpha-1/2)} \Gamma_{p,q}(\alpha)} \left[\frac{1}{p^{2\alpha-2/\alpha-2}} t^{\alpha-2} (1-qs)^{(\alpha-2)} - (t-qs)^{(\alpha-2)} \right] \\
&= \frac{1}{p^{(\alpha-1/2)} \Gamma_{p,q}(\alpha)} \left[\frac{1}{p^{2\alpha-2/\alpha-2}} t^{\alpha-2} (1-qs)^{(\alpha-2)} - t^{\alpha-2} \left(1 - q\frac{s}{t}\right)^{(\alpha-2)} \right] \\
&\geq \frac{t^{\alpha-2}}{p^{(\alpha-1/2)} \Gamma_{p,q}(\alpha)} \left[(1-qs)^{(\alpha-2)} - (1-qs)^{(\alpha-2)} \right] \\
&= 0.
\end{aligned}
\tag{22}
$$

On the other hand, for $0 \le t \le s \le 1$, it is easy to see that, from Lemma 4, the conclusion is obviously established. Therefore, $G_i(t, qs) \ge 0$, for $t, s \in [0, 1]$.

$$
\begin{aligned}
{}^t D_{p,q} G_0(t, qs) &= {}_t D_{p,q} \left\{ \frac{1}{p^{(\alpha - 1/2)} \Gamma_{p,q}(\alpha)} \left[\frac{1}{p^{2\alpha - 2/\alpha - 2}} t^{\alpha - 1}(1 - qs)^{(\alpha - 2)} - (t - qs)^{(\alpha - 1)} \right] \right\} \\
&= \left\{ \frac{1}{p^{(\alpha - 1/2)} \Gamma_{p,q}(\alpha)} \left[\frac{1}{p^{2\alpha - 2/\alpha - 2}} [\alpha - 1] t^{\alpha - 2}(1 - qs)^{(\alpha - 2)} - [\alpha - 1](t - qs)^{(\alpha - 2)} \right] \right\} \\
&= \left\{ \frac{1}{p^{(\alpha - 1/2)} \Gamma_{p,q}(\alpha)} \left[[\alpha - 1] t^{\alpha - 2}(1 - qs)^{(\alpha - 2)} - [\alpha - 1] t^{\alpha - 2} \left(1 - q\frac{s}{t} \right)^{(\alpha - 2)} \right] \right\} \\
&\ge 0.
\end{aligned}
\tag{23}
$$

For $0 \le t \le s \le 1$ and $2 < \alpha < 3$, we know that $G(t, qs) = t^{\alpha - 1}(1 - qs)^{(\alpha - 2)}$ is obviously an increasing function with respect to t.

Therefore, for $t, s \in [0, 1]$, $G_0(t, qs)$ is an increasing function with respect to t. Then, $G_0(t, qs) \le G_0(1, qs)$.

Secondly, for $0 \le s \le t \le 1$, we have

$$
\begin{aligned}
\frac{G_0(t, qs)}{G_0(1, qs)} &= \frac{1/p^{2\alpha - 2/\alpha - 2} t^{\alpha - 1}(1 - qs)^{(\alpha - 2)} - (t - qs)^{(\alpha - 1)}}{1/p^{2\alpha - 2/\alpha - 2}(1 - qs)^{(\alpha - 2)} - (1 - qs)^{(\alpha - 1)}} \\
&= \frac{t^{\alpha - 1} \left[1/p^{2\alpha - 2/\alpha - 2}(1 - qs)^{(\alpha - 2)} - (1 - q(s/t))^{(\alpha - 1)} \right]}{1/p^{2\alpha - 2/\alpha - 2}(1 - qs)^{(\alpha - 2)} - (1 - qs)^{(\alpha - 1)}} \\
&\ge \frac{t^{\alpha - 1} \left[1/p^{2\alpha - 2/\alpha - 2}(1 - qs)^{(\alpha - 2)} - (1 - qs)^{(\alpha - 1)} \right]}{1/p^{2\alpha - 2/\alpha - 2}(1 - qs)^{(\alpha - 2)} - (1 - qs)^{(\alpha - 1)}} \\
&= t^{\alpha - 1}.
\end{aligned}
\tag{24}
$$

For $0 \le t \le s \le 1$, we have

$$
\frac{G_0(t, qs)}{G_0(1, qs)} = t^{\alpha - 1}.
\tag{25}
$$

Therefore, $t^{\alpha - 1} G_0(1, qs) \le G_0(t, qs)$, for $t, s \in [0, 1]$. □

Lemma 6. *From Lemma 5, the following conclusions are established:*

$$
\begin{aligned}
t^{\alpha - 1} \theta_1(qs) &\le G(t, qs) \le \theta_1(qs) \text{ for } t, s \in [0, 1], \\
G(t, qs) &\le t^{\alpha - 1} \theta_2(qs) \text{ for } t, s \in [0, 1],
\end{aligned}
\tag{26}
$$

where

(2) Firstly, for $0 \le s \le t \le 1$, one can easily obtain that

$$
\begin{aligned}
\theta_1(s) &= G_0(1, s) + \frac{1}{A} \int_0^1 h(t) G_1(t, s) d_{p,q} s, \\
\theta_2(s) &= \frac{1}{\Gamma_{p,q}(\alpha)} \left(1 - s^{(\alpha - 2)} \right) + \frac{1}{A} \int_0^1 h(t) G_1(t, s) d_{p,q} s.
\end{aligned}
\tag{27}
$$

Lemma 7 (see [37]). *Let Ω be a bounded open set in a Banach space E, and $T: \overline{\Omega} \longrightarrow E$ is a continuous compact operator. If there exists $x_0 \in E \smallsetminus \{0\}$ such that*

$$
x - Tx \ne \mu x_0, \quad \forall x \in \partial\Omega, \mu \ge 0,
\tag{28}
$$

then the topological degree $\deg(I - T, \Omega, 0) = 0$.

Lemma 8 (see [37]). *Let Ω be a bounded open set in a Banach space E with $0 \in \Omega$, and $T: \overline{\Omega} \longrightarrow E$ is a continuous compact operator. If*

$$
Tx \ne \mu x, \quad \forall x \in \partial\Omega, \mu \ge 1,
\tag{29}
$$

then the topological degree $\deg(I - T, \Omega, 0) = 1$.

Let $E := C[0, 1], \|x\| := \max_{t \in [0,1]} |x(t)|$, and $P := \{x \in E : x(t) \ge t^{\alpha - 1} \|x\|, \forall t \in [0, 1]\}$. Then, $(E, \|\cdot\|)$ is a real Banach space and P is a cone on E. From Lemma 4, we can define operator $T: E \longrightarrow E$ as follows:

$$
(Tx)(t) := \int_0^1 G(t, qs) f\left(\frac{s}{p^{\alpha - 2}}, x\left(\frac{s}{p^{\alpha - 2}} \right) \right) d_{p,q} s, \quad x \in E,
\tag{30}
$$

where G is determined in Lemma 4. Obviously, T is a completely continuous operator.

In addition, from Lemma 4, we can obtain that the solution of BVP equation (12) is equivalent to

$$x(t) = \lambda \int_0^1 G(t, qs) g\left(\frac{s}{p^{\alpha-2}}\right) d_{p,q} s, \quad t \in [0, 1]. \tag{31}$$

For our purposes, we need to define the operator L by

$$(Lx)(t) = \int_0^1 G(t, qs) x\left(\frac{s}{p^{\alpha-2}}\right) d_{p,q} s, \quad t \in [0, 1], x \in E. \tag{32}$$

It is easy to prove that $L: E \longrightarrow E$ is a linear completely continuous operator and $L(P) \subset P$. Obviously, we know that L has a spectral radius, denoted by $r(L)$, that is not equal to 0. From Krein–Rutman theorem, we know that L has a positive eigenfunction φ_1 corresponding to its first eigenvalue $\lambda_1 = (r(L))^{-1}$, i.e., $\varphi_1 = \lambda_1 L \varphi_1$.

3. Main Results

In this section, we shall establish the existence and multiplicity results of BVP equation (1), which is based on the topological degree theory. For convenience, let λ_1 be the first eigenvalue of the following eigenvalue problem:

$$\begin{cases} D_{p,q}^\alpha x(t) + \lambda x(t) = 0, & t \in (0, 1), \\ x(0) = D_{p,q} x(0) = 0, & D_{p,q} x(1) = \int_0^1 h(t) D_{p,q} x(t) d_{p,q} t. \end{cases} \tag{33}$$

Now, let us list the following assumptions satisfied throughout the paper:

(H1) $\liminf_{x \longrightarrow 0} f(t, x)/x > \lambda_1$ uniformly with respect to $t \in [0, 1]$.

(H2) $\limsup_{x \longrightarrow \infty} f(t, x)/x < \lambda_1$ uniformly with respect to $t \in [0, 1]$.

(H3) $\limsup_{x \longrightarrow 0} f(t, x)/x < \lambda_1$ uniformly with respect to $t \in [0, 1]$.

(H4) $\liminf_{x \longrightarrow \infty} f(t, x)/x > \lambda_1$ uniformly with respect to $t \in [0, 1]$.

(H5) There exist $r^* > 0$ and a continuous function ϕ_{r^*} such that

$$f(t, x) \geq \phi_{r^*}(t), \forall t \in [0, 1], x \in [t^{\alpha-1} r^*, r^*],$$
$$\max_{t \in [0,1]} \int_0^1 t^{\alpha-1} G(1, qs) \phi_{r^*}\left(\frac{s}{p^{\alpha-2}}\right) d_{p,q} s > r^*. \tag{34}$$

(H6) There exist $r_* > 0$ and a continuous function ψ_{r_*} such that

$$f(t, x) \leq \psi_{r_*}(t), \quad \forall t \in [0, 1],$$
$$x \in [0, r_*],$$
$$\int_0^1 G(1, qs) \psi_{r_*}\left(\frac{s}{p^{\alpha-2}}\right) d_{p,q} s < r_*. \tag{35}$$

Now, we are in a position to give our main results.

Theorem 1. *Under assumptions (H1) and (H2), BVP equation (1) admits at least one positive solution.*

Proof. First, assumption (H1) implies that there exists $r > 0$ such that

$$f(t, x) > \lambda_1 x, \quad \forall x \in [0, r], t \in [0, 1]. \tag{36}$$

We claim that, for $\mu \geq 0$,

$$x(t) - Tx(t) \neq \mu \varphi_1(t), \forall x \in \partial B_r \cap P, t \in [0, 1]. \tag{37}$$

Suppose, on the contrary, that there exist $x_1 \in \partial B_r \cap P, \mu_1 > 0$ such that

$$x_1(t) - Tx_1(t) = \mu_1 \varphi_1(t), \quad t \in [0, 1]. \tag{38}$$

Without loss of generality, suppose $\mu_1 > 0$. Then, $x_1(t) \geq \mu_1 \varphi_1(t)$, for $t \in [0, 1]$.

Let

$$\mu^* = \sup\{\mu: x_1(t) \geq \mu_1 \varphi_1(t), t \in [0, 1]\}. \tag{39}$$

Obviously, $0 < \mu_1 \leq \mu^* < +\infty$ and $x_1(t) \geq \mu^* \varphi_1(t)$, for $t \in [0, 1]$.

Thus,

$$\begin{aligned} x_1(t) &= Tx_1(t) + \mu_1 \varphi_1(t) \\ &= \int_0^1 G(t, qs) f\left(\frac{s}{p^{\alpha-2}}, x_1\left(\frac{s}{p^{\alpha-2}}\right)\right) d_{p,q} s + \mu_1 \varphi_1(t) \\ &\geq \lambda_1 \int_0^1 G(t, qs) x_1\left(\frac{s}{p^{\alpha-2}}\right) d_{p,q} s + \mu_1 \varphi_1(t) \\ &\geq \lambda_1 \mu^* \int_0^1 G(t, qs) \varphi_1\left(\frac{s}{p^{\alpha-2}}\right) d_{p,q} s + \mu_1 \varphi_1(t) \\ &= (\mu^* + \mu_1) \varphi_1(t). \end{aligned} \tag{40}$$

It is a contradiction with the definition of μ^*. According to Lemma 7, one obtains

$$\deg(T, B_r \cap P, P) = 0. \tag{41}$$

On the contrary, we can choose $\varepsilon_0 > 0$ such that $0 < (\lambda_1 - \varepsilon_0)\|L\| < 1$. Then, from (H2), there exists $R > 0$ such that

$$f(t, x) \leq (\lambda_1 - \varepsilon_0)x, \quad x \geq R, t \in [0, 1]. \tag{42}$$

Let $m = \max_{(t,x) \in [0,1] \times [0,R]} f(t, x)$. Thus, one can easily find that

$$f(t, x) \leq (\lambda_1 - \varepsilon_0)x + m, \quad \forall x \geq 0, t \in [0, 1]. \tag{43}$$

Choose $R_0 > \max\{R, r, m \int_0^1 \theta_1(qs) d_{p,q} s / 1 - (\lambda_1 - \varepsilon_0)\|L\|\}$. We claim that, for $\mu \geq 1$,

$$Tx(t) \neq \mu x(t), \quad \forall x \in \partial B_{R_0} \cap P, t \in [0, 1]. \tag{44}$$

Suppose, on the contrary, that there exist $x_2 \in \partial B_{R_0} \cap P$ and $\mu_2 \geq 1$ such that

$$Tx_2(t) = \mu_2 x_2(t), \quad t \in [0,1]. \tag{45}$$

Hence,

$$
\begin{aligned}
x_2(t) &\leq \mu_2 x(t) = Tx_2(t) = \int_0^1 G(t,qs) f\left(\frac{s}{p^{\alpha-2}}, x_2\left(\frac{s}{p^{\alpha-2}}\right)\right) d_{p,q}s \\
&\leq \int_0^1 G(t,qs) \left[(\lambda_1 - \varepsilon_0) x_2\left(\frac{s}{p^{\alpha-2}}\right) + m\right] d_{p,q},
\end{aligned}
\tag{46}
$$

noticing that $0 < (\lambda_1 - \varepsilon_0)\|L\| < 1$. We know that the inverse operator of $I - (\lambda_1 - \varepsilon_0)L$ exists, and

$$[I - (\lambda_1 - \varepsilon_0)L]^{-1} = \sum_{n=0}^{\infty} (\lambda_1 - \varepsilon_0)^n L^n, \tag{47}$$

which shows that $[I - (\lambda_1 - \varepsilon_0)L]^{-1}(P) \subseteq P$.

Thus,

$$x_2(t) \leq [I - (\lambda_1 - \varepsilon_0)L]^{-1} m \int_0^1 G(t,qs) d_{p,q}s. \tag{48}$$

In addition, by $\|[I - (\lambda_1 - \varepsilon_0)L]^{-1}\| \leq 1/1 - (\lambda_1 - \varepsilon_0)\|L\|$ and Lemma 6, one can obtain

$$
\begin{aligned}
R_0 &= \|x_2(t)\| \leq \|[I - (\lambda_1 - \varepsilon_0)L]^{-1}\| m \int_0^1 \theta_1(qs) d_{p,q}s \\
&\leq \frac{m \int_0^1 \theta_1(qs) d_{p,q}s}{1 - (\lambda_1 - \varepsilon_0)\|L\|} \\
&< R_0,
\end{aligned}
\tag{49}
$$

which is a contradiction. By Lemma 8, we obtain

$$\deg\left(T, B_{R_0} \cap P, P\right) = 1. \tag{50}$$

Therefore,

$$\deg\left(T, B_{R_0} \setminus \overline{B}_r \cap P, P\right) = \deg\left(T, B_{R_0} \cap P, P\right) - \deg\left(T, B_r \cap P, P\right) = 1 - 0 = 1. \tag{51}$$

which means that BVP equation (1) has at least one positive solution. □

Theorem 2. *Under assumptions (H3) and (H4), BVP equation (1) admits at least one positive solution.*

Proof. On the one hand, assumption (H3) implies that there exist $\varepsilon \in (0, \lambda_1)$ and $r_1 > 0$ such that

$$f(t,x) < (\lambda_1 - \varepsilon), |x| < r_1. \tag{52}$$

We claim that, for $\mu \in [0,1]$,

$$x(t) \neq \mu Tx(t), \quad \forall x \in \partial B_{r_1} \cap P, t \in [0,1]. \tag{53}$$

Suppose, on the contrary, that there exist $x_1 \in \partial B_{r_1} \cap P$ and $\mu \in [0,1]$ such that

$$x_1(t) = \mu_1 Tx_1(t), \quad t \in [0,1]. \tag{54}$$

Consequently, we have

$$x_1(t) = \mu_1 Tx_1(t) < (\lambda_1 - \varepsilon) \int_0^1 G(t,qs) x_1\left(\frac{s}{p^{\alpha-2}}\right) d_{p,q}s = (\lambda_1 - \varepsilon)(Lx_1)(t). \tag{55}$$

The nth iteration of this inequality shows that

$$x_1(t) < (\lambda_1 - \varepsilon)^n (L^n x_1)(t) (n = 1, 2, \ldots,). \tag{56}$$

Then,

$$\|x_1\| < (\lambda_1 - \varepsilon)^n \|L^n\| \|x_1\|, \text{ i.e., } 1 < (\lambda_1 - \varepsilon)^n \|L^n\|. \tag{57}$$

It means that

$$1 \leq (\lambda_1 - \varepsilon) \lim_{n \to \infty} \sqrt[n]{\|L^n\|} = (\lambda_1 - \varepsilon) r(L) = \frac{(\lambda_1 - \varepsilon)}{\lambda_1} < 1, \tag{58}$$

which is a contradiction. It follows from Lemma 8 that

$$\deg\left(T, B_{r_1} \cap P, P\right) = 1. \tag{59}$$

On the other hand, let

$$L_n x(t) = \int_{1/n}^1 G(t,qs) x\left(\frac{s}{p^{\alpha-2}}\right) d_{p,q}s, \quad t \in [0,1], \tag{60}$$

where $n > 1$. It is easy to see that $L_n: P \longrightarrow P$ is completely continuous operator and spectral radius $r(L_n) > 0$, denoted by $\lambda_n = r^{-1}(L_n)$. We know $\lim_{n \to +\infty} \lambda_n = \lambda_1$.

It follows that there exist N_0, ε_0 such that $\lambda_{N_0} < \lambda_1 + \varepsilon_0$, namely, $r(L_{N_0}) > 1/r^{-1}(L) + \varepsilon_0$. From the Krein–Rutman theorem, there exists a $\varphi_{N_0}(t) \in E \setminus \{\theta\}$ such that

$$\varphi_{N_0}(t) = r^{-1}(L_{N_0}) \int_{1/N_0}^{1} G(t,qs)\varphi_{N_0}\left(\frac{s}{p^{\alpha-2}}\right)d_{p,q}s, \quad t \in [0,1]. \tag{61}$$

By the proof of Lemma 5, we know

$$G(t,qs) \geq t^{\alpha-1}G(\tau,qs). \tag{62}$$

Hence,

$$\varphi_{N_0}(t) \geq r^{-1}(L_{N_0}) \int_{1/N_0}^{1} t^{\alpha-1}G(\tau,qs)\varphi_{N_0}\left(\frac{s}{p^{\alpha-2}}\right)d_{p,q}s = t^{\alpha-1}\varphi_{N_0}(\tau), \quad \forall t, \tau \in [0,1], \tag{63}$$

which means that $\varphi_{N_0}(t) \geq t^{\alpha-1}\|\varphi_{N_0}\|$, namely, $\varphi_{N_0}(t) \in P \setminus \{\theta\}$.

Thus, from (H4), there exists $R_1 > 0$ such that

$$f(t,x) > (\lambda_1 + \varepsilon)x, \quad t \in [0,1], \forall, x \geq R_1. \tag{64}$$

Choose $\overline{R}_0 > \max\{r_1, N_0^{\alpha-1}R_1\}$. Thus,

$$x(t) \geq t^{\alpha-1}\|x\| = t^{\alpha-1}\overline{R}_0 > R_1, \quad t \in \left[\frac{1}{N_0}, 1\right], x \in \partial B_{\overline{R}_0} \cap P. \tag{65}$$

Now, we prove that, for $\mu \geq 0$,

$$x(t) - Tx(t) \neq \mu\varphi_{N_0}(t), \quad \forall x \in \partial B_{\overline{R}_0} \cap P, t \in [0,1]. \tag{66}$$

Similar to the proof of Theorem 1, this conclusion is clearly established. So, according to Lemma 7,

$$\deg\left(T, B_{\overline{R}_0} \cap P, P\right) = 0. \tag{67}$$

Therefore,

$$\deg\left(T, B_{\overline{R}_0} \setminus \overline{B}_{r_1} \cap P, P\right) = \deg\left(T, B_{\overline{R}_0} \cap P, P\right) - \deg\left(T, B_{r_1} \cap P, P\right) = 0 - 1 = -1, \tag{68}$$

which means that BVP equation (1) has at least one positive solution.

Up to now, some existence results of BVP equation (1) have been obtained by using the topological degree theory and Krein–Rutman theorem. In the following, the multiple solutions will be considered for BVP equation (1). □

Theorem 3. *Suppose that (H2), (H3), and (H5) are satisfied. Then, BVP equation (1) has at least two positive solutions.*

Proof. By (H5), we know

$$(Tx)(t) = \int_0^1 G(t,qs)f\left(\frac{s}{p^{\alpha-2}}, x\left(\frac{s}{p^{\alpha-2}}\right)\right)d_{p,q}s$$
$$\geq \int_0^1 t^{\alpha-1}G(1,qs)\phi_{r^*}\left(\frac{s}{p^{\alpha-2}}\right)d_{p,q}s, \quad x \in \partial B_{r^*} \cap P. \tag{69}$$

Consequently,

$$\|Tx\| \geq \max_{t \in [0,1]} \int_0^1 t^{\alpha-2}G(1,qs)\phi_{r^*}\left(\frac{s}{p^{\alpha-2}}\right)d_{p,q}s > r^* = \|x\|. \tag{70}$$

So, similar to the previous proof of Theorem 1, it is easy to know, for $\mu > 0$,

$$x(t) - Tx(t) \neq \mu\varphi_1(t), \quad \forall t \in [0,1], x \in \partial B_{r^*} \cap P. \tag{71}$$

By Lemma 7, one can immediately obtain that

$$\deg(T, B_r \cap P, P) = 0. \tag{72}$$

By the proof of Theorems 1 and 2, we know that there exist $r_1 \in (0, r^*)$ and $R_1 \geq \max\{r^*, R_0\}$ such that

$$\deg(T, B_{r_1} \cap P, P) = 1,$$
$$\deg(T, B_{R_1} \cap P, P) = 1. \tag{73}$$

Consequently,

$$\deg\left(T, \left(B_{r^*} \setminus \overline{B}_{r_1}\right) \cap P, P\right) = \deg(T, B_{r^*} \cap P, P) - \deg(T, B_{r_1} \cap P, P) = 0 - 1 = -1,$$
$$\deg\left(T, \left(B_{R_1} \setminus \overline{B}_{r^*}\right) \cap P, P\right) = \deg(T, B_{R_1} \cap P, P) - \deg(T, B_{r^*} \cap P, P) = 1 - 0 = 1, \tag{74}$$

which means that BVP equation (1) has at least two positive solutions. □

Theorem 4. *Suppose that (H1), (H4), and (H6) are satisfied. Then, BVP equation (1) has at least two positive solutions.*

Proof. By (H6), we know

$$(Tx)(t) = \int_0^1 G(t,qs) f\left(\frac{s}{p^{\alpha-2}}, x\left(\frac{s}{p^{\alpha-2}}\right)\right) d_{p,q}s$$

$$\le \int_0^1 G(1,qs)\psi_{r_*}\left(\frac{s}{p^{\alpha-2}}\right) d_{p,q}s, \quad x \in \partial B_{r_*} \cap P. \tag{75}$$

Therefore,

$$\|Tx\| \le \int_0^1 G(1,qs)\psi_{r_*}\left(\frac{s}{p^{\alpha-2}}\right) d_{p,q}s < r_* = \|x\|. \tag{76}$$

So, similar to the previous proof of Theorem 1, it is easy to know, for $\mu \ge 1$,

$$Tx(t) \ne \mu x(t), \quad \forall x \in \partial B_{r_*} \cap P, t \in [0,1]. \tag{77}$$

By Lemma 8, one can immediately obtain that

$$\deg(T, B_{r_*} \cap P, P) = 1. \tag{78}$$

By the proof of Theorems 1 and 2, we know that there exist $\overline{r}_1 \in (0, r_*)$ and $\overline{R}_1 \ge \max\{r_*, \overline{R}_0\}$ such that

$$\deg(T, B_{\overline{r}_1} \cap P, P) = 0,$$
$$\deg(T, B_{\overline{R}_1} \cap P, P) = 0. \tag{79}$$

Consequently,

$$\deg\left(T, \left(B_{r_*} \backslash \overline{B}_{\overline{r}_1}\right) \cap P, P\right) = \deg(T, B_{r_*} \cap P, P) - \deg(T, B_{\overline{r}_1} \cap P, P) = 1 - 0 = 1,$$
$$\deg\left(T, \left(B_{\overline{R}_1} \backslash \overline{B}_{r_*}\right) \cap P, P\right) = \deg\left(T, B_{\overline{R}_1} \cap P, P\right) - \deg(T, B_{r_*} \cap P, P) = 0 - 1 = -1, \tag{80}$$

which means that BVP equation (1) has at least two positive solutions. □

4. Examples

Example 1. Consider the following boundary value problem:

$$\begin{cases} \left(D_{(1,1/2)}^{5/2} x\right)(t) + \dfrac{28x^2 t}{x^2 + 1} = 0, \quad 0 < t < 1, \\[4mm] x(0) = D_{(1,1/2)} x(0) = 0, D_{(1,1/2)} x(1) = \displaystyle\int_0^1 t^{(1/2)} D_{(1,1/2)} x(t) d_{1,1/2} t. \end{cases} \tag{81}$$

Conclusion: BVP equation (81) has at least two positive solutions.

Proof. BVP equation (81) can be regarded as a BVP of the form of equation (1), where

$$f(t,x) = \frac{28x^2 t}{x^2 + 1}, \tag{82}$$

$p = 1, q = 1/2, \alpha = 5/2,$ and $h(t) = t^{1/2}.$ Choose $\phi_{r^*}(t) = t^2 + 2$ and $r^* = 1/5.$ Obviously, $f: [0,1] \times [1/5t^{3/2}, 1/5] \longrightarrow [0, +\infty)$ is continuous and $f(t,x) \ge \phi_{r^*}(t)$ for $(t,x) \in [0,1] \times [1/5t^{3/2}, 1/5].$

Consequently,

$$\lim_{x \longrightarrow 0} \sup_{t \in [0,1]} \frac{f(t,x)}{x} = \frac{28x^2 t}{x(x^2+1)} = 0 < \lambda_1,$$

$$\lim_{x \longrightarrow +\infty} \sup_{t \in [0,1]} \frac{f(t,x)}{x} = \frac{28x^2 t}{x(x^2+1)} = 0 < \lambda_1. \tag{83}$$

From the definition of function G, one can obtain that

$$G\left(t, \frac{s}{2}\right) = G_0\left(t, \frac{s}{2}\right) + \frac{t^{\alpha-1}}{A} \int_0^1 h(t) G_1\left(t, \frac{s}{2}\right) d_{1,1/2} t, \tag{84}$$

where

$$
G_0\left(t,\frac{s}{2}\right) = \frac{1}{1^{(\alpha/2)}\Gamma_{(1,1/2)}(5/2)}
\begin{cases}
t^{3/2}\left(1-\dfrac{s}{2}\right)^{(1/2)} - \left(t-\dfrac{s}{2}\right)^{(3/2)}, & 0 \le s \le t \le 1, \\[2mm]
t^{3/2}\left(1-\dfrac{s}{2}\right)^{(1/2)}, & 0 \le t \le s \le 1,
\end{cases}
$$

$$
G_1\left(t,\frac{s}{2}\right) = \frac{1}{1^{(\alpha/2)}\Gamma_{(1,1/2)}(5/2)}
\begin{cases}
t^{1/2}\left(1-\dfrac{s}{2}\right)^{(1/2)} - \left(t-\dfrac{s}{2}\right)^{(1/2)}, & 0 \le s \le t \le 1, \\[2mm]
t^{1/2}\left(1-\dfrac{s}{2}\right)^{(1/2)}, & 0 \le t \le s \le 1.
\end{cases}
\tag{85}
$$

Consequently,

$$
\max_{t\in[0,1]} \int_0^1 t^{\alpha-1} G\left(1,\frac{s}{2}\right)\phi_{r^*}(s)\,d_{p,q}s \approx 0.235 > \frac{1}{5} = r^*. \tag{86}
$$

Therefore, by Theorem 3, BVP equation (81) has at least two positive solutions. □

Example 2. Consider the following boundary value problem:

$$
\begin{cases}
\left(D^{5/2}_{(1,(1/2))}x\right)(t) + \left(3x^{3/2} + 2t\right) = 0, & 0 < t < 1, \\[2mm]
x(0) = D_{(1,(1/2))}x(0) = 0, \quad D_{(1,(1/2))}x(1) = \displaystyle\int_0^1 t^{(1/2)}D_{(1,(1/2))}x(t)\,d_{1,1/2}t.
\end{cases}
\tag{87}
$$

Conclusion: BVP equation (87) has at least two positive solutions.

Proof. BVP equation (87) can be regarded as a BVP of the form of equation (1), where

$$
f(t,x) = 3x^{3/2} + 2t, \tag{88}
$$

$p = 1$, $q = (1/2)$, $\alpha = (5/2)$, and $h(t) = t^{(1/2)}$. Choose $\psi_{r_*}(t) = 2t + 9$, $r_* = 3\sqrt{3}$. Obviously, $f: [0,1] \times [0, 3\sqrt{3}] \longrightarrow [0,+\infty)$ is continuous and $f(t,x) \le \psi_{r_*}(t)$ for $(t,x) \in [0,1] \times [0,3\sqrt{3}]$.

Consequently,

$$
\lim_{x\to 0}\inf_{t\in[0,1]}\frac{f(t,x)}{x} = \frac{3x^{3/2}+2t}{x} = +\infty > \lambda_1,
$$

$$
\lim_{x\to +\infty}\inf_{t\in[0,1]}\frac{f(t,x)}{x} = \frac{3x^{3/2}+2t}{x} = +\infty > \lambda_1.
\tag{89}
$$

From the definition of function G, one can obtain that

$$
G\left(t,\frac{s}{2}\right) = G_0\left(t,\frac{s}{2}\right) + \frac{t^{\alpha-1}}{A}\int_0^1 h(t)G_1\left(t,\frac{s}{2}\right)d_{1,(1/2)}t, \tag{90}
$$

where

$$
G_0\left(t,\frac{s}{2}\right) = \frac{1}{1^{(\alpha/2)}\Gamma_{(1,(1/2))}(5/2)}
\begin{cases}
t^{1/2}\left(1-\dfrac{s}{2}\right)^{(1/2)} - \left(t-\dfrac{s}{2}\right)^{(1/2)}, & 0 \le s \le t \le 1; \\[2mm]
t^{3/2}\left(1-\dfrac{s}{2}\right)^{(1/2)}, & 0 \le t \le s \le 1,
\end{cases}
$$

$$
G_1\left(t,\frac{s}{2}\right) = \frac{1}{1^{(\alpha/2)}\Gamma_{(1,(1/2))}(5/2)}
\begin{cases}
t^{1/2}\left(1-\dfrac{s}{2}\right)^{(1/2)} - \left(t-\dfrac{s}{2}\right)^{(1/2)}, & 0 \le s \le t \le 1; \\[2mm]
t^{1/2}\left(1-\dfrac{s}{2}\right)^{(1/2)}, & 0 \le t \le s \le 1.
\end{cases}
\tag{91}
$$

Thus,

$$\int_0^1 G\left(1, \frac{s}{2}\right)\psi_{r_*}(s)d_{p,q}s \approx 1.324 < 3\sqrt{3} = r_*. \qquad (92)$$

Therefore, by Theorem 4, BVP equation (87) has at least two positive solutions. □

5. Conclusions

This paper is mainly concerned with a class of fractional (p, q)-difference equations with (p, q)-integral boundary conditions. We first give the definition of fractional (p, q)-difference operator and fractional (p, q)-integral operator. Then, the existence and multiplicity of positive solutions for boundary value problems are obtained by using topological degree theory and Krein–Rutman theorem. Finally, two illustrative examples are given to show the practical usefulness of the analytical results.

Data Availability

No data were used to support this study.

Conflicts of Interest

The authors declare that they have no conflicts of interest.

Acknowledgments

References

[1] F. H. Jackson, "q-difference equations," *American Journal of Mathematics*, vol. 32, no. 4, pp. 305–314, 1910.

[2] R. Chakrabarti and R. Jagannathan, "On the representations of GL$p, q$ (2), GL$p, q$ (1 mod 1) and non-commutative spaces," *Journal of Physics A: Mathematical and General*, vol. 24, no. 24, pp. 5683–5703, 1991.

[3] R. Floreanini and L. Vinet, "q-gamma and q-beta functions in quantum algebra representation theory," *Journal of Computational and Applied Mathematics*, vol. 68, no. 1-2, pp. 57–68, 1996.

[4] V. Kac and P. Cheung, *Quantum Calculus*, Springer, New York, NY, USA, 2002.

[5] H. Cheng, *Canonical Quantization of Yang-Mills Theories, Perspectives in Mathematical Physics*, International Press, Somerville, MA, USA, 1996.

[6] G. Kaniadakis, A. Lavagno, and P. Quarati, "Kinetic model for q-deformed bosons and fermions," *Physics Letters A*, vol. 227, no. 3, pp. 227–231, 1997.

[7] W. J. Trjitzinsky, "Analytic theory of linear q-difference equations," *Acta Mathematica*, vol. 62, no. 1, pp. 167–226, 1933.

[8] J. B. Diaz and T. J. Osler, "Differences of fractional order," *Mathematics of Computation*, vol. 28, no. 125, pp. 185–202, 1974.

[9] P. Njionou Sadjang, "On the fundamental theorem of $$\varvec{(p, q)}$$ (p, q)-calculus and some $$\varvec{(p, q)}$$ (p, q)-Taylor formulas," *Results in Mathematics*, vol. 73, no. 1, p. 39, 2018.

[10] M. Mursaleen, K. J. Ansari, and A. Khan, "On (p, q)-analogue of Bernstein operators," *Applied Mathematics and Computation*, vol. 266, pp. 874–882, 2015.

[11] W. A. Al-Salam, "Some fractional q-integrals and q-derivatives," *Proceedings of the Edinburgh Mathematical Society*, vol. 15, no. 2, pp. 135–140, 1966.

[12] M. N. Hounkonnou and J. D. Kyemba, "(p, q)-calculus: differentiation and integration," *SUT Journal of Mathematics*, vol. 49, no. 2, pp. 145–167, 2013.

[13] M. Mimura, Y. Yamada, and S. Yotsutani, "Stability analysis for free boundary problems in ecology," *Hiroshima Mathematical Journal*, vol. 16, pp. 477–498, 1986.

[14] T. Brikshavana and T. Sitthiwirattham, "On fractional Hahn calculus," *Advances in Difference Equations*, vol. 2017, no. 1, p. 354, 2017.

[15] J. Soontharanon and T. Sitthiwirattham, "On fractional $ (p, q)$-calculus," *Advances in Difference Equations*, vol. 2020, no. 1, p. 35, 2020.

[16] H. Cheng and R. Yuan, "The stability of the equilibria of the Allen-Cahn equation with fractional diffusion," *Applicable Analysis*, vol. 98, no. 3, pp. 600–610, 2019.

[17] W. Cheng, J. Xu, and D. ORegan, "Positive solutions for a nonlinear discrete fractional boundary value problem with a p-laplacian operator," *Journal of Applied Analysis and Computation*, vol. 9, no. 5, pp. 1959–1972, 2019.

[18] J. Jia and H. Wang, "A fast finite volume method for conservative space-time fractional diffusion equations discretized on space-time locally refined meshes," *Computers & Mathematics with Applications*, vol. 78, no. 5, pp. 1345–1356, 2019.

[19] Y. Liu, "Positive solutions using bifurcation techniques for boundary value problems of fractional differential equations," *Abstract and Applied Analysis*, vol. 2013, Article ID 162418, 7 pages, 2013.

[20] Y. Liu, "Bifurcation techniques for a class of boundary value problems of fractional impulsive differential equations," *The Journal of Nonlinear Science and Applications*, vol. 09, no. 4, pp. 340–353, 2015.

[21] Y. Liu and H. Yu, "Bifurcation of positive solutions for a class of boundary value problems of fractional differential inclusions," *Abstract and Applied Analysis*, vol. 2013, Article ID 942831, 2013.

[22] T. Ma and B. Yan, "The multiplicity solutions for nonlinear fractional differential equations of Riemann-Liouville type," *Fractional Calculus and Applied Analysis*, vol. 21, no. 3, pp. 801–818, 2018.

[23] J. Mao and D. Zhao, "Multiple positive solutions for nonlinear fractional differential equations with integral boundary value conditions and a parameter," *Journal of Function Spaces*, vol. 2019, Article ID 2787569, 11 pages, 2019.

[24] T. Qi, Y. Liu, and Y. Cui, "Existence of solutions for a class of coupled fractional differential systems with nonlocal boundary conditions," *Journal of Function Spaces*, vol. 2017, Article ID 6703860, 9 pages, 2017.

[25] T. Qi, Y. Liu, and Y. Zou, "Existence result for a class of coupled fractional differential systems with integral boundary value conditions," *The Journal of Nonlinear Science and Applications*, vol. 10, no. 7, pp. 4034–4045, 2017.

[26] Y. Wang, Y. Liu, and Y. Cui, "Multiple solutions for a nonlinear fractional boundary value problem via critical point theory," *Journal of Function Spaces*, vol. 2017, pp. 8548975–8, 2017.

[27] Y. Wang, Y. Liu, and Y. Cui, "Infinitely many solutions for impulsive fractional boundary value problem with p-Laplacian," *Boundary Value Problems*, vol. 2018, no. 1, p. 94, 2018.

[28] Y. Wang, Y. Liu, and Y. Cui, "Multiple sign-changing solutions for nonlinear fractional Kirchhoff equations," *Boundary Value Problems*, vol. 2018, no. 1, p. 193, 2018.

[29] M. Wang, X. Qu, X. Qu, and H. Lu, "Ground state sign-changing solutions for fractional Laplacian equations with critical nonlinearity," *AIMS Mathematics*, vol. 6, no. 5, pp. 5028–5039, 2021.

[30] J. Xu, Z. Wei, Z. Wei, D. O'Regan, and Y. Cui, "Infinitely many solutions for fractional schrödinger-maxwell equations," *Journal of Applied Analysis & Computation*, vol. 9, no. 3, pp. 1165–1182, 2019.

[31] D. Zhao and Y. Liu, "Positive solutions for a class of fractional differential coupled system with integral boundary value conditions," *The Journal of Nonlinear Science and Applications*, vol. 09, no. 5, pp. 2922–2942, 2016.

[32] D. Zhao and J. Mao, "New controllability results of fractional nonlocal semilinear evolution systems with finite delay," *Complexity*, vol. 2020, Article ID 7652648, 13 pages, 2020.

[33] D. Zhao, Y. Liu, Y. Liu, and X. Li, "Controllability for a class of semilinear fractional evolution systems via resolvent operators," *Communications on Pure and Applied Analysis*, vol. 18, no. 1, pp. 455–478, 2019.

[34] Z. Zhou and W. Gong, "Finite element approximation of optimal control problems governed by time fractional diffusion equation," *Computers & Mathematics with Applications*, vol. 71, no. 1, pp. 301–318, 2016.

[35] F. Chen and X. Luo, "Existence results for nonlinear fractional difference equation," *Advances in Differential Equations*, vol. 12, Article ID 713201, 2011.

[36] M. Jagan and G. V. Deekshitulu, "Fractional order difference equations," *International Journal of Differential Equations*, vol. 2012, Article ID 780619, 11 pages, 2012.

[37] D. Guo and V. Lakshmikantham, *Nonlinear Problems in Abstract Cones*, Academic Press, New York, NY, USA, 1988.

Research Article

Analysis of a Coupled System of Nonlinear Fractional Langevin Equations with Certain Nonlocal and Nonseparated Boundary Conditions

Zaid Laadjal [iD],[1] **Qasem M. Al-Mdallal** [iD],[2] and **Fahd Jarad** [iD][3,4]

[1]*Department of Mathematics and Computer Sciences, ICOSI Laboratory, Abbes Laghrour University, Khenchela 40004, Algeria*
[2]*Department of Mathematical Sciences, United Arab Emirates University, P. O. Box 15551, Al Ain, Abu Dhabi, UAE*
[3]*Department of Mathematics, Çankaya University, Etimesgut, Ankara, Turkey*
[4]*Department of Medical Research, China Medical University, Taichung 40402, Taiwan*

Correspondence should be addressed to Qasem M. Al-Mdallal; q.almdallal@uaeu.ac.ae and Fahd Jarad; fahd@cankaya.edu.tr

In this article, we use some fixed point theorems to discuss the existence and uniqueness of solutions to a coupled system of a nonlinear Langevin differential equation which involves Caputo fractional derivatives of different orders and is governed by new type of nonlocal and nonseparated boundary conditions consisting of fractional integrals and derivatives. The considered boundary conditions are totally dissimilar than the ones already handled in the literature. Additionally, we modify the Adams-type predictor-corrector method by implicitly implementing the Gauss–Seidel method in order to solve some specific particular cases of the system.

1. Introduction

The fractional calculus is the ramification of mathematics concerning the integrals and derivatives of functions with arbitrary orders. It has a long history that goes back to more than three hundred years. Nonetheless, researchers discovered the importance and effectiveness of this calculus just a mere in the last few decades. It turned out that the fractional integrals and derivatives are very good tools in modeling some phenomena. This was concluded simply because of the amazing results obtained when some of the researchers used the implements in the fractional calculus for the sake of understanding real world problems happening in the environment surrounding. Recently, differential equations of fractional order have been applied in various fields like physical, biology, chemistry, control theory, electrical circuits, blood flow phenomena, and signal and image processing; for more details, see [1–3] and references cited therein.

In 1908, Langevin [4] formulated his famous equation containing derivative of integer order. This equation describes the evolution of certain physical phenomena in fluctuating environments [5]. The Langevin equation was used in large part to describe some phenomena such as anomalous transport [6]. The Langevin equation has been recently extended to the fractional order by Lim et al. [7]. They acquainted a new form of Langevin equations involving two different fractional order for the sake of describing the viscoelastic anomalous diffusion in the complex liquids. We refer the reader to Subsection 2.1 in [3] and the references cited therein for further details. Uranagase and Munakata [8] discussed the generalized Langevin equation with emphasis on a mechanical random force whose time evolution is not natural due to the presence of a projection operator in a propagator. Lozinski et al. [9] discussed the applications of Langevin and Fokker–Planck equations in polymer rheology and stochastic simulation techniques for solving this equation. Laadjal et al. [10] presented the

existence and uniqueness of solutions for the multiterm fractional Langevin equation with boundary conditions.

Using the tools in mathematical analysis and the theory of fixed points, discussing the qualitative specification encapsuling the behaviors of solutions of differential equations in fractional derivatives settings has attracted the attention of many scientists. To get an update about the works in the literature, we ask the readers to investigate [11] and the references cited there. On the top of this, classes of systems of fractional differential equations with separated (or nonseparated) boundary conditions have been studied intensively in literatures [12–14].

Motivated by what are mentioned above and the recent development on Langevin equations, in this paper, we discuss the existence and the uniqueness of solutions to a coupled system of fractional Langevin equations in the form as follows:

$$\begin{cases} {}^{c}D^{\alpha_1}\left({}^{c}D^{\beta_1} + \lambda\right)\psi_1(t) = f\left(t, \psi_1(t), \psi_2(t)\right), & t \in J, 0 < \alpha_1 \leq 1 < \beta_1 \leq 2, \\ {}^{c}D^{\alpha_2}\left({}^{c}D^{\beta_2} + k\right)\psi_2(t) = g\left(t, \psi_1(t), \psi_2(t)\right), & t \in J, 0 < \alpha_2 \leq 1 < \beta_2 \leq 2, \end{cases} \tag{1}$$

subject to a new type of nonlocal nonseparated boundary conditions as follows:

$$\begin{cases} \psi_1(0) = a_0, \psi_2(0) = b_0, \psi_1'(0) = \psi_2'(0) = 0, \\ \psi_1(\xi) = a\left({}^{c}D^{p}\psi_2\right)(\mu_1), \xi \in (0, 1], \mu_1 \in J, 0 < p < \beta_2, \\ \psi_2(\eta) = b\left(I^{q}\psi_1\right)[\mu_2], \eta \in (0, 1], \mu_2 \in J, q \geq 0, \end{cases} \tag{2}$$

where $J = [0, 1], \lambda, k, a_0, b_0, a, b$ are real constants, ${}^{c}D^{i}$ where $i = \alpha_1, \beta_1, \alpha_2, \beta_2, p$ are the Caputo fractional derivatives of order $\alpha_1, \beta_1, \alpha_2, \beta_2$, and p, respectively, $f, g: J \times \mathbb{R} \times \mathbb{R} \longrightarrow \mathbb{R}$ are given functions, and I^{q} is the Riemann–Liouville fractional integral of order q. By using the Banach contraction principle and Leray–Schauder alternative fixed point theorem, we investigate the existence of solutions for problems (1) and (2). We remark that the boundary value problem discussed here is distinctive of the ones discussed in literatures [12–14].

This article is organized as follows. In Section 2, we present some definitions, theorems, and related lemmas used in next sections. Section 3 discusses the existence and uniqueness of the system under consideration. In Section 4, we furnish some numerical examples. Section 5 is devoted to our concluding remarks.

2. Preliminaries

Definition 1. (see [1, 2]). Let $a, b \in \mathbb{R}$ $(-\infty < a < b < \infty)$. The Riemann–Liouville fractional integral of order $\alpha \in \mathbb{R}^{+}$ for a function $f \in L^{1}[a, b]$ is defined by

$$I_a^{\alpha}f(t) = \frac{1}{\Gamma(\alpha)}\int_a^t (t-s)^{\alpha-1}f(s)\mathrm{d}s, \quad \text{for } \alpha > 0, \text{ and } I_a^0 f(t) = f(t), \tag{3}$$

where Γ is the Euler Gamma function.

Definition 2 (see [1, 2]). The Caputo fractional derivative of order $\alpha \in \mathbb{R}^{+}$ for a function $f \in C^{n}[a, b]$ is defined by

$${}^{c}D_a^{\alpha}f(t) = I_a^{n-\alpha}D^{n}f(t), \quad \text{for } \alpha > 0, \text{ and } {}^{c}D_a^0 f(t) = f(t), \tag{4}$$

where $n - 1 < \alpha \leq n$, $n \in \mathbb{N}$, and $D^{n} = \mathrm{d}^{n}/\mathrm{d}t^{n}$.

Proposition 3 (see [2]). *For $\beta > 0$ and $\alpha > 0$ and $f \in L^{1}[a, b]$, we have the following properties:*

$$I_a^{\alpha}I_a^{\beta}f(t) = I_a^{\beta}I_a^{\alpha}f(t) = I_a^{\alpha+\beta}f(t).$$

$$I_a^{\alpha}(t-a)^{\mu} = \frac{\Gamma(\mu+1)}{\Gamma(\alpha+\mu+1)}(t-a)^{\alpha+\mu}, \mu > -1. \tag{5}$$

$${}^{c}D_a^{\alpha}\left(I_a^{\beta}f(t)\right) = I_a^{\beta-\alpha}f(t), \quad (\text{here } \beta \geq \alpha > 0).$$

Proposition 4 (see [2]). *Let $\alpha > 0$ with $n - 1 < \alpha \leq n$ and $f \in C^{n}[a, b]$. Then,*

$$I_a^{\alpha}\left[{}^{c}D_a^{\alpha}f(t)\right] = f(t) - \sum_{k=0}^{n-1} c_k(t-a)^{k}, \tag{6}$$

where $c_k = f^{(k)}(a)/k!$. In particular, when $0 < \alpha \leq 1$, we have

$$I_0^{\alpha}\left[{}^{c}D_0^{\alpha}f(t)\right] = f(t) - f(0). \tag{7}$$

Proposition 5 (see [2]). *Let $\mu > 0$ and $\alpha > 0$ with $n - 1 < \alpha \leq n$. Then,*

$${}^{c}D_a^{\alpha}(t-a)^{\mu-1} = \frac{\Gamma(\mu)}{\Gamma(\mu-\alpha)}(t-a)^{\mu-\alpha-1}, \mu > \mathrm{n},$$

$${}^{c}D_a^{\alpha}(t-a)^{k} = 0, k = 0, 1, \ldots, n-1. \tag{8}$$

Theorem 6 (Leray–Schauder alternative [15]). *Let $T: X \longrightarrow X$ be a completely continuous operator (i.e., a map that is restricted to any bounded set in X is compact). Let $M(T) = \{u \in X: u = mT(u) \text{ for some } 0 < m < 1\}$. Then, either the set $M(T)$ is unbounded or T has at least one fixed point.*

For the sake of simplicity, henceforwards we will write I^{α} and ${}^{c}D^{\alpha}$ instead of I_0^{α} and ${}^{c}D_0^{\alpha}$, respectively.

3. Main Results

In this section, we will discuss the existence and uniqueness of the solution to systems (1)-(2).

Lemma 7. *Let* $v, w \in C([0, 1], \mathbb{R})$, $0 < \alpha_1, \alpha_2 \leq 1$, $1 < \beta_1, \beta_2 \leq 2$, $q \geq 0$, $0 < p < \beta_2$, $(\overline{\alpha}_1 := \alpha_1 + \beta_1 + q, \overline{\alpha}_2 := \alpha_2 + \beta_2 - p)$, *and*

$$\Delta = \frac{\xi^{\beta_1} \eta^{\beta_2}}{\Gamma(\beta_1 + 1)\Gamma(\beta_2 + 1)} - \frac{ab\mu_1^{\beta_2 - p}\mu_2^{\beta_1 + q}}{\Gamma(\beta_1 + q + 1)\Gamma(\beta_2 - p + 1)} \neq 0. \tag{9}$$

Then, the solution of the following coupled system of fractional Langevin equations is as follows:

$$^c D^{\alpha_1}\left(^c D^{\beta_1} + \lambda\right)\psi_1(t) = v(t), \tag{10}$$

$$^c D^{\alpha_2}\left(^c D^{\beta_2} + k\right)\psi_2(t) = w(t), \tag{11}$$

equipped with the boundary condition (2) which is equivalent to the coupled system of the following integral equations:

$$\psi_1(t) = I^{\alpha_1 + \beta_1} v(t) - \lambda I^{\beta_1}\psi_1(t) + t^{\beta_1}\left\{A_1\left[aI^{\overline{\alpha}_2}w(\mu_1) - akI^{\beta_2 - p}\psi_2(\mu_1) - I^{\alpha_1 + \beta_1}v(\xi) + \lambda I^{\beta_1}\psi_1(\xi)\right]\right.$$
$$\left. + A_2\left[bI^{\overline{\alpha}_1}v(\mu_2) - b\lambda I^{\beta_1 + q}\psi_1(\mu_2) - I^{\alpha_2 + \beta_2}w(\eta) + kI^{\beta_2}\psi_2(\eta)\right] + A_3\right\} + a_0, \tag{12}$$

$$\psi_2(t) = I^{\alpha_2 + \beta_2} w(t) - kI^{\beta_2}\psi_2(t) + t^{\beta_2}\left\{B_1\left[bI^{\overline{\alpha}_1}v(\mu_2) - b\lambda I^{\beta_1 + q}\psi_1(\mu_2) - I^{\alpha_2 + \beta_2}w(\eta) + kI^{\beta_2}\psi_2(\eta)\right]\right.$$
$$\left. + B_2\left[aI^{\overline{\alpha}_2}w(\mu_1) - akI^{\beta_2 - p}\psi_2(\mu_1) - I^{\alpha_1 + \beta_1}v(\xi) + \lambda I^{\beta_1}\psi_1(\xi)\right] + B_3\right\} + b_0, \tag{13}$$

where

$$A_1 = \frac{1}{\Delta\Gamma(\beta_1 + 1)}\frac{\eta^{\beta_2}}{\Gamma(\beta_2 + 1)},$$

$$A_2 = \frac{1}{\Delta\Gamma(\beta_1 + 1)}\frac{a\mu_1^{\beta_2 - p}}{\Gamma(\beta_2 - p + 1)},$$

$$A_3 = \frac{1}{\Delta\Gamma(\beta_1 + 1)}\left[-\frac{a_0\eta^{\beta_2}}{\Gamma(\beta_2 + 1)} + \frac{a\mu_1^{\beta_2 - p}}{\Gamma(\beta_2 - p + 1)}\left(\frac{ba_0\mu_2^q}{\Gamma(q + 1)} - b_0\right)\right],$$

$$B_1 = \frac{1}{\Delta\Gamma(\beta_2 + 1)}\frac{\xi^{\beta_1}}{\Gamma(\beta_1 + 1)}, \tag{14}$$

$$B_2 = \frac{1}{\Delta\Gamma(\beta_2 + 1)}\frac{b\mu_2^{q + \beta_1}}{\Gamma(q + \beta_1 + 1)},$$

$$B_3 = \frac{1}{\Delta\Gamma(\beta_2 + 1)}\left[-\frac{ba_0\mu_2^{q + \beta_1}}{\Gamma(q + \beta_1 + 1)} + \frac{\xi^{\beta_1}}{\Gamma(\beta_1 + 1)}\left(\frac{ba_0\mu_2^q}{\Gamma(q + 1)} - b_0\right)\right].$$

Proof. Applying the operator $I^{\alpha_1 + \beta_1}$ and $I^{\alpha_2 + \beta_2}$ on (10) and (11), respectively, we get

$$\psi_1(t) = I^{\alpha_1 + \beta_1} v(t) - \lambda I^{\beta_1} \psi_1(t) + \frac{c_2 t^{\beta_1}}{\Gamma(\beta_1 + 1)} + c_1 t + c_0, \tag{15}$$

$$\psi_2(t) = I^{\alpha_2 + \beta_2} w(t) - k I^{\beta_2} \psi_2(t) + \frac{\overline{c}_2 t^{\beta_2}}{\Gamma(\beta_2 + 1)} + \overline{c}_1 t + \overline{c}_0, \tag{16}$$

where $c_i, \overline{c}_i \in \mathbb{R}$ $(i = 0, 1, 2)$. From the boundary conditions $\psi_1(0) = a_0, \psi_2(0) = b_0$, and $\psi_1'(0) = \psi_2'(0) = 0$, we get $c_0 = a_0, \overline{c}_0 = b_0$, and $c_1 = \overline{c}_1 = 0$, respectively. Next, using the nonlocal integral conditions $\psi_1(\xi) = a(^c D^p \psi_2)(\mu_1)$ and $\psi_2(\eta) = b(I^q \psi_1)(\mu_2)$, we obtain that

$$I^{\alpha_1 + \beta_1} v(\xi) - \lambda I^{\beta_1} \psi_1(\xi) + \frac{c_2 \xi^{\beta_1}}{\Gamma(\beta_1 + 1)} + a_0 = a I^{\overline{\alpha}_2} w(\mu_1)$$
$$- a k I^{\beta_2 - p} \psi_2(\mu_1) + \frac{a \overline{c}_2 \mu_1^{\beta_2 - p}}{\Gamma(\beta_2 - p + 1)}, \tag{17}$$

$$I^{\alpha_2 + \beta_2} w(\eta) - k I^{\beta_2} \psi_2(\eta) + \frac{\overline{c}_2 \eta^{\beta_2}}{\Gamma(\beta_2 + 1)} + b_0 = b I^{\overline{\alpha}_1} v(\mu_2)$$
$$- b \lambda I^{\beta_1 + q} \psi_1(\mu_2) + \frac{c_2 b \mu_2^{\beta_1 + q}}{\Gamma(\beta_1 + q + 1)} + \frac{b a_0 \mu_2^q}{\Gamma(q + 1)}. \tag{18}$$

Solving the above system, we find that

$$c_2 = \frac{1}{\Delta} \left[\frac{\eta^{\beta_2}}{\Gamma(\beta_2 + 1)} \left[a I^{\overline{\alpha}_2} w(\mu_1) - a k I^{\beta_2 - p} \psi_2(\mu_1) - I^{\alpha_1 + \beta_1} v(\xi) + \lambda I^{\beta_1} \psi_1(\xi) \right] \right.$$

$$+ \frac{a \mu_1^{\beta_2 - p}}{\Gamma(\beta_2 + 1 - p)} \left[b I^{\overline{\alpha}_1} v(\mu_2) - b \lambda I^{\beta_1 + q} \psi_1(\mu_2) - I^{\alpha_2 + \beta_2} w(\eta) + k I^{\beta_2} \psi_2(\eta) \right]$$

$$\left. - \frac{a_0 \eta^{\beta_2}}{\Gamma(\beta_2 + 1)} + \frac{a \mu_1^{\beta_2 - p}}{\Gamma(\beta_2 - p + 1)} \left(\frac{b a_0 \mu_2^q}{\Gamma(q + 1)} - b_0 \right) \right]$$

$$\overline{c}_2 = \frac{1}{\Delta} \left[\frac{\xi^{\beta_1}}{\Gamma(\beta_1 + 1)} \left[b I^{\overline{\alpha}_1} v(\mu_2) - b \lambda I^{\beta_1 + q} \psi_1(\mu_2) - I^{\alpha_2 + \beta_2} w(\eta) + k I^{\beta_2} \psi_2(\eta) \right] \right.$$

$$+ \frac{b \mu_2^{q + \beta_1}}{\Gamma(q + \beta_1 + 1)} \left[a I^{\overline{\alpha}_2} w(\mu_1) - a k I^{\beta_2 - p} \psi_2(\mu_1) - I^{\alpha_1 + \beta_1} v(\xi) + \lambda I^{\beta_1} \psi_1(\xi) \right]$$

$$\left. - \frac{a_0 b \mu_2^{q + \beta_1}}{\Gamma(q + \beta_1 + 1)} + \frac{\xi^{\beta_1}}{\Gamma(\beta_1 + 1)} \left(\frac{b a_0 \mu_2^q}{\Gamma(q + 1)} - b_0 \right) \right], \tag{19}$$

where Δ is the determinant of the matrix associated with systems (17)-(18) in the two variables c_2 and $\overline{c}_2$, and it is given by (9).

Substituting the values of $c_0, \overline{c}_0, c_1, \overline{c}_1, c_2$, and $\overline{c}_2$ in (15) and (16), we obtain the system of the integral equations (12) and (13). The proof is completed. □

The Banach space $E = C([0, 1], \mathbb{R})$ is defined with the norm $\|\psi_1\|_E = \sup_{t \in J} |\psi_1(t)|$.

So, the space $E \times E = \{(\psi_1, \psi_2), \text{s.t} (\psi_1, \psi_2) \in E \times E\}$ with the norm $\|(\psi_1, \psi_2)\|_{E \times E} = \|\psi_1\|_E + \|\psi_2\|_E$ is Banach space.

Now, let us define the operator $\mathfrak{N} \colon E \times E \longrightarrow E \times E$, by $\mathfrak{N}(\psi_1, \psi_2)(t) = (\mathfrak{N}_1(\psi_1, \psi_2)(t), \mathfrak{N}_2(\psi_1, \psi_2)(t))$, where

$$\mathfrak{N}_1(\psi_1, \psi_2)(t) = \frac{1}{\Gamma(\alpha_1 + \beta_1)} \int_0^t (t-s)^{\alpha_1+\beta_1-1} f(s, \psi_1(s), \psi_2(s)) ds - \frac{\lambda}{\Gamma(\beta_1)} \int_0^t (t-s)^{\beta_1-1} \psi_1(s) ds$$

$$+ t^{\beta_1} \left\{ A_1 \left(\frac{a}{\Gamma(\overline{\alpha}_2)} \int_0^{\mu_1} (\mu_1 - s)^{\overline{\alpha}_2 - 1} g(s, \psi_1(s), \psi_2(s)) ds - \frac{ak}{\Gamma(\beta_2 - p)} \right.\right.$$

$$\times \int_0^{\mu_1} (\mu_1 - s)^{\beta_2 - p - 1} \psi_2(s) ds - \frac{1}{\Gamma(\alpha_1 + \beta_1)} \int_0^{\xi} (\xi - s)^{\alpha_1+\beta_1-1} f(s, \psi_1(s), \psi_2(s)) ds$$

$$+ \frac{\lambda}{\Gamma(\beta_1)} \int_0^{\xi} (\xi - s)^{\beta_1 - 1} \psi_1(s) ds \Big) + A_2 \Big(\frac{b}{\Gamma(\overline{\alpha}_1)} \int_0^{\mu_2} (\mu_2 - s)^{\overline{\alpha}_1 - 1} f(s, \psi_1(s), \psi_2(s)) ds$$

$$- \frac{b\lambda}{\Gamma(\beta_1 + q)} \int_0^{\mu_2} (\mu_2 - s)^{\beta_1 + q - 1} \psi_1(s) ds - \frac{1}{\Gamma(\alpha_2 + \beta_2)} \int_0^{\eta} (\eta - s)^{\alpha_2+\beta_2-1} g(s, \psi_1(s), \psi_2(s)) ds$$

$$+ \frac{k}{\Gamma(\beta_2)} \int_0^{\eta} (\eta - s)^{\beta_2 - 1} \psi_2(s) ds \Big) + A_3 \Big\} + a_0,$$

$$\mathfrak{N}_2(\psi_1, \psi_2)(t) = \frac{1}{\Gamma(\alpha_2 + \beta_2)} \int_0^t (t-s)^{\alpha_2+\beta_2-1} g(s, \psi_1(s), \psi_2(s)) ds - \frac{k}{\Gamma(\beta_2)} \int_0^t (t-s)^{\beta_2-1} \psi_2(s) ds$$

$$+ t^{\beta_2} \left\{ B_1 \left(\frac{b}{\Gamma(\overline{\alpha}_1)} \int_0^{\mu_2} (\mu_2 - s)^{\overline{\alpha}_1 - 1} f(s, \psi_1(s), \psi_2(s)) ds - \frac{b\lambda}{\Gamma(\beta_1 + q)} \right.\right.$$

$$\times \int_0^{\mu_2} (\mu_2 - s)^{\beta_1 + q - 1} \psi_1(s) ds - \frac{1}{\Gamma(\alpha_2 + \beta_2)} \int_0^{\eta} (\eta - s)^{\alpha_2+\beta_2-1} g(s, \psi_1(s), \psi_2(s)) ds$$

$$+ \frac{k}{\Gamma(\beta_2)} \int_0^{\eta} (\eta - s)^{\beta_2 - 1} \psi_2(s) ds + B_2 \Big(\frac{a}{\Gamma(\overline{\alpha}_2)} \int_0^{\mu_1} (\mu_1 - s)^{\overline{\alpha}_2 - 1} g(s, \psi_1(s), \psi_2(s)) ds$$

$$- \frac{ak}{\Gamma(\beta_2 - p)} \int_0^{\mu_1} (\mu_1 - s)^{\beta_2 - p - 1} \psi_2(s) ds - \frac{1}{\Gamma(\alpha_1 + \beta_1)} \int_0^{\xi} (\xi - s)^{\alpha_1+\beta_1-1} f(s, \psi_1(s), \psi_2(s)) ds$$

$$+ \frac{\lambda}{\Gamma(\beta_1)} \int_0^{\xi} (\xi - s)^{\beta_1 - 1} \psi_1(s) ds \Big) + B_3 \Big\} + b_0.$$

(20)

Note that the couple (ψ_1, ψ_2) is a fixed point of the operator $\mathfrak{N}$ if only if (ψ_1, ψ_2) is a solution of systems (1)-(2). Consider the following hypotheses:

(H1). $f, g \colon J \times \mathbb{R} \times \mathbb{R} \longrightarrow \mathbb{R}$ are continuous functions, and there exist real positive constants σ_i, τ_i $(i = 0, 1, 2)$ such that

$$|f(t, \zeta, \kappa)| \le \sigma_0 + \sigma_1 |\zeta| + \sigma_2 |\kappa|,$$
$$|g(t, \zeta, \kappa)| \le \tau_0 + \tau_1 |\zeta| + \tau_2 |\kappa|,$$

(21)

for all $(t, \zeta, \kappa) \in J \times \mathbb{R} \times \mathbb{R}$.

(H2). There exist constants $K, L > 0$ such that

$$|f(t, \zeta, \kappa) - f(t, \overline{\zeta}, \overline{\kappa})| \le K(|\zeta - \overline{\zeta}| + |\kappa - \overline{\kappa}|),$$
$$|g(t, \zeta, \kappa) - g(t, \overline{\zeta}, \overline{\kappa})| \le L(|\zeta - \overline{\zeta}| + |\kappa - \overline{\kappa}|),$$

(22)

for all $(t, \zeta, \kappa), (t, \overline{\zeta}, \overline{\kappa}) \in J \times \mathbb{R} \times \mathbb{R}$.

(H3). There exist $F_0, G_0 > 0$ such that $F_0 = \sup_{t \in J} |f(t, 0, 0)|$ and $G_0 = \sup_{t \in J} |g(t, 0, 0)|$.

Remark 8. From conditions (H1) and (H2) for all $(\psi_1, \psi_2) \in E \times E$, we get

$$|f(t, \psi_1(t), \psi_2(t))| \le K \|(\psi_1, \psi_2)\|_{E \times E} + F_0,$$
$$|g(t, \psi_1(t), \psi_2(t))| \le L \|(\psi_1, \psi_2)\|_{E \times E} + G_0.$$

(23)

For computation convenience, we set the following constants:

$$Q_1 = \frac{1 + |A_1| \xi^{\alpha_1 + \beta_1}}{\Gamma(\alpha_1 + \beta_1 + 1)} + \frac{|A_2 b| \mu_2^{\overline{\alpha}_1}}{\Gamma(\overline{\alpha}_1 + 1)},$$

(24)

$$Q_2 = \frac{|a A_1| \mu_1^{\overline{\alpha}_2}}{\Gamma(\overline{\alpha}_2 + 1)} + \frac{|A_2| \eta^{\alpha_2 + \beta_2}}{\Gamma(\alpha_2 + \beta_2 + 1)},$$

$$Q_3 = \frac{|b B_1| \mu_2^{\overline{\alpha}_1}}{\Gamma(\overline{\alpha}_1 + 1)} + \frac{|B_2| \xi^{\alpha_1 + \beta_1}}{\Gamma(\alpha_1 + \beta_1 + 1)},$$

(25)

$$Q_4 = \frac{1 + |B_1| \eta^{\alpha_2 + \beta_2}}{\Gamma(\alpha_2 + \beta_2 + 1)} + \frac{|B_2 a| \mu_1^{\overline{\alpha}_2}}{\Gamma(\overline{\alpha}_2 + 1)},$$

$$Q_5 = \frac{\left(1 + |A_1|\xi^{\beta_1}\right)|\lambda|}{\Gamma(\beta_1 + 1)} + \frac{|A_2||b\lambda|\mu_2^{\beta_1 + q}}{\Gamma(\beta_1 + q + 1)},$$

$$Q_6 = \frac{|A_1||ak|\mu_1^{\beta_2 - p}}{\Gamma(\beta_2 - p + 1)} + \frac{|A_2||k|\eta^{\beta_2}}{\Gamma(\beta_2 + 1)}, \tag{26}$$

$$Q_7 = \frac{|B_2\lambda|\xi^{\beta_1}}{\Gamma(\beta_1 + 1)} + \frac{|b\lambda B_1|\mu_2^{\beta_1 + q}}{\Gamma(\beta_1 + q + 1)},$$

$$Q_8 = \frac{|B_2 ak|\mu_1^{\beta_2 - p}}{\Gamma(\beta_2 - p + 1)} + \frac{\left(1 + |B_1|\eta^{\beta_2}\right)|k|}{\Gamma(\beta_2 + 1)}, \tag{27}$$

$$\rho_1 = \max\{Q_5, Q_6\},$$
$$\rho_2 = \max\{Q_7, Q_8\}. \tag{28}$$

In the following step, we present the following result about the uniqueness of solutions for problems (1)-(2) by applying the Banach contraction principle.

Theorem 9. *Assume that (H2) and (H3) hold. If*

$$[(Q_1 + Q_3)K + (Q_2 + Q_4)L + \rho_1 + \rho_2] < 1, \tag{29}$$

where $Q_1, Q_2, Q_3,$ and Q_4 and ρ_1 and ρ_2 are, respectively, defined by (24), (25), and (28), then the boundary value problems (1)-(2) have a unique solution.

Proof. Choose a positive real constant R where

$$R \geq \frac{(Q_1 + Q_3)F_0 + (Q_2 + Q_4)G_0 + |A_3| + |B_3| + |a_0| + |b_0|}{1 - [(Q_1 + Q_3)K + (Q_2 + Q_4)L + \rho_1 + \rho_2]}. \tag{30}$$

Let $B_R = \{(\psi_1, \psi_2) \in E \times E \text{ s.t. } \|(\psi_1, \psi_2)\|_{E \times E} \leq R\}$. First, we prove that $\mathfrak{N}(B_R) \subseteq B_R$.

For all $(\psi_1, \psi_2) \in B_R$, we have

$$
\begin{aligned}
|\mathfrak{N}_1(\psi_1, \psi_2)(t)| &\leq \frac{KR + F_0}{\Gamma(\alpha_1 + \beta_1)} \int_0^t (t-s)^{\alpha_1 + \beta_1 - 1} ds + \frac{|\lambda|\|\psi_1\|_E}{\Gamma(\beta_1)} \int_0^t (t-s)^{\beta_1 - 1} ds \\
&\quad + t^{\beta_1} \left\{ |A_1| \left(\frac{|a|(LR + G_0)}{\Gamma(\overline{\alpha}_2)} \int_0^{\mu_1} (\mu_1 - s)^{\overline{\alpha}_2 - 1} ds + \frac{|ak|\|\psi_2\|_E}{\Gamma(\beta_2 - p)} \int_0^{\mu_1} (\mu_1 - s)^{\beta_2 - p - 1} ds \right. \right. \\
&\quad \left. + \frac{KR + F_0}{\Gamma(\alpha_1 + \beta_1)} \int_0^{\xi} (\xi - s)^{\alpha_1 + \beta_1 - 1} ds + \frac{|\lambda|\|\psi_1\|_E}{\Gamma(\beta_1)} \int_0^{\xi} (\xi - s)^{\beta_1 - 1} ds \right) \\
&\quad + |A_2| \left(\frac{|b|(KR + F_0)}{\Gamma(\overline{\alpha}_1)} \int_0^{\mu_2} (\mu_2 - s)^{\overline{\alpha}_1 - 1} ds + \frac{|b\lambda|\|\psi_1\|_E}{\Gamma(\beta_1 + q)} \int_0^{\mu_2} (\mu_2 - s)^{\beta_1 + q - 1} ds \right. \\
&\quad \left. \left. + \frac{LR + G_0}{\Gamma(\alpha_2 + \beta_2)} \int_0^{\eta} (\eta - s)^{\alpha_2 + \beta_2 - 1} ds + \frac{|k|\|\psi_2\|_E}{\Gamma(\beta_2)} \int_0^{\eta} (\eta - s)^{\beta_2 - 1} ds \right) + |A_3| \right\} + |a_0| \\
&\leq \frac{KR + F_0}{\Gamma(\alpha_1 + \beta_1 + 1)} + \frac{|aA_1|(LR + G_0)\mu_1^{\overline{\alpha}_2}}{\Gamma(\overline{\alpha}_2 + 1)} + \frac{|A_1|(KR + F_0)\xi^{\alpha_1 + \beta_1}}{\Gamma(\alpha_1 + \beta_1 + 1)} + \frac{|bA_2|(KR + F_0)\mu_2^{\overline{\alpha}_1}}{\Gamma(\overline{\alpha}_1 + 1)} \\
&\quad + \frac{|A_2|(LR + G_0)\eta^{\alpha_2 - \beta_2}}{\Gamma(\alpha_2 - \beta_2 + 1)} + |A_3| + |a_0| + \left(\frac{|\lambda|\left(1 + |A_1|\xi^{\beta_1}\right)}{\Gamma(\beta_1 + 1)} + \frac{|b\lambda A_2|\mu_2^{\beta_1 + q}}{\Gamma(\beta_1 + q + 1)} \right) \|\psi_1\|_E \\
&\quad + \left(\frac{|kA_2|\eta^{\beta_2}}{\Gamma(\beta_2 + 1)} + \frac{|akA_1|\mu_1^{\beta_2 - p}}{\Gamma(\beta_2 - p + 1)} \right) \|\psi_2\|_E \\
&\leq \left(\frac{K\left(1 + |A_1|\xi^{\alpha_1 + \beta_1}\right)}{\Gamma(\alpha_1 + \beta_1 + 1)} + \frac{|aA_1|\mu_1^{\overline{\alpha}_2}L}{\Gamma(\overline{\alpha}_2 + 1)} + \frac{|bA_2|\mu_2^{\overline{\alpha}_1}K}{\Gamma(\overline{\alpha}_1 + 1)} + \frac{|A_2|\eta^{\alpha_2 + \beta_2}L}{\Gamma(\alpha_2 + \beta_2 + 1)} \right) R \\
&\quad + \frac{F_0\left(1 + |A_1|\xi^{\alpha_1 + \beta_1}\right)}{\Gamma(\alpha_1 + \beta_1 + 1)} + \frac{|aA_1|\mu_1^{\overline{\alpha}_2}G_0}{\Gamma(\overline{\alpha}_2 + 1)} + \frac{|bA_2|\mu_2^{\overline{\alpha}_1}F_0}{\Gamma(\overline{\alpha}_1 + 1)} + \frac{|A_2|\eta^{\alpha_2 + \beta_2}G_0}{\Gamma(\alpha_2 + \beta_2 + 1)} + |A_3| + |a_0| + \rho_1\|(\psi_1, \psi_2)\|_{E \times E} \\
&\leq Q_1 F_0 + Q_2 G_0 + |A_3| + |a_0| + (Q_1 K + Q_2 L + \rho_1) R.
\end{aligned}
\tag{31}
$$

On the other hand, we have

$$
\begin{aligned}
\left|\mathfrak{N}_2\left(\psi_1, \psi_2\right)(t)\right| \leq &\frac{LR + G_0}{\Gamma\left(\alpha_2 + \beta_2 + 1\right)} + \frac{\left|bB_1\right|\mu_2^{\overline{\alpha}_1}\left(KR + F_0\right)}{\Gamma\left(\overline{\alpha}_1 + 1\right)} + \frac{\left|B_1\right|\left(LR + G_0\right)\eta^{\alpha_2 + \beta_2}}{\Gamma\left(\alpha_2 + \beta_2 + 1\right)} \\
&+ \frac{\left|aB_2\right|\left(LR + G_0\right)\mu_1^{\overline{\alpha}_2}}{\Gamma\left(\overline{\alpha}_2 + 1\right)} + \frac{\left|B_2\right|\left(KR + F_0\right)\xi^{\alpha_1 + \beta_1}}{\Gamma\left(\alpha_1 + \beta_1 + 1\right)} + \left|B_3\right| + \left|b_0\right| + \left(\frac{\left|b\lambda B_1\right|\mu_2^{\beta_1 + q}}{\Gamma\left(\beta_1 + q + 1\right)} + \frac{\left|\lambda B_2\right|\xi^{\beta_1}}{\Gamma\left(\beta_1 + 1\right)}\right)\left\|\psi_1\right\|_E \\
&+ \left(\frac{|k|}{\Gamma\left(\beta_2 + 1\right)} + \frac{\left|kB_1\right|\eta^{\beta_2}}{\Gamma\left(\beta_2 + 1\right)} + \frac{\left|akB_2\right|\mu_1^{\beta_2 - p}}{\Gamma\left(\beta_2 - p + 1\right)}\right)\left\|\psi_2\right\|_E \\
\leq & Q_4 G_0 + Q_3 F_0 + \left|B_3\right| + \left|b_0\right| + \left(Q_4 L + Q_3 K\right)R + \rho_2\left(\left\|\psi_1\right\|_E + \left\|\psi_2\right\|_E\right) \\
\leq & Q_4 G_0 + Q_3 F_0 + \left|B_3\right| + \left|b_0\right| + \left(Q_4 L + Q_3 K + \rho_2\right)R.
\end{aligned}
\tag{32}
$$

Consequently,

$$
\begin{aligned}
\left\|\mathfrak{N}\left(\psi_1, \psi_2\right)\right\| \leq & \left(Q_1 + Q_3\right)F_0 + \left(Q_2 + Q_4\right)G_0 + \left|A_3\right| + \left|B_3\right| + \left|a_0\right| + \left|b_0\right| + \left[\left(Q_1 + Q_3\right)K + \left(Q_2 + Q_4\right)L + \rho_1 + \rho_2\right]R, \\
\leq & R.
\end{aligned}
\tag{33}
$$

Therefore, $\mathfrak{N}\left(B_R\right) \subseteq B_R$. Next, we prove that $\mathfrak{N}$ is a contraction. Let $\left(\psi_1, \psi_2\right), \left(\overline{\psi}_1, \overline{\psi}_2\right) \in E \times E$. For all $t \in J$, we have

$$
\begin{aligned}
\left|\mathfrak{N}_1\left(\psi_1, \psi_2\right) - \mathfrak{N}_1\left(\overline{\psi}_1, \overline{\psi}_2\right)(t)\right| \leq &\frac{K\left(\left\|\psi_1 - \overline{\psi}_1\right\|_E + \left\|\psi_2 - \overline{\psi}_2\right\|_E\right)}{\Gamma\left(\alpha_1 + \beta_1 + 1\right)}t^{\alpha_1 + \beta_1} + \frac{|\lambda|\left\|\psi_1 - \overline{\psi}_1\right\|_E}{\Gamma\left(\beta_1 + 1\right)}t^{\beta_1} \\
&+ t^{\beta_1}\left\{\left|A_1\right|\left(\frac{aL\left(\left\|\psi_1 - \overline{\psi}_1\right\|_E + \left\|\psi_2 - \overline{\psi}_2\right\|_E\right)}{\Gamma\left(\overline{\alpha}_2 + 1\right)}\mu_1^{\overline{\alpha}_2} + \frac{|ak|\left\|\psi_2 - \overline{\psi}_2\right\|_E}{\Gamma\left(\beta_2 - p + 1\right)}\mu_1^{\beta_2 - p}\right.\right. \\
&+ \frac{K\left(\left\|\psi_1 - \overline{\psi}_1\right\|_E + \left\|\psi_2 - \overline{\psi}_2\right\|_E\right)}{\Gamma\left(\alpha_1 + \beta_1 + 1\right)}\xi^{\alpha_1 + \beta_1} + \left.\frac{|\lambda|\|x - \overline{x}\|_E}{\Gamma\left(\beta_1 + 1\right)}\xi^{\beta_1}\right) \\
&+ \left|A_2\right|\left(\frac{|b|K\left(\left\|\psi_1 - \overline{\psi}_1\right\|_E + \left\|\psi_2 - \overline{\psi}_2\right\|_E\right)}{\Gamma\left(\overline{\alpha}_1 + 1\right)}\mu_2^{\overline{\alpha}_1} + \frac{|b\lambda|\left\|\psi_1 - \overline{\psi}_1\right\|_E}{\Gamma\left(\beta_1 + q + 1\right)}\mu_2^{\beta_1 + q}\right. \\
&+ \left.\left.\frac{L\left(\left\|\psi_1 - \overline{\psi}_1\right\|_E + \left\|\psi_2 - \overline{\psi}_2\right\|_E\right)}{\Gamma\left(\alpha_2 + \beta_2 + 1\right)}\eta^{\alpha_2 + \beta_2} + \frac{|k|\left\|\psi_2 - \overline{\psi}_2\right\|_E}{\Gamma\left(\beta_2 + 1\right)}\eta^{\beta_2}\right) + \left|A_3\right|\right\} \\
\leq &\frac{K\left\|\left(\psi_1 - \overline{\psi}_1, \psi_2 - \overline{\psi}_2\right)\right\|_{E \times E}}{\Gamma\left(\alpha_1 + \beta_1 + 1\right)} + \frac{|\lambda|\left\|\psi_1 - \overline{\psi}_1\right\|_E}{\Gamma\left(\beta_1 + 1\right)} \\
&+ \frac{\left|aA_1\right|L\left\|\left(\psi_1 - \overline{\psi}_1, \psi_2 - \overline{\psi}_2\right)\right\|_{E \times E}}{\Gamma\left(\overline{\alpha}_2 + 1\right)}\mu_1^{\overline{\alpha}_2} + \frac{\left|akA_1\right|\left\|\psi_2 - \overline{\psi}_2\right\|_E}{\Gamma\left(\beta_2 - p + 1\right)}\mu_1^{\beta_2 - p} \\
&+ \frac{\left|A_1\right|K\left\|\left(\psi_1 - \overline{\psi}_1, \psi_2 - \overline{\psi}_2\right)\right\|_{E \times E}}{\Gamma\left(\alpha_1 + \beta_1 + 1\right)}\xi^{\alpha_1 + \beta_1} + \frac{\left|A_1\lambda\right|\left\|\psi_1 - \overline{\psi}_1\right\|_E}{\Gamma\left(\beta_1 + 1\right)}\xi^{\beta_1} \\
&+ \frac{\left|A_2 b\right|K\left\|\left(\psi_1 - \overline{\psi}_1, \psi_2 - \overline{\psi}_2\right)\right\|_{E \times E}}{\Gamma\left(\overline{\alpha}_1 + 1\right)}\mu_2^{\overline{\alpha}_1} + \frac{\left|A_2 b\lambda\right|\left\|\psi_1 - \overline{\psi}_1\right\|_E}{\Gamma\left(\beta_1 + q + 1\right)}\mu_2^{\beta_1 + q} \\
&+ \frac{\left|A_2\right|L\left\|\left(\psi_1 - \overline{\psi}_1, \psi_2 - \overline{\psi}_2\right)\right\|_{E \times E}}{\Gamma\left(\alpha_2 + \beta_2 + 1\right)}\eta^{\alpha_2 + \beta_2} + \frac{\left|A_2 k\right|\left\|\psi_2 - \overline{\psi}_2\right\|_E}{\Gamma\left(\beta_2 + 1\right)}\eta^{\beta_2} \\
\leq & \left(Q_1 K + Q_2 L + \rho_1\right)\left\|\left(\psi_1, \psi_2\right) - \left(\overline{\psi}_1, \overline{\psi}_2\right)\right\|_{E \times E}.
\end{aligned}
\tag{34}
$$

In the other respect, we have

$$
\begin{aligned}
\left|\mathfrak{N}_2\left(\psi_1, \psi_2\right)(t) - \mathfrak{N}_2\left(\overline{\psi}_1, \overline{\psi}_2\right)(t)\right| &\leq \frac{L\left(\left\|\psi_1 - \overline{\psi}_1\right\|_E + \left\|\psi_2 - \overline{\psi}_2\right\|_E\right)}{\Gamma\left(\alpha_2 + \beta_2 + 1\right)} + \frac{k\left\|\psi_2 - \overline{\psi}_2\right\|_E}{\Gamma\left(\beta_2 + 1\right)} \\
&+ \frac{\left|B_1 b\right| K\left(\left\|\psi_1 - \overline{\psi}_1\right\|_E + \left\|\psi_2 - \overline{\psi}_2\right\|_E\right)}{\Gamma\left(\overline{\alpha}_1 + 1\right)} \mu_2^{\overline{\alpha}_1 - 1} + \frac{\left|B_1 b\lambda\right|\left\|\psi_1 - \overline{\psi}_1\right\|_E}{\Gamma\left(\beta_1 + q + 1\right)} \mu_2^{\beta_1 + q} \\
&+ \frac{\left|B_1\right| L\left(\left\|\psi_1 - \overline{\psi}_1\right\|_E + \left\|\psi_2 - \overline{\psi}_2\right\|_E\right)}{\Gamma\left(\alpha_2 + \beta_2 + 1\right)} \eta^{\alpha_2 + \beta_2} + \frac{\left|B_1 k\right| K\left\|\psi_2 - \overline{\psi}_2\right\|_E}{\Gamma\left(\beta_2 + 1\right)} \eta^{\beta_2} \\
&+ \frac{\left|B_2 a\right| L\left(\left\|\psi_1 - \overline{\psi}_1\right\|_E + \left\|\psi_2 - \overline{\psi}_2\right\|_E\right)}{\Gamma\left(\overline{\alpha}_2 + 1\right)} \mu_1^{\overline{\alpha}_2} + \frac{\left|B_2 ak\right|\left\|\psi_2 - \overline{\psi}_2\right\|_E}{\Gamma\left(\beta_2 - p + 1\right)} \mu_1^{\beta_2 - p} \\
&+ \frac{\left|B_2\right| K\left(\left\|\psi_1 - \overline{\psi}_1\right\|_E + \left\|\psi_2 - \overline{\psi}_2\right\|_E\right)}{\Gamma\left(\alpha_1 + \beta_1 + 1\right)} \xi^{\alpha_1 + \beta_1} + \frac{\left|B_2 \lambda\right|\left\|\psi_1 - \overline{\psi}_1\right\|_E}{\Gamma\left(\beta_1 + 1\right)} \xi^{\beta_1},
\end{aligned}
\tag{35}
$$

$$
\begin{aligned}
&\leq \left(\frac{L}{\Gamma\left(\alpha_2 + \beta_2 + 1\right)} + \frac{\left|B_1 b\right| K}{\Gamma\left(\overline{\alpha}_1 + 1\right)} \mu_2^{\overline{\alpha}_1 - 1} + \frac{\left|B_1\right| L}{\Gamma\left(\alpha_2 + \beta_2 + 1\right)} \eta^{\alpha_2 + \beta_2}\right. \\
&\left. + \frac{\left|B_2 a\right| L \mu_1^{\overline{\alpha}_2}}{\Gamma\left(\overline{\alpha}_2 + 1\right)} + \frac{\left|B_2\right| K \xi^{\alpha_1 + \beta_1}}{\Gamma\left(\alpha_1 + \beta_1 + 1\right)}\right) \left\|\left(\psi_1 - \overline{\psi}_1, \psi_2 - \overline{\psi}_2\right)\right\|_{E \times E} \\
&\left(\frac{\left|B_1 b\lambda\right| \mu_2^{\beta_1 + q}}{\Gamma\left(\beta_1 + q + 1\right)} + \frac{\left|B_2 \lambda\right| \xi^{\beta_1}}{\Gamma\left(\beta_1 + 1\right)}\right) \left\|\psi_1 - \overline{\psi}_1\right\|_E \\
&\left(\frac{\left|k\right|\left(1 + \left|B_1\right| K \eta^{\beta_2}\right)}{\Gamma\left(\beta_2 + 1\right)} + \frac{\left|B_2 ak\right| \mu_1^{\beta_2 - p}}{\Gamma\left(\beta_2 - p + 1\right)}\right) \left\|\psi_2 - \overline{\psi}_2\right\|_E \\
&\leq \left(Q_4 L + Q_3 K + \rho_2\right) \left\|\left(\psi_1, \psi_2\right) - \left(\overline{\psi}_1, \overline{\psi}_2\right)\right\|_{E \times E}.
\end{aligned}
$$

Consequently,

$$
\begin{aligned}
\left\|\mathfrak{N}\left(\psi_1, \psi_2\right) - \mathfrak{N}\left(\overline{x}, \overline{y}\right)\right\| &\leq \left[\left(Q_1 + Q_3\right) K + \left(Q_2 + Q_4\right) L \right. \\
&\left. + \rho_1 + \rho_2\right]\left\|\left(\psi_1, \psi_2\right) - \left(\overline{\psi}_1, \overline{\psi}_2\right)\right\|_{E \times E}.
\end{aligned}
\tag{36}
$$

Therefore, the operator $\mathfrak{N}$ has a unique fixed point. Thus, we conclude that problems (1)-(2) have a unique solution on $[0, 1]$. The proof is complete.

Now, we apply the Leray-Schauder alternative theoerm to obtain the following result about the existence of solutions for problems (1)-(2).

Theorem 10. *Assume that* (H1) *holds. If*

$$
S < 1, \text{ and } \overline{S} < 1,
\tag{37}
$$

where

$$
S = Q_1 \sigma_1 + Q_2 \tau_1 + Q_3 \sigma_1 + Q_4 \tau_1 + Q_5 + Q_8,
\tag{38}
$$

$$
\overline{S} = Q_1 \sigma_2 + Q_2 \tau_2 + Q_3 \sigma_2 + Q_4 \tau_2 + Q_6 + Q_7,
\tag{39}
$$

then the boundary value problems (1)-(2) have at least one solution on $[0, 1]$.

Proof. First, we show that the operator $\mathfrak{N}$ is completely continuous.

Because f and g are continuous functions, $\mathfrak{N}$ is continuous operator as well. Let Λ be any nonempty bounded subset of $E \times E$. Then, there exists $r > 0$ such that for any $\left(\psi_1, \psi_2\right) \in \Lambda$, $\left\|\left(\psi_1, \psi_2\right)\right\|_{E \times E} \leq r$. Notice that from the condition (H1) for all $\left(\psi_1, \psi_2\right) \in \Lambda$, we have

$$
\begin{aligned}
\left|f\left(t, \psi_1(t), \psi_2(t)\right)\right| &\leq \sigma_0 + \sigma_1\left|\psi_1(t)\right| + \sigma_2\left|\psi_2(t)\right|, \\
&\leq \sigma_0 + \max\left\{\sigma_1, \sigma_2\right\}\left\|\left(\psi_1, \psi_2\right)\right\|_{E \times E} \\
&\leq \sigma_0 + r \max\left\{\sigma_1, \sigma_2\right\}
\end{aligned}
\tag{40}
$$

$$
\left|g\left(t, \psi_1(t), \psi_2(t)\right)\right| \leq \tau_0 + r \max\left\{\tau_1, \tau_2\right\}.
$$

Next, we prove that $\mathfrak{N}(\Lambda)$ is uniformly bounded. Let $\left(\psi_1, \psi_2\right) \in \Lambda$. Indeed, for any $t \in [0, 1]$, we have

$$
\begin{aligned}
\left|\mathfrak{N}_1\left(\psi_1, \psi_2\right)(t)\right| \leq & \frac{\sigma_0 + r\max\{\sigma_1, \sigma_2\}}{\Gamma(\alpha_1 + \beta_1)} \int_0^t (t-s)^{\alpha_1+\beta_1-1}\mathrm{d}s + \frac{|\lambda|\|\psi_1\|_E}{\Gamma(\beta_1)} \int_0^t (t-s)^{\beta_1-1}\mathrm{d}s \\
& + t^{\beta_1}\left\{\left|A_1\right|\left(\frac{|a|(\tau_0 + r\max\{\tau_1,\tau_2\})}{\Gamma(\overline{\alpha}_2)} \int_0^{\mu_1} (\mu_1-s)^{\overline{\alpha}_2-1}\mathrm{d}s + \frac{|ak|\|\psi_2\|_E}{\Gamma(\beta_2-p)} \int_0^{\mu_1}(\mu_1-s)^{\beta_2-p-1}\mathrm{d}s\right.\right. \\
& + \frac{\sigma_0 + r\max\{\sigma_1,\sigma_2\}}{\Gamma(\alpha_1+\beta_1)} \int_0^\xi (\xi-s)^{\alpha_1+\beta_1-1}\mathrm{d}s + \frac{|\lambda|\|\psi_1\|_E}{\Gamma(\beta_1)} \int_0^\xi (\xi-s)^{\beta_1-1}\mathrm{d}s\Big) \\
& + |A_2|\left(\frac{|b|(\sigma_0 + r\max\{\sigma_1,\sigma_2\})}{\Gamma(\overline{\alpha}_1)} \int_0^{\mu_2} (\mu_2-s)^{\overline{\alpha}_1-1}\mathrm{d}s + \frac{|b\lambda|\|\psi_1\|_E}{\Gamma(\beta_1+q)} \int_0^{\mu_2}(\mu_2-s)^{\beta_1+q-1}\mathrm{d}s\right. \\
& + \frac{\tau_0 + r\max\{\tau_1,\tau_2\}}{\Gamma(\alpha_2+\beta_2)} \int_0^\eta (\eta-s)^{\alpha_2+\beta_2-1}\mathrm{d}s + \frac{|k|\|\psi_2\|_E}{\Gamma(\beta_2)} \int_0^\eta (\eta-s)^{\beta_2-1}\mathrm{d}s\Big) + |A_3|\Big\} + |a_0|,
\end{aligned}
$$

$$
\begin{aligned}
\leq & \frac{\left(1+|A_1|\xi^{\alpha_1+\beta_1}\right)(\sigma_0 + r\max\{\sigma_1,\sigma_2\})}{\Gamma(\alpha_1+\beta_1+1)} + \frac{|aA_1|(\tau_0 + r\max\{\tau_1,\tau_2\})\mu_1^{\overline{\alpha}_2}}{\Gamma(\overline{\alpha}_2+1)} \\
& + \frac{|bA_2|(\sigma_0 + r\max\{\sigma_1,\sigma_2\})\mu_2^{\overline{\alpha}_1}}{\Gamma(\overline{\alpha}_1+1)} + \frac{|A_2|(\tau_0 + r\max\{\tau_1,\tau_2\})\eta^{\alpha_2+\beta_2}}{\Gamma(\alpha_2+\beta_2+1)} + |A_3| + |a_0| \\
& + \left(\frac{|\lambda|\left(1+|A_1|\xi^{\beta_1}\right)}{\Gamma(\beta_1+1)} + \frac{|b\lambda A_2|\mu_2^{\beta_1+q}}{\Gamma(\beta_1+q+1)}\right)\|\psi_1\|_E + \left(\frac{|kA_2|\eta^{\beta_2}}{\Gamma(\beta_2+1)} + \frac{|akA_1|\mu_1^{\beta_2-p}}{\Gamma(\beta_2-p+1)}\right)\|\psi_2\|_E \\
\leq & \left(\frac{\left(1+|A_1|\xi^{\alpha_1+\beta_1}\right)}{\Gamma(\alpha_1+\beta_1+1)} + \frac{|bA_2|\mu_2^{\overline{\alpha}_1}}{\Gamma(\overline{\alpha}_1+1)}\right)(\sigma_0 + r\max\{\sigma_1,\sigma_2\}) \\
& + \left(\frac{|aA_1|\mu_1^{\overline{\alpha}_2}}{\Gamma(\overline{\alpha}_2+1)} + \frac{|A_2|\eta^{\alpha_2+\beta_2}}{\Gamma(\alpha_2+\beta_2+1)}\right)(\tau_0 + r\max\{\tau_1,\tau_2\}) + |A_3| + |a_0| + \rho_1 r \\
\leq & +\infty.
\end{aligned}
\tag{41}
$$

Similarly,

$$
\begin{aligned}
\left|\mathfrak{N}_2\left(\psi_1, \psi_2\right)(t)\right| = & \frac{\left(1+|B_1|\eta^{\alpha_2+\beta_2}\right)(\tau_0 + r\max\{\tau_1,\tau_2\})}{\Gamma(\alpha_2+\beta_2+1)} + \frac{|bB_1|\mu_2^{\overline{\alpha}_1}(\sigma_0 + r\max\{\sigma_1,\sigma_2\})}{\Gamma(\overline{\alpha}_1+1)} \\
& + \frac{|aB_2|(\tau_0 + r\max\{\tau_1,\tau_2\})\mu_1^{\overline{\alpha}_2}}{\Gamma(\overline{\alpha}_2+1)} + \frac{|B_2|(\sigma_0 + r\max\{\sigma_1,\sigma_2\})\xi^{\alpha_1+\beta_1}}{\Gamma(\alpha_1+\beta_1+1)} + |B_3| + |b_0| \\
& + \left(\frac{|b\lambda B_1|\mu_2^{\beta_1+q}}{\Gamma(\beta_1+q+1)} + \frac{|\lambda B_2|\xi^{\beta_1}}{\Gamma(\beta_1+1)}\right)\|\psi_1\|_E + \left(\frac{|k|+|kB_1|\eta^{\beta_2}}{\Gamma(\beta_2+1)} + \frac{|akB_2|\mu_1^{\beta_2-p}}{\Gamma(\beta_2-p+1)}\right)\|\psi_2\|_E \\
\leq & \left(\frac{|bB_1|\mu_2^{\overline{\alpha}_1}}{\Gamma(\overline{\alpha}_1+1)} + \frac{|B_2|\xi^{\alpha_1+\beta_1}}{\Gamma(\alpha_1+\beta_1+1)}\right)(\sigma_0 + r\max\{\sigma_1,\sigma_2\}) \\
& + \left(\frac{|aB_2|\mu_1^{\overline{\alpha}_2}}{\Gamma(\overline{\alpha}_2+1)} + \frac{\left(1+|B_1|\eta^{\alpha_2+\beta_2}\right)}{\Gamma(\alpha_2+\beta_2+1)}\right)(\tau_0 + r\max\{\tau_1,\tau_2\}) + |B_3| + |b_0| + \rho_2 r \\
< & +\infty.
\end{aligned}
\tag{42}
$$

Consequently, $\|(\psi_1, \psi_2)\|_{E \times E} < +\infty$ for any $(\psi_1, \psi_2) \in \Lambda$. Therefore, $\mathfrak{N}(\Lambda)$ is uniformly bounded.

Now, we show that $\mathfrak{N}$ is equicontinuous on Λ. Let $(\psi_1, \psi_2) \in \Lambda$. For any $t_2, t_1 \in J$, where $t_2 > t_1$, we have

$$
\begin{aligned}
&\left| \mathfrak{N}_1(\psi_1, \psi_2)(t_2) - \mathfrak{N}_1(\psi_1, \psi_2)(t_1) \right| \\
&\leq \frac{\sigma_0 + r \max\{\sigma_1, \sigma_2\}}{\Gamma(\alpha_1 + \beta_1)} \left(\int_0^{t_1} \left[(t_2 - s)^{\alpha_1 + \beta_1 - 1} - (t_1 - s)^{\alpha_1 + \beta_1 - 1} \right] ds + \int_{t_1}^{t_2} (t_2 - s)^{\alpha_1 + \beta_1 - 1} ds \right) \\
&\quad + \frac{|\lambda| \|\psi_1\|_E}{\Gamma(\beta_1)} \left(\int_0^{t_1} \left[(t_2 - s)^{\beta_1 - 1} - (t_1 - s)^{\beta_1 - 1} \right] ds + \int_{t_1}^{t_2} (t_2 - s)^{\beta_1 - 1} ds \right) \\
&\quad + \left(t_2^{\beta_1} - t_1^{\beta_1} \right) \Bigg\{ |A_1| \Bigg(\frac{|a|(\tau_0 + r \max\{\tau_1, \tau_2\})}{\Gamma(\overline{\alpha}_2)} \int_0^{\mu_1} (\mu_1 - s)^{\overline{\alpha}_2 - 1} ds + \frac{|ak| \|\psi_2\|_E}{\Gamma(\beta_2 - p)} \int_0^{\mu_1} (\mu_1 - s)^{\beta_2 - p - 1} ds \\
&\quad + \frac{\sigma_0 + r \max\{\sigma_1, \sigma_2\}}{\Gamma(\alpha_1 + \beta_1)} \int_0^{\xi} (\xi - s)^{\alpha_1 + \beta_1 - 1} ds + \frac{|\lambda| \|\psi_1\|_E}{\Gamma(\beta_1)} \int_0^{\xi} (\xi - s)^{\beta_1 - 1} ds \Bigg) \\
&\quad + |A_2| \Bigg(\frac{|b|(\sigma_0 + r \max\{\sigma_1, \sigma_2\})}{\Gamma(\overline{\alpha}_1)} \int_0^{\mu_2} (\mu_2 - s)^{\overline{\alpha}_1 - 1} ds + \frac{|b\lambda| \|\psi_1\|_E}{\Gamma(\beta_1 + q)} \int_0^{\mu_2} (\mu_2 - s)^{\beta_1 + q - 1} ds \\
&\quad + \frac{\tau_0 + r \max\{\tau_1, \tau_2\}}{\Gamma(\alpha_2 + \beta_2)} \int_0^{\eta} (\eta - s)^{\alpha_2 + \beta_2 - 1} ds + \frac{|k| \|\psi_2\|_E}{\Gamma(\beta_2)} \int_0^{\eta} (\eta - s)^{\beta_2 - 1} ds \Bigg) + |A_3| \Bigg\} \\
&\leq \frac{[\sigma_0 + r \max\{\sigma_1, \sigma_2\}]}{\Gamma(\alpha_1 + \beta_1 + 1)} \left(-(t_2 - t_1)^{\alpha_1 + \beta_1} + t_2^{\alpha_1 + \beta_1} - t_1^{\alpha_1 + \beta_1} + (t_2 - t_1)^{\alpha_1 + \beta_1} \right) \\
&\quad + \frac{|\lambda| \|\psi_1\|_E}{\Gamma(\beta_1 + 1)} \left(-(t_2 - t_1)^{\beta_1} + t_2^{\beta_1} - t_1^{\beta_1} + (t_2 - t_1)^{\beta_1} \right) + \left(t_2^{\beta_1} - t_1^{\beta_1} \right) \\
&\quad \Bigg\{ \left(\frac{|A_1| |a| \mu_1^{\overline{\alpha}_2}}{\Gamma(\overline{\alpha}_2 + 1)} + \frac{|A_2| \eta^{\alpha_2 + \beta_2}}{\Gamma(\alpha_2 + \beta_2 + 1)} \right) (\tau_0 + r \max\{\tau_1, \tau_2\}) \\
&\quad + \left(\frac{|A_1| |ak| \mu_1^{\beta_2 - p}}{\Gamma(\beta_2 - p + 1)} + \frac{|A_2| |k| \eta^{\beta_2}}{\Gamma(\beta_2 + 1)} \right) \|\psi_2\|_E + \left(\frac{|A_1| |\lambda| \xi^{\beta_1}}{\Gamma(\beta_1 + 1)} + \frac{|A_2| |b\lambda| \mu_2^{\beta_1 + q}}{\Gamma(\beta_1 + q + 1)} \right) \|\psi_1\|_E \\
&\quad + \left(\frac{|A_2| |b| \mu_2^{\overline{\alpha}_1}}{\Gamma(\overline{\alpha}_1 + 1)} + \frac{|A_1| \xi^{\alpha_1 + \beta_1}}{\Gamma(\alpha_1 + \beta_1 + 1)} \right) (\sigma_0 + r \max\{\sigma_1, \sigma_2\}) + |A_3| \Bigg\} \\
&\leq \frac{\sigma_0 + r \max\{\sigma_1, \sigma_2\}}{\Gamma(\alpha_1 + \beta_1 + 1)} \left(t_2^{\alpha_1 + \beta_1} - t_1^{\alpha_1 + \beta_1} \right) + \frac{|\lambda| r}{\Gamma(\beta_1 + 1)} \left(t_2^{\beta_1} - t_1^{\beta_1} \right) \\
&\quad + \left(t_2^{\beta_1} - t_1^{\beta_1} \right) \Bigg\{ \left(\frac{|A_1| |a| \mu_1^{\overline{\alpha}_2}}{\Gamma(\overline{\alpha}_2 + 1)} + \frac{|A_2| \eta^{\alpha_2 + \beta_2}}{\Gamma(\alpha_2 + \beta_2 + 1)} \right) (\tau_0 + r \max\{\tau_1, \tau_2\}) \\
&\quad + r \max \Bigg\{ \left(\frac{|A_1| |ak| \mu_1^{\beta_2 - p}}{\Gamma(\beta_2 - p + 1)} + \frac{|A_2| |k| \eta^{\beta_2}}{\Gamma(\beta_2 + 1)} \right), \left(\frac{|A_1| |\lambda| \xi^{\beta_1}}{\Gamma(\beta_1 + 1)} + \frac{|A_2| |b\lambda| \mu_2^{\beta_1 + q}}{\Gamma(\beta_1 + q + 1)} \right) \Bigg\} \\
&\quad + \left(\frac{|A_2| |b| \mu_2^{\overline{\alpha}_1}}{\Gamma(\overline{\alpha}_1 + 1)} + \frac{|A_1| \xi^{\alpha_1 + \beta_1}}{\Gamma(\alpha_1 + \beta_1 + 1)} \right) (\sigma_0 + r \max\{\sigma_1, \sigma_2\}) + |A_3| \Bigg\} \\
&\longrightarrow 0, \quad \text{as } t_2 \longrightarrow t_1.
\end{aligned}
\tag{43}
$$

Analogously,

$$\left|\mathfrak{N}_2\left(\psi_1,\psi_2\right)\left(t_2\right)-\mathfrak{N}_2\left(\psi_1,\psi_2\right)\left(t_1\right)\right|\leq\frac{\tau_0+r\max\{\tau_1,\tau_2\}}{\Gamma\left(\alpha_2+\beta_2+1\right)}\left(t_2^{\alpha_2+\beta_2}-t_1^{\alpha_2+\beta_2}\right)+\frac{|k|r}{\Gamma\left(\beta_2+1\right)}\left(t_2^{\beta_2}-t_1^{\beta_2}\right)$$

$$+\left(t_2^{\beta_2}-t_1^{\beta_2}\right)\left\{\left(\frac{|bB_1|\mu_2^{\overline{\alpha}_1}}{\Gamma\left(\overline{\alpha}_1+1\right)}+\frac{B_2\xi^{\alpha_1+\beta_1}}{\Gamma\left(\alpha_1+\beta_1+1\right)}\right)\left(\sigma_0+r\max\{\sigma_1,\sigma_2\}\right)\right.$$

$$+r\max\left\{\left(\frac{|B_2\lambda|\xi^{\beta_1}}{\Gamma\left(\beta_1+1\right)}+\frac{|b\lambda B_1|\mu_2^{\beta_1+q}}{\Gamma\left(\beta_1+q+1\right)}\right),\left(\frac{|B_2ak|\mu_1^{\beta_2-p}}{\Gamma\left(\beta_2-p+1\right)}+\frac{|B_1k|\eta^{\beta_2}}{\Gamma\left(\beta_2+1\right)}\right)\right\} \qquad (44)$$

$$+\left(\frac{|B_1|\eta^{\alpha_2+\beta_2}}{\Gamma\left(\alpha_2+\beta_2+1\right)}+\frac{|B_2a|\mu_1^{\overline{\alpha}_2}}{\Gamma\left(\overline{\alpha}_2+1\right)}\right)\left(\tau_0+r\max\{\tau_1,\tau_2\}\right)+\left.|B_3|\right\}$$

$$\longrightarrow 0,\quad \text{as}\, t_2\longrightarrow t_1,$$

which imply that $\left|\mathfrak{N}\left(\psi_1,\psi_2\right)\left(t_2\right)-\mathfrak{N}\left(\psi_1,\psi_2\right)\left(t_1\right)\right|\longrightarrow 0$ as $t_2\longrightarrow t_1$. Thus, the operator $\mathfrak{N}$ is equicontinuous. Hence, by Arzela–Ascoli theorem, we deduce that the operator $\mathfrak{N}$ is completely continuous.

Finally, we will verify that the set $M\left(\mathfrak{N}\right)$ $=\{(\psi_1,\psi_2)\in E\times E\colon (\psi_1,\psi_2)=m\mathfrak{N}\left(\psi_1,\psi_2\right)\text{ for some }0<m<1\}$ is bounded. For all $(\psi_1,\psi_2)\in M\left(\mathfrak{N}\right)$ and for any $t\in J$, we have $m\mathfrak{N}\left(\psi_1,\psi_2\right)=\left(m\mathfrak{N}_1\left(\psi_1,\psi_2\right),m\mathfrak{N}_2\left(\psi_1,\psi_2\right)\right)$. Then,

$$\left|\psi_1\left(t\right)\right|=m\left|\mathfrak{N}_1\left(\psi_1,\psi_2\right)\left(t\right)\right|\leq\frac{\sigma_0+\sigma_1\|\psi_1\|_E+\sigma_2\|\psi_2\|_E}{\Gamma\left(\alpha_1+\beta_1+1\right)}+\left(\frac{|A_1||a|\mu_1^{\overline{\alpha}_2}}{\Gamma\left(\overline{\alpha}_2+1\right)}+\frac{|A_2|\eta^{\alpha_2+\beta_2}}{\Gamma\left(\alpha_2+\beta_2+1\right)}\right)$$

$$\times\left(\tau_0+\tau_1\|\psi_1\|_E+\tau_2\|\psi_2\|_E\right)+\left(\frac{|A_1||ak|\mu_1^{\beta_2-p}}{\Gamma\left(\beta_2-p+1\right)}+\frac{|A_2||k|\eta^{\beta_2}}{\Gamma\left(\beta_2+1\right)}\right)\|\psi_2\|_E$$

$$(45)$$

$$+\left(\frac{|A_1||\lambda|\xi^{\beta_1}}{\Gamma\left(\beta_1+1\right)}+\frac{|A_2||b\lambda|\mu_2^{\beta_1+q}}{\Gamma\left(\beta_1+q+1\right)}+\frac{|\lambda|}{\Gamma\left(\beta_1+1\right)}\right)\|\psi_1\|_E$$

$$+\left(\frac{|A_2||b|\mu_2^{\overline{\alpha}_1}}{\Gamma\left(\overline{\alpha}_1+1\right)}+\frac{|A_1|\xi^{\alpha_1+\beta_1}}{\Gamma\left(\alpha_1+\beta_1+1\right)}\right)\left[\sigma_0+\sigma_1\|\psi_1\|_E+\sigma_2\|\psi_2\|_E\right]+|A_3|+|a_0|.$$

This yields that

$$\|\psi_1\|_E=m\|\mathfrak{N}_1\left(\psi_1,\psi_2\right)\|$$
$$\leq Q_1\left(\sigma_0+\sigma_1\|\psi_1\|_E+\sigma_2\|\psi_2\|_E\right)+Q_2\left(\tau_0+\tau_1\|\psi_1\|_E+\tau_2\|\psi_2\|_E\right)+Q_5\|\psi_1\|_E+Q_6\|\psi_2\|_E+|A_3|+|a_0|. \qquad (46)$$

In the same way, we deduce that

$$\|\psi_2\|_E=m\|\mathfrak{N}_2\left(\psi_1,\psi_2\right)\|$$
$$\leq Q_4\left(\tau_0+\tau_1\|\psi_1\|_E+\tau_2\|\psi_2\|_E\right)+Q_3\left(\sigma_0+\sigma_1\|\psi_1\|_E+\sigma_2\|\psi_2\|_E\right)+Q_7\|\psi_2\|_E+Q_8\|\psi_1\|_E+|B_3|+|b_0|. \qquad (47)$$

Hence, we have

$$\begin{aligned}
\left\|(\psi_1, \psi_2)\right\|_{E \times E} &= \left\|\psi_1\right\|_E + \left\|\psi_2\right\|_E \\
&\leq Q_1\left[\sigma_0 + \sigma_1\left\|\psi_1\right\|_E + \sigma_2\left\|\psi_2\right\|_E + Q_2\left(\tau_0 + \tau_1\left\|\psi_1\right\|_E + \tau_2\left\|\psi_2\right\|_E\right)\right. \\
&\quad + Q_5\left\|\psi_1\right\|_E + Q_6\left\|\psi_2\right\|_E + Q_4\left(\tau_0 + \tau_1\left\|\psi_1\right\|_E + \tau_2\left\|\psi_2\right\|_E\right) + Q_3\left(\sigma_0 + \sigma_1\left\|\psi_1\right\|_E + \sigma_2\left\|\psi_2\right\|_E\right) \\
&\quad + Q_7\left\|\psi_2\right\|_E + Q_8\left\|\psi_1\right\|_E + \left|A_3\right| + \left|B_3\right| + \left|a_0\right| + \left|b_0\right|,
\end{aligned} \tag{48}$$

which yields

$$\left\|(\psi_1, \psi_2)\right\|_{E \times E}$$

$$\leq \frac{Q_3\sigma_0 + Q_4\tau_0 + Q_1\sigma_0 + Q_2\tau_0 + \left|A_3\right| + \left|B_3\right| + \left|a_0\right| + \left|b_0\right|}{1 - \max\{S, \overline{S}\}}, \tag{49}$$

where S and $\overline{S}$ are given by (36) and (38), respectively, which proves that $M(\mathfrak{N})$ is bounded. Thus, as a consequence of Leray–Schauder alternative theorem, $\mathfrak{N}$ has more than one fixed point. Hence, the boundary value problems (1)-(2) have one solution at the very least on $[0, 1]$.

4. Applications and Numerical Examples

In this section, we solve the integral equations (12) and (13) using the Adams-type predictor-corrector method with step size $h = 0.01$ (for details, see [16–18] and the references therein). Briefly, we aim to approximate the solution of the following fractional initial value problem:

$$D^\alpha y(t) = f(t, y(t)), \ y(t_0) = y_0, \ t \in (t_0, T], \quad \alpha \in (0, 1), \tag{50}$$

at the grid points $t_m = t_0 + mh$, $m \geq 0$, with h is a uniform step size. It is found that

$$y(t_m) \approx Y(t_m) = y(t_0) + \frac{1}{\Gamma(\alpha)} \sum_{j=0}^{m} R_{m,j} f_j, \tag{51}$$

where

$$R_{m,j} = \begin{cases} W0_{m,0}, & \text{if } j = 0, \\ W1_{m,j-1} + W0_{m,j}, & \text{if } 1 \leq j \leq m-1, \\ W1_{m,m-1}, & \text{if } j = m. \end{cases}$$

$$W1_{m,j} = \frac{(-\alpha + j - m)(h(-j + m - 1))^\alpha + (m - j)(h(m - j))^\alpha}{\alpha(\alpha + 1)}$$

$$W0_{m,j} = \frac{(\alpha + j - m + 1)(h(m - j))^\alpha + (h(-j + m - 1))^{\alpha+1}/h}{\alpha(\alpha + 1)}. \tag{52}$$

To measure the accuracy of the present algorithm, we calculated the residual function as follows:

$$R(t) := D^\alpha Y(t) - f(t, Y(t)), \tag{53}$$

at the grid points t_m for $m > 0$, i.e.,

$$\begin{aligned}
R(t_m) &= \frac{1}{\Gamma(1-\alpha)} \int_{t_0}^{t_m} (t_m - \tau)^{-\alpha} Y'(\tau) d\tau - f(t_m, Y(t_m)), \\
&= \frac{1}{\Gamma(1-\alpha)} \sum_{j=0}^{m-1} \int_{t_j}^{t_{j+1}} (t_m - \tau)^{-\alpha} Y'(\tau) d\tau - f(t_m, Y(t_m)), \\
&= \frac{h^{-\alpha}}{2\Gamma(1-\alpha)} \sum_{j=0}^{m-1} \left((m - j - 1)^{-\alpha} Y'(t_{j+1}) - (m - j)^{-\alpha} Y'(t_j)\right) - f(t_m, Y(t_m)),
\end{aligned} \tag{54}$$

after using the trapezoidal rule.

Consider the following coupled system of fractional Langevin equations:

$$\begin{cases}
{}^cD^{\alpha_1}\left({}^cD^{\beta_1} + \frac{1}{8}\right)\psi_1(t) = \frac{\left|\psi_2(t)\right|}{7(1 + t^2)(1 + \left|\psi_2(t)\right|)} - \frac{\psi_1(t)}{5} + \ln(1 + t), \quad t \in [0, 1], \\
\\
{}^cD^{\alpha_2}\left({}^cD^{\beta_2} + \frac{1}{7}\right)\psi_2(t) = \frac{\left|\psi_1(t)\right|}{14\sqrt{1 - t + \psi_1^2(t)}} - \frac{3 \sin \psi_2(t)}{5 + t} - 1 - t^2.
\end{cases} \tag{55}$$

Equipped with the nonlocal nonseparated fractional integral and fractional derivative boundary conditions,

$$\begin{cases} \psi_1(0) = 1, \psi_2(0) = 3, \psi_1'(0) = \psi_2'(0) = 0, \\\\ \psi_1\left(\dfrac{9}{10}\right) = \dfrac{1}{4}\left({}^c D^{1/4}\psi_2\right)\left(\dfrac{1}{5}\right), \\\\ \psi_2(1) = 2\left(I^{5/4}\psi_1\right)\left(\dfrac{1}{8}\right). \end{cases} \tag{56}$$

Here, $\lambda = 1/8, k = 1/7, a = 1/4, b = 2, a_0 = 1, b_0 = 3, p = 1/4, q = 5/4, \xi = 9/10, \eta = 1, \mu_1 = 1/5, \mu_2 = 1/8$, and

$$f(t, \psi_1, \psi_2) = \frac{|\psi_2|}{7(1+t^2)(1+|\psi_2|)} - \frac{\psi_1}{5} + \ln(1+t),$$

$$g(t, \psi_1, \psi_2) = \frac{|\psi_1|}{14\sqrt{1-t+\psi_1^2}} - \frac{3\sin\psi_2}{5+t} - 1 - t^2. \tag{57}$$

On the other part, for $(t, \zeta, \kappa), (t, \overline{\zeta}, \overline{\kappa}) \in [0, 1] \times \mathbb{R} \times \mathbb{R}$, we get

$$|f(t, \zeta, \kappa) - f(t, \overline{\zeta}, \overline{\kappa})| \le \frac{1}{5}\left(|\zeta - \overline{\zeta}| + |\kappa - \overline{\kappa}|\right),$$

$$|g(t, \zeta, \kappa) - g(t, \overline{\zeta}, \overline{\kappa})| \le \frac{3}{5}\left(|\zeta - \overline{\zeta}| + |\kappa - \overline{\kappa}|\right),$$

$$|f(t, \zeta, \kappa)| \le \sigma_0 + \frac{1}{5}|\zeta| + \frac{1}{7}|\kappa|, \tag{58}$$

$$|g(t, \zeta, \kappa)| \le \tau_0 + \frac{1}{14}|\zeta| + \frac{3}{5}|\kappa|,$$

so $\sigma_1 = 1/5, \sigma_2 = 1/7, \tau_1 = 1/14, \tau_2 = 3/5, K = 1/5$, and $L = 3/5$.

Case i. In order to illustrate Theorem 9, we take $\alpha_1 = 1/2, \beta_1 = 3/2, \alpha_2 = 3/4$, and $\beta_2 = 7/4$. Thus, $\overline{\alpha}_1 = 13/4$, and $\overline{\alpha}_2 = 9/4$. By using the Matlab program, we found that

$$\Delta \simeq 0.399301327423794,$$

$$A_1 \simeq 1.171331813010056,$$

$$A_2 \simeq 0.031689241829108,$$

$$A_3 \simeq -1.262241885268691,$$

$$B_1 \simeq 1.000100634730081,$$

$$B_2 \simeq 0.002312772254050,$$

$$B_3 \simeq -2.871400693622515,$$

$$Q_1 \simeq 00.974398268143493,$$

$$Q_2 \simeq 0.043889448160305,$$

$$Q_3 \simeq 0.001217044521056,$$

$$Q_4 \simeq 0.601838570591574,$$

$$Q_5 \simeq 0.188078540898721,$$

$$Q_6 \simeq 0.005629381698062,$$

$$Q_7 \simeq 3.713645478256922 \times 10^{-4},$$

$$Q_8 \simeq 0.177657802566698,$$

$$\rho_1 \simeq 0.188078540898721, \tag{59}$$

$$\rho_2 \simeq 0.0.177657802566698,$$

$$(Q_1 + Q_3)K + (Q_2 + Q_4)L + \rho_1 + \rho_2$$

$$\simeq 0.948296217249456 < 1.$$

Thus, the hypothesis of Theorem 9 holds. Then, problems (55)-(56) have a unique solution on $[0, 1]$. The behavior of the solutions $\psi_1(t)$ and $\psi_2(t)$ for Case i is presented in Figure 1. Table 1 displays the residuals $R_{\psi_1}(t_m)$ and $R_{\psi_2}(t_m)$ for the couple of equations given in (55) which clearly indicates the accuracy of the present algorithm.

Case ii. In order to illustrate Theorem 10, we take $\alpha_1 = 1/4, \beta_1 = 5/4, \alpha_2 = 1/2$, and $\beta_2 = 2$.

Thus, $\overline{\alpha}_1 = 11/4$ and $\overline{\alpha}_2 = 5/4$.

By using the Matlab program, we found that

$$\Delta \simeq 0.386787685580080,$$

$$A_1 \simeq 1.140949096832007,$$

$$A_2 \simeq 0.021215616584967,$$

$$A_3 \simeq -1.201812441154092,$$

$$B_1 \simeq 1.000159825315441,$$

$$B_2 \simeq 0.004297601923856,$$

$$B_3 \simeq -2.873555329197462,$$

$$Q_1 \simeq 1.485098417429794,$$

$$Q_2 \simeq 0.056422691832900,$$

$$Q_3 \simeq 0.004245829991826, \tag{60}$$

$$Q_4 \simeq 0.601861587859298,$$

$$Q_5 \simeq 0.220678979659357,$$

$$Q_6 \simeq 0.003030802369281,$$

$$Q_7 \simeq 8.31262586410917 \times 10^{-4},$$

$$Q_8 \simeq 0.142874266998083,$$

$$\rho_1 \simeq 0.220678979659357,$$

$$\rho_2 \simeq 0.142874266998083,$$

$$S \simeq 0.708442401834063 < 1,$$

$$\overline{S} \simeq 0.611596096688384 < 1.$$

Thus, all the conditions of Theorem 10 are satisfied. Then, problems (55)-(56) have one solution at the least $[0, 1]$. In addition, both solutions $\psi_1(t)$ and $\psi_2(t)$ for Case ii are sketched in Figure 2.
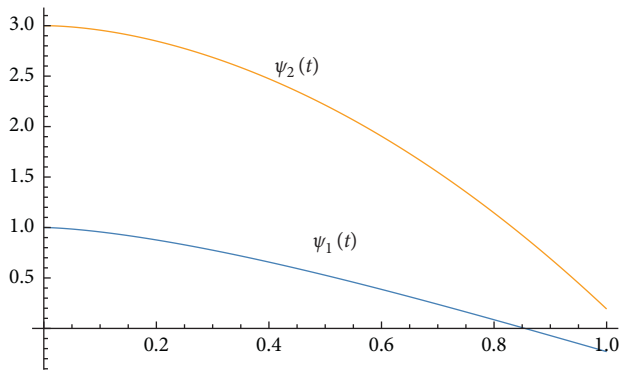
Figure 1: Graphs of the approximated solutions $\psi_1(t)$ and $\psi_2(t)$ for Case i.

Table 1: Residuals $R_{\psi_1}(t_m)$ and $R_{\psi_2}(t_m)$ for example 1.

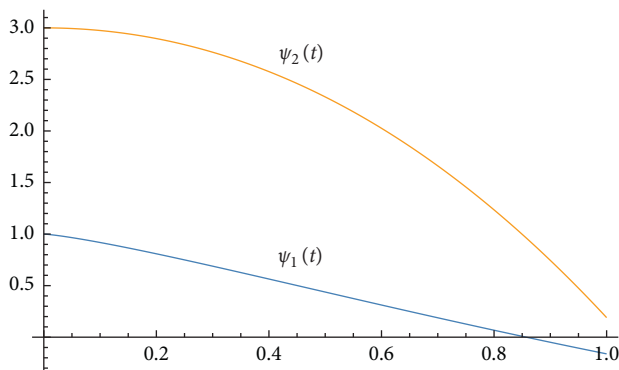| t_m	$R_{\psi_1}(t_m)$	$R_{\psi_2}(t_m)$
0.2	0.64265×10^{-4}	2.33263×10^{-4}
0.2	3.61491×10^{-3}	1.51331×10^{-4}
0.6	2.96055×10^{-3}	7.53023×10^{-3}
0.3	5.12564×10^{-3}	2.02533×10^{-3}
1.0	3.69052×10^{-3}	5.32055×10^{-3}

Figure 2: Graphs of the approximated solutions $\psi_1(t)$ and $\psi_2(t)$ for Case ii.

5. Conclusion

The most important features of differential equations subject to either initial or boundary conditions are the existence and uniqueness of their solutions. In this paper, we discussed the existence and uniqueness of solutions of specific type of the couple system of the Langevin differential equation in the framework of Caputo fractional derivatives and under the suzerainty of nonlocal and nonseparated boundary conditions. The boundary value problem we studied contained 6 different parameters. Because of the complexity, we were forced to use computer programs in order to find examples that would support our results. We discussed these examples from the theoretical point and solved numerically using the Adams-type predictorcorrector method by implicitly implementing the Gauss–Seidel method.

It is recommended to consider the same problem in the frame of other fractional derivatives especially the ones with no singular kernels and compare their results to the ones discussed in this paper.

Data Availability

The data used to support the findings of this study are included within the article in the references.

Conflicts of Interest

The authors declare that they have no conflicts of interest.

Acknowledgments

References

[1] S. G. Samko, A. A. Kilbas, and O. I. Marichev, *Fractional Integrals and Derivatives: Theory and Applications*, Gordon & Breach, Yverdon, Switzerland, 1993.

[2] A. Kilbas, H. M. Srivastava, and J. J. Trujillo, *Theory and Application of Fractional Differential Equations, North Holland Mathematics Studies*, Elsevier, Amsterdam, Netherlands, 2006.

[3] H. Sun, Y. Zhang, D. Baleanu, W. Chen, and Y. Chen, "A new collection of real world applications of fractional calculus in science and engineering," *Communications in Nonlinear Science and Numerical Simulation*, vol. 64, pp. 213–231, 2018.

[4] P. Langevin, "Sur la théorie du mouvement brownien (in French) [On the theory of Brownian motion]," *Comptes Rendus de l'Académie des Sciences*, vol. 146, pp. 530–533, 1908.

[5] W. Coffey, Y. Kalmykov, and J. Waldron, "The Langevin equation," *With applications to stochastic problems in physics, chemistry and electrical engineering, World Scientific Series in Contemporary Chemical Physics*, World Scientific, vol. 14, World Scientific, River Edge, NJ, USA, 2nd edition, 2004.

[6] R. Klages, G. Radons, and M. Sokolov, *Anomalous Transport: Foundations and Applications*, Wiley VCH, Weinheim, Germany, 2008.

[7] S. C. Lim, M. Li, and L. P. Teo, "Langevin equation with two fractional orders," *Physics Letters A*, vol. 372, no. 42, pp. 6309–6320, 2008.

[8] M. Uranagase and T. Munakata, "Generalized Langevin equation revisited: mechanical random force and self-consistent structure," *Journal of Physics A: Mathematical and Theoretical*, vol. 43, no. 45, p. 11, Article ID 455003, 2010.

[9] A. Lozinski, R. G. Owens, and T. N. Phillips, "The Langevin and fokker-planck equations in polymer rheology," *Numerical Methods for Non-Newtonian Fluids*, vol. 16, pp. 211–303, 2011.

[10] Z. Laadjal, B. Ahmed, and N. Adjeroud, "Existence and uniqueness of solutions for multi-term fractional Langevin equation with boundary conditions," *Dynamics of Continuous Discrete and Impulsive Systems: Series A - Mathematical Analysis*, vol. 27, no. 5, pp. 339–350, 2020.

[11] C. Torres, "Existence of solution for fractional Langevin equation: variational approach," *Electronic Journal of Qualitative Theory of Differential Equations*, vol. 54, no. 54, pp. 1–14, 2014.

[12] B. Ahmad, S. K. Ntouyas, and A. Alsaedi, "On fully coupled nonlocal multi-point boundary value problems of nonlinear mixed-order fractional differential equations on an arbitrary domain," *Filomat*, vol. 32, no. 13, pp. 4503–4511, 2018.

[13] H. Li and J. Zhang, "Positive solutions for a system of fractional differential equations with two parameters," *Journal of Function Spaces*, vol. 2018, Article ID 1462505, 9 pages, 2018.

[14] S. N. Rao and M. M. Zico, "Positive solutions for a coupled system of nonlinear semipositone fractional boundary value problems," *International Journal of Differential Equations*, vol. 2019, Article ID 2893857, 9 pages, 2019.

[15] A. Granas and J. Dugundji, *Fixed Point Theory*, Springer-Verlag, New York, NY, USA, 2003.

[16] S. Abbas, M. Banerjee, and S. Momani, "Dynamical analysis of fractional-order modified logistic model," *Computers & Mathematics with Applications*, vol. 62, no. 3, pp. 1098–1104, 2011.

[17] F. A. Rihan, Q. M. Al-Mdallal, H. J. AlSakaji, and A. Hashish, "A fractional-order epidemic model with time-delay and nonlinear incidence rate," *Chaos, Solitons & Fractals*, vol. 126, pp. 97–105, 2019.

[18] Q. M. Al-Mdallal, M. A. Hajji, and T. Abdeljawad, "On the iterative methods for solving fractional initial value problems: new perspective," *Journal of Fractional Calculus and Nonlinear Systems*, vol. 2, no. 1, pp. 76–81, 2021.

Research Article

Existence and Uniqueness Results of Volterra–Fredholm Integro-Differential Equations via Caputo Fractional Derivative

Ameth Ndiaye [1] **and Fulgence Mansal**[2]

[1]*Département de Mathématiques, FASTEF, UCAD, Dakar, Senegal*
[2]*Département de Mathématiques et Informatique, UCAO, Dakar, Senegal*

Correspondence should be addressed to Ameth Ndiaye; ameth1.ndiaye@ucad.edu.sn

In this paper, we study a Volterra–Fredholm integro-differential equation. The considered problem involves the fractional Caputo derivatives under some conditions on the order. We prove an existence and uniqueness analytic result by application of the Banach principle. Then, another result that deals with the existence of at least one solution is delivered, and some sufficient conditions for this result are established by means of the fixed point theorem of Schaefer. Ulam stability of the solution is discussed before including an example to illustrate the results of the proposal.

1. Introduction

Fractional calculus and differential equations of fractional order are of great importance since they can be used in analyzing and modeling real word phenomena [1–3]. Recently, there has been a very important progress in the study of the theory of differential equations of fractional order. The theory of differential equations of arbitrary order has been recently proved to be an important tool for modeling many physical phenomena. For more details, refer to [4–9].

The fractional integro-differential equations have been recently used as effective tools in the modeling of many phenomena in various fields of applied sciences and engineering such as acoustic control, signal processing, electrochemistry, viscoelasticity, polymer physics, electromagnetics, optics, medicine, economics, chemical engineering, chaotic dynamics, and statistical physics (see [10–16]).

Hattaf in [17] proposed a new definition of fractional derivative that generalizes the fractional derivatives [18, 19] with nonsingular kernel for both Caputo and Riemann–Liouville types.

The efficient numerical method based on a novel shifted piecewise cosine basis for solving Volterra–Fredholm integral equations of the second kind is investigated (see [20]).

Recently, Wang et al. in [21] studied a nonlinear fractional differential equations with Hadamard derivative and Ulam stability in the weighted space of continuous functions. Some sufficient conditions for existence of solutions are given by using fixed point theorems via a prior estimation in the weighted space of the continuous functions. Ahmad et al. in [22] discussed the existence of solutions for an initial value problem of nonlinear hybrid differential equations of Hadamard type.

Ahmed et al. [23] discussed the existence of solutions by means of endpoint theory for initial value problem of

Hadamard and Riemann–Liouville fractional integro-differential inclusion of the form as follows:

$$
\begin{cases}
D^{\alpha}\left(x(t) - \sum_{i=1}^{m} I^{\rho_i} G_i(t, x(t)) \right) \in F(t, x(t)), & t \in J = [1, T], 0 < \alpha \leq 1, \\
x(1) = 0,
\end{cases}
\tag{1}
$$

where D^{α} denotes the Hadamard fractional derivative of order α for $0 < \alpha \leq 1$. I^{φ} is the Riemann–Liouville integral of order $\varphi > 0$, $\varphi \in \{\rho_1, \rho_2, \ldots, \rho_m\}$, $G_i \in C(J \times \mathbb{R}, \mathbb{R})$ with $G_i(1, 0) = 0$ for $i = 1, 2, 3 \ldots, m$.

Very recent work like Hamoud et al. [24] established some new conditions for the existence and uniqueness of solutions for a class of nonlinear Hadamard fractional Volterra–Fredholm integro-differential equations with initial conditions. The homotopy perturbation method has been successfully applied to find the approximate solution of a Caputo fractional Volterra–Fredholm integro-differential equation.

Motivated by the above works, we will study the following problem of fractional integro-differential equations in the context of Caputo fractional derivative called Caputo fractional Volterra–Fredholm integro-differential equations of the form as follows:

$$
\begin{cases}
D^{\alpha}\left(x(t) - \sum_{i=1}^{m} I^{\rho_i} f_i(t, x(t)) \right) = g(t, x(t), Kx(t), Hx(t)), & t \in J = [0, 1], \\
x(0) = 0, \\
D^{\alpha} x(0) = \eta, \quad 1 < \alpha < 2,
\end{cases}
\tag{2}
$$

where D^{α} is in the sense of Caputo, $f: J \times \mathbb{R}^n \times \mathbb{R}^n \longrightarrow \mathbb{R}^n$ is a given function, K and H are linear integral operators defined by $Kx(t) = \int_0^t k(t, \tau) x(t) \mathrm{d}\tau$ and $Hx(t) = \int_0^t h(t, \tau) x(t) \mathrm{d}\tau$, and its called Volterra–Fredholm integro-differential with $\theta_1 = \sup\{|k(t, \tau)|: (t, \tau) \in J \times J\}$ and $\theta_2 = \sup\{|h(t, \tau)|: (t, \tau) \in J \times J\}$.

The paper is organised as follows. In Section 2, we recall some definitions and lemmas that are used for the proof of our main results. In Section 3, we prove the main theorems of this paper by the existence and uniqueness of the solution which have been proved and some numerical simulation of the solution. A brief conclusion is given in Section 6.

2. Preliminaries

In this section, we introduce some definitions, lemmas, and preliminaries facts which are used throughout this paper (see [7] for more information). Let $|.|$ be a suitable norm in $\mathbb{R}^n$ and $\|.\|$ be the matrix norm. Let $E = C(J, \mathbb{R})$ denote the Banach space of continuous function on J with the norm

$$
\|x\| = \sup\{|x|, x \in J\}.
\tag{3}
$$

Definition 1. The Riemann–Liouville integral of order $\alpha > 0$ for a continuous function $\varphi \in L^1((0, 1], \mathbb{R})$ is given by

$$
I^{\alpha} \varphi(t) = \frac{1}{\Gamma(\alpha)} \int_0^t (t - \tau)^{\alpha - 1} \varphi(t) \mathrm{d}\tau, \quad \forall t \in (0, 1],
\tag{4}
$$

with $\Gamma(\alpha): = \int_0^{\infty} e^{-u} u^{\alpha - 1} \mathrm{d}u$.

Definition 2. If $\varphi \in C^n([0, 1], \mathbb{R})$ and $n - 1 < \alpha \leq n$, then the Caputo fractional derivative is given by

$$
D^{\alpha} \varphi(t) = I^{n - \alpha} \frac{\mathrm{d}^n}{\mathrm{d}t^n} (\varphi(t))
$$
$$
= \frac{1}{\Gamma(n - \alpha)} \int_0^t (t - s)^{n - \alpha - 1} \varphi^{(n)}(s) \mathrm{d}s,
\tag{5}
$$

where the parameter α is the order of the derivative and is allowed to be real or even complex.

Lemma 1. *Let $n \in \mathbb{N}^*$ and $n - 1 < \alpha < n$, then the general solution of $D^{\alpha} u(t) = 0$ is given by*

$$
u(t) = \sum_{i=0}^{n-1} c_i t^i,
\tag{6}
$$

such that $c_i \in \mathbb{R}, i = 0, 1, 2, \ldots, n - 1$.

Lemma 2. *Taking $n \in \mathbb{N}^*$ and $n - 1 < \alpha < n$, then we have*

$$
I^{\alpha} D^{\alpha} u(t) = u(t) + \sum_{k=0}^{n-1} \frac{u^{(k)}(0)}{k!} t^k,
\tag{7}
$$

with $t > 0$, $n - 1 < \alpha < n$.

Definition 3. Let X be a Banach space. Then, a map $T: X \longrightarrow X$ is called a contraction mapping on X if there exists $q \in [0, 1)$ such that

$$
\|T(x) - T(3y)\| \leq q\|x - y\|,
\tag{8}
$$

for all $x, y \in X$.

Theorem 1 (Banach's fixed point theorem, see [25]). *Let Ω be a nonempty closed subset of a Banach space X. Then, any*

contraction mapping T of Ω into itself has a unique fixed point.

Theorem 2 (Schaefer's fixed point theorem, see [25]). *Let X be a Banach space, and let $N\colon X \longrightarrow X$ be a completely continuous operator. If the set $E = \{y \in X\colon y = \lambda N y \text{ for some } \lambda \in (0,1)\}$ is bounded, then N has fixed points.*

$$
\begin{cases}
D^\alpha\left(x(t) - \sum_{i=1}^{m} I_i^p f_i(t, x(t))\right) = G(t), & t \in J = [0,1], \\
x(0) = 0, D^\alpha x(0) = \eta,
\end{cases}
\tag{9}
$$

admits as integral solution the following representation:

$$
x(t) = \frac{1}{\Gamma(\alpha)} \int_0^t (t-\tau)^{\alpha-1} G(\tau) d\tau + \sum_{i=1}^{m} I^{\rho_i} f_i(t, x(t)).
\tag{10}
$$

Proof. Using Lemma 2, we get

$$
I^\alpha D^\alpha \left(x(t) - \sum_{i=1}^{m} I_i^p f_i(t, x(t))\right) = I^\alpha G(t),
$$

$$
x(t) - \sum_{i=1}^{m} I_i^p f_i(t, x(t)) = I^\alpha G(t) + c_1 t + c_0,
\tag{11}
$$

$$
x(t) = I^\alpha G(t) + \sum_{i=1}^{m} I_i^p f_i(t, x(t)) + c_1 t + c_0.
$$

Using the initial conditions $x(0) = 0$ and $D^\alpha x(0) = \eta$, we get $c_1 = c_2 = 0$ which implies that the proof is completed.

$$
\left|g(t, x, y, z)\right| \le c_1(t) + c_2(t)|y| + c_2(t)|z|, \quad \forall (t, x, y, z) \in I \times \mathbb{R}^3,
$$
$$
\left|f_i(t, x)\right| \le a_i(t), \quad \forall (t, x) \in I \times \mathbb{R}.
\tag{14}
$$

Set $\sup_{i \in I} |c_1(t)| = \|c_1\|$, $\sup_{i \in I} |c_2(t)| = \|c_2\|$, $\sup_{i \in I} |c_3(t)| = \|c_3\|$, and $\sup_{i \in I} |a_i(t)| = \|a_i\|, i = 1, \ldots, m$.

Also, we consider the quantity:

$$
R = \frac{L_1}{\Gamma(\alpha+1)} + \frac{\theta_1 L_2 + \theta_2 L_3}{\Gamma(\alpha)} + \sum_{i=1}^{m} \frac{L_f}{\Gamma(\rho_i + 1)}.
\tag{16}
$$

$\square$

3. Existence and Uniqueness Results

We begin this section by some result that helps us for solving the problem considered in (2).

Lemma 3. *Let $1 < \alpha < 2$ and $G \in C(J, \mathbb{R}^n)$. Then, we can state that the problem*

Let us now transform the above problem to a fixed point one. Consider the nonlinear operator $T\colon E \longrightarrow E$ defined by

$$
Tx(t) = \frac{1}{\Gamma(\alpha)} \int_0^t (t-\tau)^{\alpha-1} g(\tau, x(\tau), Kx(\tau), Hx(\tau)) d\tau
$$
$$
+ \sum_{i=1}^{m} I^{\rho_i} f_i(t, x(t)).
\tag{12}
$$

To prove the main results, we need to work with the following hypotheses:

(H1) There exists a constant $L_f > 0$, such that

$$
\left|f_i(t, x(t)) - f_i(t, y(t))\right| \le L_f |x(t) - y(t)|.
\tag{13}
$$

(H2) There exist functions $c_1(t)$, $c_2(t)$, $c_3(t)$, and $a_i(t) \in C(J, \mathbb{R})$ such that

(H3) There exist constants $L_1, L_2, L_3 > 0$ such that

$$
\left|g(t, x_1, y_1, z_1) - g(t, x_2, y_2, z_2)\right| \le L_1 |x_1 - x_2| + L_2 |y_1 - y_2| + L_3 |z_1 - z_2|, \quad \forall t \in J, x_i, y_i, z_i \in \mathbb{R}, i = 1, 2.
\tag{15}
$$

Theorem 3. *Assume that the hypothesis (H1)-(H2) are fulfilled, and if*

$$
L_f \sum_{i=1}^{m} \frac{1}{\Gamma(\rho_i + 1)} < 1,
\tag{17}
$$

then there exists at least one solution for the problem (2).

Proof. Consider the ball $B_r = \{x \in E: \|x\| \le r\}$ with $r > 0$, where

$$r \ge \frac{\sum_{i=1}^{m} \left(\|a_i\|/\Gamma(\rho_i + 1)\right) + \left(\|c_1\|/\Gamma(\alpha + 1)\right)}{1 - (1/\Gamma(\alpha))\left(\|c_2\|\theta_1 + \|c_3\|\theta_2\right)}. \qquad (18)$$

We define the operators P and Q such that $T = P + Q$, by

$$Px(t) = \frac{1}{\Gamma(\alpha)} \int_0^t (t - \tau)^{\alpha - 1} g(\tau, x(\tau), Kx(\tau), Hx(\tau)) d\tau,$$

$$Qx(t) = \sum_{i=1}^{m} \frac{1}{\Gamma(\rho_i)} \int_0^t (t - \tau)^{\rho_i - 1} f_i(t, x(t)) d\tau. \qquad (19)$$

For any $x \in B_r$, we have

$$|Tx(t)| \le \frac{1}{\Gamma(\alpha)} \int_0^t (t - \tau)^{\alpha - 1} |g(\tau, x(\tau), Kx(\tau), Hx(\tau))| d\tau + \sum_{i=1}^{m} \frac{1}{\Gamma(\rho_i)} \int_0^t (t - \tau)^{\rho_i - 1} |f_i(\tau, x(\tau))| d\tau$$

$$\le \frac{1}{\Gamma(\alpha)} \int_0^t (t - \tau)^{\alpha - 1} \left(|c_1(\tau)| + |c_2(\tau)||Kx(\tau)| + |c_3(\tau)||Hx(\tau)|\right) d\tau \qquad (20)$$

$$+ \sum_{i=1}^{m} \frac{1}{\Gamma(\rho_i)} \int_0^t (t - \tau)^{\rho_i - 1} |a_i(\tau)| d\tau$$

$$\le \frac{\|c_1\|}{\Gamma(\alpha + 1)} + \left(\|c_2\|\theta_1 + \|c_3\|\theta_2\right) \frac{r}{\Gamma(\alpha)} + \sum_{i=1}^{m} \frac{\|a_i\|}{\Gamma(\rho_i + 1)}, |Px(t) + Qx(t)| \le r.$$

Now, we will show that P is continuous and compact. The operator P is obviously continuous. Also, P is uniformly bounded on B_r as

$$\|Px\| \le \frac{\|c_1\|}{\Gamma(\alpha + 1)} + \left(\|c_2\|\theta_1 + \|c_3\|\theta_2\right) \frac{r}{\Gamma(\alpha)}. \qquad (21)$$

Let $t_1, t_2 \in J$ with $t_1 < t_2$ and $x \in B_r$. Then, we have

$$|Px(t_2) - Px(t_1)| = \frac{1}{\Gamma(\alpha)} \int_0^{t_2} (t_2 - \tau)^{\alpha - 1} g(\tau, x(\tau), Kx(\tau), Hx(\tau)) d\tau$$

$$- \frac{1}{\Gamma(\alpha)} \int_0^{t_1} (t_1 - \tau)^{\alpha - 1} g(\tau, x(\tau), Kx(\tau), Hx(\tau)) d\tau, \qquad (22)$$

$$|Px(t_2) - Px(t_1)| \le \frac{\|c_1\| + \|c_2\|\theta_1 + \|c_3\|\theta_2}{\gamma(\alpha + 1)} (t_2^{\alpha} - t_1^{\alpha}).$$

We remark that when $t_2 \longmapsto t_1$, the quantity $\|Px(t_2) - Px(t_1)\| \longmapsto 0$.

Thus, P is equicontinuous and relatively compact on B_r. Then, we show by the Arzelà–Ascoli theorem that P is

compact on B_r. Let us show now that Q is a contraction mapping and consider $x, y \in B_r$.

$$|Qx(t) - Qy(t)| = \left| \sum_{i=1}^{m} \frac{1}{\Gamma(\rho_i)} \int_0^t (t-\tau)^{\rho_i-1} f_i(\tau, x(\tau)) d\tau - \sum_{i=1}^{m} \frac{1}{\Gamma(\rho_i)} \int_0^t (t-\tau)^{\rho_i-1} f_i(\tau, y(\tau)) d\tau \right|$$

$$\leq \sum_{i=1}^{m} \frac{1}{\Gamma(\rho_i)} \int_0^t (t-\tau)^{\rho_i-1} |f_i(\tau, x(\tau)) - f_i(\tau, y(\tau))| d\tau$$

$$\leq \sum_{i=1}^{m} \frac{1}{\Gamma(\rho_i)} \int_0^t (t-\tau)^{\rho_i-1} L_f \|x-y\|$$

$$\leq L_f \sum_{i=1}^{m} \frac{1}{\Gamma(\rho_i+1)} \|x-y\|. \tag{23}$$

We can therefore deduce that T is a contraction map. Since all the assumptions of the Krasnoselskii fixed point theorem are now satisfied, problem (2) then admits at least one solution on J which ends the proof. $\square$

Theorem 4. *Assume that (H1) and (H3) are satisfied. Then, problem (2) has a unique solution, provided that $R < 1$.*

Proof. We show that T has a unique fixed point, which is unique solution of problem (2).

Our objective is to show that $TB_r \subset B_r$.

Let $B_r = \{x \in E : \|x\| \leq r\}$ with $r > 0$, where

Then, for $t \in J$, we have

$$r \geq \frac{(\mu/\Gamma(\alpha+1)) + \sum_{i=1}^{m} (\nu_i/\Gamma(\rho_i+1))}{(L_1/\Gamma(\alpha+1)) + (\theta_1 L_2 + \theta_2 L_3/\gamma(\alpha)) + L_f \sum_{i=1}^{m} (1/\Gamma(\rho_i+1))}. \tag{24}$$

Let us set now

$$\mu = \sup_{i \in J} |g(t, 0, 0, 0)|,$$

$$\nu_i = \sup_{i \in J} |f_i(t, 0)|. \tag{25}$$

For $x \in B_r$, we have

$$|Tx(t)| = \left| \frac{1}{\Gamma(\alpha)} \int_0^t (t-\tau)^{\alpha-1} g(\tau, x(\tau), Kx(\tau), Hx(\tau)) d\tau + \sum_{i=1}^{m} \frac{1}{\Gamma(\rho_i)} \int_0^t (t-\tau)^{\rho_i-1} f_i(\tau, x(\tau)) d\tau \right|$$

$$\leq \sup_{t \in J} \left[\frac{1}{\Gamma(\alpha)} \int_0^t (t-\tau)^{\alpha-1} |g(\tau, x(\tau), Kx(\tau), Hx(\tau))| d\tau + \sum_{i=1}^{m} \frac{1}{\Gamma(\rho_i)} \int_0^t (t-\tau)^{\rho_i-1} |f_i(\tau, x(\tau))| d\tau \right]$$

$$\leq \sup_{t \in J} \left\{ \frac{1}{\Gamma(\alpha)} \int_0^t (t-\tau)^{\alpha-1} |g(\tau, x(\tau), Kx(\tau), Hx(\tau)) - g(\tau, 0, 0, 0)| d\tau \right\} \tag{26}$$

$$+ \sum_{i=1}^{m} \frac{1}{\Gamma(\rho_i)} \int_0^t (t-\tau)^{\rho_i-1} |f_i(\tau, x(\tau)) - f_i(\tau, 0)| d\tau$$

$$\leq \frac{1}{\Gamma(\alpha+1)} (L_1 r + \mu) + (\theta_1 L_2 + \theta_2 L_3) \frac{r}{\Gamma(\alpha)} + \sum_{i=1}^{m} \frac{L_f r + \nu_i}{\Gamma(\rho_i+1)} \leq r,$$

which implies that $TB_r \subset B_r$.

Now, for $x, y \in X$ and for each $t \in J$, we obtain

$$|Tx(t) - Ty(t)| \leq \sup_{t \in J} \left\{ \frac{1}{\Gamma(\alpha)} \int_0^t (t-\tau)^{\alpha-1} |g(\tau, x(\tau), Kx(\tau), Hx(\tau)) - g(\tau, (\tau), Kx(\tau), Hx(\tau))| d\tau \right\}$$

$$+ \sum_{i=1}^{m} \frac{1}{\Gamma(\rho_i)} \int_0^t (t-\tau)^{\rho_i-1} |f_i(\tau, x(\tau)) - f_i(\tau, y(\tau))| d\tau \tag{27}$$

$$\leq \left(\frac{L_1}{\Gamma(\alpha+1)} + \frac{\theta_1 L_2 + \theta_2 L_3}{\Gamma(\alpha)} + \sum_{i=1}^{m} \frac{L_f}{\Gamma(\rho_i+1)} \right) \|x-y\| \leq R\|x-y\|.$$

Consequently, we observe that $\|Tx - Ty\| \le R\|x - y\|$. Since $R < 1$, the operator T is a contracting mapping. Hence, we conclude that the operator T has a unique fixed point $x \in X$. $\quad\square$

Definition 4. The Equation in (2) is Ulam–Hyers stable if there exists a real number $C_f > 0$ such that for each $\varepsilon > 0$ and for each solution $y \in C(J, \mathbb{R})$ of inequality (28), there exists a solution $x \in C(J, \mathbb{R})$ of equation (2) with

$$|y(t) - x(t)| \le \varepsilon C_f, \quad t \in J. \tag{29}$$

Theorem 5. *Assume that (H1) and (H3) are fulfilled. Then, problem (2) is Ulam–Hyers stable if $R < 1$.*

Proof. Let $\varepsilon > 0$, and let $y \in C(J, \mathbb{R})$ be a function which satisfies inequality (28), and let $x \in C(J, \mathbb{R})$ be the unique solution of the following problem. Then, we recall that

4. Ulam Stability Results

In this section, we will study the Ulam stability of problem (2). Let us consider the following inequality:

$$\left| D^\alpha \left(x(t) - \sum_{i=1}^m I^{\rho_i} f_i(t, x(t)) \right) - g(t, x(t), Kx(t), Hx(t)) \right| \le \varepsilon. \tag{28}$$

$$x(t) = \frac{1}{\Gamma(\alpha)} \int_0^t (t - \tau)^{\alpha-1} g(\tau, x(\tau), Kx(\tau), Hx(\tau)) \mathrm{d}\tau$$

$$+ \sum_{i=1}^m I^{\rho_i} f_i(t, x(t)). \tag{30}$$

Integrating inequality (28) and using the initial condition of problem (2), we get

$$\left| y(t) - \sum_{i=1}^m I^{\rho_i} f_i(t, y(t)) - \frac{1}{\Gamma(\alpha)} \int_0^t (t - \tau)^{\alpha-1} g(\tau, y(\tau), Ky(\tau), Hy(\tau)) \mathrm{d}\tau \right| \le \frac{\varepsilon t^\alpha}{\Gamma(\alpha+1)}. \tag{31}$$

Now, we have

$$|y(t) - x(t)| \le \left| y(t) - \sum_{i=1}^m I^{\rho_i} f_i(t, y(t)) - \frac{1}{\Gamma(\alpha)} \int_0^t (t - \tau)^{\alpha-1} g(\tau, y(\tau), Ky(\tau), Hy(\tau)) \mathrm{d}\tau \right|$$

$$+ \sum_{i=1}^m \frac{1}{\Gamma(\rho_i)} \int_0^t (t - \tau)^{\alpha-1} |f_i(t, y(t)) - f_i(t, x(t))| \mathrm{d}\tau + \frac{1}{\Gamma(\alpha)} \int_0^t (t - \tau)^{\alpha-1} \tag{32}$$

$$\times |g(\tau, y(\tau), Ky(\tau), Hy(\tau)) - g(\tau, x(\tau), Kx(\tau), Hx(\tau))| \mathrm{d}\tau.$$

Using hypothesis (H1) and (H3) and inequality (31), we obtain

$$\|y - x\| \le \frac{\varepsilon}{\Gamma(\alpha+1)} + \left(\sum_{i=1}^m \frac{L_f}{\Gamma(\rho_i+1)} + \frac{L_1}{\Gamma(\alpha+1)} + \frac{\theta_1 L_2 + \theta_2 L_3}{\Gamma(\alpha)} \right) \|y - x\|, \tag{33}$$

and consequently we get

$$\|y - x\| \leq \frac{\varepsilon}{\Gamma(\alpha + 1)(1 - R)} = \varepsilon C, \tag{34}$$

where $C = (1/\Gamma(\alpha + 1)(1 - R))$.

Thus, the considered problem (2) has the Ulam–Hyers stability. □

$$\begin{cases} D^{(3/2)}\left(x(t) - \sum_{i=1}^{2} I^{((3i+2)/3)} f_i(t, x(t))\right) = g(t, x(t), Kx(t), Hx(t)), \quad t \in J = [0, 1], \\ x(0) = 0, \\ D^{(3/2)}x(0) = \eta, \quad 1 < \alpha < 2, \end{cases} \tag{35}$$

where

$$f_i(t, x(t)) = \frac{2x(t)}{(2i + t\sqrt{3})(23 + i)},$$

$$g(t, x(t), y(t), z(t)) = \frac{|x(t)|}{100(1 + |x(t)|)} + \frac{2y(t)}{30(1 + y^2(t))} + \frac{2z(t)}{55(1 + z^2(t))} - \cos t, \quad \forall t \in J; x, y, z \in \mathbb{R}. \tag{36}$$

Then, we have

$$\left| f_i(t, x(t)) - f_i(t, y(t)) \right| \leq L_f |x - y|. \tag{37}$$

An easy computation gives

$$L_f = \frac{2}{2 + \sqrt{3}},$$

$$L_1 = \frac{1}{100},$$

$$L_2 = \frac{1}{30},$$

$$L_3 = \frac{1}{55}, \tag{38}$$

$$\theta_1 = \frac{\ln 2}{3},$$

$$\theta_2 = \frac{\ln 2}{5}.$$

Then, we have $R = (L_1/\Gamma(\alpha + 1)) + (\theta_1 L_2 + \theta_2 L_3/\Gamma(\alpha)) + \sum_{i=1}^{m}(L_f/\Gamma(\rho_i + 1)) = 0.398 < 1$.

By Theorem 1, we see that problem (2) has a unique solution and has also the Ulam–Hyers stability.

6. Conclusion

In this work, we have considered a coupled Volterra–Fredholm integro-differential equation, and we have used the Caputo derivative operator. We prove two theorems and

5. Illustrative Example

In this section, an application of the results which have proved is provided. Let us consider Caputo fractional integro-differential equation as follows:

an example to illustrate our results. In the first theorem, we prove the existence and uniqueness of the solution, and the second theorem deals with the existence of at least one solution. The methods used here are Banach's fixed point theorem and Schaefer's fixed point theorem. Here, two Caputo derivative operators of different fractional orders were used in the considered equation, and it would be relevant to generalize this idea by considering several Caputo operators of different fractional orders. The example given on this work establishes the precision and efficiency of the proposed technique and shows that the problem has a unique solution. Before that, we have discussed the Ulam stability of the solution of problem (2).

Data Availability

No data were used to support this study.

Conflicts of Interest

The authors declare that they have no conflicts of interest.

References

[1] R. C. Calleja, A. R. Humphries, and B. Krauskopf, "Resonance phenomena in a scalar delay differential equation with two state-dependent delays," *SIAM Journal on Applied Dynamical Systems*, vol. 16, no. 3, Article ID 14741513, 2017.

[2] A. Carpinteri and F. Mainardi, *Fractional Calculus in Continuum Mechanics*, Springer, Berlin, Germany, 1997.

[3] D. Kumar, J. Singh, S. D. Purohit, and R. Swroop, "A hybrid analytical algorithm for nonlinear fractional wave-like

equations," *Mathematical Modelling of Natural Phenomena*, vol. 14, no. 3, p. 304, 2019.

[4] Z. Dahmani and A. Taieb, "New existence and uniqueness results for high dimensional fractional differential systems," *Facta Universitatis–Series: Mathematics and Informatics*, vol. 30, no. 3, pp. 281–293, 2015.

[5] M. Feckan, J. Wang, and M. Pospísil, "Fractional-order equations and inclusions," *Fractional Calculus in Applied Sciences and Engineering*, De Gruyter, Berlin, Germany, 2017.

[6] Y. Gouari, Z. Dahmani, and A. Ndiaye, "A generalized sequential problem of Lane Emden type via fractional calculus," *Moroccan Journal of Pure and Applied Analysis*, vol. 6, no. 2, Article ID 168183, 2020.

[7] A. A. Kilbas, H. M. Srivastava, and J. J. Trujillo, *Theory and Applications of Fractional Differential Equations*, Elsevier B.V., Amsterdam, Netherlands, 2006.

[8] K. S. Miller and B. Ross, *An Introduction to the Fractional Calculus and Fractional Differential Equations*, Wiley, Hoboken, NJ, USA, 1993.

[9] N. Sene and A. Ndiaye, "On class of fractional-order chaotic or hyperchaotic systems in the context of the Caputo fractional-order derivative," *Journal of Mathematics*, vol. 2020, Article ID 8815377, 15 pages, 2020.

[10] A. Hamoud, "Existence and uniqueness of solutions for fractional neutral Volterra-Fredholm integro-differential equations," *Advances in the Theory of Nonlinear Analysis and its Application*, vol. 4, no. 4, pp. 321–331, 2020.

[11] A. Hamoud, N. Mohammed, and K. Ghadle, "Existence and uniqueness results for Volterra-Fredholm integro-differential equations," *Advances in the Theory of Nonlinear Analysis and its Application*, vol. 4, no. 4, pp. 361–372, 2020.

[12] A. Hamoud and K. Ghadle, "The approximate solutions of fractional Volterra-Fredholm integro-differential equations by using analytical techniques," *Problemy Analiza-Issues of Analysis*, vol. 7, no. 25, pp. 41–58, 2018.

[13] A. Hamoud and K. Ghadle, "Modified Laplace decomposition method for fractional Volterra-Fredholm integro-differential equations," *Journal of Mathematical Modeling*, vol. 6, no. 1, pp. 91–104, 2018.

[14] A. Hamoud and K. Ghadle, "Usage of the homotopy analysis method for solving fractional Volterra-Fredholm integro-differential equation of the second kind," *Tamkang Journal of Mathematics*, vol. 49, no. 4, pp. 301–315, 2018.

[15] A. Hamoud and K. Ghadle, "Existence and uniqueness of solutions for fractional mixed Volterra-Fredholm integro-differential equations," *Indian Journal of Mathematics*, vol. 60, no. 3, pp. 375–395, 2018.

[16] A. Hamoud, K. Ghadle, and S. Atshan, "The approximate solutions of fractional integro-differential equations by using modified Adomian decomposition method," *Khayyam Journal of Mathematics*, vol. 5, no. 1, pp. 21–39, 2019.

[17] K. Hattaf, "A new generalized definition of fractional derivative with non-singular kernel," *Computation*, vol. 8, no. 2, p. 49, 2020.

[18] A. Atangana and D. Baleanu, "New fractional derivatives with nonlocal and non-singular kernel: theory and application to heat transfer model," *Thermal Science*, vol. 20, no. 2, pp. 763–769, 2016.

[19] A. Caputo and M. Fabrizio, "A new definition of fractional derivative without singular kernel," *Progress in Fractional Differentiation and Applications*, vol. 1, pp. 73–85, 2015.

[20] S. Amiri, M. Hajipour, and D. Baleanu, "A spectral collocation method with piecewise trigonometric basis functions for nonlinear Volterra–Fredholm integral equations," *Applied Mathematics and Computation*, vol. 370, Article ID 124915, 2020.

[21] J. Wang, Y. Zhou, and M. Medved, "Existence and stability of fractional differential equations with Hadamard derivative," *Topological Methods in Nonlinear Analysis*, vol. 41, no. 1, pp. 113–133, 2013.

[22] B. Ahmad and S. Ntouyas, "Initial-value problems for hybrid Hadamard fractional differential equations," *The Electronic Journal of Differential Equations*, vol. 2014, no. 161, pp. 1–8, 2014.

[23] B. Ahmad, S. K. Ntouyas, and J. Tariboon, "A study of mixed Hadamard and Riemann-Liouville fractional integro-differential inclusions via endpoint theory," *Applied Mathematics Letters*, vol. 52, pp. 9–14, 2016.

[24] A. Hamoud, A. A. Charif, A. K. Ghadle, and K. P. Ghadle, "Existence and uniqueness results of hadamard fractional volterra-fredholm integro-differential equations," *Konuralp Journal of Mathematics*, vol. 9, no. 1, pp. 143–147, 2021.

[25] Y. Zhou, *Basic Theory of Fractional Differential Equations*, World Scientific, Singapore, 2014.